

**“SYNTHESIS OF LANTHANIDE COMPLEXES WITH
BIOLOGICALLY ACTIVE ORGANIC LIGANDS: THEIR SPECTRAL
AND CHEMICAL KINETIC STUDIES”**

by

RUOKUOSENUEO ZATSU



Submitted to

NAGALAND UNIVERSITY

In Partial Fulfilment of the Requirements for Award of the Degree

of

DOCTOR OF PHILOSOPHY IN CHEMISTRY

**DEPARTMENT OF CHEMISTRY
NAGALAND UNIVERSITY
LUMAMI-798627
NAGALAND, INDIA**

Sept - 2021



NAGALAND UNIVERSITY

(A Central University, Estd. By the Act of Parliament No. 35 of 1989)

Lumami – 798627, Nagaland, India

Department of Chemistry

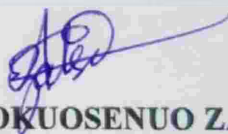
Declaration

I, RUOKUOSENUE ZATSU, hereby declare that the matter illustrated in this Thesis entitled “SYNTHESIS OF LANTHANIDE COMPLEXES WITH BIOLOGICALLY ACTIVE ORGANIC LIGANDS: THEIR SPECTRAL AND CHEMICAL KINETIC STUDIES” submitted by me for the degree of Doctor of Philosophy in Chemistry is the result of investigations carried out by me in the Department of Chemistry, Nagaland University under the Supervision of **Dr. MADDELA PRABHAKAR**, Assistant Professor, Department of Chemistry, Nagaland University and **Prof. M. INDIRA DEVI**, Professor Department of Chemistry, Nagaland University.

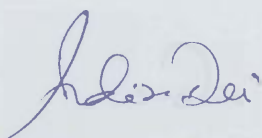
I further declare that in keeping with the general practice of reporting scientific observations, due acknowledgments have been made wherever the work described is based on the findings of other investigators and the contents of this thesis did not form the basis for award of any degree to me or to the best of my knowledge to anybody else.

Date: 15/09/2021

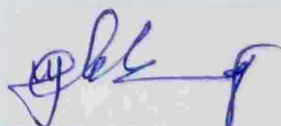
Lumami


(RUOKUOSENUE ZATSU)

Candidate


(Prof. M. Indira Devi)

(M. INDIRA DEVI)
Co-Supervisor
Professor
Department of Chemistry
Nagaland University
Hqrs: Lumami-798627


(Dr. Maddela Prabhakar)

Dr. M. PRABHAKAR
Assistant Professor
Department of Chemistry
Nagaland University
Hqrs: Lumami-798627, Nagaland


(Prof. M. Indira Devi)

Head Department of Chemistry
Nagaland University
Lumami - 798627



NAGALAND UNIVERSITY

(A Central University, Estd. By the Act of Parliament No. 35 of 1989)

Lumami – 798627, Nagaland, India

Department of Chemistry

Certificate

It is to certify that the Ph. D. Thesis entitled “*Synthesis of Lanthanide Complexes with Biologically Active Organic Ligands: their Spectral and Chemical Kinetic Studies*” is based on the original work done by **Ms. Ruokuosenuo Zatsu** (Ph. D. Reg. No. 703/2016; dated: 27-05-2015) under our direct Supervision in the Department of Chemistry, Nagaland University, Lumami, Nagaland, hence this research work leading to advancement of knowledge in the fields of Lanthanide Metal Complexes, Material Chemistry, Photo Chemistry and Medicinal Chemistry.

This work has not previously formed the basis for any degree, diploma, associateship, fellowship or any other similar title and that it represents entirely an independent work on the part of the candidate. We certify that the candidate has fulfilled all the necessary conditions/requirements as laid down by the Nagaland University for the purpose of submission of Ph. D. Thesis.

(Prof. M. Indira Devi)

(M. INDIRA DEVI)

Professor
Co-Supervisor
Department of Chemistry
Nagaland University
Hqrs: Lumami-798627

(Dr. Maddela Prabhakar)

Dr. M. PRABHAKAR

Supervisor
Asstt. Professor
Department of Chemistry
Nagaland University
Hqtrs: Lumami-798627, Nagaland



NAGALAND UNIVERSITY

(A Central University, Estd. By the Act of Parliament No. 35 of 1989)

Lumami – 798627, Nagaland, India

Department of Chemistry

Course Completion Certificate

This is to certify that **Ms. Ruokuosenuo Zatsu** has satisfactorily completed all the courses offered in the Pre-Ph. D. course work programme in Chemistry.

The courses include:

CHEM-601	Research Methodology
CHEM-602	Advances in Chemistry
CHEM-603	Literature review, Report writing and Presentation

(Prof. M. Indira Devi)

Head
विभागाध्यक्ष / Head
Department of Chemistry
विभाग / Department of Chemistry
Nagaland University / University
लुनामी / Lumami - 798 627

Acknowledgements

*First and foremost I give thanks to **God Almighty**, the source of strength in my life. Thank you Lord for your wisdom and knowledge upon me, my state of good health and peace of mind for which I was able to witness this day of completion of my Ph. D. research.*

*With great pleasure, I acknowledge my utmost gratitude and indebtedness to my esteemed Research Supervisor, **Dr. Maddela Prabhakar**, Asstt. Professor, Dept. of Chemistry, Nagaland University and **Prof. M Indira Devi**, Professor, Dept. of Chemistry, Nagaland University, under whose expert supervision/guidance I made my own beginnings. Their positive attitude, patience, enthusiasm and dedication to research have really inspired me. They gave me the confidence and mould me well for a career path on which I am about to embark. Their critical remarks and suggestions have helped me a lot in shaping this work and thus making it a success. Thank you Sir and Madam!*

*I am extremely thankful to **Mom** and **Dad** for their love, their prayers and sacrifices and preparing me for my future. Who has always supported me and encouraged me. Your love, prayers, patience and understanding during my research work have brought me thus far making this work a success. I also thank all my family members for their love and support and who have always stood by my side, encouraging me and supporting me through prayers.*

I give thanks to Professor Indira Devi, Head of Department of Chemistry, Prof. Dipak Sinha, prof. Upasana Bora Sinha, Dr. I. Tavishe Phucho, Dr. N. A. Choudhury and Dr. Seram Dushila Devi for their help, advices and moral support.

I sincerely acknowledge the DST-SERB, Govt. of India and Nagaland University for the financial support and assistance which contributed much to the smooth work flow of my research programme.

I gratefully acknowledge the help provided by the technical and office staff, Mr. S. Bendangtemsu, Ms. Sunepjungla, Ms. Temsuienla Amer, Mr. Puloto, Mr. Johnny Yanthan, and Mr. Phyobemo Patton of the Department of Chemistry, Nagaland University.

I take this opportunity to thank my fellow lab mates Thechno, Shurhovolie, Melevolu and Veto for maintaining a warm and encouraging environment, making my work enjoyable and their patience throughout my anxieties for the past few years.

I would also like to express my thanks to all my research colleagues and friends for their kind support and timely help.

My heartfelt gratitude goes to Aunty Toheli Kiyelho and my Exodus sisters for their constant prayers, love, support and encouragement. It was indeed a wonderful journey together.

Last but not the least; I humbly apologize to those whose contribution should have been acknowledged but escaped mentioning inadvertently. I express my sincere thanks to all.

(RUOKUOSENUEO ZATSU)

Dedicated
to
My Parents
Mr. Ketoulhoulie Zatsu
&
Mrs. Lhoukhrienuo Zatsu

Table of Contents

	List of Abbreviations	Page no.
Chapter 1:	Introduction	1-27
1.1.	History and Chemistry of Lanthanide	1-2
1.2.	Lanthanide Contraction and Coordination Number	2-3
1.2.1.	Large Coordination Numbers	3
1.2.2.	Variable Coordination Numbers	3
1.3.	Magnetic and Spectroscopic Properties of Lanthanides	3-5
1.4.	Synthesis and Importance of Lanthanide Complexes	5-16
1.5.	Chemical Kinetics	16-17
1.6.	Scope and Aim of the Study	17
1.7.	References	18-27
Chapter 2:	Microwave-Assisted Green Synthesis of Curcumin Lanthanide (Pr^{3+}, Nd^{3+}, Eu^{3+} and Gd^{3+}) Complexes and Investigation of their Spectroscopic and Kinetic Studies	28-62
	Abstract	28
2.1.	Introduction	28-31
2.2.	Experimental	31-32
2.2.1.	Materials and Methods	31
2.2.2.	General Microwave-assisted Green Synthesis of Curcumin Lanthanide(III) Complexes [$\text{L}^1_3\text{LnCl}_3 \cdot x\text{H}_2\text{O}$] (2.1a-d)	32
2.3.	Results and Discussion	32-56
2.3.1.	FT-IR Spectral Characterization Studies	34-39
2.3.1.1.	FT-IR Spectra of Curcumin ligand (L^1)	34
2.3.1.2.	FT-IR Spectra of Curcumin Praseodymium Complex [$\text{L}^1_3\text{PrCl}_3$] (2.1a)	35
2.3.1.3.	FT-IR Spectra of Curcumin Neodymium Complex [$\text{L}^1_3\text{NdCl}_3$] (2.1b)	36
2.3.1.4.	FT-IR Spectra of Curcumin Europium Complex [$\text{L}^1_3\text{EuCl}_3 \cdot 6\text{H}_2\text{O}$] (2.1c)	37
2.3.1.5.	FT-IR Spectra of Curcumin Gadolinium Complex [$\text{L}^1_3\text{GdCl}_3 \cdot 6\text{H}_2\text{O}$] (2.1d)	38
2.3.2.	UV-Vis Spectral Characterization Studies	40-41
2.3.3.	Fluorescence Spectral Characterization Studies	42-43
2.3.4.	Thermogravimetric Analysis	43-45
2.3.5.	Chemical Kinetic and Thermodynamic Studies	46-56
2.4.	Conclusion	57
2.5.	References	58-62
Chapter 3:	Synthesis of Curcumin-thiosemicarbazone Lanthanide (Pr^{3+}, Nd^{3+}, Eu^{3+} and Gd^{3+}) Complexes and Investigation of their Spectroscopic and Kinetic Studies	63-99
	Abstract	63
3.1.	Introduction	63-67
3.2.	Experimental	67-69
3.2.1.	Materials and Methods	67
3.2.2.	Synthesis of Curcumin-thiosemicarbazone Ligand (L^2)	67-68

3.2.3.	General Synthesis of Curcumin-thiosemicarbazone Lanthanide(III) Complexes [$L^2_3LnCl_3$] (3.1a-d)	68-69
3.3.	Results and Discussion	69-94
3.3.1.	FT-IR Spectral Characterization Studies	71-76
3.3.1.1.	FT-IR Spectra of Curcumin-thiosemicarbazone Ligand(L^2)	71
3.3.1.2.	FT-IR Spectra of Curcumin-thiosemicarbazone Praseodymium Complex [$L^2_3PrCl_3$] (3.1a)	72
3.3.1.3.	FT-IR Spectra of Curcumin-thiosemicarbazone Neodymium Complex [$L^2_3NdCl_3$] (3.1b)	73
3.3.1.4.	FT-IR Spectra of Curcumin-thiosemicarbazone Europium Complex [$L^2_3EuCl_3$] (3.1c)	74
3.3.1.5.	FT-IR Spectra of Curcumin-thiosemicarbazone Gadolinium Complex [$L^2_3GdCl_3$] (3.1d)	75
3.3.2.	UV-Vis Spectral Characterization Studies	77-78
3.3.3.	Fluorescence Spectral Characterization Studies	79-80
3.3.4.	Thermogravimetric Analysis	81-83
3.3.5.	Chemical Kinetic and Thermodynamic Studies	84-94
3.4.	Conclusion	95
3.5.	References	96-99
Chapter 4:	Synthesis of Curcumin-pyrazole Lanthanide (Pr^{3+} , Nd^{3+} , Eu^{3+} and Gd^{3+}) Complexes and Investigation of their Spectroscopic Studies	100-126
	Abstract	100
4.1.	Introduction	100-105
4.2.	Experimental	105-107
4.2.1.	Materials and Methods	105-106
4.2.2.	Synthesis of Curcumin-pyrazole Ligand (L^3)	106
4.2.3.	General Synthesis of Curcumin-pyrazole Lanthanide(III) Complexes [$L^3_3LnCl_3 \cdot xH_2O$] (4.1a-d)	107
4.3.	Results and Discussion	107-
4.3.1.	FT-IR Spectral Characterization Studies	109-115
4.3.1.1.	FT-IR Spectra of Curcumin-pyrazole Ligand (L^2)	109
4.3.1.2.	FT-IR Spectra of Curcumin-pyrazole Praseodymium Complex [$L^3_3PrCl_3 \cdot H_2O$] (4.1a)	110-111
4.3.1.3.	FT-IR Spectra of Curcumin-pyrazole Neodymium Complex [$L^3_3NdCl_3 \cdot 6H_2O$] (4.1b)	111-112
4.3.1.4.	FT-IR Spectra of Curcumin-pyrazole Europium Complex [$L^3_3EuCl_3 \cdot 6H_2O$] (4.1c)	112-113
4.3.1.5.	FT-IR Spectra of Curcumin-pyrazole Gadolinium Complex [$L^3_3GdCl_3 \cdot 6H_2O$] (4.1d)	113-114
4.3.2.	UV-Vis Spectral Characterization Studies	116-117
4.3.3.	Fluorescence Spectral Characterization Studies	118-119
4.3.4.	Thermogravimetric Analysis	120-122
4.4.	Conclusion	123
4.5.	References	124-126

Chapter 5:	Synthesis of Curcumin-diethanolimine Lanthanide (Pr^{3+}, Nd^{3+}, Eu^{3+} and Gd^{3+}) Complexes and Investigation of their Spectroscopic Studies	126-151
	Abstract	126
5.1.	Introduction	126-131
5.2.	Experimental	132-134
5.2.1.	Materials and Methods	132
5.2.2.	Synthesis of Curcumin-diethanolimine Ligand (L^4)	132-133
5.2.2.	General Synthesis of Curcumin-diethanolimine Lanthanide(III) Complexes [$\text{L}^4\text{LnCl}_3 \cdot x\text{H}_2\text{O}$] (5.1a-d)	133-134
5.3.	Results and Discussion	134-147
5.3.1.	FT-IR Spectral characterization studies:	135-141
5.3.1.1.	FT-IR Spectra of Curcumin-diethanolimine Ligand (L^4)	135-136
5.3.1.2.	FT-IR Spectra of Curcumin-diethanolimine praseodymium complex [$\text{L}^4_2\text{PrCl}_3 \cdot \text{H}_2\text{O}$] (5.1a)	136-137
5.3.1.3.	FT-IR Spectra of Curcumin-diethanolimine neodymium complex [$\text{L}^4_2\text{NdCl}_3 \cdot 6\text{H}_2\text{O}$] (5.1b)	137-138
5.3.1.4.	FT-IR Spectra of Curcumin-diethanolimine europium complex [$\text{L}^4_2\text{EuCl}_3 \cdot 6\text{H}_2\text{O}$] (5.1c)	138-139
5.3.1.5.	FT-IR Spectra of Curcumin-diethanolimine gadolinium complex [$\text{L}^4_2\text{GdCl}_3 \cdot 6\text{H}_2\text{O}$] (5.1d)	139-140
5.3.2.	UV-Vis Spectral Characterization Studies	142-143
5.3.3.	Fluorescence Spectral Characterization Studies	144-145
5.3.4.	Thermogravimetric Analysis	145-147
5.4.	Conclusion	148
5.5.	References	149-151
Chapter 6:	Synthesis of Flavanone-thiosemicarbazone Lanthanide (Pr^{3+}, Nd^{3+}, Eu^{3+} and Gd^{3+}) Complexes and Investigation of their Spectroscopic Studies	152-180
	Abstract	152
6.1.	Introduction	152-155
6.2.	Experimental	156-158
6.2.1.	Materials and Methods	156
6.2.2.	Synthesis of Flavanone-thiosemicarbazone Ligand (L^5)	156-157
6.2.2.	General Synthesis of Flavanone-thiosemicarbazone Lanthanide(III) Complexes [$\text{L}^5_3\text{LnCl}_3 \cdot x\text{H}_2\text{O}$] (6.1a-d)	157-158
6.3.	Results and Discussion	158-176
6.3.1.	Crystal Structure and Hirshfeld Surface Analysis of Flavanone-thiosemicarbazone Ligand (L^5)	160-164
6.3.2.	FT-IR Spectral Characterization Studies	165-171
6.3.2.1.	FT-IR Spectra of Flavanone-thiosemicarbazone Ligand (L^5)	165
6.3.2.2.	FT-IR Spectra of Flavanone-thiosemicarbazone Praseodymium Complex [$\text{L}^5_3\text{PrCl}_3 \cdot \text{H}_2\text{O}$] (6.1a).	166-167
6.3.2.3.	FT-IR Spectra of Flavanone-thiosemicarbazone Neodymium complex [$\text{L}^5_3\text{NdCl}_3 \cdot 6\text{H}_2\text{O}$] (6.1b).	167-168
6.3.2.4.	FT-IR Spectra of Flavanone-thiosemicarbazone Europium Complex [$\text{L}^5_3\text{EuCl}_3 \cdot 6\text{H}_2\text{O}$] (6.1c).	168-169

6.3.2.5.	FT-IR Spectra of Flavanone-thiosemicarbazone Gadolinium Complex [$L^5_3GdCl_3 \cdot 6H_2O$] (6.1d).	169-170
6.3.3.	UV-Vis Spectral Characterization Studies	172-173
6.3.4.	Thermogravimetric Analysis Studies	174-176
6.4.	Conclusion	177
6.5.	References	178-180
Appendix 1	Plagiarism Checked Proof	181-182
Appendix 2	List of Publications and Conferences/ Seminars/ workshops attended	183-184

Abbreviations

Å	Angstrom
CHN	Carbon Hydrogen Nitrogen
cm	Centimetre
CN	Coordination Number
DMF	N,N-Dimethylformamide
DMSO	Dimethyl Sulfoxide
DNA	Deoxyribonucleic acid
DTA	Differential Thermal Analysis
Ea	Activation Energy
Et ₃ N	Triethylamine
EtOH	Ethanol
Eu ⁺³	Europium
FT-IR	Fourier Transfer Infrared
Gd ⁺³	Gadolinium
La ⁺³	Lanthanum
Ln ⁺³	Lanthanide
Lu ⁺³	Lutetium
MeOH	Methanol
Nd ⁺³	Neodymium
nm	Nanometre
NMR	Nuclear Magnetic Resonance
pm	Pico meter
ppm	Parts per million
Pr ⁺³	Praseodymium
TGA	Thermogravimetric Analysis
THF	Tetrahydrofuran
Uv-Vis	Ultraviolet-Visible
z	Atomic number
β	Nephelauxetic
ΔG°	Gibbs free energy change
ΔH°	Enthalpy change
ΔS°	Entropy change

INTRODUCTION

1.1. History and Chemistry of Lanthanides

Lanthanide was discovered by Lieutenant Karl Axel Arrhenius way back in 1787 as an unusual black mineral near Ytterby, Sweden. The mineral was studied by Swedish chemist Johan Gadolin in 1794 and found it to contain a new element and after the name of the village, called it as Yttria.¹ The discovery of the rare mineral did not straight away isolate all the elements; it took a decade to separate them all. One of the problems at that time was that the scientist did not know that they have been working with a complete group of metal and so they were classified as 'rare earth metal'. After discovery of Lutetium, Henry Mosely discovered that on bombarding the sample of an element with cathode ray there was fifteen rare earth elements with atomic no. 57 (Lanthanum) to 71 (Lutetium) out of which element with atomic no. 61 (Promethium) was missing. From the laboratory in Tennessee, during fission of Uranium atoms, Marinsky, Glendenin and Coryell discovered an isotope of element 61. The element was classified and named as Promethium in 1947 and with this discovery the Lanthanide series were completed.^{2,3} They are extremely similar to each other in properties and are assembled in a same substance so the Lanthanides are rare but are not paucity as they are difficult to derive the elements in its pure form. It was hard to distinguish the element of Lanthanide, but with the introduction of the spectroscopy in nineteen century each Lanthanide was well defined by its spectroscopic properties.⁴ The word Lanthanide is from a Greek word "*lanthanein*" which means "*lying hidden*" introduced by Victor Goldschmidt in 1925.⁵ The Lanthanides are broadly distributed on the earth crust with a concentration of 10-300 ppm. The most abundant element Cerium is found in a concentration of 60-80 ppm, and then comes the Neodymium and Lanthanum with half abundance of Cerium. Praseodymium, Samarium, Gadolinium and Dysprosium with abundance of 5-10 ppm and the other element with less abundance, the least abundance is Lutetium ($> 0.05\text{ppm}$).⁶

Lanthanides are found to be present in monazite sand, sediments and coal fly ash.^{7,8} Lanthanides have a similar physico-chemical properties as they occur together in the earth crust and they are classified as f-block elements as the valence electron of the elements lies in the 4f orbital. These f-block are called the inner transition elements as they lie much deeper than that of the d-orbitals.^{9,10} Bohr stated that the Lanthanides have a

ground state configuration $[\text{Xe}]4f^n 5d^1 6s^2$ (where $n=0-14$) and have a changeable oxidation state i.e. +2, +3 and +4 oxidation states and among them the most stable one is +3 oxidation state because the inner shell of the 4f sub-shell is a part of the inner Xenon core. Lanthanides are a group of 15 elements that are located between Barium and Hafnium as one series in the 6th row of the periodic table.¹¹

1.2. Lanthanide Contraction and Coordination Number

On moving from the left to right in the periodic table with the increase in the atomic number of the element i.e. from La^{+3} to Lu^{+3} there is a steady decrease in the covalent and ionic radii, this phenomenon is known as the Lanthanide contraction. The contraction in the Lanthanides occurs as the extra orbital electron in the nuclear charge which is incompletely shielded by the 4f-electron resulting in the smaller atomic radii as the electron 6s are pulled towards the nucleus.^{12,13}

The atomic radii of La^{+3} is 1.061 Å, where as the Lu^{+3} has 0.850 Å. The radii of these rare earth ions are about the same size because of the Lanthanide contraction.¹⁴ Due to these interesting features of Lanthanides, the elements present resemble each other and so it is difficult to isolate them individually.¹⁵ The contraction does not only affect the Lanthanides but also the elements beyond. According to Fajan's rule, decrease in size increase the covalent character and decreases the basicity of the Lanthanides. As the size of the ionic radii decrease it has the tendency to form more stable complexes and there is a small increase in electronegativity of the trivalent ions.¹⁶ Similar structures are shown when any compounds of the rare earth are crystallized but the crystal dense towards the series as the lattice parameters decrease. Due to contraction across the Lanthanide series, the parameters determining the properties of the Lanthanide can be kept constant, while small increment can be varied in the lattice spacing, which has attracted the attention of scientists for research.¹⁷

In 1960s, the coordination number (CN) of Lanthanides was found to be much higher than 6 and how the complex with lower coordination number such as 2, 3 and 4 are possible for the research to synthesize.¹⁸ The coordination number of a complex can be affected by different factors such as relative size of the metal, charge which depends on the electronic configuration of the metal and the ligand.¹⁹ Aqueous solution of Lanthanides have a coordination number 9 and 8 which can be elevate to 12 on inclusion of ligand.²⁰ In most of the Lanthanide complexes, coordination number were found to be between 2 to

12, out of which the 8 coordination number is the most common one. Lanthanide coordination number shows two distinguishable features than that of the other transition metals:

1.2.1. Large Coordination Numbers

Lanthanides mostly show 8 or 9 coordination number while that of other transition metals show 4 or 6 coordination number. One of the factors that affect the large coordination number is the large ionic radii of Lanthanides. For example Iron and Copper shows 55 and 54 Å respectively while that of the Lanthanides shows around 80-110 Å.

1.2.2. Variable Coordination Numbers

Comparing with the transition metals, crystal field stabilization energy of Lanthanides shows much smaller stabilization energy, therefore, the bonding of lanthanide are not directional and so the coordination number varies from 2 to 12.²¹

The Lanthanide contraction phenomena shows that, with the increase in the atomic number (Z) decreases the ionic radii, it can be expected that around the central metal ion less anion will be present and so the coordination will be lesser with increase Z value. The halides and the oxides shows this behavior, as for example the LaCl_3 shows 9 coordination number while that of LuCl_3 shows 8 coordination number. Similar changes can be observed in many complexes of transition metals. The hydrated Ln^{3+} ions of the earlier lanthanide series ($\text{Ln}=\text{La-Gd}$) shows nine-coordinate $[\text{Ln}(\text{OH}_2)_9]^{3+}$ ions while those in the later ($\text{Ln}=\text{Tb-Lu}$) shows eight-coordinate $[\text{Ln}(\text{OH}_2)_8]^{3+}$ ions with an aggregate of intermediate metal. Sometimes the coordination numbers are also found to be constant throughout the series.²²

1.3. Magnetic and Spectroscopic Properties of Lanthanides

Lanthanides have fascinating electromagnetic and light properties as Ln^{3+} ions have unpaired electrons in the f-orbital. The ground state and the excitation state of the Lanthanides are well separated from each other that it is thermally out of reach, so the magnetic properties are determined with ground state. From the coupling of spin and orbital angular momentum the magnetic moments of Ln^{3+} can be well described.²³ Consequences of the spin-spin, spin-orbital and orbital-orbital interactions gives the magnetic compartment of the transition metals or the Lanthanides.²⁴ All the Lanthanides

elements except for Lu^{3+} shows paramagnetic at higher temperature while at lower the temperature they shows anti-ferromagnetism and on lowering temperature they may show ferromagnetism.²⁵

Lanthanide ions have a noticeable colour both in solid and aqueous state due to f-f transitions as they have partly filled f-orbitals. Almost all the ions show absorption near UV region of the spectrum or in the visible region except for Lu^{3+} which have a full f-shell.²⁶

In **1866**, Busen observed a sharp absorption line of a rare compound which was further analyzed by J. Becquerel in **1906**. But the genesis of the spectra remained unrevealed until in 1930s when Kramers and Becquerel and Bethe put forward that all the provenance were due to the electronic structure of the 4f-configuration (f-f transition).²⁷ The studies continues and in the early **1940**, the first spectroscopic studies of the Lanthanide ion in aqueous solution were observed using purified Eu^{3+} and with the change in the solvent and the concentration there is a difference in the absorption spectrum of the element and when excited with ultraviolet light they were found to have a high luminescent properties. Organic ligand having a light-harvesting chromophore with suitable photophysical properties when coupled with Lanthanides, the Ln^{3+} has the ability to produce luminescence by photosensitization. Lanthanides possess excellent photophysical properties as they have a distinctive colour, which has attractive Ln^{3+} ions to be used in imaging, colour reproduction and lighting.^{28,29}

Lanthanide ions have two transition states which affect the electronic spectra; they are the allowed and forbidden transition. Allowed transitions are the f-d transition which exhibits a strong broad band and intense band. Lanthanides involved a large energy level and they differ with the change in the ligand, while the forbidden transitions are the f – f transition with sharp and narrow spectral bands. For example taking the characteristic of Eu^{3+} in UV, they give a spin and electric-dipole transition which do not show a splitting and so the selection rule (Laporte, spin and selection rule for orbital angular momentum) are relaxed.³⁰ The internal 4f-transition in the spectral region of the Lanthanides and the sensitivity of this transition towards coordination to the ligand makes it an interesting property to investigate the coordination chemistry of Lanthanides in aqueous, semi aqueous and non-aqueous solution. Many applications of the Lanthanides have been discovered for the last few decades and it's found that most of the applications are concerned with the spectral properties of Lanthanides. Progress in the theory and practice

of Lanthanide absorption spectroscopy come across some of the difficulties which can be corrected using the optical spectroscopy. One of the characteristic properties of Lanthanide is the weak narrow absorption in Ultra-violet and Infra-Red region of the spectrum.³¹

1.4. Synthesis and Importance of Lanthanide Complexes

The chemistry of the Lanthanides has been achieving much progress in different studies and researches. They have the achievements in the field in of coordination chemistry,³² inorganic chemistry,³³ application in industries and agriculture,³⁴ medical and biological application,³⁵ magnetic resonance imaging agent (MRI),^{36,37} bio-imaging,³⁸ lighting devices,³⁹ lasers,⁴⁰ telecommunications⁴¹ and the application of the Lanthanides are also remarkably increasing as an excellent diagnostics and prognostic probe in biological and clinical aspects.⁴² Lanthanides are also found to have excellent physical and chemical properties because its electronic configuration is special.⁴³

For the last 20 years, the Lanthanide complexes in the organic solution and aqueous solution are attracting much interest as their ground state and excited state have many activities.⁴² Lanthanides are mostly ionic salts and are hard acceptors. Lanthanide ions form stable complexes with oxygen and nitrogen donor ligands and form 9 or 8 coordinations. When Lanthanide complexes synthesized with monodentate ligand they formed weak complexes but when they are synthesized with chelated ligands, result in stronger complexes because of the chelate effect.⁴⁴ Lanthanide ions possess smaller atomic radii with high positive charge, satisfying the optimum condition for resulting in a higher coordination number,^{45,47} so they are used for the formation of coordination compounds and supramolecular system like the helicate, grids, interlock and bundle molecule which cannot be attained applying frequently used templating ions (ligand-based reactions on the coordination site of the metal) and so utilizing of the Lanthanide ions result in distinctive and stable complexes with functional and flexible structure.⁴⁸ Lanthanide complexes in solution manifest many properties and the complexes usually exhibits a narrow emission band, large Stokes's shifts, long excited lifetime and emit in the red and green region. Although the excitation of the Lanthanide ions itself have a weak luminescence signal due to the fact that the absorption band within the 4f-electrons are forbidden.^{49,50}

The formation of Lanthanide complexes with oxygen, sulfur and nitrogen donor atoms as ligands can be a good factor as the Lanthanide ions favor to coordinate to this site

of the ligand due to its high charge density, Lewis acids and are reactive metals. As the ligands acts as transmitter for the complexation, they are used for the transportation of energy in order to attain systematic excitation state.^{51,54} Lanthanide ions have a similar characteristic with that of the other elements such as calcium and magnesium, so they have the ability to replace them with Ln^{3+} ions and can be utilized as probe in place of Ca and Mg metals for the investigation of the structural functions of bimolecular reactions.^{55,57}

In 1999, P. R. Maravalli *et al.* synthesized a series of Lanthanide(III) complexes using 3-N-methyl piperidion-4-salicylidene amino- 5- mercapto- 1, 2, 4-trazole ligand with Ln (III) nitrate; where Ln = La, Ce, Pr, Nd, Sm, Gd, Tb, Dy, ER, Yb and Y by direct reaction method (**Figure 1.1**). The complexes prepared were characterized by different methods and suggested the structure of the complexes. The spectral studies show that the coordination bonding between the metal and the ligand is a bidentate one and proposed the complexes to have coordination number six.⁵⁸

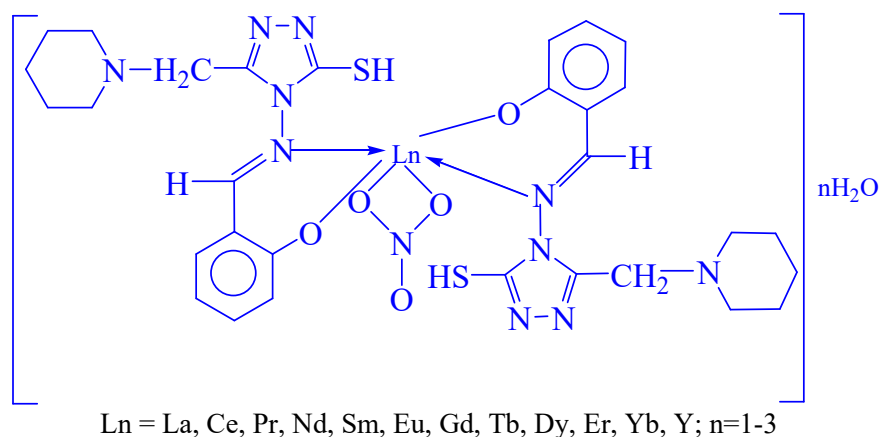


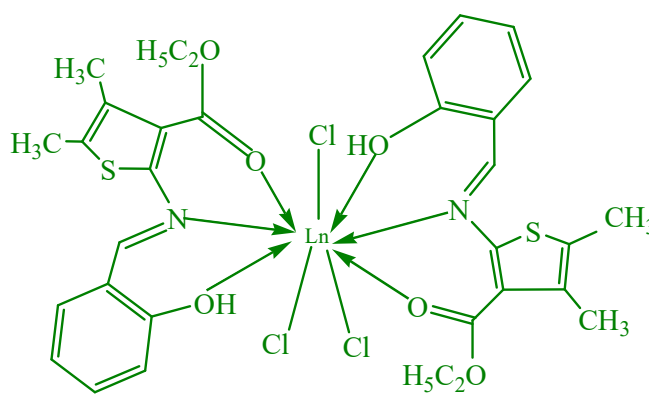
Figure 1.1. Proposed Structures of the Complexes.

In 2001, I. P. Kostova *et al.* reported the synthesized Lanthanide(III) complexes with 4-methyl-7-hydrocoumarin ligand and studied their thermal analysis and the various spectral properties using different spectroscopic methods. The synthesized complexes were identified and characterized by elemental analysis, IR, NMR, conductivity, Mass spectroscopy, DTA and TGA.⁵⁹ Irena Kostova and group in 2005 synthesized some of the Lanthanide complexes and disclosed its antineoplastic activity and its cytotoxic effect. The complexes were found to have metal-ligand coordination through hydroxyl group.^{60,61}

As Lanthanide(III) complexes were used as a detector of natural sugar and as a cancer biomarker at a certain pH, O. Alpturk and co-workers in 2006 designed complexes

of Lanthanide which shows a successful detection of natural sugar and exhibits enhanced fluorescence emission.⁶²

B. S. Kumari *et al.* (2009) synthesized a series of Lanthanide(III) chloride complexes with heterocyclic Schiff base (2-(N-salicylideneamino)-3-carboxyethyl-4,5-dimethylthiophene) base under microwave irradiation in solid state (**Figure 1.2**). The spectral studies showed that the metals were coordinated at the ONO donor site of the ligand acting as a neutral tridentate and studies shown from the X-ray diffraction of the lanthanide (III) complexes results in orthorhombic. The synthesized complexes were also reported to be a promising antimicrobial agents.⁶³



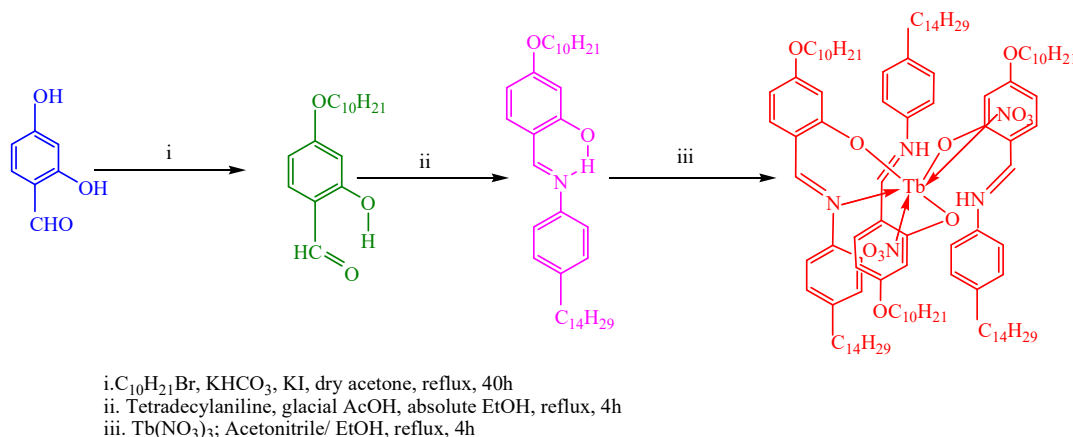
Ln = La(III), Ce(III), Pr(III), Nd(III), Sm(III), Eu(III), Gd(III)

Figure 1.2. Structure of the Lanthanide(III) Complexes.

In 2009, T. Moaienla and co-workers studied the comparative absorption spectra of Lanthanide with L-phenylalanine, L-glycine, L-alanine, and L-aspartic in the presence and absence of Ca^{2+} in organic solvents. The investigation shows that 4f-4f transition Lanthanides can be utilized to study the binding nature of biologically important ligands. From the different studies and evaluated parameters (Slator-Condon F_k , Racah E^k , spin-orbit coupling constant ξ_{4f} , Nephelauxetic β , oscillator strength and Judd-Ofelt T_λ) it is found that the absorption spectra of Lanthanide complexes in DMF solvent was the most favorable one among the organic solvents used.⁶⁴

N. V.S. Rao and co-workers (2010) synthesized new Lanthanide complexes, Tb(III), Dy(III), and Gd(III) of N-aryl base showing mesomorphism (**Scheme 1.1**); all the synthesized complexes were characterized and it is observed that electronic properties are dominated by the donor-acceptor of the organic chromophore ligand and the emission maxima shows a ligand-driven strong fluorescence with large Stokes shift. The nature of

the interaction (Vander Waals interaction, electrostatic interaction) between the coordinated ligand and the Lanthanide ions leads to an increase transition temperature and thermal stability.⁶⁵



Scheme 1.1. Synthesis of Lanthanide(III) complexes.

M. R. Anoop *et al.* (2011), reported the synthesis, thermal and spectral study of 1,2-diphenyl-4-butyl-3,5-pyrazolidione(phenylbutazone) Lanthanide(III) complexes which were characterized by elemental analysis, IR, molar conductance, Uv-Vis and NMR spectra. In their study the spectra show that the phenylbutazones act as a bidentate and mono-ionic ligand coordinating at the carbonyl oxygen of the ligand ring. TGA analysis showed the thermal stability of the complex and the kinetic and thermodynamic parameters were also evaluated for the dehydration and decomposition state of the complexes. From the different spectral characterizations analysis data they have given the possible structure of the complexes which is shown in **Figure 1.3**.⁶⁶

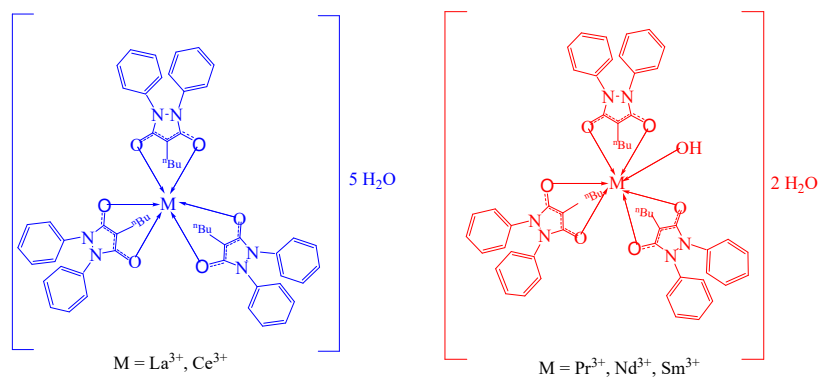


Figure 1.3. Possible Structures of Lanthanide(III) Complexes.

V. C. Devi and R. N. Singh studied on the change in coordination of Pr(III) and uracil in different organic solvents and observed the absorption bands. The energy interaction and energy dipole intensity parameter were calculated using 4f-4f transition spectra as a probe. From the study, it was reported that minor change in the coordination of the Pr(III) complexes were affected by different coordination site depending on the nature of the bonding between the metal and the ligand and the organic solvents used in **2011**.⁶⁷ Using furan-2-carboxylic acid as a ligand, R. Gupta and his group synthesized a biologically active La(III), Sm(III), Gd(III) and Dy(III) complexes and their spectral were characterized and reported in **2012**. The synthesized complexes were found to have more promising activity then that of the ligand itself.⁶⁸

A. Hussain *et al.* (**2012**) synthesized Lanthanide(III) complexes (**Figure 1.4**) with 4-phenyl-2,2,6,2-terpyridine, curcumin and diglucosylcurcumin and studied their DNA photocleavage and photocytotoxicity activity. The coordination between the ligands and the Ln^{3+} ions increase the hydrolytic stability and photocytotoxicity of the ligands. This study made a way for the Lanthanide(III) complexes to the field of photochemotherapeutic applications as the synthesized complexes were found to be suitable for photochemotherapeutic applications as it doesn't show any hydrolytic DNA cleavage activity and it also show photocytotoxicity in HeLa cancer cells.⁶⁹

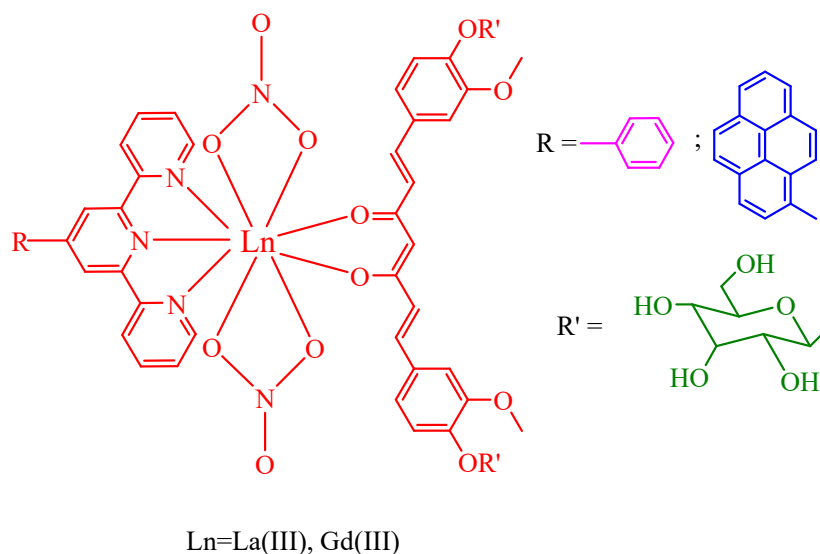
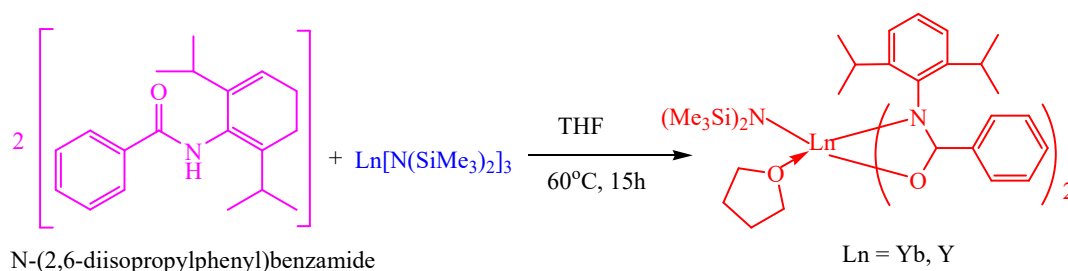


Figure 1.4. Schematic Structures of Lanthanide Complexes.

X. Hu *et al.* (2013) successfully synthesized series of Lanthanide amidate complexes by direct protonolysis and studied its structural diversity. The characterization data show that the complexes possessed abundant and different structures with varying coordination mode. Coordinations at the carbonyl oxygen site of the ligand both in the anionic and neutral with rare earth metal complexes, high molecular weight and low distributions of molecular weight of heterotactic-rich polymers and the ability for the ring-opening polymerization of rac-lactide using lanthanide amidate complexes as a catalyst were also reported in this study.⁷⁰ Again in 2014, L. Zhao *et al.* by simple silylamine elimination prepared two novel amidate rare-earth metal amide of $\text{Ln}[\text{SiMe}_3)_2)_3$ and proligand N-(2,6-diisopropylphenyl) benzamide (Scheme 1.2), both the complexes were reported to have two chelating amidate; coordinated tetrahydrofuran and amino group molecule. Complexes were also found to have an excellent catalytic activity for aldehydes and a moderate activity for inactivated ketones.⁷¹



Scheme 1.2. Synthesis of Earth Metal Complexes.

S. M. A. Barody and H. Ahmad, (2015) synthesized four Ln (III) complexes [where $\text{Ln} = \text{La(III)}, \text{Ce(III)}, \text{Sm(III)}$ and Gd(III)]. The ligand used was a new mesogen Schiff base name N-N-di-(pentyloxybenzoate) salicylidene-1,3-diamino propane which was prepared by 1:2 reaction of 4-pentyloxy(4'-formyl-3'-hydroxy)-benzoate and 1,3-diaminopropane. The complexes are characterized by FT-IR, elemental analysis, NMR, Mass, magnetic susceptibility and molar conductivity. Investigation of the data collected shows that two of the ligand is bonding to the metal in stereochemistry: one deprotonated phenolic oxygen and the other bidentate through phenolic oxygen (Figure 1.5). From the studies of thermal stability TGA/DSC curve of the complexes, it was found to be very stable thermally.⁷²

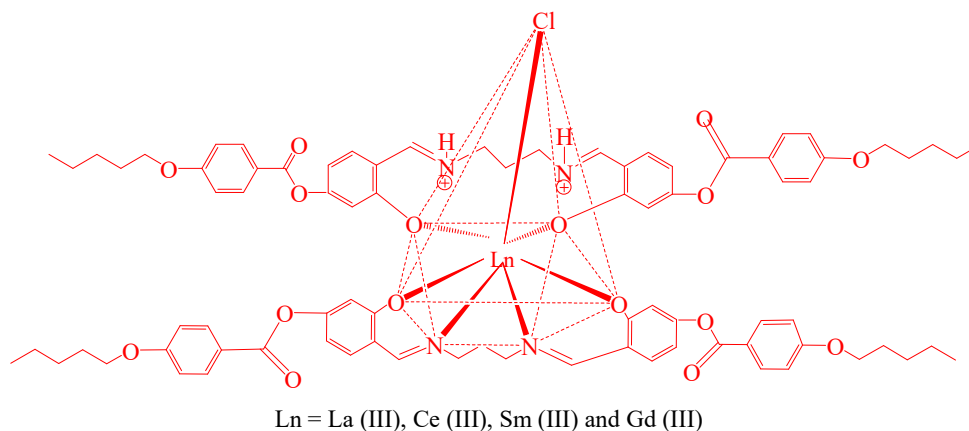


Figure 1.5. Suggested Molecular Structure of the Lanthanide Complexes.

R. Su *et al.* (2016), reported a Lanthanide polymer nanostructure by template-free solvothermal methods using DMF as a solvent and ligand 2-methyl benzoic acid. The outcome of the reaction was characterized by elemental analysis, powder X-ray diffraction, scanning electron microscopy and downward luminescence which give a characteristic transitions.⁷³ Berezhnytska *et al.* (2017), synthesized a series of polycomplexes of Neodymium(III) nitrate with 2-methyl-5-phenylpenten-1-3,5-dione and allyl-3-oxo-butanoate. The nature and the structure of the coordination were found to be dependent on the ligand and they remain constant on polymerization which was important for the investigation of the coordination and the structure of the polyhydra.⁷⁴ C. Lian *et al.* (2017), reported a synthesized and characterized novel coordinated polymer of Ln(III) (Ln=Pr(III), Gd(III) and Yb(III)) and 1,1-(2,4,6-trimethylbenzene-1,3,5-triyl(methylene))-tris (pyridine-4-carboxylic acid) and N,N-dimethylacetamide as ligand. Examining the polymer, they are found to be iso-morphous and iso-structural exhibiting the cavate 14-membered cages which gives infinite 1D metallic chain through two COO⁻ groups that later interlinks to polymerize into 3D porous scaffold. The study also shows that they can be used as a luminescent probe toward Pd²⁺ ions.⁷⁵

Single-crystal to single-crystal phase transition phase of a newly anion Lanthanide(III) complexes were synthesized (Figure 1.6), characterized and reported by I. Olyshevets *et al.* (2018) using dimethyl[(4-methylphenyl)sulfonyl] amido phosphate as a ligand. The study leads to a highly thermal stability, red luminescence dominated by ⁵D₀ - ⁷F₄ transition and a longer emission decay period which support the complexes for further application in light-emitting diode.⁷⁶

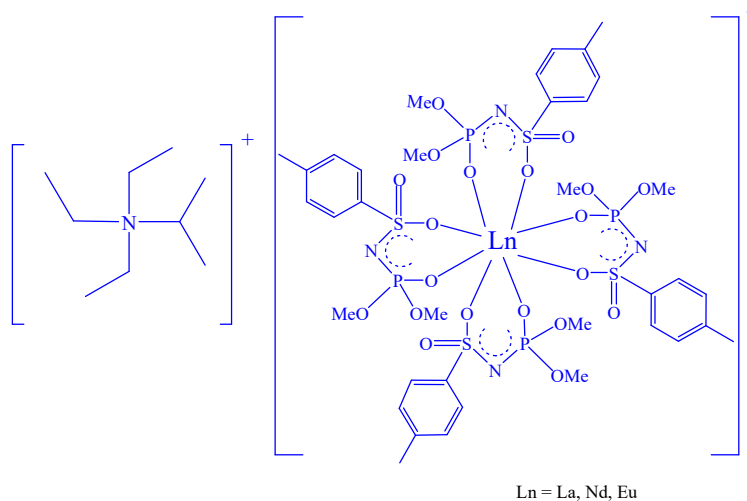


Figure 1.6. Schematic Representations of Lanthanide(III) Complexes.

M. P. C. Campello *et al.* (2019), reported a series of Lanthanide (III) complexes which were stabilized by mixed ligand of three β -diketonate units and a phenanthroline derivative (Figure 1.7). Using DMSO and PBS as a solvent UV-Vis and florescent spectra were recorded exhibiting an absorption and emission bands at 350 nm and 520 nm respectively. The complexes show a similar cytotoxic activity towards ovarian cancer cells and the effect of the complexes particularly the Eu (III) complex in the mitochondria and lysosome which were determined through the Transition Electron Microscopy (TEM). These studies pointed out the potentiality of the complexes as an anticancer agent which could challenge for future investigations.⁷⁷

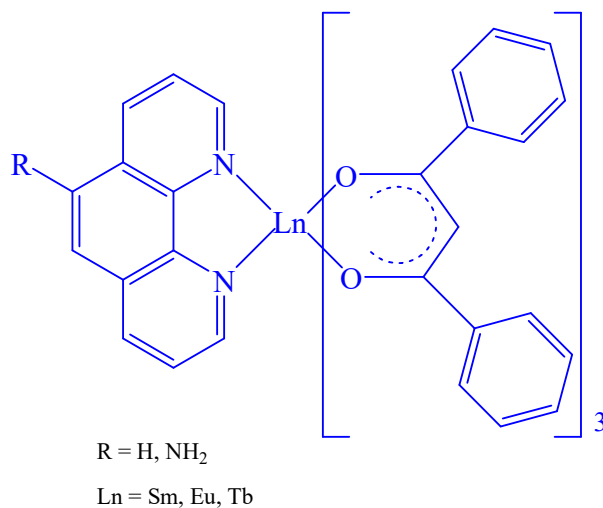


Figure 1.7. Molecular Structures of the Complexes.

Lanthanide complexes are making a remarkable way into synthetic clay as they exhibit a charismatic trait. Y. Wang *et al.* (2019), outline the development of the luminescent organic – inorganic material using Lanthanide complexes as the host. The study provides excellent aqueous solubility, hydrogel with self sustaining, and thin, flexible and independent films of the hybrid material. The luminescent properties of the Lanthanide complexes retained even on the impact of the clay and so, it boosted the luminescence of the hybrid material which were used for the chemical molecule and the sensing of metal ions luminescent. In view of the different trait that the hybrid exhibit, its novel material were reported to be auspicious in the field of biology, therapeutic, security and solar cells.⁷⁸

In 2020, R. Li *et al.* reported the synthesis of Lanthanide(III) complexes as a suitor for the photoluminescence device and a photo-magnetic functional using Ln(III), Sm(III), Dy(III) and 2,2'-bipyridine-6,6'-dicarboxylic acid. Their magnetic properties, florescent properties and crystallography of the compounds were examined; showing a long lasting luminescent, excellent quantum capability and a strong f-f transition. Dy(III) complex shows a single magnetic manner and were moderate in magnetization, which can be served as the photo-magnetic activity.⁷⁹ A unique potential biological agents of Lanthanide(III) complexes were synthesized through reaction between two biologically active molecules 2-carbaldehyde thiophene and salicylic acid hydrazide, and Sm(NO₃)₃.6H₂O, Eu(NO₃)₃.6H₂O, Dy(NO₃)₃.6H₂O, and LaCl₃.6H₂O which were set-forth by R. Fouad in 2020. On exploring the complexes, it was disclosed that the coordination was at the OONS site of the donor ligand (**Figure 1.8**) and characterization were done through different methods such as the FT-IR, Mass, H¹ NMR, molar conductance and elemental analysis for further studies. The complexes were also reported to exhibit promising anti-tumor, anti-microbial, anti-oxidant agent and anti-microbial agent against bacteria which are more convincing than that of the reference drug.⁸⁰

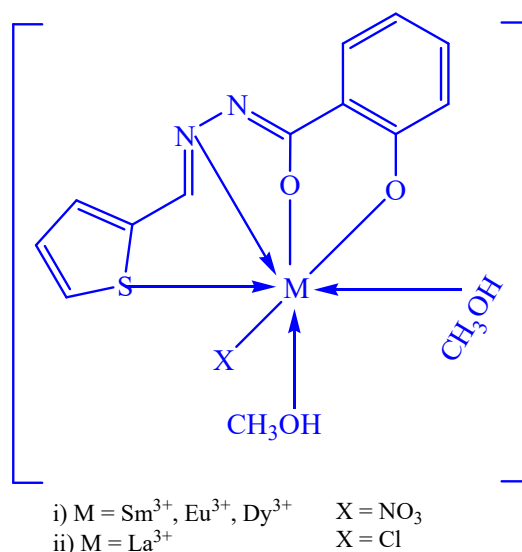
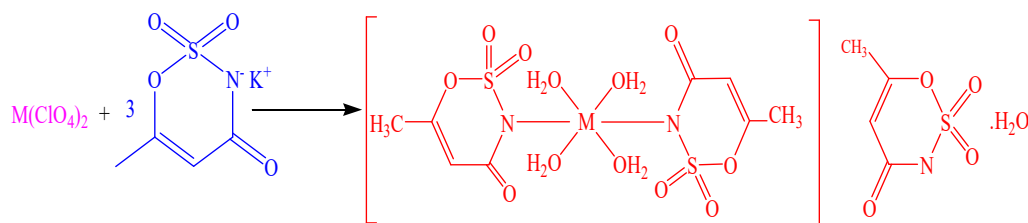


Figure 1.8. Structure of Lanthanide Metal Complexes.

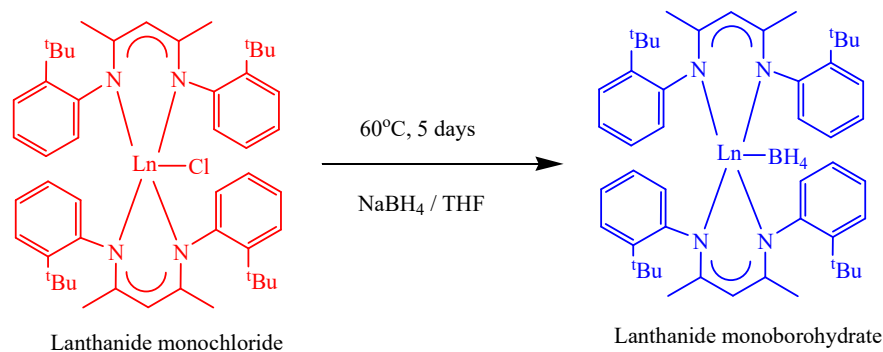
T.D. Nguyen and group in **2020** synthesized a highly-purified f-element nitrate using Lanthanides as there is a struggle to obtain it in a pure form which mostly preferred sophisticated apparatus with high temperature. Using an aqueous reaction, the lanthanide complexes were prepared by combining Lanthanide salts (Lanthanum, Cerium, Praseodymium, Neodymium and Europium) and a ligand which holds high nitrogen (5,5'-bis(tetrazolato)amine monohydrate). Nano-structural lanthanide nitrate, formed were obtained on dehydration of the synthesized complexes as under an inert environment, they have the ability to go through self-extension burning reaction. The study shows that the Ln^{3+} ions possessed a very low reduction potential and so they have the courtesy to react with the nitrogen to give Ln(III) nitrate rather than Lanthanide itself. This new way of producing an authentic Lanthanides/Actinides nitrate may provide a way into the application in nuclear fuels in the coming days.⁸¹

L. Zeybel and D. A. Köse in the beginning of **2021** reported a hydrothermal synthesis of Lanthanide cations (Eu, Tb, Ho, Er, Yb) with acesulfame-K (**Scheme 1.3**). The synthesized complexes were analyzed and characterized through Mass, NMR, IR, Solid state UV-Vis and elemental analysis. On examining the TGA curve shows that the hydrated water coordinates outside the coordination sphere. The coordination of the complexes were found to be six coordinates.⁸²



Scheme 1.3. Synthesis of Acesulfame Lanthanide Metal Complexes.

Lanthanide complexes have drawn the interest of many researchers to synthesize, characterize and investigate its applications, and with it L. Zhu *et al.* (2021) reported a satisfactory coordination for stabilizing Lanthanide monochloride and monoborohydrate using β -diketiminato as the ligand (**Scheme 1.4**). On the investigation of the ring opening polymerization in lactide, Lanthanide monoborohydrate were found to have an efficient capability for L-lactide and rac-lactide to give the α,ω -telechelic polylactide diols with high molecule weight and moderate molecular weight distribution.⁸³



Ln=Yb, Sm, Nd, La, THF =Tetrahydrofuran, NaBH₄=Sodium borohydride and ^tBu= tert- butyl group

Scheme 1.4. Synthesis of Lanthanide Monoborohydrate from Lanthanide Monochloride Complexes.

Lanthanide complexes have many other implementations in different fields. Complexes of Lanthanides have made its way into the field of nano science and technology as the complexes can decompose to oxide molecule of nano size.⁸⁴ Lanthanide complexes were also found to have DNA cleaving ability and with increase in time the potentiality of the complexes also increases due to the change in the DNA strain on the insertion of the complex into the DNA.^{85,86} The complexes of Lanthanides were found to have capability to act as antibacterial agents to fight pathogenic strains that causes urinary tract infections.⁸⁷ Currently hydrolysis is securing a lot of interest in biotechnology and as

the lanthanide ions have been discovered to obtain phosphodiesterolytic activity with increasing pH, they made a way into biotechnology province.⁸⁸ As Lanthanides hold a long lifetime period of emission, they applied as luminescent biolabeling. They can be found in the market as Lanthanide label kit which can be utilized for the labeling.⁸⁹

1.5. Chemical Kinetics

Chemical Kinetics can be defined as the study of chemical rate of a reaction. It is also known as the reaction kinetics and it complement with thermodynamic which have to do with the overall change in the reaction i.e. from initial state to final state for a synthesis but it does not concern with the reaction rate directly as the rate is examined by chemical kinetics. Comprehension of the process of the reaction is must in chemistry, so the chemical kinetics was added in the syllabus of the chemistry discipline with different features respective to the course of study and the level of education. To develop reaction mechanism kinetics is adapted such as in organic synthesis, chemical engineering, chemical mechanism, analytical, stability of commercial products as of pharmaceutical drugs. Further, they are applied for the rate theories for the evaluation of equilibrium, solvent properties, and analysis of solution depending on the rate of the reaction.^{90,91}

With the change in temperature, concentration and amount of catalyst added, the rate of reaction change; this is due to the fact that on increasing temperature it increases the collision resulting in increase of the numbers of molecule intersecting the threshold energy. In order to complete a reaction a molecule need to have a certain amount of energy to break a bond and coordinate with other molecule to develop the required compound. That certain amount of energy required to start the chemical reaction is known as the Activation Energy (E_a) which varies with different type of reactions.^{92,93}

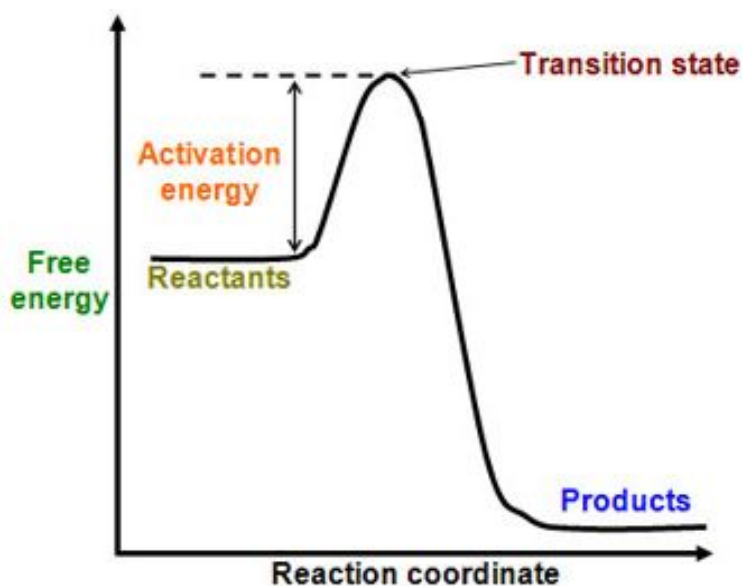


Figure 1.9. Schematic Representations of Activation Energy for a Reaction.

1.6. Scope and Aim of the study

Over the past few decades, Lanthanide complexes have gained a lot of attention in various researches due to its implementation in Inorganic chemistry, Organometallic, Industries, Agriculture, Biotechnology, Biomolecular, Lighting Device, Imaging, Labeling and nano-sciences. Currently one of the most needed magnetic and luminescent materials for LEDs, Bio-medical, NMR shift reagent, MRI contrast agent, telecommunication and lasers need to be synthesized with Lanthanide ions which has a unique magnetic and photophysical properties that could offer a charm and attraction to many researcher's interest. Lanthanide ions are known to be one of the best non-enzymatic agents for DNA and RNA hydrolysis; they can also interact with peroxide and free radical without forming into radicals.

Because of the vast applications and importance of Lanthanide complexes our interest is to synthesize a series of Lanthanide complexes using Praseodymium, Neodymium, Europium and Gadolinium with different biologically active organic ligands and the spectral characterization were done through IR, UV-vis, Fluorescence and CHN-analysis for conformations of the complexation and coordination of the metal and ligand. Chemical kinetics and thermodynamic parameters were also evaluated to provide the details of the reaction mechanism.

1.7. References

1. R. W Hakala. "Letters". *J. Chem. Educ.*, 1952, **29(11)**, 581-582.
<https://pubs.acs.org/doi/pdf/10.1021/ed029p581.2>
2. N. E. Holden and T. Coplen, The Periodic Table of the Elements Chemistry, Int. *J. Chem. Int. Newsmagazine for IUPAC*, 2004. **26(1)**.
<https://doi.org/10.1515%2Fci.2004.26.1.8>
3. S. Cotton, The Periodic Table and the Lanthanides, *Sci. tech.*, 2019.
<https://blog.degruyter.com/the-periodic-table-and-the-lathanides/>
4. D. A. Atwood, *The Rare Earth Element Fundamentals and Applications*. John Wiley & Sons, 2012, ISBN 978-1-119-95097-4
<https://www.wiley-vch.de/de/fachgebiete/naturwissenschaften/chemie-11ch/anorganische-chemie-11ch7/the-rare-earth-elements-978-1-119-95097-4>
5. C.K. Jorgensen, *The Inner Mechanism of Rare Earth Elucidated by Photo-Electronic Spectra*, Springer, Berlin/Heidelberg, 1973.
https://link.springer.com/chapter/10.1007%2F3-540-06125-8_4
6. J. Leduc, Y. Geoneulleu, A. Raauf, T. Fisher and S. Mathur, Chapter-5 Rare-Earth-Containing Materials for Photoelectrochemical Water Splitting Applications, *Semicond. Semimet.*, 2017, **97**, 185-219.
<https://doi.org/10.1016/bs.semsem.2017.05.001>
7. G. Venkateswarlu, P. R. Mamatha, S. Thangavel, and A. C. Sahayam, Determination of Lanthanides in Coal Fly Ash, Sediment and Monazite Sand by Inductively Coupled Plasma Optical Emission Spectrometry after Separation Using Oxalate form of Ion-Exchange Resin, *J. Anal. Chem.*, 2021, **76**, 180-184
<https://doi.org/10.1134/S1061934821020155>
8. W. Franus, M. Małgorzata, W. Motyka and M. Wdowin, Coal fly ash as a resource for rare earth elements, *Environ. Sci. Pollut. Res.*, 2015, **22(12)**, 9464-9474.
<https://link.springer.com/article/10.1007/s11356-015-4111-9>
9. Z. Hubicki and M. Olszak, Studies on Separation of Rare Earth Elements on Various types of Anion-exchangers in the C₃H₇OH-7 M HNO₃ Systems, *J. Chromatogr. A.*, 2002, **955(2)**, 257-262.
[https://doi.org/10.1016/S0021-9673\(02\)00212-1](https://doi.org/10.1016/S0021-9673(02)00212-1)
10. Science Motive Online,

- <https://www.sciencemotive.com/class-12-chemistry/f-block-elements-and-properties/>, (November 2020).
11. <http://students.open.ac.uk/omresources/periodictable/ellaac/core.pdf>
12. P. S. Bagus, Y. S. Lee and K. S. Pitzer, Effects of Relativity and of the Lanthanide Contraction on the Atoms from Hafnium to Bismuth, *Chem. Phys. Lett.*, 1975, **33(3)**, 408-411.
[https://ui.adsabs.harvard.edu/link_gateway/1975CPL....33..408B/doi:10.1016/0009-2614\(75\)85741-1](https://ui.adsabs.harvard.edu/link_gateway/1975CPL....33..408B/doi:10.1016/0009-2614(75)85741-1)
13. Chemistry Libre Texts Online,
[https://chem.libretexts.org/Bookshelves/Inorganic_Chemistry/Supplemental_Modules_and_Websites_\(Inorganic_Chemistry\)/Descriptive_Chemistry/Elements_Organized_by_Block/4_fBlock_Elements/The_Lanthanides/aLanthanides%3A_Properties_and_Reactions/Lanthanide_Contraction](https://chem.libretexts.org/Bookshelves/Inorganic_Chemistry/Supplemental_Modules_and_Websites_(Inorganic_Chemistry)/Descriptive_Chemistry/Elements_Organized_by_Block/4_fBlock_Elements/The_Lanthanides/aLanthanides%3A_Properties_and_Reactions/Lanthanide_Contraction), (August 2020).
14. Britannica, <https://www.britannica.com/science/lanthanoid-contraction>
15. https://www.zigya.com/study/book?class=12&board=cbse&subject=Chemistry&book=Chemistry+I&chapter=The+d-And-f-Block+Elements&q_type=&q_topic=The+Lanthanoids&q_category=&question_id=CHEN12069304
16. ExpertsMind.com, <http://www.expertsmind.com/learning/lanthanide-contraction-effect-assignment-help-7342871223.aspx>
17. H. Frank, Lanthanide Contraction, *Access Science*, 2020.
<https://doi.org/10.1036/1097-8542.370700>
18. S. A. Cotton, Establishing Coordination Numbers for the Lanthanides in simple Complexes, *Comptes. Rendus. Chimie*, 2005, **8(2)**, 129-145.
<https://doi.org/10.1016/j.crci.2004.07.002>
19. [https://chem.libretexts.org/Bookshelves/Inorganic_Chemistry/Supplemental_Modules_and_Websites_\(Inorganic_Chemistry\)/Coordination_Chemistry/Structure_and_Nomenclature_of_Coordination_Compounds/Coordination_Numbers_and_Geometry](https://chem.libretexts.org/Bookshelves/Inorganic_Chemistry/Supplemental_Modules_and_Websites_(Inorganic_Chemistry)/Coordination_Chemistry/Structure_and_Nomenclature_of_Coordination_Compounds/Coordination_Numbers_and_Geometry)
20. S. A. Cotton, *Scandium, Yttrium & the Lanthanides: Inorganic & Coordination Chemistry*, Willy online Library, 2011.
<https://doi.org/10.1002/9781119951438.eibc0195>
21. C. Huang and Z. Bian, *Rare Earth Coordination Chemistry: Fundamentals and Applications*, Edited by Chunhui Huang, Asia, John Wiley & Sons Pte Ltd., 2010

- <https://catalogimages.wiley.com/images/db/pdf/9780470824856.excerpt.pdf>
22. S. A. Cotton, *Lanthanide and Actinide Chemistry*, Wiley online Library, 2006, Chapter 4, 35-60. <https://doi.org/10.1002/0470010088.ch4>
23. S. A. Cotton, *Lanthanide and Actinide Chemistry*, Wiley online Library, 2006, Chapter 5, 61-87. <https://doi.org/10.1002/0470010088.ch5>
24. M. Dalal, *A Text book of Physical Chemistry – Volume 1*, 2012, chapter-9, 359-361. <https://www.dalalinstitute.com/wp-content/uploads/Books/A-Textbook-of-Inorganic-Chemistry-Volume-1/ATOICV1-9-4-Magnetic-Properties-of-Free-Ions.pdf>
25. Pakistan Science Mission <https://psm.org.pk/magnetic-properties-of-lanthanides/> (June 2019)
26. Chemistry LibreTexts, <https://chem.libretexts.org/@go/page/1762?pdf> (August 2020)
27. M. H. V. Werts, Making Sense of Lanthanide Luminescence, *Science Progress*, 2005, **88(2)**, 101-131. <https://doi.org/10.3184%2F003685005783238435>
28. S. Freed, S. I. Weissman, F. E. Fortess, and H. F. Jacobson, Ions of Europium Distributed Between Different Configurations in Homogeneous Solutions, *J. Chem. Phys.*, 1939, **7**, 824-828. <https://doi.org/10.1063/1.1750532>
29. S. I. Weissman, Intramolecular Energy Transfer the Fluorescence of Complexes of Europium, *J. Chem. Phys.*, 1942, **10**, 213-217. <https://doi.org/10.1063/1.1723709>
30. S. Purohit and N. Bhojak, The Absorption Spectra of Some Lanthanide (III) Ions, Research and Reviews, *J. Chem.*, 2013, **2(2)**, 1-3. <https://www.rroij.com/open-access/the-absorption-spectra-of-some-lanthanide-iii-ions-.php?aid=33850>
31. S. N. Misra and S. O. Sommerer, Absorption Spectra of Lanthanide Complexes in Solution, *Appl. Spectrosc. Rev.*, 1991, **26(3)**, 151-202. <http://dx.doi.org/10.1080/05704929108050880>
32. M. D. M. C. Ribeiro da Silva, N. R. M. Araujo, A. L. R. Silva, L. C. M. da Silva, N. P. S. M. Barros, J. M. Goncalves and M. A. V. Ribeiro da Silva, Three N2O2 ligands Derived from the Condensation of 1,2-cyclohexanediaminewith Salicylaldehyde, Acetylacetone and Benzoylacetone. *J. Therm. Anal. Calorim.*, 2007, **87**, 291-296. <https://doi.org/10.1007/s10973-006-7808-7>
33. I. P. Kostova, I. I. Manolov and M. K. Radulova, Stability of the Complexes of some Lanthanides with Coumarin Derivatives. I. Cerium(III)-4-methyl-7-hydroxycoumarin, *Acta. Pharm.*, 2004, **54**, 37-47. <https://hrcak.srce.hr/16660>

34. V. Gonzalez , D. A. L. Vignati , C. Leyval and L. Giamberini, Environmental Fate and Ecotoxicity of Lanthanides: Are they a Uniform Group Beyond Chemistry?, *Environ. Int.*, 2014, **71**, 148-157. <https://doi.org/10.1016/j.envint.2014.06.019>
35. C. X. Zhang, X. M. Qiao, H. W. Chen and Y. Y. Zhang, Synthesis and Biological Activities of Lanthanide Metal Complexes with Nitronly Nitroxide, Synthesis and Reactivity in Inorganic, *Met. Org. Nano-Met. chem.*, 2015, **45**, 145-150. <http://doi.org/10.1080/155333174.2013.819914>
36. P. Caravan, J. J. Ellison, T. J. McMurry and R. B. Lauffer, Gadolinium(III) Chelates as MRI Contrast Agents: Structure, Dynamics, and Applications, *Chem.rev.*, 1999, **99**, 2293-2352 . <https://doi.org/10.1021/cr980440x>
37. A. E. Merbach, L. Helm and E. Toth, *The Chemistry of contrast agents in medical magnetic resonance imaging*, Wiley, New York, 2001.
<http://dx.doi.org/10.1002/9781118503652>
38. X. Qin, J. Wang and Q. Yuan, Synthesis and Biomedical Applications of Lanthanides-Doped Persistent Luminescence Phosphors With NIR Emissions, *Front. Chem.*, 2020, **8**, 1-17. <https://doi.org/10.3389/fchem.2020.608578>
39. J. C. G. Buzli, *Lanthanides*, Krik-Othmer encyclopedia of Chemical Teachnology, Wiley, New York, 2013.
https://www.researchgate.net/publication/257921324_Lanthanides
40. M. Osawa, M. Hoshino, T. Wada, F. Hayashi, and S. Osanai, Intra-Complex Energy Transfer of Europium(III) Complexes Containing Anthracene and Phenanthrene Moieties, *J. Phys. Chem. A.*, 2009, **113(41)**, 10895-10902.
<https://doi.org/10.1021/jp905160w>
41. J. C. G. Bünzli and S. V. Eliseeva, Lanthanide NIR Luminescence for Telecommunications, Bioanalyses and Solar Energy Conversion. *J. Rare Earths.*, 2010, **28(6)**, 824-842. [https://doi.org/10.1016/S1002-0721\(09\)60208-8](https://doi.org/10.1016/S1002-0721(09)60208-8)
42. S. N. Misra, M. A. Gagnani, M. Indira and R. S. Shukla, Biological and Clinical Aspects of Lanthanide Coordination Compounds, *Biochem. Appl.*, 2004, **2**, 3-4.
<https://doi.org/10.1155/S1565363304000111>
43. L. Zapala, M. Kosinska, E. Woznicka, L. Byczynski and W. Zapala, Synthesis, Spectral and Thermal Study of Ln(III), Nd(III), Sm(III) Eu(III), Gd(III), and Tb(III) Complexes with Mefenamic acids. *J. Therm. Anal. Calrim.*, 2016, **124**, 363-374.
<http://Doi.10.1007/s10973-015-5120-0>

44. J. Burgess, *Metal ions in solution*, New York, Ellis Horwood, 1978.
45. R. K. Agarwal, k. Arora and P. Dutt, Some high Coordination Compound of Thorium (IV) and Dioxouranium (VI) with Schiff Bases Derived from 4- aminoantipyrine, *Synth. React. Inorg. Met.-Org. Chem.*, 1994, **24(2)**, 301-324.
<https://doi.org/10.1080/00945719408000112>
46. R. K. Agarwal, G. Rajeev and S. K. Sindhu, Synthesis, Spectral and thermal Properties of some High Coordinated Complexes of Thorium (IV) and Dioxouranium (VI) derive from 4[n-(2'-hydroxy-1'-naphthalidene) aminol] antipyrinethiosemicardazone, *Bull. Chem. Soc. Ethiop.*, 2005, **19(2)**, 185-195. <https://doi.org/10.4314/bcse.v19i2.21124>
47. L. Singh, N. Tyagi and N. P. Dhaka, Synthesis and Physico-Chemical Characteristic of some Dioxouranium (VI) complexes of N-isonicotinamido-3-Methoxy-4-hydroxy Benzaladimine and N-isonicotinamidocinnamalaldinime, *Asian J. Chem.*, 1998, **10**, 915-921. <https://www.osti.gov/etdeweb/biblio/294128>
48. D. E. Barry, D. F. Caffrey and T. Gunnlaugsson, Lanthanide-directed Synthesis of Luminescent Self-assembly Supramolecular Structures and Mechanically Bonded Systems from Acyclic Coordinating Organic Ligands, *Chem. Soc Rev.*, 2016, **45**, 3244-3274. <https://doi.org/10.1039/C6CS00116E>
49. D. Parker, R. S. Dickins, H. Puschmann, C. Crossland, and J. A. K. Howard, Being Excited by Lanthanide Coordination Complexes: Aqua Species, Chirality, Excited-State Chemistry, and Exchange Dynamics, *Chem. Rev.*, 2002, **102**, 1977-2010.
<https://doi.org/10.1021/cr010452+>
50. B. C. Roy, M. Santos, S. Mallik, and A. D. Campiglia, Synthesis of Metal-Chelating Lipids to Sensitize Lanthanide Ions, *J. Org. Chem.*, 2003, **68**, 3999-4007.
<https://doi.org/10.1021/jo026833k>
51. A. El-Anasry and N. S. Abdel-Kader, Synthesis, Characterization of Ln(III), Nd(III), and Er(III) Complexes with Schiff Bases Derived from Benzopyran-4-one and their Florescence Study, *Int. J. Inorg. Chem.*, 2012, 1-13.
<https://doi.org/10.1155/2012/901415>
52. A. Carac, R. Boscencu, G. Carac and S. G. Bungau, Spectral Study of Some Lanthanide Complexes with Quaternary Pyridinium Ligands, *Rev. Chem.*, 2017, **68(10)**, 2265-2269. <http://www.revistadechimie.ro>
53. A. N. Gusev, M. Hasegawa, T. Shimizu, T. Fukawa, S. Sakurai, G. A. Nishchymenko, V. F. Shulgin, S. B. Meshkova and W. Linert, Synthesis, Structure and Luminescence

- studies of Eu(III), Tb(III), Sm(III), Dy(III), Cationic Complexes with Acetylacetone and Bis(5-(pyridine-2-yl)-1,2,4-triazol-3-yl)propane, *Inorg. Chimica Acta*, 2013, **406**, 276-284. <https://www.sciencedirect.com/science/article/pii/S0020169313001965>
54. S. Alghool, F. Hanan, A. EL-Halim, M.S. Abd El-sadek, L.S. Yahia, and L.A. Wahab, Synthesis, Thermal Characterization, and Antimicrobial Activity of Lanthanum, Cerium and Thorium Complexes of Amino Acid Schiff Base Ligand, *J. Therm. Anal. Calorim.*, 2013, **112**, 671-681. <https://link.springer.com/article/10.1007/s10973-012-2628-4>
55. X. L. Wang, H. Chao, H. Li, X.L. Hong, L.N. Ji, X.Y. Li, Synthesis, Crystal Structure and DNA Cleavage Activities of Copper(II) Complexes with Asymmetric Tridentate Ligands, *J. Inorgn. Biochem.*, 2004, **98**, 423-429. <https://www.sciencedirect.com/science/article/pii/S0162013403004562>
56. D.F. Xu, S.Z. Ma, Q.Z. He, G.Y. Du, Synthesis, Characterization and Anticancer Properties of Rare Earth Complexes with Schiff Base and o-phenanthroline, *J. Rare Earths.*, 2008, **26**, 643-647. <https://www.sciencedirect.com/science/article/pii/S1002072108601532>
57. J. Easmon, G. Purstinger, G. Heinisch, T. Roth, H.H. Fiebig, W. Holzer, et al., Synthesis, Cytotoxicity, and Antitumor Activity of Copper(II) and Iron(II) Complexes of (4)N-azabicyclo[3.2.2]nonane Thiosemicarbazones derived from Acyl Diazines, *J. Med. Chem.*, 2001, **44**, 2164-2171. <https://pubs.acs.org/doi/abs/10.1021/jm000979z>
58. P.R. Maravalli, S.D. Dhumwad and T.R. Goudar, Synthesis, Spectral, Thermal and Biological Studies of Lanthanide (III) Complexes with a Schiff Base derived from 3-N-Yetaylpiperidino-4-Amino-5-Yercapto-1,2,4-Traizole, *Synth. React. Inorg. Met. Org. Chem.*, 1999, **29(3)**, 525-540. <http://dx.doi.org/10.1080/00945719909349467>
59. I. Kostovaa, I. Manolovb and I. Nicolovac, S. Konstantinovc and M. Karaivanovac, New lanthanide Complexes of 4-methyl-7-hydroxycoumarin and their Pharmacological Activity, *Eur. J. Med. Chem.*, 2001, **36**, 339-347. [https://doi.org/10.1016/S0223-5234\(01\)01221-1](https://doi.org/10.1016/S0223-5234(01)01221-1)
60. I. Kostovaa, R.Kostova, G. Momekov, N. Trendafilova and M. Karaivanovac, Antineoplastic Activity of New lanthanide (cerium, Lanthanum and Neodymium) Complex Compounds, *J. Trace. Elem. Med. Biol.*, 2005, **18**, 219-226. <https://doi.org/10.1016/j.jtemb.2005.01.002>

61. I. Kostovaa, N. Trendafilova and G. Momekov, Theoretical and Spectroscopic Evidence for Coordination ability of 3,3'-benzylidenedi-4-hydroxycoumarin. New neodymium(III) Complex and its Cytotoxic Effect, *J. Inorg. Biochem.*, 2005, **99**, 477-487. <https://doi.org/10.1016/j.jinorgbio.2004.10.022>
62. O. Alpturk, O. Rusin, S. O. Fakayode, W. Wang, J. O. Escobedo, I. M. Warner, W. E. Crowe, Vladimir, J. M. Pruet and R. M. Strongin, Lanthanide Complexes as Flourscent Indicatorsa for Neutral Sugars and Cancer Biomarkers, *PNAS*, 2006, **103(26)**, 9756-9760. www.pnas.org/cgi/doi/10.1073/pnas.0603758103
63. B. S. Kumari, G. Rijulal and K. Mohanan, Microwave Assited Synthesis, Spectroscopic, thermal and Biological studies of some Lanthanide (III) Chloride Complexes with a Heterocyclic Schiff Base, *Synth. React. Inorg. Met. Org. Nano Met. Chem.*, 2009, **39(1)**, 24-30. <https://doi.org/10.1080/15533170802679550>
64. T. Moaienla, T. D. Singh, N. R. Singh and M. I. Devi, Computation Energy Interaction Parameters as well as Electric Dipole Intensity Parameters for Absorption Spectral Study of the Interaction of Pr(III) with L-phenylalanine, L-glycin, L-alanine and L-aspartic acid in the Presence and Absence of Ca^{2+} in Organic Solvents, *Spectrochem. Acta A Mol. Biomol. Spectroscopy*, 2009, **74**, 434-440. <https://doi.org/10.1016/j.saa.2009.06.039>
65. N. V.S. Rao, T. D. Choudhury, R. Deb, M. K. Paul, T. R. Rao, T. Francis and I. I. Smalyukh, Flourescent Lanthanide Complexex of Schiff Base Ligand Possessing N-Aryl: influence of Chain Length on Crossover (calamitic to discotic) phase behavior, *Liq. Cryst.*, 2010, **37(11)**, 1393-1410. <https://doi.org/10.1080/02678292.2010.517328>
66. M. R. Anoop, P. S. Binil, K. R. Jisha, S. Suma, and M. R. Sudarsanakumar, Synthesis, Spectral and Thermal Studies of Lanthanide(III) Complexes of Phenylbutazone, *J. Korean Chem. Soc.*, 2011, **55(4)**, 612- 619. <https://doi.org/10.5012/jkcs.2011.55.4.612>
67. V. Ch. Devi And R. N. Singh, Calculation of Energy Interaction and Electric Dipole Intensity Parameters to Explore the Interaction between the Trivalent Praseodymium and Uracil Using 4f-4f Transition Spectra as an Absorption Probe, *ICCCP.*, 2011, **10**, 195-199. <http://www.ipcbee.com/vol10/37-V10018.pdf>
68. R. Gupta, N. Agrawal and K. C. Gupta, Synthesis, IR Spectral Studies and Biological Activities of Some Rare Earth Metal Complexes with Biochemically relevant Ligand, 2012, **3(2)**, 50-56. <https://elibrary.ru/item.asp?id=20764587>

69. A. Hussain, K. Somyajit, B. Banik, S. Banerjee, G. Nagaraju and A. R. Chakravarty, Enhancing the photocytotoxic potential of Curcumin on Terpyridyl Lanthanide (III) Complex formation, *Dal. Tran.*, 2013, **42**, 182-195.
<https://doi.org/10.1039/C2DT32042H>
70. X. HU, C. Lu, B. Wu, H. Ding, B. Zhao, Y. Yao and Q. Shen, Synthesis and Structural Diversity Amidate Complexes and their Catalytic Activities for the Ring Opening Polymerization of rac-lactide, *J.organomet. Chem.*, 2013, **732**, 92-101.
<http://dx.doi.org/10.1016/j.jorganchem.2013.02.022>
71. L. Zhao, H. Ding, B. Zhao, C. Lu and Y. Yao, Synthesis and Characterization of Amidate Rare-Earth Metal Amides and their Catalytic Activities towards Hydrophosphonylation of Aldehydes and Unactivated Ketones, *Polyhedron*, 2014, **83**, 50-59. <https://doi.org/10.1016/j.poly.2014.04.018>
72. S. M. Al-Barody & H. Ahmad, Synthesis, Structural Characterization and Thermal Studies of Lanthanide complexes with Schiff Base Ligand N,N'-di-(4'-pentyloxybenzoate)-salicylidene-1,3-diaminopropane, *Cogent Chem.*, 2015, **1**, 1093920. <http://dx.doi.org/10.1080/23312009.2015.1093920>
73. R. R. Su, P. Tao, Y. Han, C. H. Zeng, and S. L. Zhong, Lanthanide Coordination Polymer Nanosheet Aggregates: Solvothermal Synthesis and Downconversion Luminescence, *J. Nanomat.*, 2016, 1-5. <https://doi.org/10.1155/2016/3714041>
74. O. Berezhnyska, I. Savchenko, N. Ivakha, O. Trunova, N. Rusakova, S. Smola and O. Rogovtsov, Synthesis, Characterization, and Luminescent Properties of Polymer Complexes of Nd(III) with β -Dicarbonyl Ligands, *Nanoscale Res. Lett.*, 2017, **12**, 1-8. <https://doi.org/10.1186/s11671-017-2074-0>
75. C. Lian, Y. Chen, S. Li, M. Hao, F. Gao and L. Yang, Synthesis and Characterization of Lanthanide-Based Coordination Polymers for Highly Selective and Sensitive Luminescent Sensor for Pb²⁺ over mixed Metal ions, *J. Alloys Comp.*, 2017, **702**, 303-308. <https://doi.org/10.1016/j.jallcom.2017.01.260>
76. I. Olyshevets, N. Kariaka, K. Znovjyak, N. Gerasimchuk, S. Lindeman, S. Smola, M. Seredyuk, T. Y. Sliva, and V. M. Amirkhanov, Synthesis and Characterization of Anionic Lanthanide (III) Complexes With Bidentate SAPH (sulfonamidophosphate), *Ligand, Inorg. Chem.* 2020, **59(1)**, 76-85.
<https://doi.org/10.1021/acs.inorgchem.8b02846>

77. M. P. C. Campello, E. Palma, I. Correia, P. M. R. Paulo, A. Matos, J. Rino, J. Coimbra, J. C. Pessoa, D. Gambino, A. Paulo and F. Marques, Lanthanide Complexes with Phenanthroline-based Ligands: insights into Cell death Mechanisms by Microscopy Techniques, *Dalton Trans.*, 2019, **48**, 4611-4624.
<https://doi.org/10.1039/C9DT00640K>
78. Y. Wang, P. Li, S. Wang and H. Li, Recent Progress in the Luminescent Materials Based on Lanthanide Complexes Intercalated Synthetic Clays, *J. Rare Earths*, 2019, **37(5)**, 451-467. <https://doi.org/10.1016/j.jre.2018.09.004>
79. R. F. Li, R. H. Li, X. F. Liu, X. H. Chang and X. Feng, Lanthanide complexes based on a Conjugated Pyridine Carboxylate Ligand: Structure, Luminescence and Magnetic Properties, *RSC Adv.*, 2020, **10**, 6192-6199.
<https://doi.org/10.1039/C9RA10975G>
80. R. Fouad, Synthesis and Characterization of Lanthanide Complexes as Potential Therapeutic Agents, *J. Coord. Chem.*, 2020, **73(14)**, 201-202.
<https://doi.org/10.1080/00958972.2020.1808629>
81. T. D. Nguyen, J. M. Veauthier, D. E. Chavez, B. C. Tappan, A. H. Mueller, B. L. Scott and D. A. Parrish, Lanthanide Complexes of Bis(tetrazolato)amine: A Route to Lanthanide Nitride Foams, *Inorg. Chem.* 2020, **59(22)**, 16109-16116.
[HTTPS://DOI.ORG/10.1021/ACS.INORGCHEM.0C02480](https://doi.org/10.1021/ACS.INORGCHEM.0C02480)
82. L. Zeybel and D.A. Köse, Acesulfame Complex Compounds of some Lanthanide group Metal cations. Synthesis and Characterization, *J. Mol. Struct.*, 2021, **1226**, 1-8.
<https://doi.org/10.1016/j.molstruc.2020.129399>
83. L. Zhu, Y. Xu, D. Yuan, Y. Wang and Y. Yao, Synthesis and Structural Characterization of Lanthanide Monoborohydride Complexes Supported by 2-tertbutylphenyl substituted β -diketiminate, and their Application in the Ring Opening Polymerization of Lactide, *J. Organomet. Chem.* 2020, 934, 121662.
<https://doi.org/10.1016/j.jorganchem.2020.121662>
84. S. Devipriya, N. Arunadevi and S. Vairam, Synthesis and Thermal Characterization of Lanthanide (III) Complexes with Mercaptosuccinic Acid and Hydrazine as Ligand, *J. Chem.*, 2013, article ID 497956. <http://dx.doi.org/10.1155/2013/497956>
85. M. A. Subhan, K. Alam, M.s. Rahaman, M.A. Rahaman and M.R. Awal, Synthesis and Characterization of Metal Complexes Containing Curcumin ($C_{12}H_{20}O_6$) and Study of

- their Anti-microbial Activity and DNA Binding Properties, *J. Sci. Res.* 2014, **6(1)**, 97-109. <http://dx.doi.org/10.3329/jsr.v6i1.15381>
86. L. F. Chu, Y. Shi, D. F. Xu, H. Yu, J. R. Lin and Q. Z. He, Synthesis and Biological Studies of Some Lanthanide Complexes of Schiff Base, *Synth. React. Inorg., Met. Org. Nano-Met. Chem.*, 2015, **45(110)**, 1617- 1626.] <http://dx.doi.org/10.1080/15533174.2015.1031048>
87. k.Arun, S. Bootwala, M. Tariq, C. Frenandes and S. Somasundaran, Synthesis, Characterization, Thermal and Kinetic studies of Lanthanum(III), Thorium (IV) and Dioxouranium (VI) chelates with Multidentate Ligand and its in vitro Antibacterial analysis, *Int. J. Pharm. Sci. Res.*, 2014, **5(2)**, 400-409. [http://dx.doi.org/10.13040/IJPSR.0975-8232.5\(2\).400-409](http://dx.doi.org/10.13040/IJPSR.0975-8232.5(2).400-409)
88. J. Torres, M. Brusoni, F. Peluffo, C. Kremer, S. Dominguez, A. Mederos and E. Kremer, Phosphodiesterolytic Activity of Lanthanide (III) Complexes with α -Amino Acids. *Inorg. Chimica Acta*, 2005, **358**, 3320-3328. <https://doi.org/10.1016/j.ica.2005.05.003>
89. G. R. Motson, J. S. Fleming and Sally Brooker, Potential Application for the use of Lanthanide Complexes as Luminescence Biolabels, *Adv. Inorg. Chem.*, 2004, **55**, 361-432. [https://doi.org/10.1016/S0898-8838\(03\)55007-3](https://doi.org/10.1016/S0898-8838(03)55007-3)
90. James E. House, Principle of Chemical Kinetics Second Edition, Academic Press Publication, USA, ISBN: 978-0-12-356787-1, 2007. https://books.google.co.in/books?hl=en&lr=&id=Df2B4Il_h_EC&oi=fnd&pg=PP1&dq=chemical+kinetics+concepts&ots=MR5h7hfULJ&sig=GIfls2NNC3voy4Kq3lu9BpD8UKQ
91. R. Justi, Teaching and Learning Chemical Kinetics, *Sci. Tech. Edu. Lib.*, 2002, **17**, 293-315. https://doi.org/10.1007/0-306-47977-X_13
92. K. Bain and M. H. Towns, A review of Research on the Teaching and Learning of Chemical Kinetics, *Chem. Educ. Res. Pract.*, 2016, **17**, 246-262. <https://doi.org/10.1039/C5RP00176E>
93. Connors and K. Antonio, Chemical kinetics: the Study of Reaction Rates in Solution, New York. 1990, 480. https://books.google.com/books/about/Chemical_Kinetics.html?id=nHux3YED1HsC

Microwave-assisted Fast and Efficient Green Synthesis of Curcumin Lanthanide (Pr^{3+} , Nd^{3+} , Eu^{3+} and Gd^{3+}) Complexes and Investigation of their Spectroscopic and Kinetic Studies

Abstract

In the present study, we report the Microwave-assisted green synthesis of curcumin lanthanide complexes from curcumin ligand (L^1) and lanthanide chlorides ($\text{LnCl}_3 \cdot x\text{H}_2\text{O}$; where; $\text{Ln}=\text{Pr}^{3+}$, Nd^{3+} , Eu^{3+} and Gd^{3+}) in presence of triethylamine (Et_3N) in ethanol at 180 °C for 5 min and investigated their spectroscopic and chemical dynamic studies. The spectroscopic and physico-chemical properties of the curcumin ligand (L^1) and its lanthanide(III) complexes $[\text{L}^1_3\text{PrCl}_3]$ (**2.1a**), $[\text{L}^1_3\text{NdCl}_3]$ (**2.1b**), $[\text{L}^1_3\text{EuCl}_3 \cdot 6\text{H}_2\text{O}]$ (**2.1c**), $[\text{L}^1_3\text{GdCl}_3 \cdot 6\text{H}_2\text{O}]$ (**2.1d**) were studied by various means IR, UV-Vis, Fluorescence, TGA-DTA and elemental analysis. The IR-spectra of curcumin lanthanide complexes; $\text{L}^1_3\text{LnCl}_3 \cdot x\text{H}_2\text{O}$ (**2.1a-d**) were well interpreted based on the comparison of free curcumin ligand (L^1) spectrum which predicts the formation of complexes (**2.1a-d**). The fluorescence spectral studies of the curcumin lanthanide complexes demonstrate that there is a quenching in fluorescence spectra with respect to the free curcumin ligand.

2.1. Introduction

Curcumin is one of the promising agent for the treatment of many diseases which was first isolated in 1815 by Vogel and Pelletier¹ from the rhizome of turmeric herb *Curcuma longa* and its medicinal properties are known for thousands of years, where it is traditionally used as antiseptic, anti-inflammatory, for the relief of gastrointestinal discomfort, analgesic and in cosmetics in India and China.² For the last decade, scientifically, curcumin has been investigated for its remarkable therapeutic potentiality against cardiovascular, nervous systems, obesity and diabetes.³ Curcumin is well recognized as photosensitizer showing significant anti-cancer activity.^{4,5} Unfortunately, its applications in clinical trials hindered due to its poor bioavailability.⁶ Henceforth, there are many strategies to overcome these poor solubility and higher stability factor and recently curcumin and its derivatives were used as ligands with most of the transition metals for the synthesis of curcumin metal complexes and reported their numerous spectroscopic and medicinal properties.⁷ Apart from transition metals, curcumin with alkali metals such as Na, Be, Mg, Ca and Ba complexes were described and among the other main group elements, curcumin boron complexes have been most comprehensively investigated.⁸

Notably, very few reports were found on curcumin lanthanide complexes ($\text{Ln}=\text{La}$, Y, Lu, Gd, Eu) with different synthetic methods and some curcumin complexes were described with the spectator ligands which brings together in the coordination sphere for the formation of stable curcumin lanthanide complexes due to large ionic radii, steric saturation of lanthanide ions and also the Ln^{3+} generally prefer high coordination numbers such as 8 or 9.⁹ With regard to its importance and applications some of the current survey on curcumin metal complexes are thrashed out below.

With the innumerable studies and incept of curcumin and its metal complexes, an innovative synthesis of a soluble and crystallizable substituted curcumin metal complexes were foreground by S. Waniner in **2015 (Figure 2.1)**. These substituted curcumin metal complexes were found to have binate character and as an MRI agent they have the ability to detect the tumour but cannot vandalized the tumour. In this study curcumin metal complexes were also reported to have anti-oxidant properties and can be used as a drug transporter. On reviewing the applications and importance pointed by different researcher, curcumin complexes were speculated to be a “multi-anti” agent in the time to come.¹⁰

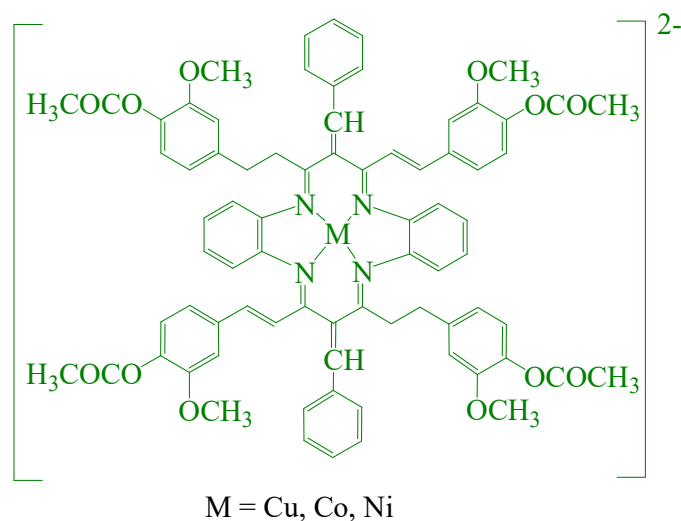


Figure 2.1. Structure of the Substituted Metal complexes.

B. Dinesh and R. Saraswathi in **2017** synthesized a nano-structured copper curcumin complex by electrochemical methods. The complexes in the aqueous solution shows a potential electrochemical determination of 4-nitrophen due to its anti-interference ability which can be utilized as an electrode sensor in various industrial applications with high durable ability, inexpensive and effortless preparation.¹¹ N. Bicer *et al.* (**2018**) synthesized

curcumin complexes with Iron(III) and Manganese(II) and were characterized showing an octahedral geometry and two H_2O molecules coordinating to the central metal (**Figure 2.2**). The complexes were reported to reduce the built-up of Beta Amyloid protein which root Alzheimer and Dementia.¹²

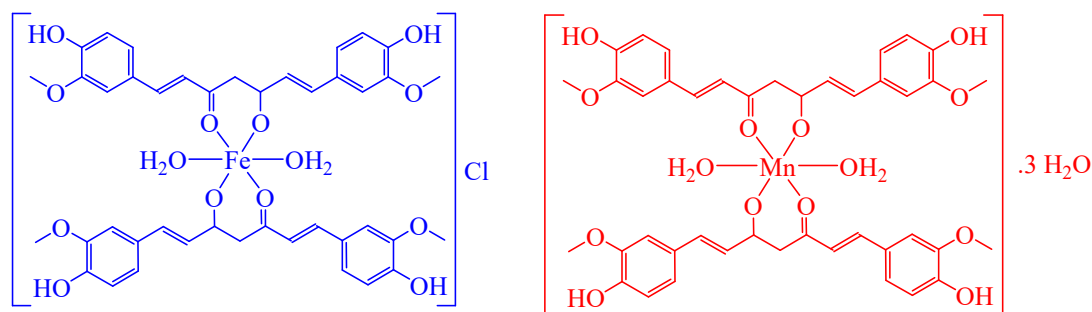


Figure 2.2. Structures of Curcumin Fe(III) and Mn(II) Complexes.

Chemistry of lanthanide(III) and how they are capable of affecting photocytotoxicity of the photo-active curcumin based ligand were discussed in 2020 by D. Musib and co-workers. Curcumin based lanthanum (III) complexes (**Figure 2.3**) were synthesized, characterized and on examining the complexes, in visible light, the complex containing the curcumin base ligand were found to have photo-cytotoxicity activity against HELA (Cervical Cancer) and MCF-7 (Breast Cancer) cell line.¹³

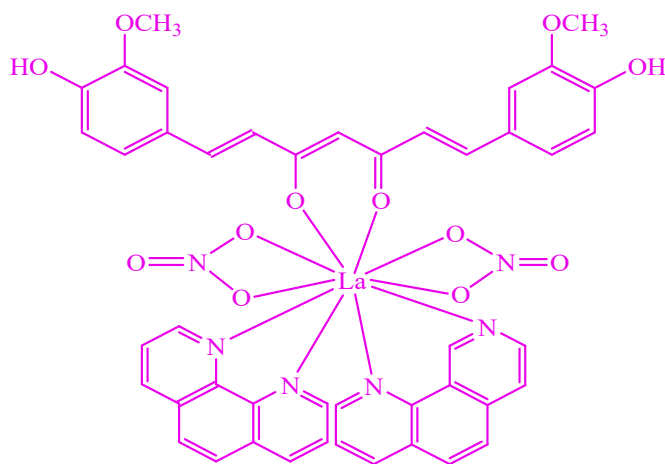


Figure 2.3. Schematic Structure of Curcumin based Lanthanum(III) Complexes.

In the last few years, curcumin is getting a lot of attention traditionally and scientifically due to its multi characteristic and benefits. Nevertheless, they have some

shortcoming due to its hydrophobia, water insolubility, fast reaction and feeble bioavailability. To overcome these drawbacks of curcumin, curcumin metal complexes were created. S. Prasad *et al.* (2021) elaborated on how the curcumin metal complexes and its applications in chemo preventive, therapeutic and pharmacologically became one of the most necessities. Further discussion was done on curcumin metal complexes biological activities and its importance in the radio imaging and also predicted for better treatment and prevention of chronic diseases.¹⁴

The potential applications of curcumin and its metal complexes prompted us to develop the synthesis of curcumin lanthanide complexes. Therefore, the aim of the present work is to describe the Microwave-assisted fast and efficient green synthesis of curcumin lanthanide complexes (**2.1a-b**) and investigate their spectroscopic, physico-chemical and kinetic studies.

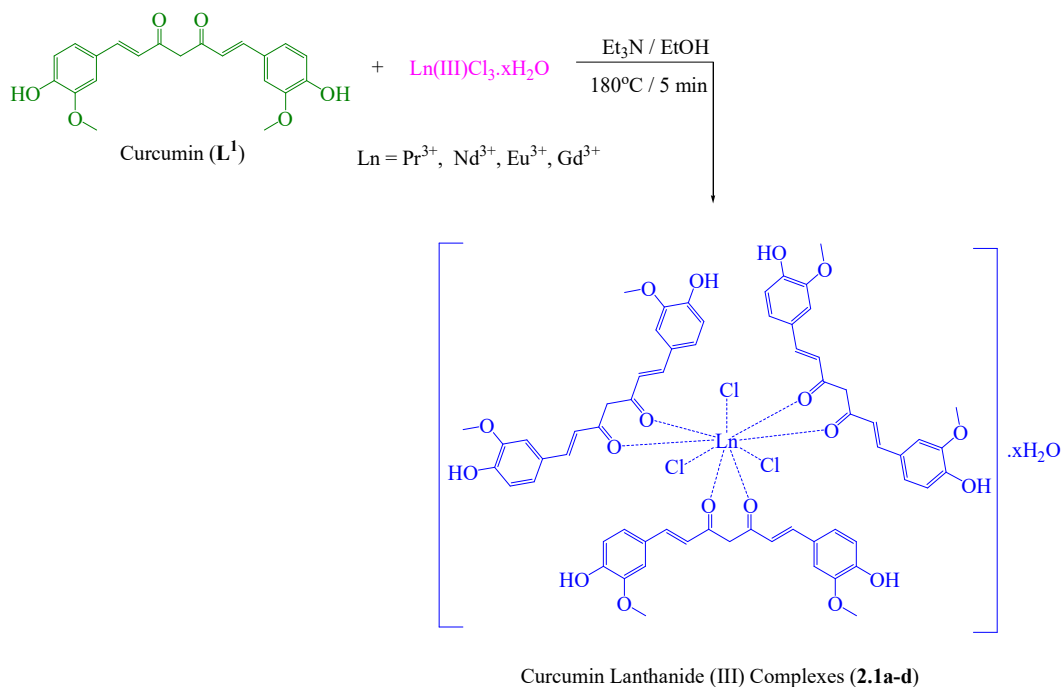
2.2. Experimental

2.2.1. Materials and Methods

All the reagents and solvents were purchased from commercially available sources and used without further purification. Melting points were recorded in open capillaries using IKON melting point apparatus and are uncorrected. FT-IR spectra of the curcumin ligand and its lanthanide complexes were recorded on Perkin-Elmer spectrophotometer (Spectrum-Two) using KBr disk and values are expressed in cm^{-1} . Micro analytical (CHN) data were obtained with a FLASH EA 1112 Series CHNS analyzer. UV-visible spectrophotometer (Double Beam) Perkin Elmer, Lambda-35 is used for recording the absorption bands of the curcumin ligand and its lanthanide complexes. All fluorescence emission spectra of curcumin ligand and its lanthanide complexes were recorded using fluorescence spectrophotometer Shimadzu RF- 6000 which is followed by the evaluation of their quantum yields. pH values of the reactions were recorded using EUTECH instrument pH 700. The TGA-DTA measurements of curcumin ligand and its lanthanide complexes were performed on a Perkin-Elmer analyzer with the temperature range of 25 – 900°C.

2.2.2. General Microwave-assisted Green Synthesis of Curcumin Lanthanide Complexes $[L_3LnCl_3 \cdot xH_2O]$ (2.1a-d)

Curcumin ligand (L^1) (0.368 g, 1 mmol) and $Ln(III)Cl_3 \cdot xH_2O$ (where; $Ln=Pr^{3+}$, Nd^{3+} , Eu^{3+} and Gd^{3+}) (0.33 mmol) were mixed in a microwave reaction vial in which it was added catalytic amount of trimethylamine (Et_3N) in ethanol (2 mL). The reaction mixture was mixed thoroughly with glass rod and was irradiated in a microwave reactor under $180^\circ C$ for 5 minutes. After completion of the reaction, the solid compound obtained was washed with hexane for several times and collected through filtration. The yielded solid of curcumin lanthanide complexes; $[L_3PrCl_3]$ (2.1a), $[L_3NdCl_3]$ (2.1b), $[L_3EuCl_3 \cdot 6H_2O]$ (2.1d), $[L_3GdCl_3 \cdot 6H_2O]$ (2.1d) were allowed to air dried.



Scheme 2.1. Microwave-assisted Synthesis of the Curcumin Lanthanide Complexes (2.1a-d).

2.3. Results and Discussion

Herein, we report the microwave-assisted fast and efficient green synthesis of curcumin chelated lanthanide complexes (2.1a-d). The Curcumin lanthanide metal complexes were synthesized from curcumin (1,7-bis(4-hydroxyl-3-methoxyphenyl)-1,6-heptadiene-3,5-dione) as ligand (L^1) and lanthanide metal chlorides ($LnCl_3 \cdot xH_2O$; $Ln = Pr^{3+}$, Nd^{3+} , Eu^{3+} and Gd^{3+}) in 1:3 ratio in presence of catalytic amount of Et_3N in ethanol

under microwave irradiation at 180 °C for 5 min. The synthesized solid lanthanide complexes were collected through filtration method from the reaction mixture by the complete removal of the solvent followed by washing with the hexane for several times and air dried at room temperature. The yielded curcumin lanthanide complexes (**2.1a-d**) were stable at room temperature, which were analyzed through for various spectroscopic properties. The resulting curcumin lanthanide complexes were well studied with FT-IR spectroscopy, UV-Visible spectroscopy, Fluorescence spectroscopy, TGA-DTA analysis and elemental analysis. The physico-analytical data of free curcumin ligand (**L¹**) and curcumin lanthanide complexes (**2.1a-d**) were represented in **Table 2.1**.

Table 2.1. Physico-analytical data of free Curcumin Ligand (**L¹**) and its Lanthanide Complexes (**2.1a-d**).

Compounds	Yield (%)	Colour	CHN Analysis (%) Found(Calculated)		
			Carbon	Hydrogen	Nitrogen
Curcumin(L¹)	-	Bright orange	68.52 (68.47)	5.42 (5.47)	-
[L¹ ₃ PrCl ₃](2.1a)	86	Brown	55.86 (55.95)	4.41 (4.47)	-
[L¹ ₃ NdCl ₃](2.1b)	90	Brown	55.74 (55.81)	4.51 (4.46)	-
[L¹ ₃ EuCl ₃ ·6H ₂ O](2.1c)	93	Dark brown	51.48 (51.42)	4.86 (4.93)	-
[L¹ ₃ GdCl ₃ ·6H ₂ O](2.1d)	95	Dark brown	51.32 (51.24)	4.85 (4.91)	-

2.3.1. FT-IR Spectral Characterization Studies

2.3.1.1. FT-IR Spectra of Curcumin Ligand (L^1)

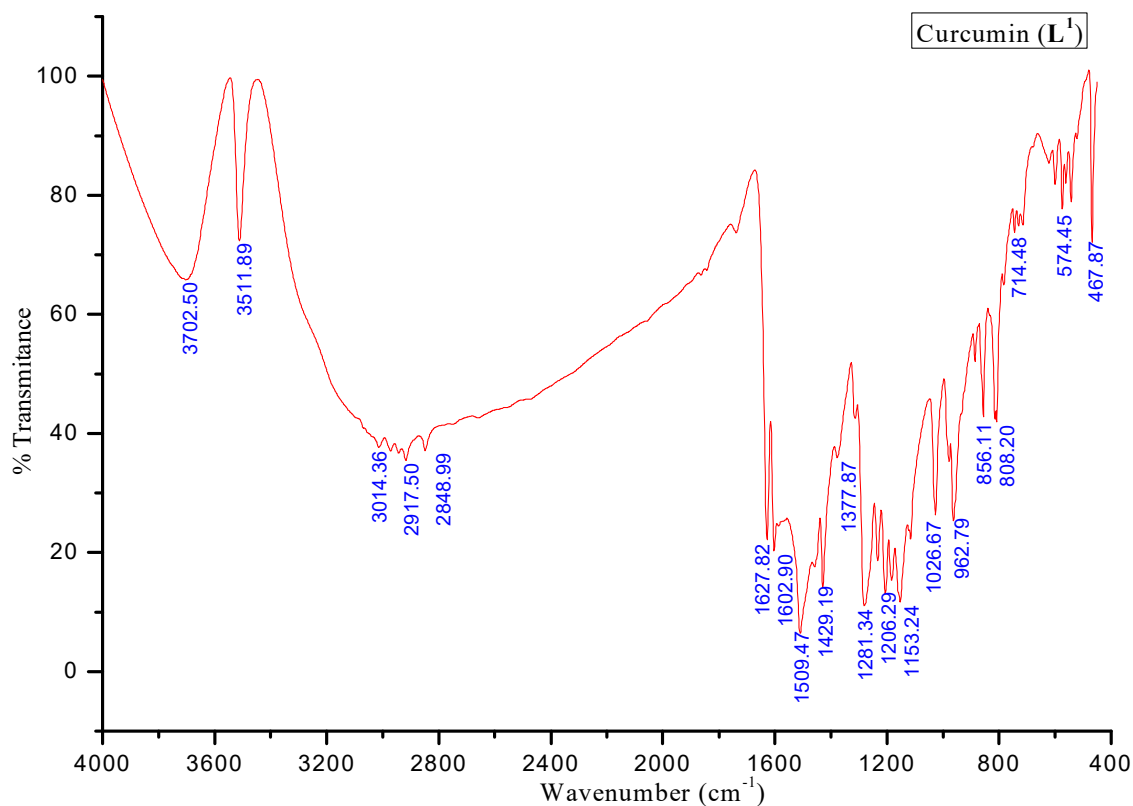


Figure 2.4. FT-IR Spectra of Curcumin Ligand (L^1).

The FT-IR spectrum of the free curcumin ligand (L^1) showed a broad vibrational peak at 3702 cm^{-1} correspond to free phenolic OH group and a sharp peak at 3511 cm^{-1} attributing to the enolic-OH stretching vibrations. The bands observed at 1627 cm^{-1} and 1602 cm^{-1} indicated the mixed vibrations of $\nu(\text{C}=\text{O})$ and band at 1509 cm^{-1} frequency was the most prominent which attributed to mixed vibrations of $\nu(\text{C}=\text{C})$ bonds, and the band at 1429 cm^{-1} correspond to the $\nu(\text{CCC})$ bonds. The bands at 1281 cm^{-1} and 1206 cm^{-1} are mixed vibrations aromatic C-O stretching. The peak observed at 1153 cm^{-1} frequency corresponds to the enolic C-O stretching vibrations. The mixed bending vibrations observed for C=C and C-H bonds at 1026 cm^{-1} , 962 cm^{-1} , 856 cm^{-1} and 808 cm^{-1} (**Figure 2.4** and **Table 2.2**).

2.3.1.2. FT-IR Spectra of Curcumin Praseodymium Complex $[L^1_3PrCl_3]$ (**2.1a**)

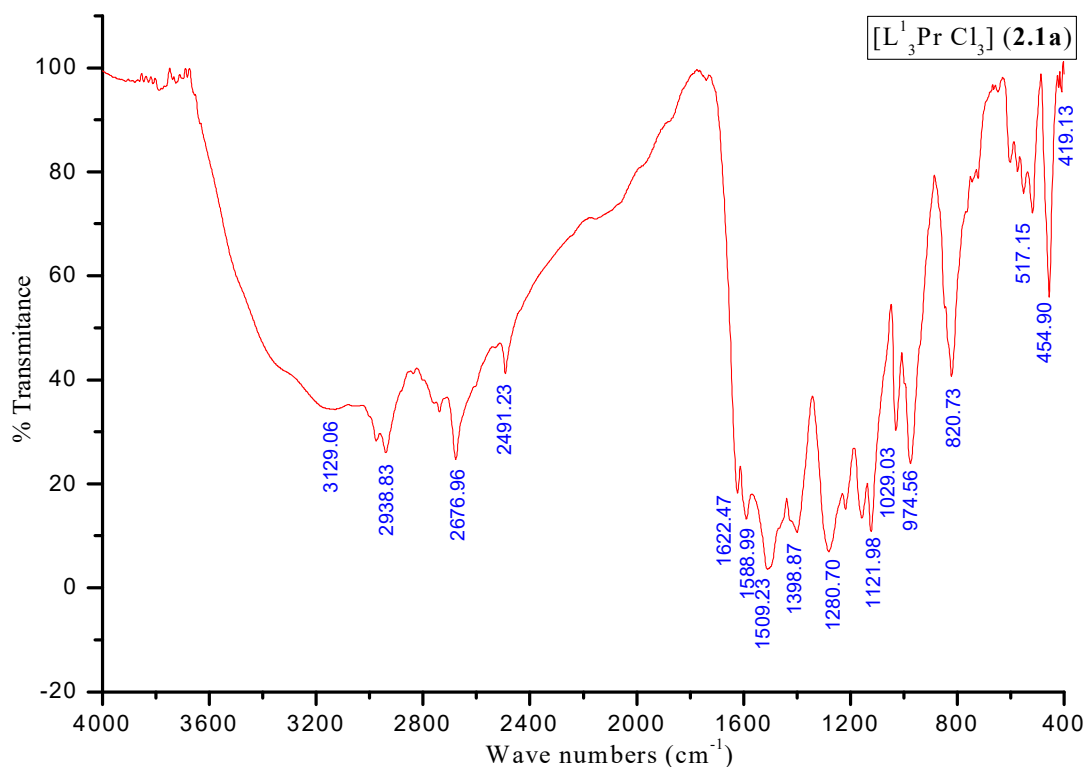


Figure 2.5. FT-IR Spectra of Curcumin Praseodymium Complex $[L^1_3PrCl_3]$ (**2.1a**).

The curcumin praseodymium complex $[L^1_3PrCl_3]$ (**2.1a**) was characterized by recording the FT-IR spectra. It was found that the prominent bands appeared in the free curcumin ligand indicating the mixed vibrations of C=O stretching at 1627 cm^{-1} and 1602 cm^{-1} were completely shifted to lower frequencies values at 1622 cm^{-1} and 1588 cm^{-1} . The shifting of the bands in the complex IR spectra strongly signify that the formation of complex with praseodymium metal at β -diketonate coordination site of the curcumin ligand (L^1). The OH stretching at 3511 cm^{-1} which appeared in the free Curcumin ligand is disappeared in the complex and a new band appearing at 419 cm^{-1} supported the formation of the M-O bond which supports the ligand coordination to the metal where this band was not observed in the free Curcumin ligand (**Figure 2.5** and **Table 2.2**).

2.3.1.3. FT-IR Spectra of Curcumin Neodymium Complex $[L^1_3NdCl_3]$ (**2.1b**)

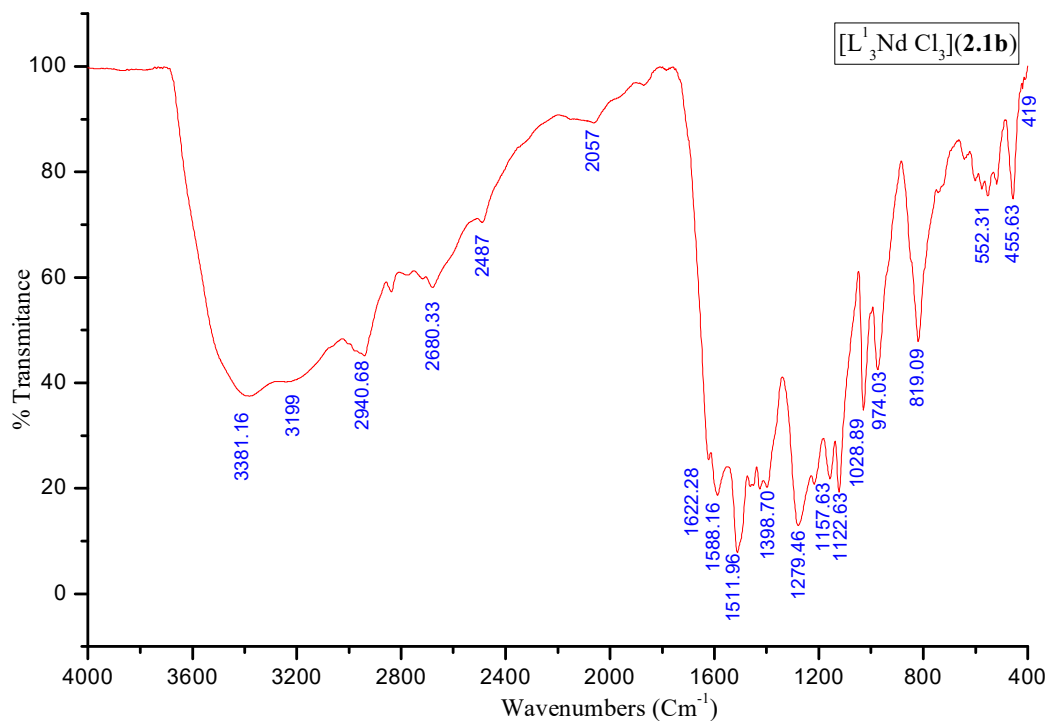


Figure 2.6. FT-IR Spectra of Curcumin Neodymium Complex $[L^1_3NdCl_3]$ (**2.1b**).

The characteristic FT-IR spectrum of the curcumin neodymium complex $[L^1_3NdCl_3]$ (**2.1b**) showed that the most prominent bands at 1627 cm^{-1} and 1602 cm^{-1} which appear in the free ligand indicating the C=O stretching shifted to lower frequencies at 1623 cm^{-1} and 1588 cm^{-1} in the curcumin neodymium complex compound and a new band appearing at 412 cm^{-1} due to M-O bond which suggests the ligand coordination with the metal which band was not found in the free curcumin ligand (**Figure 2.6** and **Table 2.2**).

2.3.1.4. FT-IR Spectra of Curcumin Europium Complex $[L^1_3EuCl_3 \cdot 6H_2O]$ (2.1c)

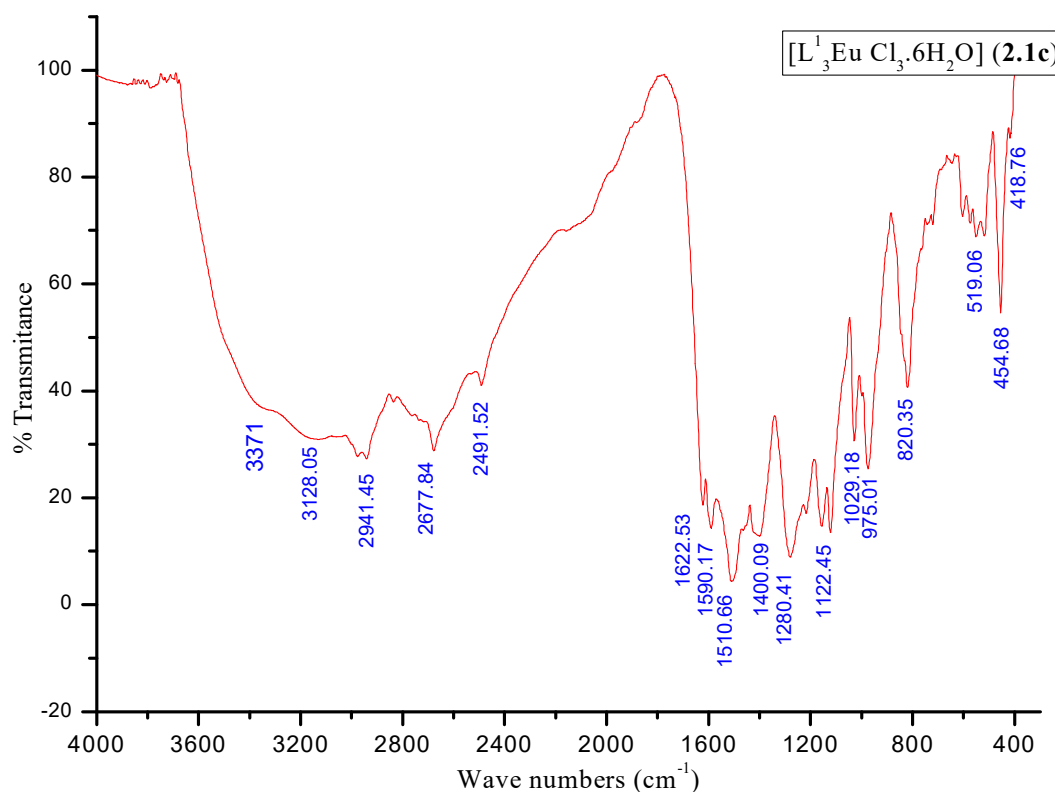


Figure 2.7. FT-IR Spectra of Curcumin Europium Complex $[L^1_3EuCl_3 \cdot 6H_2O]$ (2.1c).

Similarly for the IR spectra of the curcumin europium complex $[L^1_3EuCl_3 \cdot 6H_2O]$ (2.1c) (Figure 2.7 and Table 2.2) shows that the band at 1627 cm^{-1} and 1602 cm^{-1} in free ligand indicating the (C=O) stretching shifted to lower wavelength at 1622 cm^{-1} and 1590 cm^{-1} in complex supporting the formation of the curcumin europium complex and the new band appearing at 418 cm^{-1} supports the formation of the M-O bond.

2.3.1.5. FT-IR Spectra of Curcumin Gadolinium Complex $[L^1_3GdCl_3 \cdot 6H_2O]$ (2.1d)

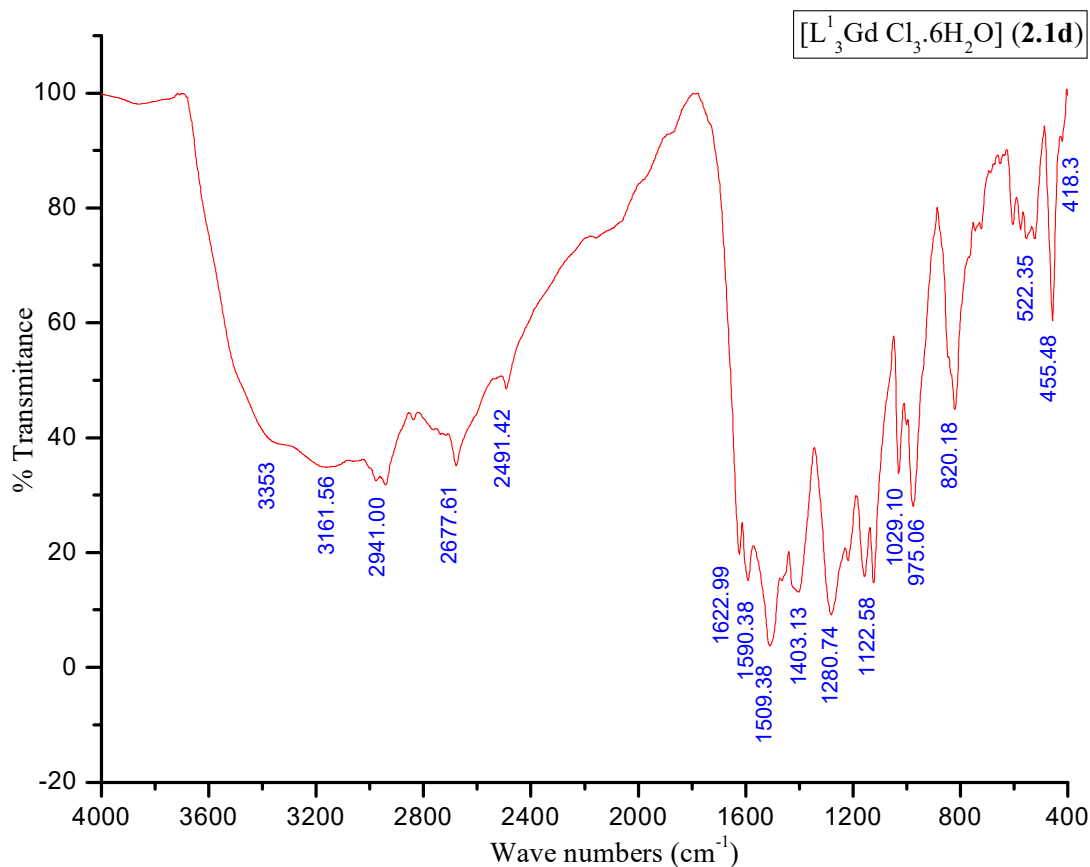


Figure 2.8. FT-IR Spectra of Curcumin Gadolinium Complex $[L^1_3GdCl_3 \cdot 6H_2O]$ (2.1d).

In the IR spectra of $[L^1_3GdCl_3 \cdot 6H_2O]$ (2.1d), the band at 1627 cm^{-1} and 1602 cm^{-1} in free curcumin ligand (L^1) shifted to a lower frequency at 1622 cm^{-1} and 1590 cm^{-1} respectively after complexation which attribute to the C=O stretching and appearance of the new band attributing M-O bond at 418 cm^{-1} support the coordination of the curcumin and gadolinium.

The supporting information for the FT-IR spectra for all the different stretching bands of the free Curcumin ligand (L^1), $[L^1_3PrCl_3]$ (2.1a), $[L^1_3NdCl_3]$ (2.1b), $[L^1_3EuCl_3 \cdot 6H_2O]$ (2.1c) and $[L^1_3GdCl_3 \cdot 6H_2O]$ (2.1d) were provided in Table 2.2

Table 2.2. Major FT-IR Spectral data of the Curcumin (**L¹**) and its Lanthanide Complexes (**2.1a-d**) (cm⁻¹).

Compound	$\nu(\text{ArOH, OH})$	Ar $\nu(\text{CH})$	$\nu(\text{C=O})(\text{C=C})$	Ar $\nu(\text{CC})$	$\nu(\text{C-O})$	$\nu(\text{C-H})$	$\nu(\text{M-O})$
Curcumin (L¹)	3702, 3511	3014	1627, 1602, 1509	1429	1281, 1153	1026, 962, 856, 808	-
[L¹ ₃ PrCl ₃] (2.1a)	-	3129	1622, 1588, 1509	1398	1280, 1121	1029, 974, 820	419
[L¹ ₃ NdCl ₃] (2.1b)	-	3127	1623, 1588, 1510	1426	1280, 1121	1028, 971, 816	412
[L¹ ₃ EuCl ₃ ·6H ₂ O] (2.1c)	3371	3128	1622, 1590, 1510	1400	1280, 1122	1029, 975, 820	418
[L¹ ₃ GdCl ₃ ·6H ₂ O] (2.1d)	3353	3161	1622, 1590, 1509	1403	1280, 1122	1029, 975, 820	418

2.3.2. UV-Vis Spectroscopic Studies

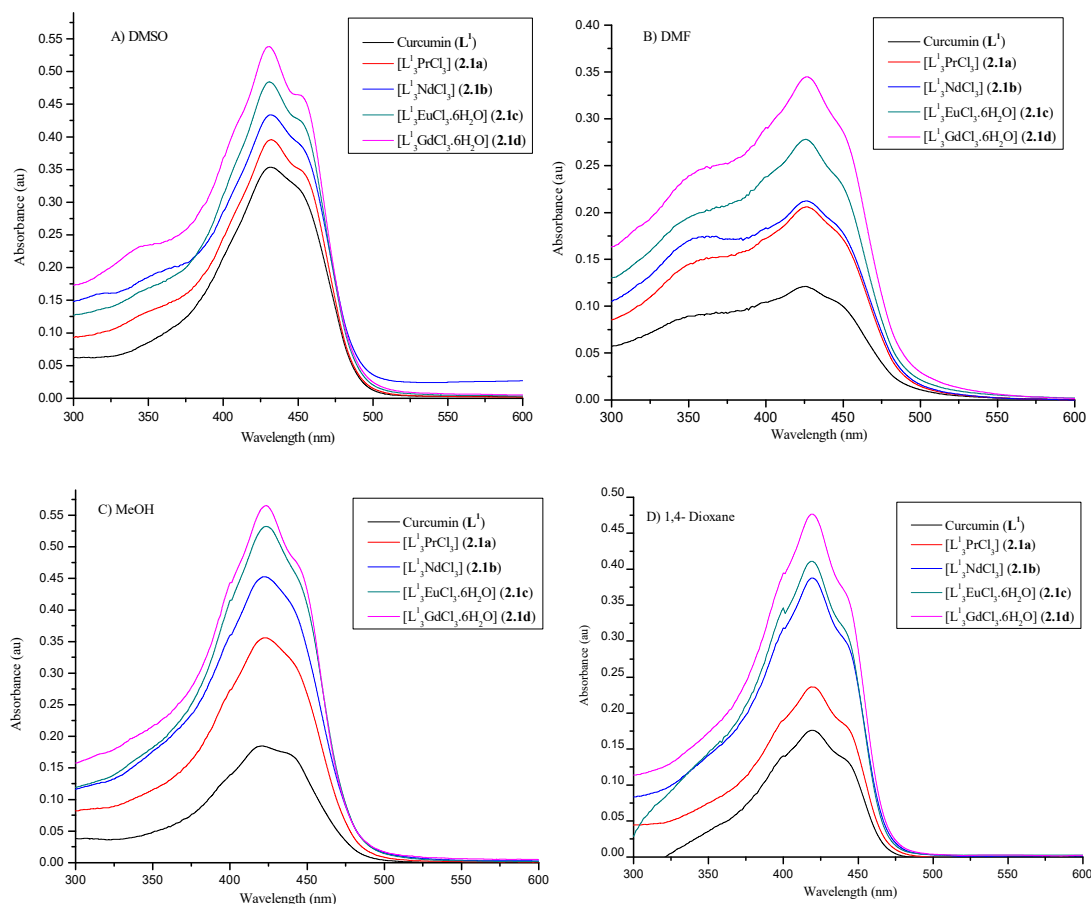


Figure 2.9. UV-VisS of Curcumin ligand (L^1) and its Lanthanide Complexes (**2.1a-d**) in different solvents (conc. 1×10^{-5} M).

UV-Vis Spectra of Curcumin ligand (L^1) and its Lanthanide complexes (**2.1a-d**) in different solvents such as dimethyl sulfoxide (DMSO), dimethylformamide (DMF), methanol (MeOH) and 1,4-dioxane were recorded at conc. 1×10^{-5} M. A maximum absorption bands occur at around 431 nm to 418 nm and an insignificant shoulder band at around 440 nm on recording the electronic spectra of free curcumin ligand (L^1) in different solvent medium. We observed that the increase in polarity of the solvent the absorption band move toward the higher intensity. This happen due to $\pi-\pi^*$ transition as π^* orbitals are more stabilized by hydrogen bonding with polar solvent and so it required a small energy for transition. Similarly, we have recorded for the curcumin lanthanide complexes (**2.1a-d**) in dimethyl sulfoxide (DMSO), methanol, dimethylformamide (DMF) and 1,4-dioxane solvents at same 1×10^{-5} M concentrations and found that with the increase

in polarity of the solvent, the higher intensification of the absorption bands, found in all the curcumin lanthanide complexes compared to the pure curcumin ligand (L^1) shown in **Figure 2.9** and **Table 2.3**. When there is complexation, the atomic radii of central metal, Ln(III) expands thereby reducing the bond distance between the metal and the ligand (curcumin) shows by the higher intensification of the absorption bands, known as the Nephelauxetic effect (β).

We observed that the absorption intensity of the free curcumin ligand and its lanthanide complexes increases in the order as curcumin (L^1) < $[L^1_3PrCl_3]$ (**2.1a**) < $[L^1_3NdCl_3]$ (**2.1b**) < $[L^1_3EuCl_3 \cdot 6H_2O]$ (**2.1c**) < $[L^1_3GdCl_3 \cdot 6H_2O]$ (**2.1d**) which is due to the increasing of electronegativity of the metals in the periodic table.

Table 2.3. UV-Vis Spectral values of Curcumin Ligand (L^1) and its Lanthanide Complexes (**2.1a-d**).

Compound	DMSO $\lambda_{max}(a.u)$	DMF $\lambda_{max}(a.u)$	MeOH $\lambda_{max}(a.u)$	1,4-Dioxane $\lambda_{max}(a.u)$
Curcumin (L^1)	431.50 (0.3536)	425.5 (0.1209)	419.35 (0.1842)	418.35 (0.1758)
$[L^1_3PrCl_3]$ (2.1a)	431.50 (0.3953)	426.7 (0.2059)	422.35 (0.3559)	418.75 (0.2364)
$[L^1_3NdCl_3]$ (2.1b)	431.50 (0.4337)	426.1 (0.2123)	422.35 (0.4525)	419.35 (0.3875)
$[L^1_3EuCl_3 \cdot 6H_2O]$ (2.1c)	430.80 (0.4841)	425.5 (0.2779)	422.95 (0.5321)	418.75 (0.4110)
$[L^1_3GdCl_3 \cdot 6H_2O]$ (2.1d)	430.20 (0.5381)	426.7 (0.3447)	423.55 (0.5652)	419.35 (0.4764)

2.3.3. Fluorescence Spectral Characterization Studies

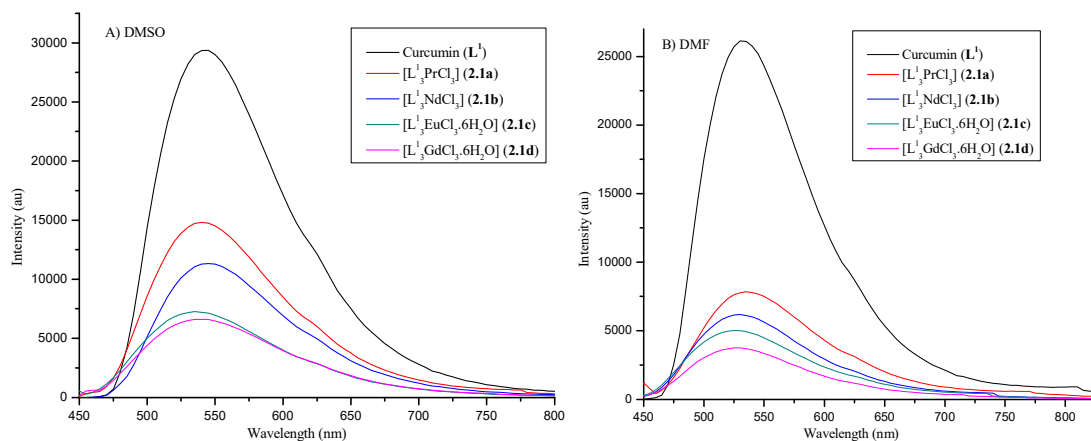


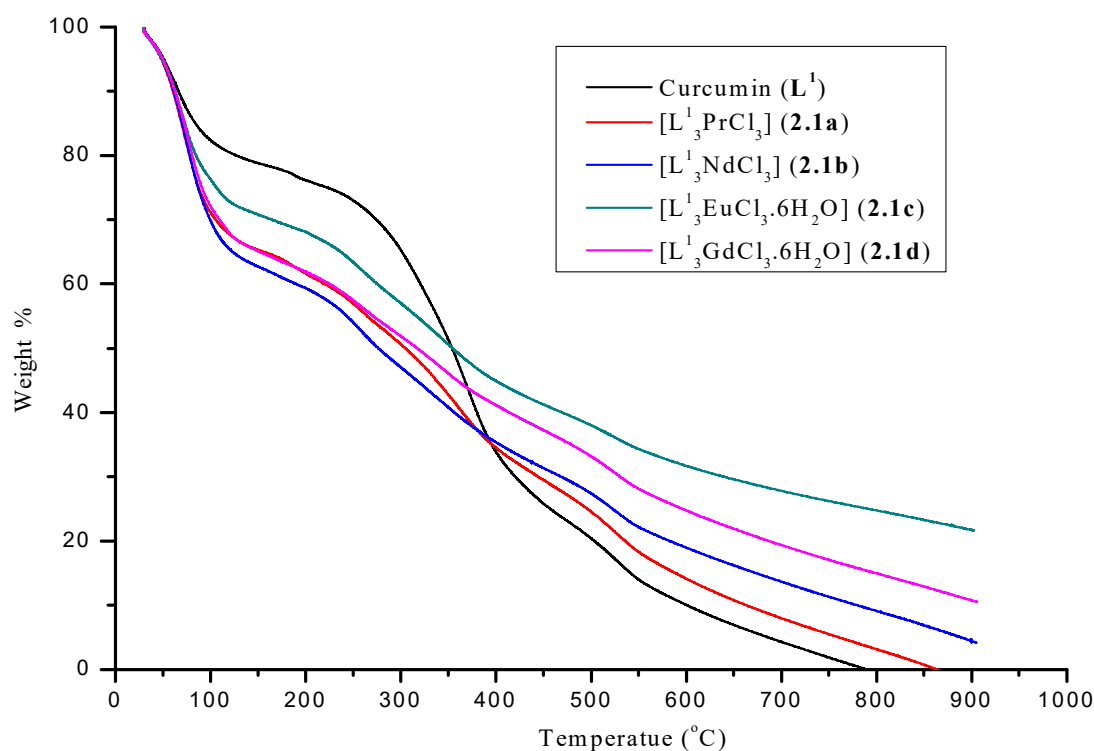
Figure 2.10. Fluorescence spectra of Curcumin Ligand (L^1) and its Lanthanide Complexes (2.1a-d).

The emission spectra of the curcumin ligand (L^1) and its lanthanide metal complexes (2.1a-d) were recorded at concentration 1×10^{-4} M using DMSO and DMF as the solvents. The maximum absorption of the complexes is different and so the excitation wavelength varied. The intensity of the higher polarity shows higher intensity and excitation wavelength. Interestingly, we observed that there is drastic fluorescence decline in the curcumin lanthanide complexes (2.1a-d) compared with that of free curcumin ligand (L^1). With the increase in the electronegativity of the lanthanide metals in the periodic table the intensity of the complexes decreases giving the descending order: Curcumin (L^1) > $[L^1_3PrCl_3]$ (2.1a) > $[L^1_3NdCl_3]$ (2.1b) > $[L^1_3EuCl_3 \cdot 6H_2O]$ (2.1c) > $[L^1_3GdCl_3 \cdot 6H_2O]$ (2.1d). The Quantum yield of the Curcumin lanthanide complexes (2.1a-d) compared to the free ligand curcumin (L^1) gives the same quenching order as that of the intensity of the fluorescence spectra (Figure 2.10 and Table 2.4).

Table 2.4. Florescence Spectral data of the Curcumin Ligand (L^1) and its Lanthanide Complexes (**2.1a-d**).

Compound	Solvent	Excitation (nm)	Emission (nm)	Intensity (au)	Quantum Yield (Φ_f)
Curcumin (L^1)	DMSO	432	545	29361.2	0.0142
	DMF	425	530	26127.5	0.0053
[$L^1_3PrCl_3$] (2.1a)	DMSO	432	540	14814.4	0.0099
	DMF	426	535	7838.2	0.0036
[$L^1_3NdCl_3$] (2.1b)	DMSO	432	540	11286.2	0.0058
	DMF	426	525	6145.4	0.0023
[$L^1_3EuCl_3 \cdot 6H_2O$] (2.1c)	DMSO	430	535	7255.4	0.0038
	DMF	427	525	5022.9	0.0020
[$L^1_3GdCl_3 \cdot 6H_2O$] (2.1d)	DMSO	430	535	6611.0	0.0034
	DMF	426	525	375.1	0.0018

2.3.4. Thermogravimetric Analysis

**Figure 2.11.** TGA curve for the free Curcumin Ligand (L^1) and its Lanthanide Complexes (**2.1a-d**).

The thermo gravimetric analysis was recorded at 10°C/minute at a temperature range from 29°C to 900°C in nitrogen atmosphere in order to study the thermal behavior of

curcumin ligand (L^1) and its lanthanide(III) complexes (**2.1a-d**) at different temperature. From the obtained TGA curve the weight loss of the free curcumin ligand and the lanthanide complexes at different temperature were analyzed experimentally and theoretically.

The free curcumin ligand under goes five stages while those of the synthesized metal complexes under goes more than five stages of decompositions. The first decomposition was found at around 100 °C involving the loss of OH and H₂O followed by decomposition of the remaining composition of the curcumin ligand and the complexes. In all most all the lanthanide metal complexes the metal oxide remained as the residue except for the praseodymium complex [$L^1_3PrCl_3$] (**2.1a**) which fully decomposed at 863.01 °C. The detail decomposition of the compounds respected to the temperature is tabulated in **Table 2.5**.

Table 2.5. Thermo Gravimetric Analysis of Curcumin ligand (**L⁵**) and its Lanthanide complexes (**2.1a-d**).

Compound	Temperature(° C)	Weight Lost (%) (Experiment/Theoretical)	Decomposed Compound
Curcumin (L¹)	29.00 – 90.22	16.011% / 16.835%	2(CH ₃ O)
	90.22 – 222.61	09.979% / 09.220%	2OH
	222.61 – 432.38	46.213% / 46.720%	C ₆ H ₃ CH=CH-CO-CH ₂ -CO
	432.38 – 637.94	20.351% / 20.375%	C ₆ H ₃
	637.94 – 790.86	07.538% / 07.063%	HC=CH
[L ¹ ₃ PrCl ₃] (2.1a)	29.00 – 101.15	28.845% / 28.815%	6(OCH ₃), 6(OH) and C ₆ H ₃ CH=CH
	101.15 – 172.95	07.204% / 07.418%	C ₆ H ₃ CH=CH
	172.95 – 281.41	11.009% / 11.116%	2(C ₆ H ₃)
	281.41 – 551.54	35.067% / 35.148%	C ₆ H ₃ CH=CH-C-CH ₂ -C-CH=CH- C ₆ H ₃ , C-CH ₂ -C, CH=CH-C-CH ₂ -C-CH=CH and Cl ₃
			PrO ₆
[L ¹ ₃ NdCl ₃] (2.1b)	551.54 – 863.01	17.875% / 17.476%	6(OCH ₃), 6(OH) and 2(C ₆ H ₃ CH)
	29.00 – 114.84	34.705% / 34.238%	C ₆ H ₃
	114.84 – 174.94	05.300% / 05.536%	C ₆ H ₃ CH=CH and 3(CH)
	174.94 – 276.87	10.771% / 10.334%	C ₆ H ₃ CH=CH-C-CH ₂ -C-CH=CH C ₆ H ₃ 2(C-CH ₂ -C), CH and Cl ₃
	276.87 – 47.03	27.346% / 27.861%	NdO ₆
[L ¹ ₃ EuCl ₃ ·6H ₂ O] (2.1c)	547.03 – 12.85	05.360% / 05.230%	
	712.85.....	17.172% / 17.719%	
	29.00 – 93.32	22.500% / 22.292%	6(H ₂ O), 6(OCH ₃) and 2OH
	93.32 – 122.50	05.108% / 05.100%	C ₆ H ₃
	122.50 – 173.82	03.192% / 03.465%	3(OH)
[L ¹ ₃ GdCl ₃ ·6H ₂ O] (2.1d)	173.82 – 267.46	08.301% / 08.024%	HO-C ₆ H ₃ CH=CH
	267.46 – 388.81	15.178% / 15.506%	2(C ₆ H ₃ CH=CH) and CH=CH
	388.81 – 540.30	10.728% / 10.201%	2(C ₆ H ₃)
	540.30 – 828.71	10.987% / 10.405%	3(C-CH ₂ -C-CH)
	828.71.....	24.006% / 24.077%	Cl ₃ and EuO ₆
	29.00 – 95.120	26.285% / 26.816%	6(H ₂ O), 6(OCH ₃) and 6(OH)
	95.120 – 127.19	06.677% / 06.844%	C ₆ H ₃ CH=CH
	127.19 – 195.80	05.248% / 05.082%	C ₆ H ₃
	195.80 – 276.49	07.402% / 07.725%	C ₆ H ₃ CH=CH
	276.49 – 547.92	27.092% / 27.445%	3(C ₆ H ₃ CH=CH), CH=CH, 2(C-CH ₂ -C)
	547.92 – 732.76	09.915% / 09.776%	C-CH ₂ -C and Cl ₃
	732.76.....	17.976% / 17.196%	GdO ₆

2.3.5. Chemical Kinetic and Thermodynamic Studies

A chemical reaction is lead by stretching, bending and ultimately breaking of bonds when molecules collide and the kinetic energy of the molecule is utilized. The minimum energy required for a chemical reaction to occur is called activation energy (E_a).¹⁵ Or it is the difference between the threshold energy and the activation energy of the reactant molecule. Considering the Arrhenius Equation, the activation energy of the chemical reaction can be evaluated.¹⁶

Which is represented as: $k = Ae^{-E_a/RT}$ (1)

Where A = frequency factor or the pre exponential factor, T = temperature, R = universal gas constant, E_a = activation energy and k = rate constant.¹⁷

Applying the Arrhenius rate equation the activation energy (E_a) of the complexation of curcumin lanthanides complexes were evaluated by plotting $\log k$ (k =rate constant) against $1/T \times 10^{-3}$.

$E_a = \text{Slope} \times 2.303 \times R$ (2)

Using Van't Hoff plot of $\log k$ against $1/T$,¹⁷ the thermodynamic parameters for the complexation were calculated.¹⁸

$$\ln k = -\frac{\Delta H^\circ}{RT} + \Delta S^\circ R$$

Or $\ln k = -\Delta G^\circ/RT$ (3)

Experimentally the studies of chemical dynamics have been performed by recording the pH value of curcumin lanthanides complexes; $[L^1_3PrCl_3]$ (**2.1a**), $[L^1_3NdCl_3]$ (**2.1b**), $[L^1_3EuCl_3 \cdot 6H_2O]$ (**2.1c**) and $[L^1_3GdCl_3 \cdot 6H_2O]$ (**2.1d**) at different temperatures for a time interval of 10 minutes in ethanol medium which is shown in **Table 2.6** and a plot of pH against time were plotted (**Figure 2.12, 2.14, 2.16 and 2.18**) in order to analyze the rate of the reaction or complexation at different temperature (288K, 298K, 308K, 318K and 328K) utilizing which the activation energy E_a were evaluated plotting the graph of $\log k$ against $1/T \times 10^{-3}$. From **Table 2.6** we can see that the pH values of the complexes increase with increase in temperatures and time intervals in all the cases which show that the rate of the complexation (k) of curcumin with the lanthanide in the formation of complexes in ethanol medium increases as shown in **Table 2.7, 2.9, 2.11 and 2.13** respectively, which is inconsistent with the theoretical prediction of Arrhenius rate equation. The intercepts of the plot $\log k$ versus $1/T \times 10^{-3}$ provide the frequency factor or the pre exponential factor (A). From the values of the activation energy (E_a) as tabulated in **Table 2.7, 2.9, 2.11 and 2.13**, the negligibly low value of E_a signified that the reactions involved are fast ones. Observing

the value of activation energy (E_a), evaluated from the graph, the order of the increasing rate in the formation of complexes are in the sequence $[L^1_3PrCl_3]$ (**2.1a**) > $[L^1_3NdCl_3]$ (**2.1b**) > $[L^1_3EuCl_3 \cdot 6H_2O]$ (**2.1c**) > $[L^1_3GdCl_3 \cdot 6H_2O]$ (**2.1d**).

From the Van't Hoff plot of $\ln k$ against $1/T$, (**Figure 2.13, 2.15, 2.17 and 2.19**) the thermodynamic parameters such as Enthalpy change (ΔH°) entropy change (ΔS°) and Gibbs free energy change (ΔG°) of the complexation of $[L^1_3PrCl_3]$ (**2.1a**), $[L^1_3NdCl_3]$ (**2.1b**), $[L^1_3EuCl_3] \cdot 6H_2O$ (**2.1c**), $[L^1_3GdCl_3] \cdot 6H_2O$ (**2.1d**), were evaluated which are tabulated in **Table 2.8, 2.10, 2.12 and 2.14**. The negative value of the Gibbs free energy change (ΔG°) indicates that the reaction is a spontaneous and also favorable one associated with the positive values of Enthalpy change (ΔH°) conveying the complexation as endothermic one and the entropy change (ΔS°) value as entropy driven one.

Table 2.6. pH value of Curcumin Lanthanide Complexes (**2.1a-d**) at different temperature with 10 minutes of time interval.

Compound	Temperature °C	pH at different time interval (minutes)						
		0	10	20	30	40	50	60
[L ¹ ₃ PrCl ₃] (2.1a)	15	1.08	1.10	1.15	1.19	1.22	1.25	1.29
	25	1.11	1.14	1.19	1.22	1.27	1.30	1.32
	35	1.12	1.16	1.21	1.26	1.29	1.31	1.34
	45	1.15	1.20	1.23	1.28	1.31	1.35	1.38
	55	1.19	1.22	1.27	1.30	1.35	1.39	1.42
[L ¹ ₃ NdCl ₃](2.1b)	15	2.70	2.72	2.74	2.79	2.83	2.84	2.86
	25	2.77	2.78	2.85	2.88	2.90	2.93	2.94
	35	2.89	2.91	2.95	2.99	3.02	3.04	3.08
	45	3.03	3.07	3.13	3.16	3.18	3.21	3.23
	55	3.06	3.10	3.15	3.19	3.22	3.25	3.28
[L ¹ ₃ EuCl ₃ ·6H ₂ O](2.1c)	15	1.88	1.90	1.94	1.97	2.03	2.09	2.13
	25	2.30	2.34	2.38	2.43	2.48	2.52	2.58
	35	2.70	2.75	2.79	2.82	2.88	2.97	3.00
	45	2.80	2.84	2.90	2.96	3.01	3.05	3.12
	55	2.84	2.86	2.92	3.05	3.09	3.13	3.17
[L ¹ ₃ GdCl ₃ ·6H ₂ O](2.1d)	15	1.61	1.65	1.70	1.72	1.78	1.81	1.84
	25	2.02	2.09	2.15	2.18	2.20	2.24	2.30
	35	2.08	2.11	2.19	2.23	2.29	2.34	2.38
	45	2.10	2.14	2.20	2.27	2.32	2.37	2.41
	55	2.15	2.19	2.26	2.30	2.38	2.43	2.48

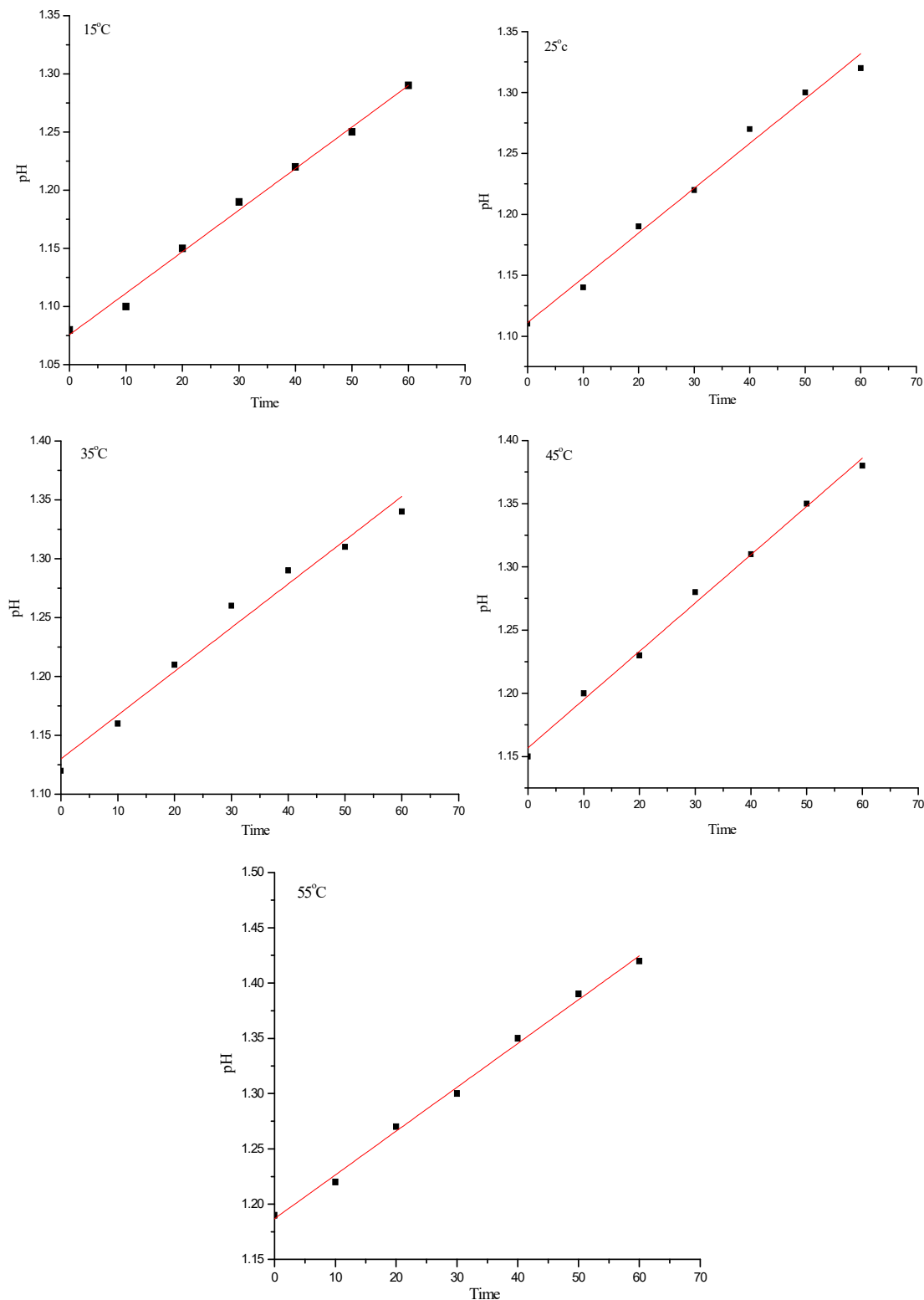
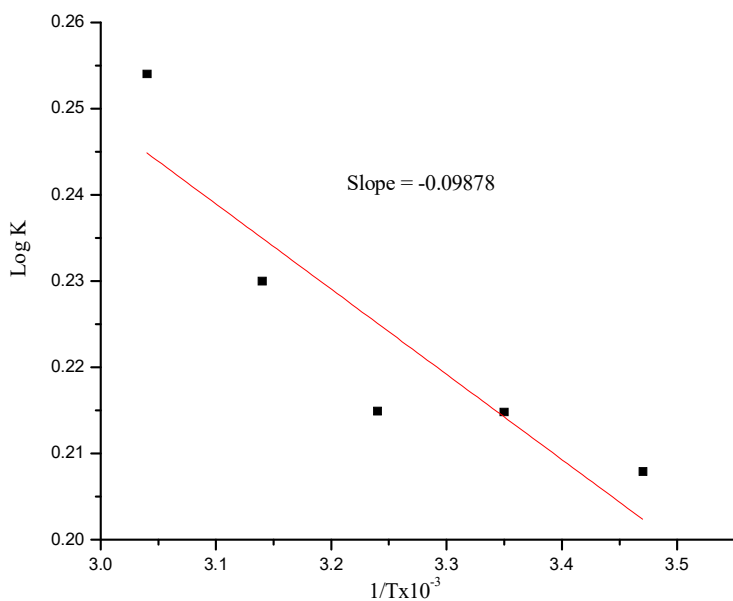


Figure 2.12. Plot of pH and Time (10 minutes) for the complexation of $[L_3PrCl_3]$ (2.1a) at different temperatures.

Table 2.7. Rate (k) at different temperature; i.e. 288K, 298K, 308K, 318K, and 328K and Activation energy (Ea) of $[L^1_3PrCl_3]$ (**2.1a**).

Temperature K	1/T K ⁻¹ x10 ⁻³	Rate (k) Mol L ⁻¹ Min ⁻¹	Rate (k) Mol L ⁻¹ S ⁻¹ x10 ⁻³	Log k	Activation Energy (Ea) (KJ)
288	3.47	0.09684	1.61400	0.20790	0.00189
298	3.35	0.09805	1.63400	0.21484	
308	3.24	0.09842	1.64033	0.21493	
318	3.14	0.10190	1.69850	0.23006	
328	3.24	0.1770	1.79500	0.25400	

**Figure 2.13.** Plot of log k versus $(1/T) \times 10^{-3}$ for the complexation of $[L^1_3PrCl_3]$ (**2.1a**) in EtOH.**Table 2.8.** Rate (k) and Thermodynamics parameter for the complexation of $[L^1_3PrCl_3]$ (**2.1a**) at different temperature.

Temperature (K)	Rate (k) MolL ⁻¹ S ⁻¹ x10 ⁻³	ΔH° (kJmol ⁻¹)	ΔS° (JK ⁻¹ mol ⁻¹)	ΔG° (kJmol ⁻¹)
288	1.61400	0.00189	0.00398	-1.14703
298	1.63400		0.00411	-1.22646
308	1.64033		0.00412	-1.26812
318	1.69850		0.00455	-1.40144
328	1.79500		0.00486	-1.59591

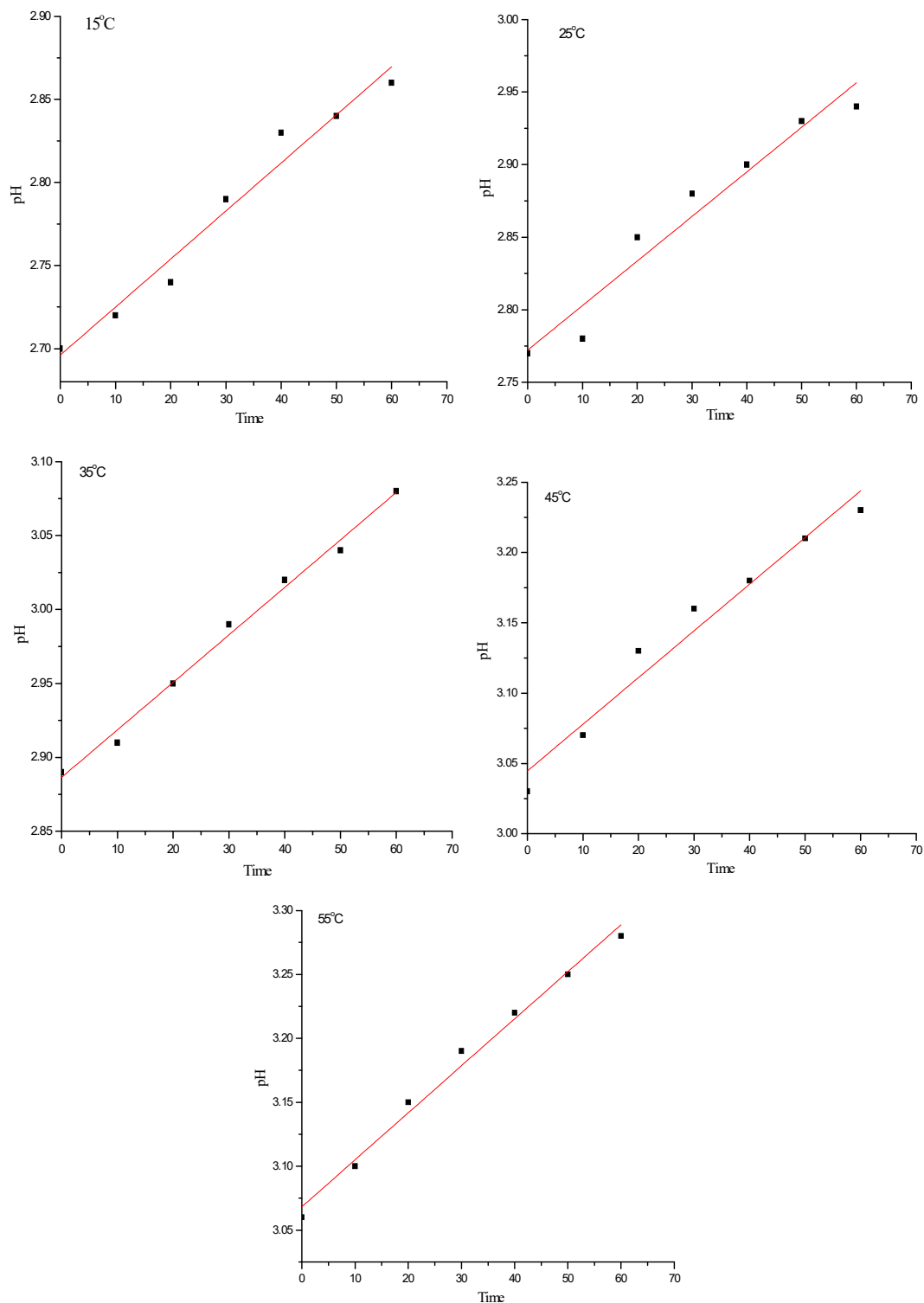
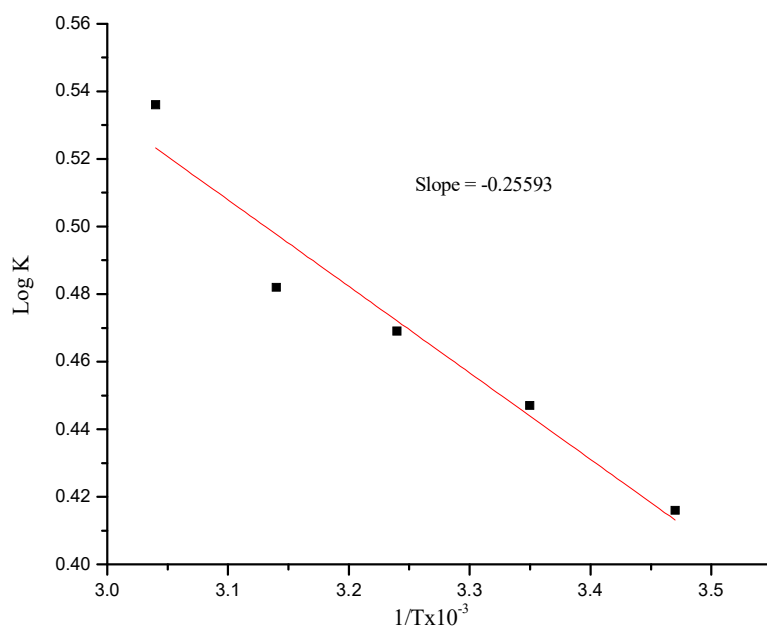


Figure 2.14. Plot of pH and Time (10 minutes) for the complexation of $[L^1_3NdCl_3]$ (2.1b) at different temperatures.

Table 2.9. Rate (k) at different temperature; i.e. 288K, 298K, 308K, 318K, and 328K and Activation energy (Ea) of $[L^1_3NdCl_3]$ (**2.1b**).

Temperature K	1/T $k^{-1} \times 10^{-3}$	Rate (k) $Mol\ L^{-1}\ Min^{-1}$	Rate (k) $Mol\ L^{-1}\ S^{-1} \times 10^{-3}$	Log k	Activation Energy (Ea) (KJ)
288	3.47	0.15645	2.60750	0.41622	0.00490
298	3.35	0.16804	2.80066	0.44725	
308	3.24	0.17669	2.94483	0.46901	
318	3.14	0.18221	3.03683	0.48241	
328	3.04	0.20638	3.43966	0.53647	

**Figure 2.15.** Plot of log k versus $(1/T) \times 10^{-3}$ for the complexation of $[L^1_3NdCl_3]$ (**2.1b**) in EtOH.**Table 2.10.** Rate (k) and Thermodynamics parameter for Complexation of $[L^1_3NdCl_3]$ (**2.1b**) at different temperature.

Temperature (K)	Rate (k) $Mol\ L^{-1}\ S^{-1} \times 10^{-3}$	ΔH° ($kJmol^{-1}$)	ΔS° ($JK^{-1}\ mol^{-1}$)	ΔG° ($kJmol^{-1}$)
288	2.60750	0.00490	0.00798	-2.29638
298	2.80066		0.00858	-2.55550
308	2.94483		0.00896	-2.76724
318	3.03683		0.00925	-2.93867
328	3.43966		0.01028	-3.37071

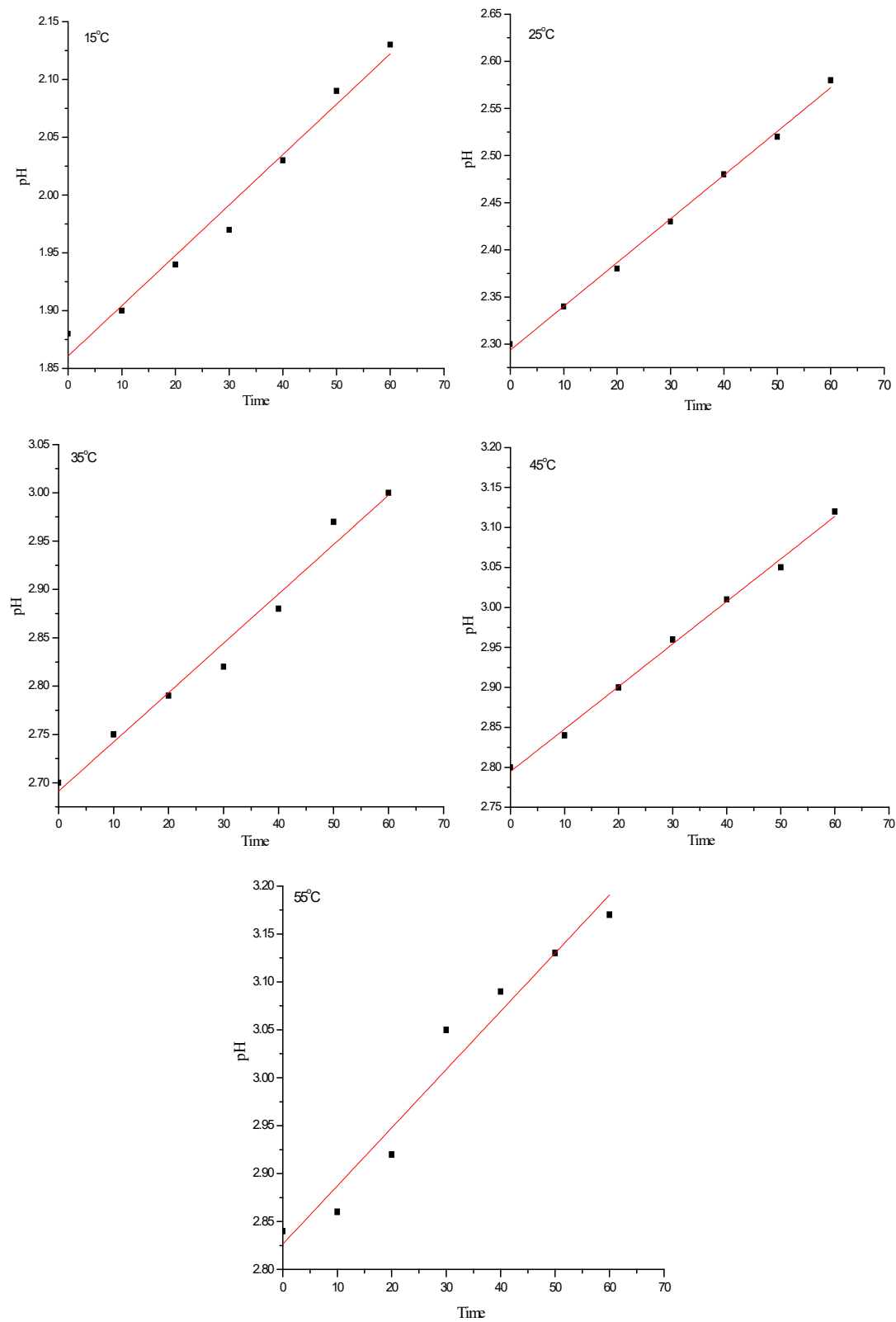


Figure 2.14. Plot of pH and Time (10 minutes) for the complexation of $[L^1_3EuCl_3 \cdot 6H_2O]$ (2.1c) at different temperatures.

Table 2.11. Rate (k) at different temperature; i.e. 288K, 298K, 308K, 318K, and 328K and Activation energy (Ea) of $[L^1_3EuCl_3 \cdot 6H_2O]$ (**2.1c**).

Temperature K	$1/T \text{ K}^{-1} \times 10^{-3}$	Rate (k) $\text{Mol L}^{-1} \text{ Min}^{-1}$	Rate (k) $\text{Mol L}^{-1} \text{ S}^{-1} \times 10^{-3}$	Log k	Activation Energy (Ea) (KJ)
288	3.47	0.25102	4.18366	0.62155	0.00685
298	3.35	0.28188	4.69800	0.67193	
308	3.24	0.31559	5.25983	0.72097	
318	3.14	0.32608	5.43466	0.73517	
328	3.04	0.36206	6.03433	0.78062	

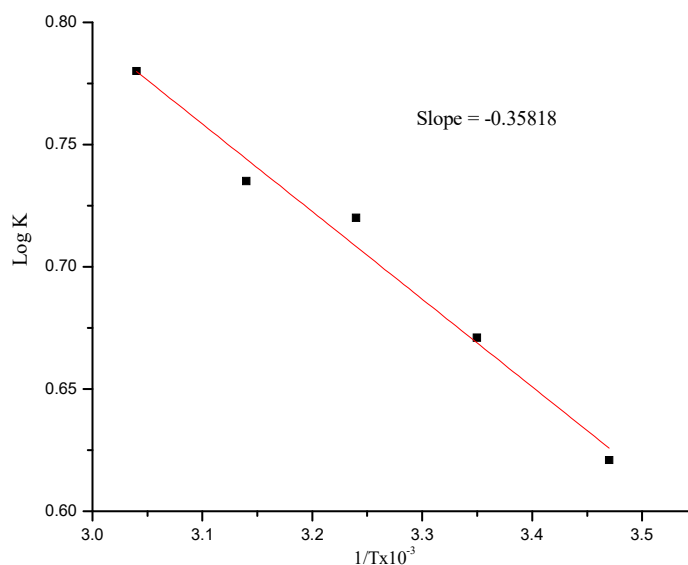


Figure 2.15. Plot of log k versus $(1/T) \times 10^{-3}$ for the complexation of $[L^1_3EuCl_3 \cdot 6H_2O]$ (**2.1c**) in EtOH.

Table 2.12. Rate (k) and Thermodynamics parameter for the complexation of $[L^1_3EuCl_3 \cdot 6H_2O]$ (**2.1c**) at different temperature.

Temperature (K)	Rate (k) $\text{Mol L}^{-1} \text{ S}^{-1} \times 10^{-3}$	ΔH° (kJ mol^{-1})	ΔS° ($\text{JK}^{-1} \text{ mol}^{-1}$)	ΔG° (kJ mol^{-1})
288	4.18366	0.00685	0.01192	-3.42897
298	4.69800		0.01288	-3.83568
308	5.25983		0.01382	-4.25344
318	5.43466		0.01409	-4.47798
328	6.03433		0.01496	-4.90461

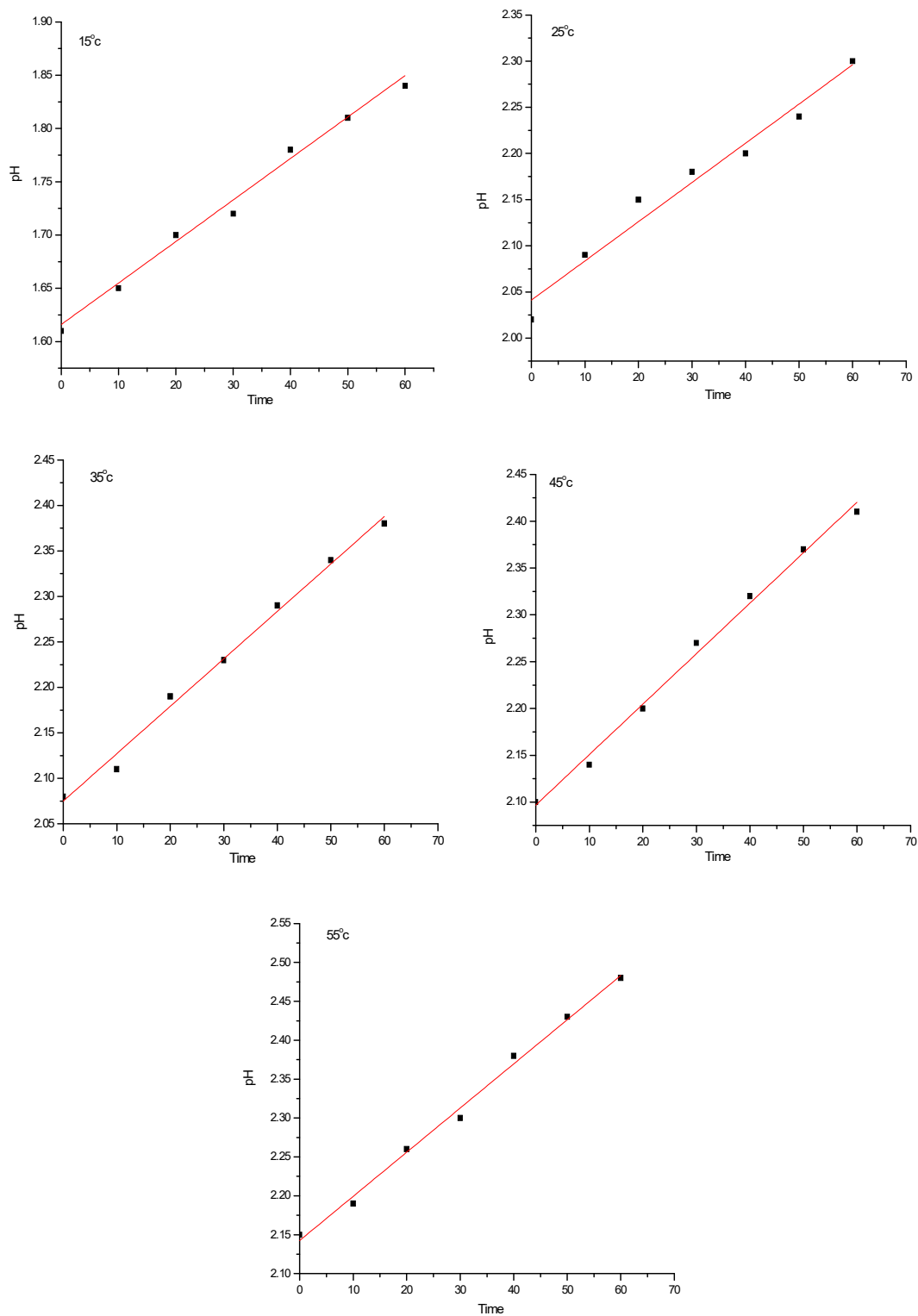
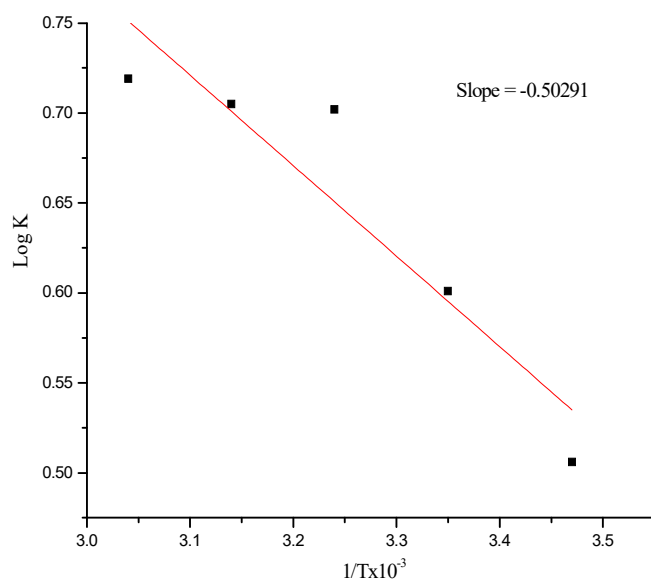


Figure 2.18. Plot of pH and time (10 minutes) for the complexation of $[L_3GdCl_3 \cdot 6H_2O]$ (2.1d) at different temperatures.

Table 2.13. Rate (k) at different Temperature; i.e. 288K, 298K, 308K, 318K, and 328K and Activation energy (Ea) of $[L^1_3GdCl_3 \cdot 6H_2O]$ (**2.1d**).

Temperature K	1/T $k^{-1} \times 10^{-3}$	Rate (k) $Mol\ L^{-1}\ Min^{-1}$	Rate (k) $Mol\ L^{-1}\ S^{-1} \times 10^{-3}$	Log k	Activation Energy (Ea) (KJ)
288	3.47	0.19247	3.20783	0.50621	0.00962
298	3.35	0.23937	3.98950	0.60091	
308	3.24	0.30270	5.04500	0.70286	
318	3.14	0.30439	5.07316	0.70527	
328	3.04	0.31425	5.23750	0.71912	

**Figure 2.19.** Plot of log k versus $(1/T) \times 10^{-3}$ for the complexation of $[L^1_3GdCl_3 \cdot 6H_2O]$ (**2.1d**) in EtOH.**Table 2.14.** Rate (k) and Thermodynamics parameter for the complexation of $[L^1_3GdCl_3] \cdot 6H_2O$ (**2.1d**) at different temperature.

Temperature (K)	Rate (k) $Mol\ L^{-1}\ S^{-1} \times 10^{-3}$	ΔH° ($kJmol^{-1}$)	ΔS° ($JK^{-1}mol^{-1}$)	ΔG° ($kJmol^{-1}$)
288	3.20783	0.00962	0.00972	-2.79288
298	3.98950		0.01154	-3.43385
308	5.04500		0.01348	-4.14700
318	5.07316		0.01353	-4.29626
328	5.23750		0.01379	-4.51832

2.4. Conclusion

In conclusion, we report the novel microwave-assisted fast and efficient green synthesis of curcumin lanthanide complexes (**2.1a-d**). All the synthesized curcumin lanthanide complexes were well investigated for their various spectroscopic studies. In IR spectra of all complexes, there is a chelate band shift in complexes comparing with that of free curcumin ligand which reveals the possibility of the formation of complex. The UV-Vis absorption spectra of the complexes increased to higher intensity with the increase in the polarity of the solvents in all the curcumin lanthanide complexes. Interestingly, the fluorescence spectroscopic studies were found that there is a quenching in curcumin lanthanide complexes (**2.1a-d**) intensity comparing with that of free curcumin ligand (**L¹**). The negligibly low value of activation energy (E_a) signified that the reactions involved are fast ones. The negative value of the Gibbs free energy change (ΔG°) indicated that the reaction is spontaneous and also favorable one. Positive values of Enthalpy change (ΔH°) shows the complexation is endothermic one and the entropy change (ΔS°) value shows the reaction is entropy driven.

2.5. References

1. Vogel and E. Pelletier, Curcumin-Biological and Medicinal Properties, *J. Pharm.* 1815, **2**, 50-54.
2. L. Baum and A. Ng, Curcumin interaction with copper and iron suggests one possible mechanism of action in Alzheimer's disease animal models, *J. Alzheimer's Dis.* 2004, **6(4)**, 367-377.
<https://content.iospress.com/articles/journal-of-alzheimers-disease/jad00330>
3. S. C. Gupta, S. Patchva, W. Koh and B. B. Aggarwal, Discovery of Curcumin, a Component of the Golden Spice, and Its Miraculous Biological Activities, *Clin. Exp. Pharmacol. Physiol.*, 2012, **39(3)**, 283-299.
<https://doi.org/10.1111/j.1440-1681.2011.05648.x>
4. (a) P. Anand, C. Sundaram, S. Jhurani, A. B. Kunnumakkara and B. B. Aggarwal, Curcumin and cancer: An "old-age" disease with an "ageold" solution, *Cancer Lett.* 2008, **267(1)**, 133-164. <https://doi.org/10.1016/j.canlet.2008.03.025>
(b) A. Goel and B. B. Aggarwal, Curcumin, the Golden Spice from Indian saffron, is a Chemosensitizer and Radiosensitizer for Tumors and Chemoprotector and Radioprotector for Normal Organs, *Nutr. Cancer.*, 2010, **62(7)**, 919-930.
<https://doi.org/10.1080/01635581.2010.509835>
(c) K. M. Dhandapani, V. B. Mahesh and D. W. Brann, Curcumin suppresses growth and Chemoresistance of Human Glioblastoma Cells via AP-1 and NFkappaB Transcription Factors, *J. Neuroche.*, 2007, **102(2)**, 522-538.
<https://doi.org/10.1111/j.1471-4159.2007.04633.x>
(d) M. Li, Z. Zhang, D. L. Hill, H. Wang and R. Zhang, Curcumin, a Dietary Component, has Anticancer, Chemosensitization, and Radiosensitization effects by Down-regulating the MDM2 Oncogene through the PI3K/mTOR/ETS2 Pathway, *Cancer Res.* 2007, **67(5)**, 1988-1996.
<https://cancerres.aacrjournals.org/content/67/5/1988>
(e) P. Javvadi, A. T. Segan, S. W. Tuttle and C. Koumenis, The Chemopreventive Agent Curcumin is a Potent Radiosensitizer of Human Cervical Tumor cells via increased Reactive Oxygen Species Production and Overactivation of the Mitogen-Activated Protein Kinase Pathway, *Mol. Pharmacol.*, 2008, **73(5)**, 1491-1501.
<https://molpharm.aspetjournals.org/content/73/5/1491.short>

- (f) A. Khafif, R. Hurst, K. Kyker, D. M. Fliss, Z. Gil and J. E. Medina, Curcumin: A New Radiosensitizer of Squamous Cell Carcinoma Cells, *Otolaryngol. Head Neck Surg.*, 2005, **132**(2), 317-321.
<https://journals.sagepub.com/doi/abs/10.1016/j.otohns.2004.09.006>
- (g) B. B. Patel, R. Sengupta, S. Qazi, H. Vachhani, Y. Yu, A. K. Rishi and A. P. Majumdar, Curcumin Enhances the Effects of 5-fluorouracil and Oxaliplatin in Mediating Growth Inhibition of Colon Cancer Cells by Modulating EGFR and IGF-1R, *Int. J. Cancer.*, 2008, **122**(2), 267-273.
<https://onlinelibrary.wiley.com/doi/abs/10.1002/ijc.23097>
5. (a) M. M. Yallapu, M. Jaggi and S. C. Chauhan, Curcumin Nano formulations: A Future Nanomedicine for Cancer *Drug Discov. Today*, 2012, **17**, 71-80.
<https://www.sciencedirect.com/science/article/pii/S1359644611002996>
- (b) M. H. Teiten, S. Eifes, M. Dicato and M. Diederich, Curcumin—The Paradigm of a Multi-Target Natural Compound with Applications in Cancer Prevention and Treatment *Toxins*, 2010, **2**, 128-162.
https://res.mdpi.com/d_attachment/toxins/toxins-02-00128/article_deploy/toxins-02-00128.pdf
- (c) B. B. Aggarwal, A. Kumar and A. C. Bharti, Anticancer Potential of Curcumin: Preclinical and Clinical Studies, *Anticancer Res.*, 2003, **23**, 363-393.
<https://pubmed.ncbi.nlm.nih.gov/12680238/>
- (d) A. Goel, A. B. Kunnumakkara and B. B. Aggarwal, Curcumin as "Curecumin": from Kitchen to Clinic, *Biochem. Pharmacol.*, 2008, **75**, 787-809.
<https://pubmed.ncbi.nlm.nih.gov/17900536/>
- (e) G. Sa and T. Das, Anti Cancer Effects of Curcumin: Cycle of Life and Death, *Cell Div.*, 2008, **3**, 1-14. <https://pubmed.ncbi.nlm.nih.gov/18834508/>
- (f) A. Shehzad, F. Wahid and Y. S. Lee, Curcumin in Cancer Chemoprevention: Molecular Targets, Pharmacokinetics, Bioavailability, and Clinical Trials, *Arch. Pharm. Chem. Life Sci.*, 2010, **343**, 489-499. <https://pubmed.ncbi.nlm.nih.gov/20726007/>
- (g) F. Yang, P. L. G. P. Lim, A. N. Begum, O. J. Ubeda, M. R. Simmons, S. S. Ambegaokar, P. Chen, R. Kaye, C. G. Glabe, S. A. Frautschy and G. M. Cole, Curcumin Inhibits Formation of Amyloid beta Oligomers and Fibrils, Binds Plaques, and Reduces Amyloid in vivo, *J. Biol. Chem.*, 2005, **280**, 5892-5901.
<https://pubmed.ncbi.nlm.nih.gov/15590663/>

- (h) M. G. Alloza, L. A. Borrelli, A. Rozkalne, B. T. Hyman and B. J. Bacscai, Curcumin Labels Amyloid Pathology *in vivo*, Disrupts Existing Plaques and Partially Restores Distorted Neurites in an Alzheimer mouse model, *J. Neurochem.*, 2007, **102**, 1095-1104. <https://onlinelibrary.wiley.com/doi/abs/10.1111/j.1471-4159.2007.04613.x>
- (i) N. Dhillon, B. B. Aggarwal, R. A. Newman, R. A. Wolff, A. B. Kunnumakkara, J. L. Abbruzzese, C. S. Ng, V. Badmaev and R. Kurzrock, Phase II trial of Curcumin in Patients with Advanced Pancreatic Cancer, *Clin. Cancer Res.*, 2008, **14**, 4491-4499. <https://pubmed.ncbi.nlm.nih.gov/18628464/>
- (j) R. A. Sharma, S. A. Euden, S. L. Platton, D. N. Cooke, A. Shafayat, H. R. Hewitt, T. H. Marczylo, B. Morgan, D. Hemingway, S. M. Plummer, M. Pirmohamed, A. J. Gescher and W. P. Steward, Phase I Clinical Trial of Oral Curcumin: Biomarkers of Systemic Activity and Compliance, *Clin. Cancer Res.*, 2004, **10**, 6847- 6854. <https://pubmed.ncbi.nlm.nih.gov/15501961/>
- (k) C. H. Hsu and A. L. Cheng, Clinical Studies with Curcumin, *Adv. Exp. Med. Biol.*, 2007, **595**, 471-480. https://link.springer.com/chapter/10.1007%2F978-0-387-46401-5_21
6. L. Shen and H. F. Ji, The Pharmacology of Curcumin: Is It the Degradation Products? *Trends Mol. Med.*, 2012, **18**, 138-144. <https://www.sciencedirect.com/science/article/pii/S147149141200007X>
7. (a) P. Jeyaraman, A. Alagarraj and R. Natarajan, In silico and in vitro Studies of Transition Metal Complexes Derived from Curcumin-isoniazid Schiff base, *J. Biomol. Struct. Dyn.*, 2019, **15**, 1-15. <https://cogentoa.tandfonline.com/doi/full/10.1080/07391102.2019.1581090>
- (b) S. Borowska, M. M. Brzoska and M. Tomczyk, Complexation of Bioelements and Toxic Metals by Polyphenolic Compounds-Implications for Health, *Curr Drug Targets.*, 2018, **19(14)**, 1612-1638. <https://pubmed.ncbi.nlm.nih.gov/29611487/>
- (c) F. S. Yan, J. L. Sun, W. H. Xie, L. Shen and H. F. Ji, Neuroprotective Effects and Mechanisms of Curcumin-Cu(II) and Zn(II) Complexes Systems and Their Pharmacological Implications, *Nutrients.*, 2017, **10(1)**, 2-11. <https://pubmed.ncbi.nlm.nih.gov/29283372/>
- (d) U. Bhattacharyya, B. Kumar, A. Garai, A. Bhattacharyya, A. Kumar, S. Banerjee, P. Kondaiah and A. R. Chakravarty, Curcumin "Drug" Stabilized in Oxidovanadium (IV)-

- BODIPY Conjugates for Mitochondria-Targeted Photocytotoxicity, *Inorg Chem.* 2017, **56**(20), 12457-12468. <https://pubs.acs.org/doi/abs/10.1021/acs.inorgchem.7b01924>
- (e) R. Sareen, N. Jain and K. L. Dhar, Curcumin-Zn(II) complex for Enhanced Solubility and Stability: an Approach for Improved Delivery and Pharmacodynamic Effects, *Pharm Dev Technol.*, 2016, **21**(5), 630-635.
<https://www.tandfonline.com/doi/abs/10.3109/10837450.2015.1041042>
- (f) S. Banerjee and A. R. Chakravarty, Metal complexes of curcumin for cellular imaging, targeting, and photoinduced anticancer activity, *Acc. Chem. Res.*, 2015, **48** (7), 2075-2083. <https://pubs.acs.org/doi/abs/10.1021/acs.accounts.5b00127>
- (g) A. Hussain, K. Somyajit, B. Banik, S. Banerjee, G. Nagaraju and A. R. Chakravarty, Enhancing the Photocytotoxic Potential of Curcumin on Terpyridyl Lanthanide (III) complex Formation, *Dalton Trans.*, 2013, **42**(1), 182-195.
<https://pubs.rsc.org/en/content/articlehtml/2013/dt/c2dt32042h>
8. (a) H. J. Roth and B. Miller, To know the Color Reaction Between Boric Acid and Curcumin. I. Boric Acid-curcumin Complexes, *Arch. Pharm.*, 1964, **297**, 660-673.
<https://doi.org/10.1002/ardp.19642971007>
- (b) Z. Sui, R. Salto, J. Li, C. Craik and P. R. Ortiz de Montellano, Inhibition of the HIV-1 and HIV-2 Proteases by Curcumin and Curcumin Boron Complexes, *Bioorg. Med. Chem.*, 1993, **1**, 415-422.
<https://www.sciencedirect.com/science/article/pii/S0968089600821525>
9. (a) Y. Mawani and C. Orvig, Improved Separation of the Curcuminoids, Syntheses of their Rare Earth Complexes, and Studies of Potential Antiosteoporotic Activity, *J. Inorg. Biochem.*, 2014, **132**, 52-58. <https://pubmed.ncbi.nlm.nih.gov/24387940/>
- (b) Y. M. Song, J. P. Xu, L. Ding, Q. Hou, J. W. Liu and Z. L. Zhu, Syntheses, Characterization and Biological Activities of Rare Earth Metal Complexes with Curcumin and 1,10-phenanthroline-5,6-dione, *J. Inorg. Biochem.*, 2009, **103**, 396-400.
<https://www.ncbi.nlm.nih.gov/pubmed/19135257>
- (c) M. A. Subhan, K. Alam, M. S. Rahaman, M. A. Rahman and M. R. Awal, Synthesis and Characterization of Metal Complexes Containing Curcumin (C₂₁ H₂₀ O₆) and Study of their Anti-microbial Activities and DNA Binding Properties *J. Sci. Res.*, 2014, **6**, 97-109. <http://dx.doi.org/10.3329/jsr.v6i1.15381>

- (d) S. S. Zhou, X. Xue, J. F. Wang, Y. Dong, B. Jiang, D. Wei, M. L. Wan and Y. Jia, Synthesis, Optical Properties and Biological Imaging of the Rare Earth Complexes with Curcumin and Pyridine, *J. Mater. Chem.*, 2012, **22**, 22774-22780.
<https://pubs.rsc.org/en/content/articlehtml/2012/jm/c2jm34117d>
- (e) A. Hussain, K. Somyajit, B. Banik, S. Banerjee, G. Nagaju and A. R. Chakravarty, Enhancing the Photocytotoxic Potential of Curcumin on Terpyridyl Lanthanide(III) complex Formation, *Dalton Trans.*, 2013, **42**, 182–195. <https://doi.org/10.1039/C2DT32042H>
10. S. Wanninger, V. Lorenz, A. Subhan and F. T. Edlmann, Metal Complexes of Curcumin-Synthetic Strategies, Structure and Medicinal Application, *Chem. Soc. Rev.*, 2015, **44**, 4986. <https://doi.org/10.1039/C5CS00088B>
11. B. Dinesh and R. Saraswathi, Electrochemical Synthesis of Nanostructured Copper-Curcumin Complex and its Electrocatalytic Application towards Reduction of 4-Nitrophenol, *Sens. Actuators B Chem.*, 2017, **253**, 502-512.
<https://doi.org/10.1016/j.snb.2017.06.149>
12. N. Bicer, E. Yildiza, A. A. Yegani and F. Aksu, Synthesis of Curcumin Complexes with Iron(III) and Manganese(II) and Curcumin-iron(III) effects on Alzheimer's Disease, *New J. Chem.*, 2018, **42**, 8098-8104. <https://doi.org/10.1039/C7NJ04223J>
13. D. Musib, M. Pal, M. K. Raza, and M. Roy, Photo-physical, Theoretical and Photo-Cytotoxic Evaluation of a New Class of Lanthanide (III)–curcumin/diketone complexes for PDT Application, *Dalton Trans.*, 2020, **49**, 10786-10798.
<https://doi.org/10.1039/D0DT02082F>
14. S. Prasad, D. D. Bourdieu, A. Srivastava, P. Kumar and R. Lall, Metal–Curcumin Complexes in Therapeutics: An Approach to Enhance Pharmacological Effects of Curcumin, *Int. J. Mol. Sci.*, 2021, **22(13)**, 1-24. <https://doi.org/10.3390/ijms22137094>
15. <https://www.britannica.com/science/activation-energy>
16. <https://www.chem.fsu.edu/chemlab/chm1046course/activation.html>
17. <https://www.thoughtco.com/arrhenius-equation-4138629>
18. <https://www.priyamstudycentre.com/2019/09/vant-hoff-equation.htm>

Synthesis of Curcumin-thiosemicarbazone Lanthanide (Pr^{3+} , Nd^{3+} , Eu^{3+} and Gd^{3+}) Complexes and Investigation of their Spectroscopic and Kinetic Studies

Abstract

In this chapter, we report the synthesis of curcumin-thiosemicarbazone lanthanide complexes from curcumin-thiosemicarbazone ligand (L^2) and lanthanide chlorides ($\text{LnCl}_3 \cdot x\text{H}_2\text{O}$; where; $\text{Ln} = \text{Pr}^{3+}$, Nd^{3+} , Eu^{3+} and Gd^{3+}) in presence of triethylamine (Et_3N) in ethanol reflux for 24 hours and investigated their spectroscopic and kinetic studies. The spectroscopic and physic-chemical properties of the curcumin-thiosemicarbazone ligand (L^2) and its lanthanide(III) complexes $[\text{L}^2_3\text{PrCl}_3]$ (**3.1a**), $[\text{L}^2_3\text{NdCl}_3]$ (**3.1b**), $[\text{L}^2_3\text{EuCl}_3]$ (**3.1c**), $[\text{L}^2_3\text{GdCl}_3]$ (**3.1d**) were studied by various methods of IR, UV-Vis, Fluorescence, TGA-DTA and elemental analysis. The FT-IR spectra of curcumin-thiosemicarbazone lanthanide complexes were well interpreted based on the comparison of free curcumin ligand spectrum which confirms the formation of complexes (**3.1a-d**).

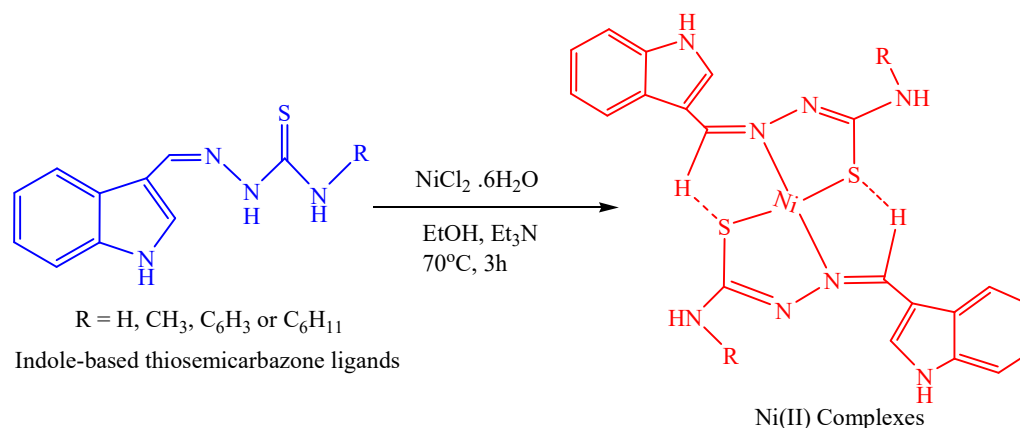
3.1. Introduction

Thiosemicarbazone is an organic compound that embrace sulfur in it and consist N, S-donor as a ligand. They are commonly synthesized by condensing thiosemicarbazide alone with aldehydes and ketones. Investigation of this compound has been done for the last few decades individually or with organic as well as inorganic compound or with metal as metal complexes and discovered to possess a variety of biological activities together with the application of treatment of numerous diseases. Regarding to the applications, first reported in 1950s for the treatment of leprosy and tuberculosis and also further studies shows their multiple applications as drug, anti-cancer, anti-tumor activities.¹⁻⁴ Chemistry, Pharmacology, and Biology are granting much interest towards thiosemicarbazone and its derivatives as they possessed a diverse activities toward many diseases and not only that they have several other applications.⁵ Thiosemicarbazone coordinate with metallic cation as a chelating ligand to give complexes which are broadly utilized by medicinal chemistry for the development of drug and bioactive materials.⁶

Apart from the applications in medicinal chemistry, thiosemicarbazone are acquiring multiple attentions because of its liability to change the bonding mode, structural variance, and ion-sensing potentiality.⁷⁻⁹ Their applications were also found in analytical chemistry

and industries.¹⁰ Due to flexibility as ligand with regard to metal ions they are titled as superior coordination liability, constancy and finer selectivity and with its photoluminescence properties they were utilized for tracking of drug in cancer cell.¹¹ Looking on to its numerous potentiality some of lately synthesized and application of thiosemicarbazone metal complexes were reviewed.

With the opportunities put forwarded by bioinorganic chemistry towards thiosemicarbazone transition metal complexes, J. Haribabu *et.al.* **2017** synthesized Ni(II) complexes of thiosemicarbazone ligand (**Scheme 3.1**) and examine some of its potentiality biologically. X-ray crystallographies of the complexes shows square planar geometry and were found to have significant binding affinity toward the targeted protein, together with it they were found to have anti-oxidant activity and cytotoxicity activity against human lung and breast cancer cell line.¹²



Scheme 3.1. Schematic Synthesis of Ni(II) complexes.

The advances in mining and industries cause heavy metal ions pollution which is becoming hazardous to human health as well as other living organisms because of its high toxicity. Over viewing these disadvantage of the heavy metals, S. S. Panja and group in **2018** has developed and reported a multi-approachable thiosemicarbazone-based chemo sensor for the recognition and exposure of 12 metal ions. The metal-ligand complexes were found to have a potential probe and along with it they were found to be a good detector for the metal ions individually or as a group.¹³ As the coordination chemistry of manganese ions are becoming an interest because of its biological activity and catalytic potentiality. M. K. Bharty and co-worker in **2019** work on the synthesis of Mn(III) complexes using 4-phenyl (phenyl-acetyl)-3-thiosemicarbazide (**Figure 3.1**) and 4-amino-

5-phenyl-1,2,4-triazole-3-thiolate and further studied their potentiality towards electrochemical oxygen reductions. X-ray crystallography shows an octahedral geometry along with it the crystal structures were found stabilized by the inter-molecular and intra-molecular interaction by hydrogen bonding. As electrocatalyst with affordable and systematic methods, the complexes may be utilized as an oxygen reduction in fuel cells, batteries and electrolytes.¹⁴

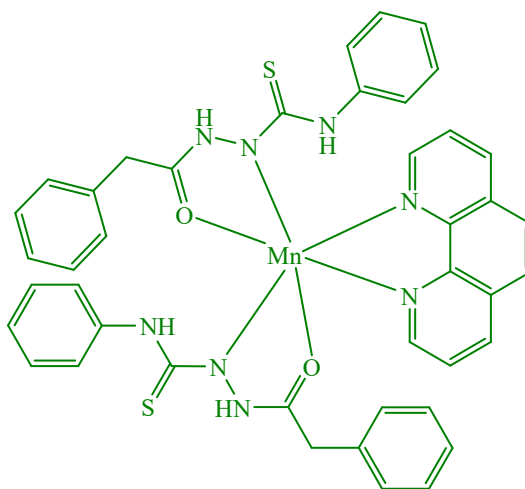


Figure 3.1. Structure of 4-phenyl (phenyl-acetyl)-3-thiosemicarbazide Mn(III) complexes.

Similar studies on the possible usage of the thiosemicarbazone metal complexes for electrocatalyst along with the applications as energy storage devices and electro-sensor were reported by B. Kaya *et al.* (2020) and found that the synthesized complexes as proposed shows the potentiality towards the electrochemical technology.¹⁵ As pointed out before thiosemicarbazone metal complexes at present are gaining lots of attention due to its nitrogen and sulphur donor ligand capability of cytotoxicity activity which increases on coordinating with metal ions such as the copper and nickel. Considering the potentiality D. Sarker and co-workers in 2020 synthesized and characterized metal complexes of thiosemicarbazone and put-forward a possible structure confirm by elemental analysis and mass spectroscopy as shown in **Figure 3.2** along with its investigation of its antibacterial activity shows an average activity.¹⁶

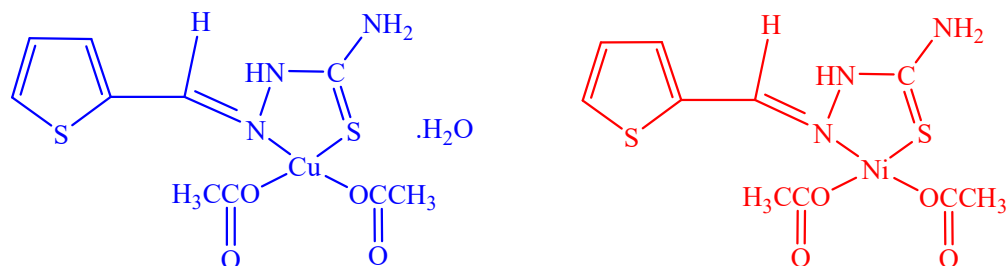
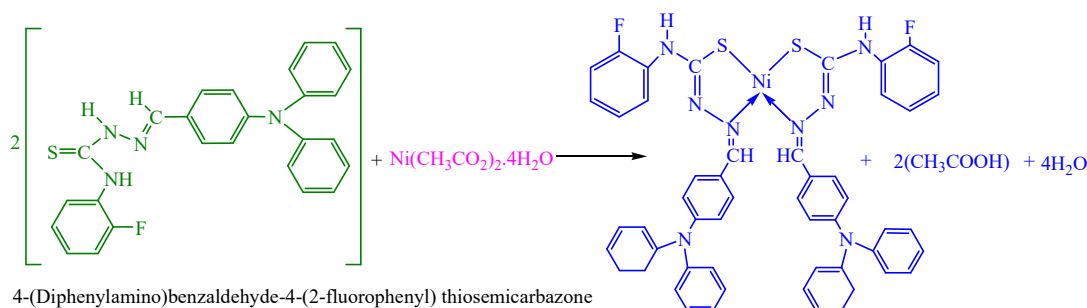


Figure 3.2. Proposed Structures of Synthesized Thiosemicarbazone Metal Complexes.

U. M. Osman *et al.* (2021) using a conventional methods synthesized a Ni(II) complex with thiosemicarbazone as ligand (**Scheme 3.2**). The synthesized complex was identified by different spectroscopic methods. Single crystal X-ray of the crystallized complex shows disfigured square planner geometry together with the coordination of the metal to nitrogen and sulphur site of the donor ligand.¹⁷



Scheme 3.2. Chemical equation for the Synthesis of Thiosemicarbazone Ni(II) Complex.

S. Savir *et al.* (2021) synthesized a series of Ni(II) complexes with oxygen, nitrogen and sulfur tridentate thiosemicarbazone and polyhydroxybenzaldehyde and characterized by various spectroscopic methods. The complexes were found to be square planar geometry and they were found to have cytotoxic activity. The interaction of the complexes with the DNA were confirmed through molecular docking studies.¹⁸ With the increase of the heavy metal contaminations, Y. Yue and group recently (2021) have synthesized a new mobile, high-precision and recyclable hydrogel sensor for the detection of Cu^{2+} ions in environment which was further coordinated with thiosemicarbazone complexes and found to give an excellent hydrogel. The complex hydrogel was discovered to be reversible from liquid state at high temperature to solid state on cooling. The complexes were also found to possess anti-bacterial activity.¹⁹

Other than the mentioned importance and application of thiosemicarbazone complexes, they were found to be utilized for anti-cancer, anti-tumor, anti-oxidant, hemolytic, bio-molecular interaction, drug for prediction of activity spectra of substance analysis and cross-coupling catalytic reaction.²⁰⁻²⁵ In viewing the potentiality of thiosemicarbazone complexes have lead us to synthesize novel lanthanide complexes of curcumin-thiosemicarbazone and characterized its spectroscopic, physico-chemical and kinetics studies.

3.2. Experimental

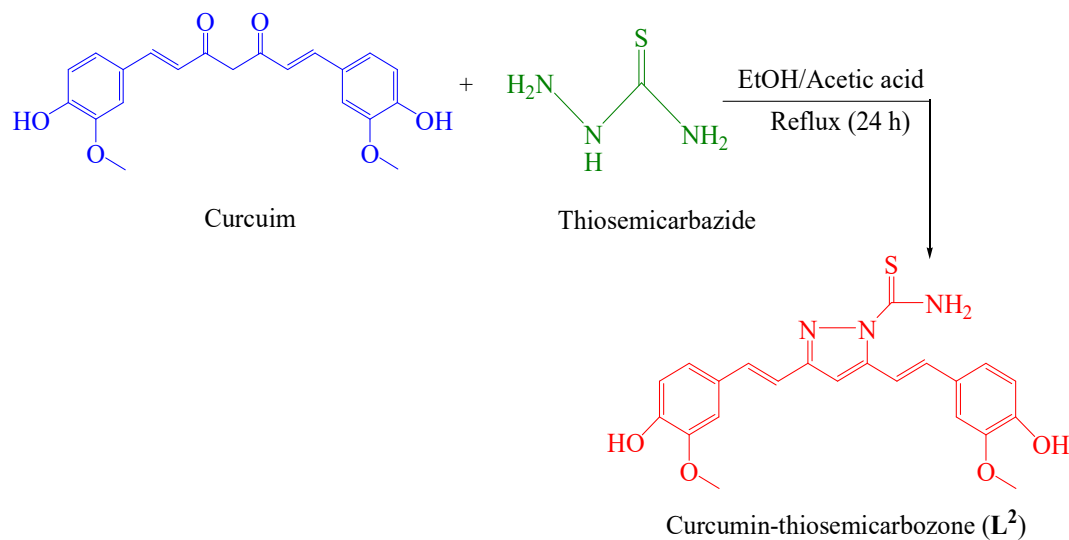
3.2.1. Materials and Methods

All the reagents and solvents were purchased from commercially available sources and used without further purification. Melting points were recorded in open capillaries using IKON melting point apparatus and are uncorrected. FTIR spectra of the curcumin-thiosemicarbazone ligand (L^2) and its lanthanide complexes (**3.1a-d**) were recorded on Perkin-Elmer spectrophotometer (Spectrum-Two) using KBr disk and values are expressed in cm^{-1} . Micro analytical (CHN) data were obtained with a FLASH EA 1112 Series CHNS analyzer. UV-visible spectrophotometer (Double Beam) Perkin Elmer, Lambda-35 is used for recording the absorption bands of the curcumin-thiosemicarbazone ligand and its lanthanide complexes. All fluorescence emission spectra of curcumin-thiosemicarbazone ligand and its lanthanide complexes were recorded using fluorescence spectrophotometer Shimadzu RF- 6000 which is followed by the evaluation of their quantum yields. pH values of the reactions were recorded using EUTECH instrument pH 700. The TGA-DTA measurements of curcumin-thiosemicarbazone ligand and its lanthanide complexes were performed on a Perkin-Elmer analyzer in air over the temperature range of 25-900°C.

3.2.2. Synthesis of Curcumin-thiosemicarbazone Ligand (L^2)

Solution of curcumin [1, 7- bis(4- hydroxyl-3-methoxyphenyl)-1, 6- heptadiene-3, 5-dione] (1mmol, 0.368g) in ethanol medium was kept with continuous stirring in a magnetic stirrer. Then, to it was added (3 mmol, 0.264g) of thiosemicarbazide and catalytic amount of acetic acid. The reaction mixture was bright orange with some insoluble solid residue which completely gets dissolved in the solvent after an hour of refluxing. After keeping the reaction for about two and a half hours, precipitate started to be formed. The resulting mixture was kept under reflux condition for 24 hours. On evaporation of the

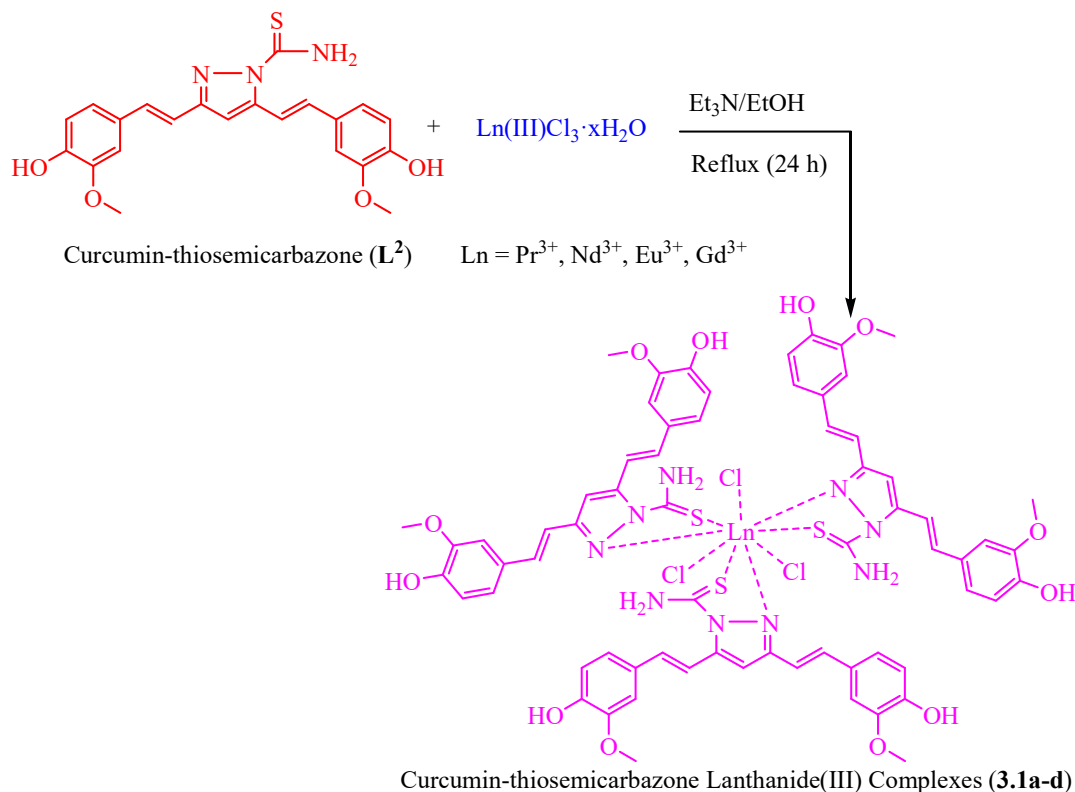
solvent, it gives a pale yellow compound; it was added ice cold water converting to a solid which was collected through filtration and air dried after washing several times with water (**Scheme 3.3**).



Scheme 3.3. Synthesis of Curcumin-thiosemicarbazone Ligand (L^2).

3.2.3 General Synthesis of Curcumin-thiosemicarbazone Lanthanide Complexes [$L_3 LnCl_3$] (**3.1a-d**)

The complex of the lanthanide was prepared by taken curcumin thiosemicarbazone (3 mmol) in ethanol medium in a round bottom flask at 100°C to it was added $LnCl_3 \cdot xH_2O$; (where; $Ln = Pr^{3+}$, Nd^{3+} , Eu^{3+} and Gd^{3+}) (1 mmol). To the reaction mixture was added catalytic amount of triethylene amine (Et_3N) and was keep for refluxing for 24 hours. After which the reaction was allowed to evaporate the solvent completed on evaporation the reaction mixture form a yellow compound which was washed with hexane for several time and on washing with hexane the compound form a yellowish green which was collected trough filtration. The complexes [$L^2_3PrCl_3$] (**3.1a**), [$L^2_3NdCl_3$] (**3.1b**), [$L^2_3EuCl_3$] (**3.1c**), [$L^2_3GdCl_3$] (**3.1d**) were allowed to air dried and stored in a glass vial for further investigation (**Scheme 3.4**).



Scheme 3.4. Schematic synthesis of Curcumin-thiosemicarbazone Lanthanide Complexes (**3.1a-d**).

3.3. Results and Discussion

Herein, we report synthesis of curcumin-thiosemicarbazone lanthanide complexes (**3.1a-d**). The ligand curcumin-thiosemicarbazone (L^2) was prepared from a reaction of curcumin and thiosemicarbazide with a catalytic amount of CH_3COOH in ethanol and reflux for 24 hours. The Curcumin lanthanide metal complexes were then synthesized using curcumin-thiosemicarbazone ligand (L^2) and lanthanide metal chlorides ($LnCl_3 \cdot xH_2O$; $Ln = Pr^{3+}, Nd^{3+}, Eu^{3+}$ and Gd^{3+}) in 3:1 ratio in presence of catalytic amount of Et_3N in ethanol and reaction mixture was kept under reflux condition for 24 hours. The solvent was completely evaporated by removing the condenser after 24 hours of refluxing. The yielded solid, collected through filtration was washed with hexane for several times and is allowed to air dried and then collected. The synthesized solid curcumin-thiosemicarbazone lanthanide complexes (**3.1a-d**) were stable at room temperature, which were characterised for various spectroscopic properties. The resulting curcumin lanthanide complexes were well studied through FT-IR spectroscopy, UV-Visible spectroscopy, Fluorescence spectroscopy, TGA-DTA analysis and elemental analysis. The chemical

kinetics and thermodynamic parameters were evaluated by recording pH of the reactions at different temperature. The physico-analytical data of free curcumin-thiosemicarbazone ligand (L^2) and curcumin-thiosemicarbazone lanthanide complexes (**3.1a-d**) were represented in **Table 3.1**.

Table 3.1. Physico-analytical data of Curcumin-thiosemicarbazone ligand (L^1) and its Lanthanide complexes (**3.1a-d**).

Compounds	Yield (%)	Colour	CHN Analysis (%) Found(calculated)			
			Carbon	Hydrogen	Nitrogen	Sulphur
Curcumin-thiosemicarbazone (L^2)	-	Pale yellow	62.34 (62.40)	5.06 (5.00)	9.98 (9.92)	7.51 (7.57)
[$L^2_3PrCl_3$] (3.1a)	98.00	Yellowish green	52.41 (52.33)	3.94 (3.99)	8.27 (8.32)	6.41 (6.35)
[$L^2_3NdCl_3$] (3.1b)	97.67	Yellowish green	52.31 (52.22)	3.94 (3.98)	8.36 (8.30)	6.41 (6.34)
[$L^2_3EuCl_3$] (3.1c)	98.45	Brown	51.85 (51.96)	3.92 (3.96)	8.21 (8.26)	6.35 (6.30)
[$L^2_3GdCl_3$] (3.1d)	86.56	Pale yellow	51.68 (51.78)	3.91 (3.95)	8.19 (8.23)	6.23 (6.28)

3.3.1. FT-IR Spectral Characterization Studies

3.3.1.1. FT-IR Spectra of Curcumin-thiosemicarbazone Ligand (L^2)

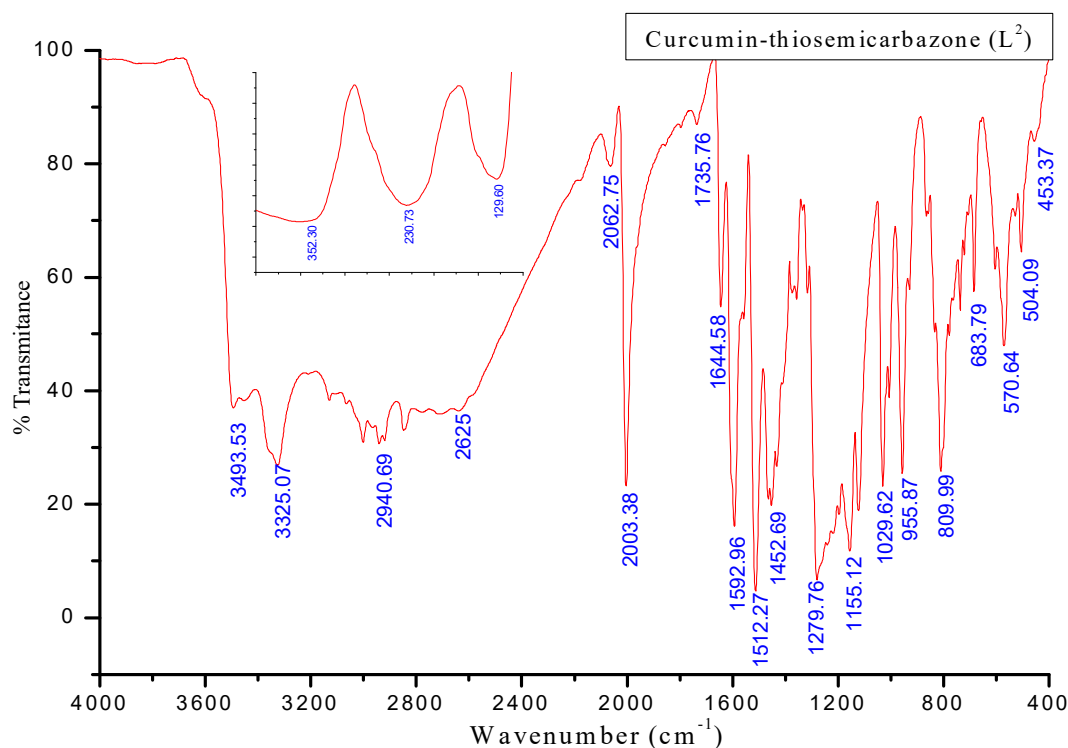


Figure 3.3. FT-IR spectra of Curcumin-thiosemicarbazone ligand (L^2).

The FT-IR spectrum of the curcumin-thiosemicarbazone (L^2) showed a peak at 3493 cm^{-1} attributing to the OH stretching and absorption at 3325 cm^{-1} and 3000 cm^{-1} attributing to NH and CH. The absorption band at 2062 cm^{-1} and 2003 cm^{-1} indicating the thiocyanate i.e. $\nu(\text{N-C}\equiv\text{S})$ of the compound. The band observed at 1644 cm^{-1} , 1592 cm^{-1} and the most prominent band at 1512 cm^{-1} indicating the mixed vibration of $\nu(\text{C}=\text{C})$ and $\delta(\text{C}=\text{N})$. The bands at 1452 cm^{-1} and 1429 cm^{-1} are corresponding to the vibration of $\nu(\text{CCC})$ bond. The peak observed at 1279 cm^{-1} and 1155 cm^{-1} correspond to C-O stretching and the mixed bend vibrations of the C=C and C-H bond is observed at 1029 cm^{-1} , 955 cm^{-1} and 809 cm^{-1} (**Figure 3.3** and **Table 3.2**).

3.3.1.2. FT-IR Spectra of Curcumin-thiosemicarbazone Praseodymium Complex $[L^2_3PrCl_3]$ (3.1a)

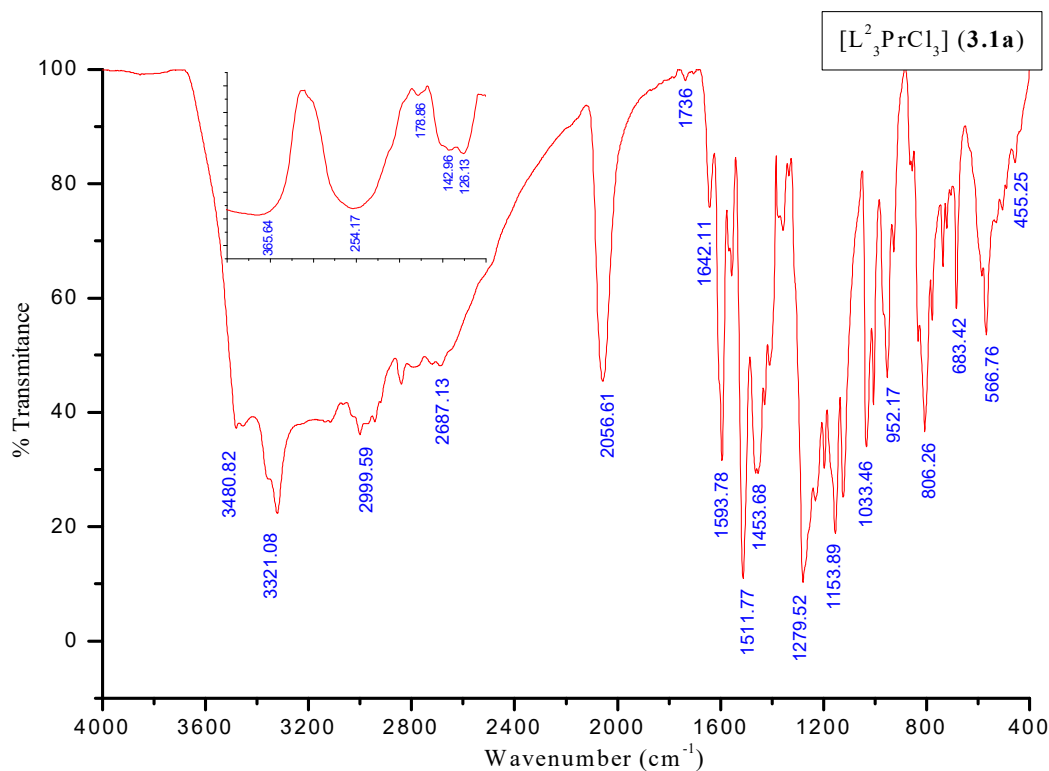


Figure 3.4. FT-IR spectra of Curcumin-thiosemicarbazone Praseodymium Complex $[L^2_3PrCl_3]$ (3.1a).

The FT-IR spectra characterization of curcumin-thiosemicarbazone praseodymium complex $[L^2_3PrCl_3]$ (3.1a) shows that the sharp band at 2003 cm^{-1} and a band at 2062 cm^{-1} merge to form a sharp at 2056 cm^{-1} . The prominent bands appeared in the free curcumin-thiosemicarbazone ligand indicating the mixed vibrations of C=N and C=C stretching at 1644 cm^{-1} and 1512 cm^{-1} were completely shifted to lower frequencies values at 1642 cm^{-1} and 1511 cm^{-1} . The shifting of the bands in the complex IR spectra is strongly signifying that the formation of complex with praseodymium metal at N and S coordination site of the curcumin-thiosemicarbazone ligand (L^2) and new bands appearing at 365 cm^{-1} and 142 cm^{-1} supports the formation of the M-N bond and M-S bond respectively supporting the ligand coordination to the metal where this band was not observed in the free curcumin-thiosemicarbazone ligand (Figure 3.4 and Table 3.2).

3.3.1.3. FT-IR Spectra of Curcumin-thiosemicarbazone Neodymium Complex $[L^2_3NdCl_3]$ (3.1b)

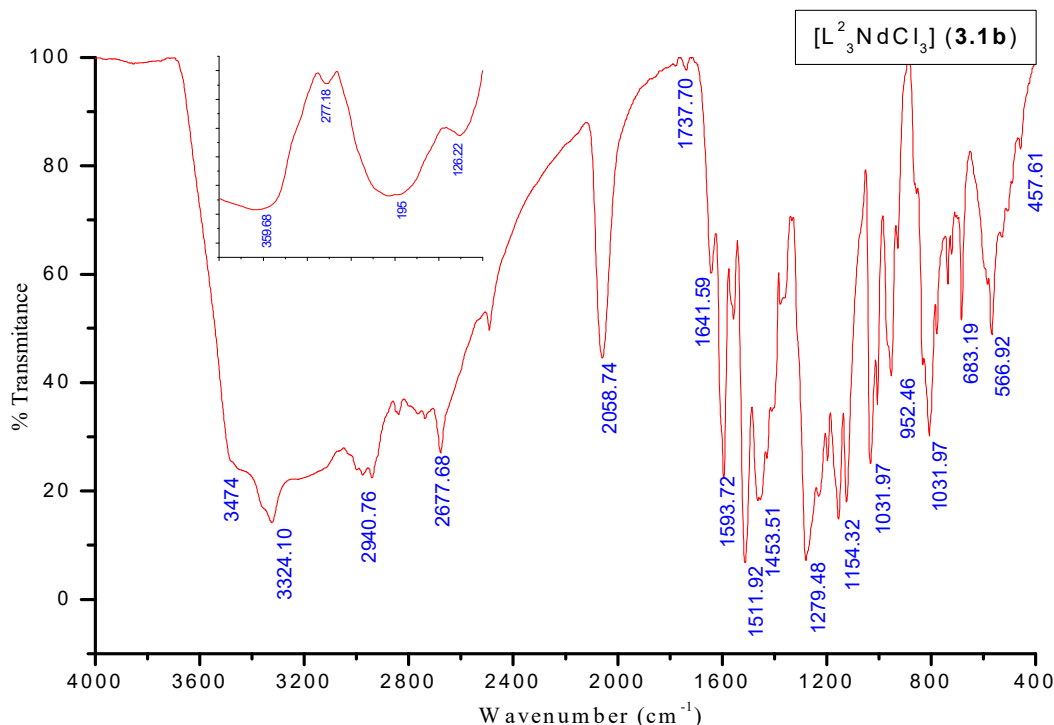


Figure 3.5. FT-IR spectra of Curcumin-thiosemicarbazone Neodymium complex $[L^2_3NdCl_3]$ (3.1b).

Analysing the FT-IR spectra of curcumin-thiosemicarbazone neodymium complex $[L^2_3NdCl_3]$ (3.1b) also showed that the sharp band at 2003 cm^{-1} and a band at 2062 cm^{-1} integrate to form a sharp peak at 2058 cm^{-1} and the prominent bands appeared in the free curcumin-thiosemicarbazone ligand at 1644 cm^{-1} and 1512 cm^{-1} indicating the mixed vibrations of C=N and C=C stretching completely shifted to lower frequencies values at 1641 cm^{-1} and 1511 cm^{-1} . The shifting of the bands in the complex IR spectra strongly supported the formation of complex with neodymium metal at N and S coordination site of the curcumin-thiosemicarbazone ligand (L^2) and new bands arising at 359 cm^{-1} and 172 cm^{-1} supports the formation of the M-N bond and M-S bond respectively supporting the coordination of the lanthanide to the free curcumin-thiosemicarbazone ligand (Figure 3.5 and Table 3.2).

3.3.1.4. FT-IR Spectra of Curcumin-thiosemicarbazone Europium Complex $[L^2_3NdCl_3]$ (3.1c)

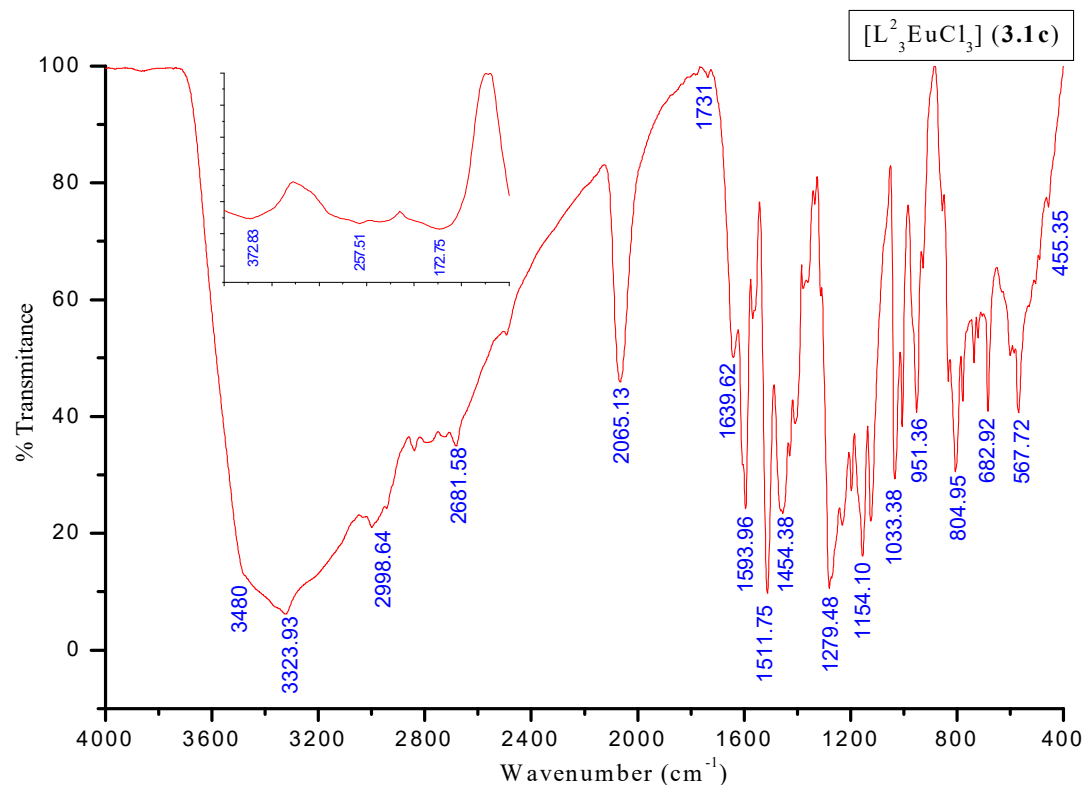


Figure 3.6. FT-IR spectra of Curcumin-thiosemicarbazone Europium Complex $[L^2_3EuCl_3]$ (3.1c).

The FT-IR spectrum of curcumin-thiosemicarbazone europium complex $[L^2_3EuCl_3]$ (3.1c) showed that the prominent bands at 1639 cm^{-1} and 1511 cm^{-1} attributing to the mixed vibrations of C=N and C=C stretching which was shifted to a lower wavelength as compared curcumin-thiosemicarbazone ligand (L^2). Integration of the sharp band at 2003 cm^{-1} and a band at 2062 cm^{-1} of the free ligand resulting in a sharp at 2058 cm^{-1} in the complex. The shifting of the frequencies values fortify the coordination of curcumin-thiosemicarbazone and europium metal and new bands arising at 372 cm^{-1} and 172 cm^{-1} confirm the formation of the M-N bond and M-S bond respectively supporting the coordination of the lanthanide to the free curcumin-thiosemicarbazone ligand (Figure 3.6 and Table 3.2).

3.3.1.5. FT-IR Spectra of Curcumin-thiosemicarbazone Gadolinium Complex $[L^2_3GdCl_3]$ (3.1d)

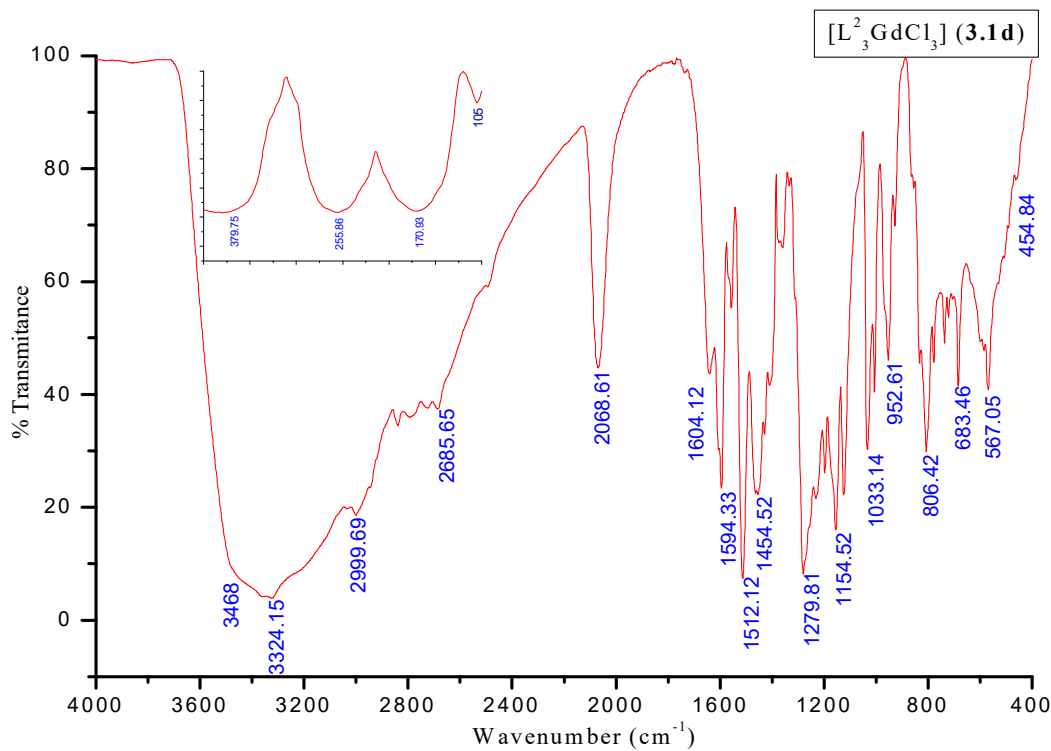


Figure 3.7. FT-IR spectra of Curcumin-thiosemicarbazone Gadolinium Complex $[L^2_3GdCl_3]$ (3.1d).

The sharp band at 2003 cm^{-1} and a band at 2062 cm^{-1} of the free ligand come together result in a sharp band at 2068 cm^{-1} after complexation and the bands at 1644 cm^{-1} and 1512 cm^{-1} attributing to the mixed vibrations of C=N and C=C stretching shown in curcumin-thiosemicarbazone ligand (L^2) was shifted to a lower wavelength at 1640 cm^{-1} and 1511 cm^{-1} after complexation of curcumin-thiosemicarbazone gadolinium complex $[L^2_3EuCl_3]$ (3.1d). The shifting of the bands signifies the coordination of curcumin-thiosemicarbazone and gadolinium metal and new bands arising at 387 cm^{-1} and 170 cm^{-1} confirm the formation of the M-N bond and M-S bond respectively supporting the coordination of the gadolinium to the free Curcumin thiosemicarbazone ligand (Figure 3.7 and Table 3.2).

The results of the FT-IR spectra of all the curcumin-thiosemicarbazone complexes (3.1a-d) along with curcumin-thiosemicarbazone (L^2) are tabulated in Table 3.2

Table 3.2. Major FT-IR spectral data of the Curcumin-thiosemicarbazone (L^2) and its Lanthanide complexes (**3.1a-d**) (cm^{-1}).

Compound	$\nu(\text{ArOH, OH})$	$\nu(\text{NH, CH})$	$\nu(\text{N-C=S})$	$\nu(\text{C=N, C=C})$	$\nu(\text{CC})$	$\nu(\text{C-O})$	$\nu(\text{C-H})$	$\nu(\text{M-N})$	$\nu(\text{M-Cl})$	$\nu(\text{M-S})$
Curcumin-thiosemicarbazone(L^2)	3493	3325, 3000	2062, 2003	1644, 1592, 1512	1452	1279, 1155	1029, 955, 809	-	-	-
$[\text{L}^2_3\text{PrCl}_3]$ (3.1a)	3480	3321, 2999	2056	1642, 1593, 1511	1453	1279, 1153	1033, 952, 806	365	254	178
$[\text{L}^2_3\text{NdCl}_3]$ (3.1b)	3474	3324, 2998	2058	1641, 1593, 1511	1453	1279, 1154	1031, 952, 806	359	277	172
$[\text{L}^2_3\text{EuCl}_3]$ (3.1c)	3480	3323, 2998	2065	1639, 1593, 1511	1454	1279, 1154	1033, 951, 804	372	257	172
$[\text{L}^2_3\text{GdCl}_3]$ (3.1d)	3468	3324, 2999	2068	1640, 1594, 1511	1453	1279, 1154	1033, 952, 806	387	255	170

3.3.2. UV-Vis Spectral Characterization Studies

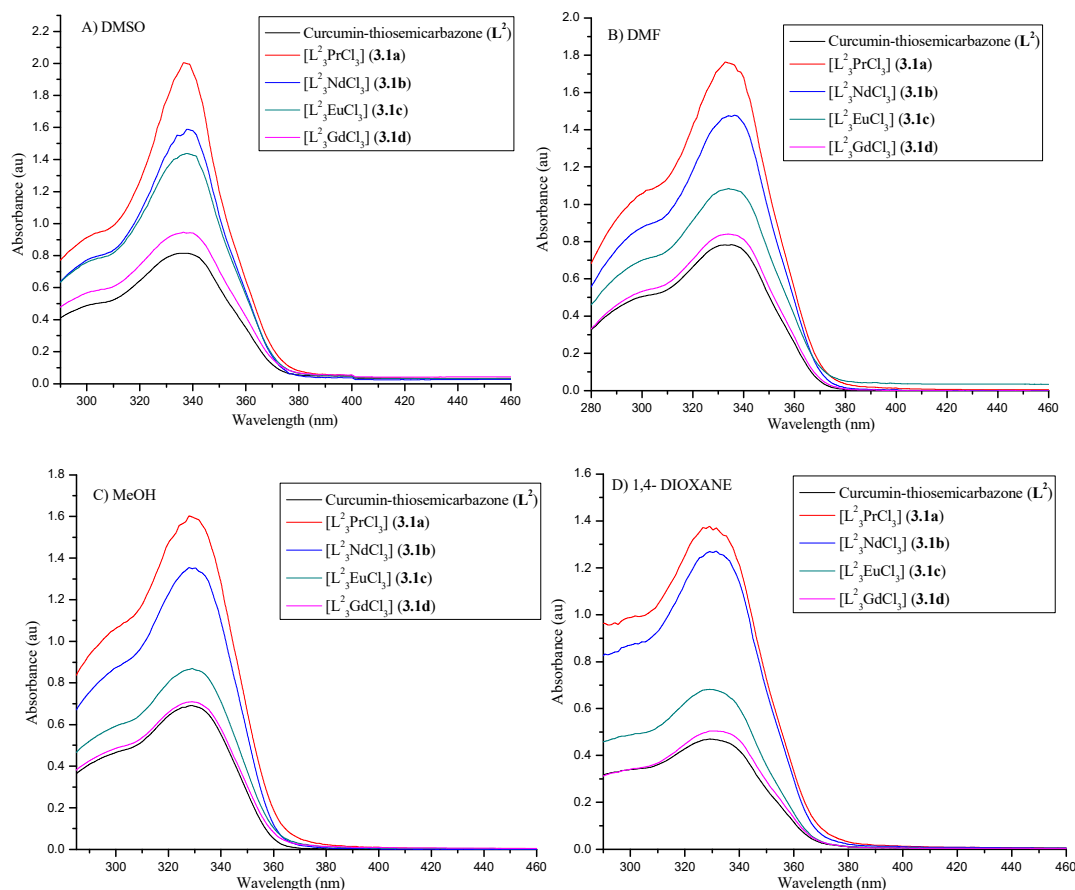


Figure 3.8. UV-Vis spectra of Curcumin-thiosemicarbazone Ligand (L^2) and its Lanthanide Complexes ($3.1a-d$) in solvents (conc. $1 \times 10^{-5} M$).

UV-Vis spectra of curcumin-thiosemicarbazone ligand (L^2) and its lanthanide complexes (($1-4$)) in different solvents such as dimethyl-sulfoxide (DMSO), dimethylformamide (DMF), methanol (MeOH) and 1,4-dioxane were recorded at concentration of $1 \times 10^{-5} M$. A maximum absorption band occurs at around 327 nm to 336 nm on recording the electronic spectra of free curcumin-thiosemicarbazone ligand (L^2) in different solvents. We observed that on increasing the polarity of the solvent the absorption band move to the higher intensity. Similarly, on recording the curcumin-thiosemicarbazone lanthanide complexes ($3.1a-d$) in dimethyl sulfoxide (DMSO), methanol, dimethylformamide (DMF) and 1,4-dioxane solvents at same $1 \times 10^{-5} M$ concentrations and found that with the increase in polarity of the solvent the absorption bands move toward

higher wavelength indicating bathochromic shift or the red shift in all the curcumin-thiosemicarbazone lanthanide complexes (**3.1a-d**) as revealed in **Figure 3.8** and **Table 3.3**. When ligand interacts with the metal ($\text{Ln}=\text{Pr}^{3+}$, Nd^{3+} , Eu^{3+} and Gd^{3+}) and forms complex, the metal- ligand bond length is shortened and a strong bond is formed there by increasing the absorption intensity of UV-Vis spectra of the complex compared to the intensity of the absorption spectra of ligand alone (Nephelauxetic Effect). In all the solvents (DMF, DMSO, MeOH and 1,4-Dioxane), the intensity of the pure ligand and complexes are in the order $\text{L}^2 < [\text{L}_3\text{PrCl}_3]$ (**3.1a**) $< [\text{L}_3\text{NdCl}_3]$ (**3.1b**) $< [\text{L}_3\text{EuCl}_3]$ (**3.1c**) $< [\text{L}_3\text{GdCl}_3]$ (**3.1d**) which signifies the formation of the complexes of lanthanide with curcumin-thiosemicarbazone ligand (L^2) which is in the same order of the electronegativity in the periodic table.

Table 3.3. UV-Vis spectral values of Curcumin-thiosemicarbazone Ligand (L^2) and its Lanthanide Complexes (**3.1a-d**).

Compound	DMSO	DMF	MeOH	1,4-Dioxane
	$\lambda_{\text{max}}(\text{a.u})$	$\lambda_{\text{max}}(\text{a.u})$	$\lambda_{\text{max}}(\text{a.u})$	$\lambda_{\text{max}}(\text{a.u})$
Curcumin-thiosemicarbazone(L^2)	336.35 (0.8142)	332.70 (0.7821)	328.80 (0.6412)	327.75 (0.4676)
$[\text{L}_3\text{PrCl}_3]$ (3.1a)	338.05 (0.9411)	334.15 (0.8396)	329.05 (0.7096)	328.80 (0.5043)
$[\text{L}_3\text{NdCl}_3]$ (3.1b)	338.05 (1.4365)	334.15 (1.0839)	329.15 (0.8688)	328.90 (0.6820)
$[\text{L}_3\text{EuCl}_3]$ (3.1c)	338.40 (1.5869)	335.60 (1.4734)	329.85 (1.3518)	328.95 (1.2689)
$[\text{L}_3\text{GdCl}_3]$ (3.1d)	338.40 (1.9962)	333.40 (1.7611)	329.80 (1.5935)	328.65 (1.3746)

3.3.3. Fluorescence Spectral Characterization Studies

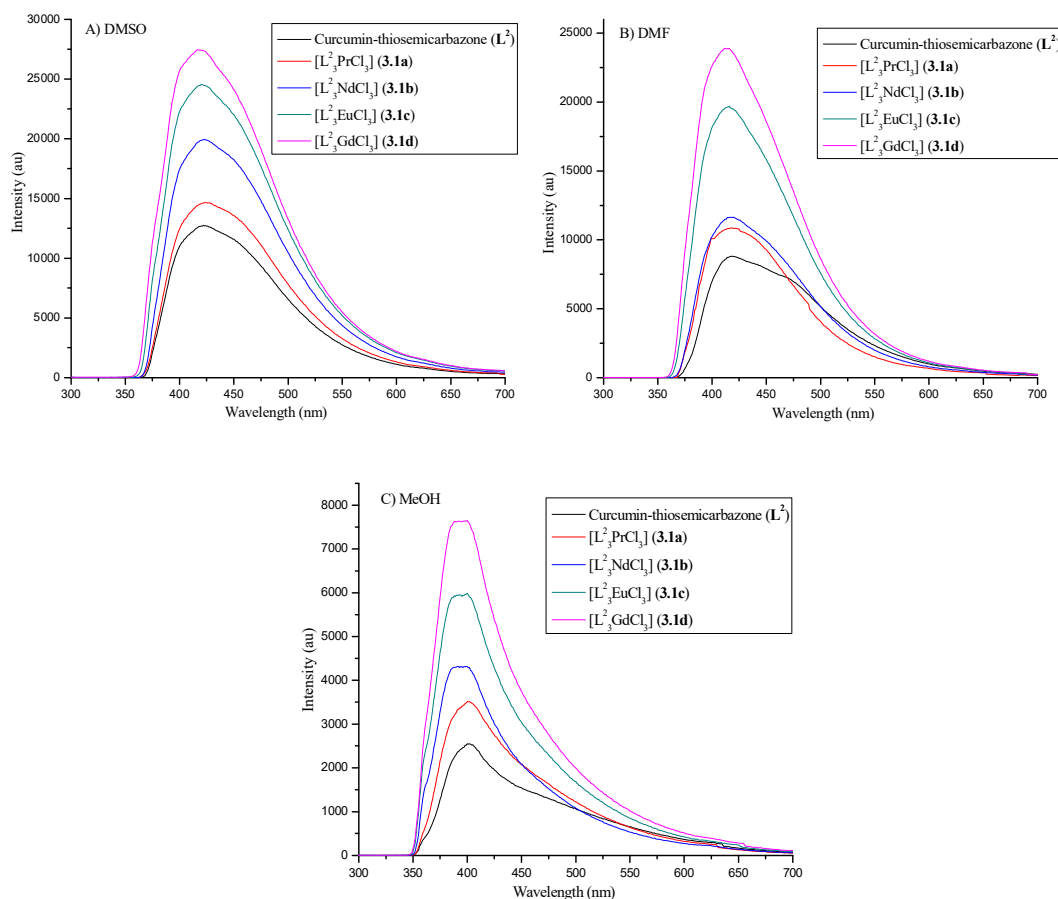


Figure 3.9. Fluorescence spectra of Curcumin-thiosemicarbazone Ligand (L^2) and its Lanthanide Complexes (**3.1a-d**) in different solvents.

The photoluminescence spectra of the curcumin-thiosemicarbazone ligand (L^2) and its lanthanide(III) complexes (**3.1a-d**) were recorded in DMSO, DMF and MeOH medium at concentration of 1×10^{-4} M. As the absorption coefficients of the lanthanide complexes are larger than the organic ligand, the lanthanide ions play an important role to enhance the quantum yield of luminescence emission for the complexes. The differences in the maximum absorption intensity of the complexes and the excitation wavelength showing a red shift after complexation in all the solvents used confirmed the co-ordination nature as well as the transfer of energy of ligand with lanthanide ions. The intensity of the higher polarity solvents shows higher intensity and excitation wavelength. Interestingly, we observed that the fluorescence intensity increases after complexation of curcumin-thiosemicarbazone lanthanide complexes (**3.1a-d**) compared with that of free curcumin-

thiosemicarbazone ligand (L^2). With the increase in the electronegativity of the lanthanide metals in the periodic table the intensity of the complexes increase as curcumin-thiosemicarbazone (L^2) < [$L^2_3PrCl_3$] (**3.1a**) < [$L^2_3NdCl_3$] (**3.1b**) < [$L^2_3EuCl_3$] (**3.1c**) < [$L^2_3GdCl_3$] (**3.1d**). The Quantum yield of the Curcumin lanthanide complexes (**1-4**) compared to the free ligand curcumin-thiosemicarbazone (L^2) also gives the same ascending orders as that of the intensity of the florescence spectra as revealed in **Figure 3.9** and **Table 3.4**. The higher the quantum yield of luminescent, the higher the sensitivity of the applications and so [$L^2_3GdCl_3$] (**3.1d**) may have higher potentiality than that of the other complexes and the curcumin-thiosemicarbazone.

Table 3.4. Florescence Spectra and Quantum yield for Curcumin-thiosemicarbazone Ligand (L^2) and its Lanthanides Complexes (**3.1a-d**).

Compound	Solvent	Emission (nm)	Excitation (nm)	Intensity (a.u)	Quantum Yield (Φ_f)
Curcumin-thiosemicarbazone (L^2)	DMSO	422	370	12739.9	0.0024
	DMF	417	373	8761.4	0.0017
	MeOH	400	355	2546	0.0010
[$L^2_3PrCl_3$] (3.1a)	DMSO	424	367	14652.3	0.0099
	DMF	418	376	10865.1	0.0036
	MeOH	400	355	3512	0.0022
[$L^2_3NdCl_3$] (3.1b)	DMSO	423	370	19961.4	0.0058
	DMF	417	368	11649	0.0023
	MeOH	400	355	4317.1	0.0019
[$L^2_3EuCl_3$] (3.1c)	DMSO	421	369	24529.4	0.0038
	DMF	417	364	19558.9	0.0020
	MeOH	400	355	5983.6	0.0018
[$L^2_3GdCl_3$] (3.1d)	DMSO	420	366	27406.2	0.0034
	DMF	417	366	23802.4	0.0018
	MeOH	400	355	7651.1	0.0011

3.3.4. Thermogravimetric Analysis

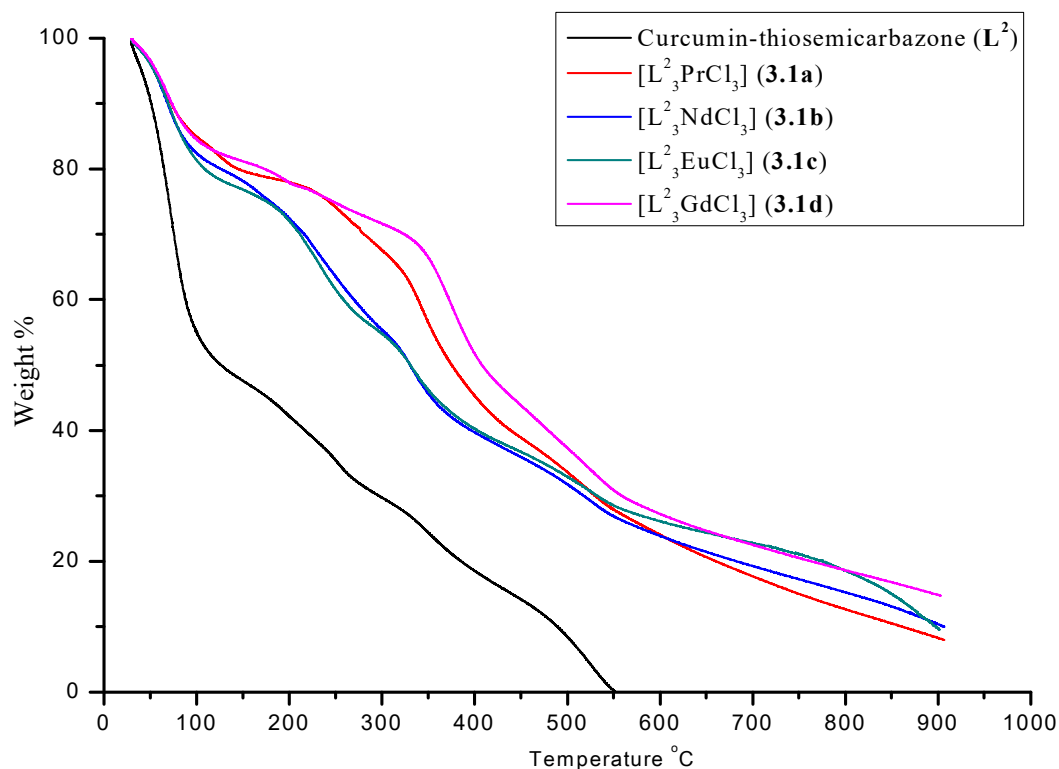


Figure 3.10. TGA curve for Curcumin-thiosemicarbazone Ligand (L^2) and its Lanthanide Complexes (3.1a-d).

Thermogravimetric analysis (weight change) were recorded at 10°C/minute at a temperature range from 29°C to 900°C under nitrogen atmosphere in order to study the thermal behaviour of curcumin-thiosemicarbazone (L^2) and its lanthanide(III) complexes (3.1a-d) at different temperatures. The thermal stability of the complexes were specified by the ligand to a great extent and at an average temperature the decomposition of the lanthanide complexes begins step by step and yield a residue of metal complexes even at high temperature showing its thermal stability. From the obtained TGA curve the weight loss of the free ligand and the metal complexes at different temperature were analyzed experimentally and theoretically. The typical thermograms of the curcumin-thiosemicarbazone and its lanthanide complexes $[L^2_3PrCl_3]$ (3.1a), $[L^2_3NdCl_3]$ (3.1b), $[L^2_3EuCl_3]$ (3.1c), and $[L^2_3GdCl_3]$ (3.1d) are represented in **Figure 3.10** and the detail decomposition of the compounds with respect to the temperature is tabulated in **Table 3.5**.

The first decomposition of the curcumin thiosemicarbazone (L^2) was observed at temperature between 30°C-94°C with weight loss of 43.18%. Followed by second

decomposition of 23.91% weight loss at temperature between 94 °C-266 °C and the third decomposition at temperature ranging between 266 °C-369 °C, finally with complete decomposition at 547 °C.

While those of the curcumin-thiosemicarbazone lanthanides complexes (**3.1a-d**) showing five stages of decomposition with the left residue supporting the content of metal for every end of the decomposition curve. In all the complexes the decomposition starts with 18%-19% of weight loss with a temperature range between 30°C-150°C, decomposition of the complexes continue till the fourth stage at around 530 °C-555 °C corresponding to the molecules of the organic ligand and shows its thermal stability thereafter with a residue of metal alone with the nitrogen and sulphur of the ligand coordinated to it.

Table 3.5. Thermo gravimetric analysis of the Curcumin-thiosemicarbazone Ligand (**L²**) and its Lanthanide Complexes (**3.1a-d**).

Compound	Temperature (° C)	Weight Loss (%) (Experiment/Theoretical)	Decomposed Compound
Curcumin-thiosemicarbazone (L²)	30.00 – 94.82	43.18 % / 43.97%	2 (OCH ₃), 2 (OH), C ₆ H ₃ and NH ₂
	94.82 – 266.48	23.91% / 23.64%	C ₆ H ₃ -CH=CH and CH ₂
	266.84 – 369.99	13.31% / 13.71%	CH=CH and S
	369.99 – 547.71	19.60% / 19.14%	2N and 3C
[L ₃ PrCl ₃] (3.1a)	30.00 – 137.82	19.50% / 19.41%	6 (OCH ₃) and 6 (OH),
	137.82 – 304.24	13.47% / 13.07%	2 (C ₆ H ₃) and 3 (NH ₂)
	304.24 – 448.77	28.03% / 28.46%	2 (C ₆ H ₃ -CH) and 2 (C ₆ H ₃)
	448.77 – 543.20	10.46% / 10.36%	2 (CH-CH) and 3 Cl
	543.20.....	28.54% / 28.86%	3 (N-N-C-S) , 3 (C-CH-C) and Pr
[L ₃ NdCl ₃] (3.1b)	30.00 – 109.15	18.39% / 18.97%	6 (OCH ₃) and 6 (OH),
	109.15 – 276.46	22.49% / 22.92%	4 (C ₆ H ₃) and 3 (NH ₂)
	276.46 – 375.22	16.48% / 16.73%	2 (C ₆ H ₃ -CH) and 6 (CH)
	372.22 – 537.18	13.66% / 13.10%	2 (CH-CH),CH and 3 Cl
	900.....	28.00% / 28.52%	3 (N-N-C-S), 6 C and Nd
[L ₃ EuCl ₃] (3.1c)	30.00 – 108.84	19.99% / 19.27%	6 (OCH ₃) and 6 (OH),
	108.84 – 290.65	24.19% / 24.59%	5 (C ₆ H ₃)
	290.64 – 382.09	13.86% / 13.18%	3 (NH ₂) 2(C ₆ H ₃ -CH) and 5 (CH)
	382.09 – 553.21	12.41% / 12.19%	3(CH-CH),3H and 3 Cl
	553.21.....	29.53% / 29.04%	3 (N-N-C-S), 6 C and Eu
[L ₃ GdCl ₃] (3.1d)	30.00 – 119.13	17.23% / 17.70%	6 (OCH ₃) and 5 (OH),
	119.13 – 204.11	5.16% / 5.09%	(C ₆ H ₃) and 3H
	204.11 – 411.32	28.27% / 28.85%	3 (NH ₂) , 5 (C ₆ H ₃) and OH
	411.32 – 530.11	16.01% / 16.85%	4(CH-CH),3c and 3 Cl
	530.11.....	33.33% / 32.50%	3 (N-N-C-S), 3C and Gd

3.3.5. Chemical Kinetic and Thermodynamic Studies

A chemical reaction is lead by stretching, bending and ultimately breaking of bonds when molecules collide and the kinetic energy of the molecule is utilized. The minimum energy required for a chemical reaction to occur is called activation energy (E_a).²⁶ Or it is the difference between the threshold energy and the activation energy of the reactant molecule. Considering the Arrhenius Equation, the activation energy of the chemical reaction can be evaluated.²⁷

$$\text{Which is represented as: } k = Ae^{-E_a/RT} \quad (1)$$

Where A= frequency factor or the pre exponential factor, T= temperature, R= universal gas constant, E_a = activation energy and k= rate constant.

Applying the Arrhenius rate equation the activation energy (E_a) of the complexation of curcumin lanthanides complexes were evaluated by plotting $\log k$ (k= rate constant) against $1/T \times 10^{-3}$

$$E_a = \text{Slope} \times 2.303 \times R \quad (2)$$

Using Van't Hoff plot of $\log k$ against $1/T$, the thermodynamic parameters for the complexation were calculated.²⁸

$$\ln k = -\frac{\Delta H^\circ}{RT} + \Delta S^\circ R$$

$$\text{Or } \ln k = -\Delta G^\circ RT \quad (3)$$

Experimentally the studies of chemical dynamics have been performed by recording the pH value of curcumin-thiosemicarbazone lanthanides complexes; $[L^2_3PrCl_3]$ (**3.1a**), $[L^2_3NdCl_3]$ (**3.1b**), $[L^2_3EuCl_3]$ (**3.1c**) and $[L^2_3GdCl_3]$ (**3.1d**) at different temperatures for a time interval of 10 minutes in ethanol medium which is shown in **Table 3.6** and a plot of pH against time were plotted (**Figure 3.11, 2.13, 2.15 and 2.17**) in order to analyze the rate of the reaction or complexation at different temperature (288K, 298K, 308K, 318K and 328K) utilizing which the activation energy (E_a) were evaluated plotting the graph of $\log k$ against $1/T \times 10^{-3}$. From **Table 3.6** we can see that the pH values of the complexes increase with increase in temperatures and time intervals in all the cases which show that the rate of the complexation (k) of curcumin with the lanthanide in the formation of complexes in ethanol medium increases as shown in **Table 3.7, 3.9, 3.11 and 3.13** respectively which is inconsistent with the theoretical prediction of Arrhenius. The intercepts of the plot $\log k$ versus $1/T \times 10^{-3}$ provide the frequency factor or the pre exponential factor (A). From the values of the activation energy (E_a) as tabulated in **Table 3.7, 3.9, 3.11 and 3.13**, the negligibly low value of E_a signified that the reactions involved

are fast ones. Observing the value of activation energy, evaluated from the graph, the order of the increasing rate in the formation of complexes are in the sequence $[L^2_3PrCl_3]$ (**3.1a**) < $[L^2_3NdCl_3]$ (**3.1b**) < $[L^2_3EuCl_3]$ (**3.1c**) < $[L^2_3GdCl_3]$ (**3.1d**).

From the Van't Hoff plot of $\ln k$ against $1/T$, (**Figure 2.12, 2.14, 2.16 and 2.18**) the thermodynamic parameters such as Enthalpy change (ΔH°) entropy change (ΔS°) and Gibbs free energy change (ΔG°) of the complexation of $[L^2_3PrCl_3]$ (**3.1a**), $[L^2_3NdCl_3]$ (**3.1b**), $[L^2_3EuCl_3]$ (**3.1c**) and $[L^2_3GdCl_3]$ (**3.1d**) were evaluated which are tabulated in **Table 3.8, 3.10, 3.12 and 3.14**. The negative value of the Gibbs free energy change (ΔG°) indicates that the reaction is a spontaneous and also favourable one associated with the positive values of Enthalpy change (ΔH°) revealing the complexation as endothermic one and the entropy change (ΔS°) value as the reaction to be entropy driven.

Table 3.6. pH value of the Curcumin-thiosemicarbazone Complexes (**3.1a-d**) at different temperature with 10 minutes of time interval.

Compound	Temperature °C	pH at different time interval (minutes)						
		0	10	20	30	40	50	60
[L ² ₃ PrCl ₃](3.1a)	15	2.28	2.32	2.35	2.38	2.40	2.43	2.45
	25	2.37	2.42	2.44	2.46	2.48	2.53	2.58
	35	2.43	2.47	2.50	2.53	2.57	2.60	2.63
	45	2.45	2.50	2.54	2.56	2.60	2.63	2.67
	55	2.52	2.56	2.59	2.62	2.68	2.71	2.75
[L ² ₃ NdCl ₃](3.1b)	15	2.23	2.28	2.34	2.37	2.39	2.41	2.45
	25	2.25	2.29	2.35	2.38	2.40	2.47	2.49
	35	2.27	2.32	2.38	2.41	2.47	2.49	2.53
	45	2.38	2.41	2.49	2.57	2.60	2.63	2.65
	55	2.42	2.48	2.53	2.59	2.62	2.67	2.73
[L ² ₃ EuCl ₃](3.1c)	15	3.37	3.43	3.48	3.53	3.58	3.6	3.62
	25	3.42	3.45	3.52	3.60	3.66	3.68	3.70
	35	3.50	3.59	3.66	3.70	3.75	3.79	3.83
	45	3.63	3.71	3.79	3.85	3.87	3.93	3.97
	55	3.78	3.84	3.92	3.96	4.03	4.09	4.12
[L ² ₃ GdCl ₃](3.1d)	15	4.10	4.13	4.19	4.23	4.29	4.31	4.33
	25	4.22	4.26	4.28	4.34	4.4	4.42	4.48
	35	4.31	4.36	4.39	4.44	4.48	4.54	4.59
	45	4.41	4.44	4.49	4.51	4.57	4.65	4.70
	55	4.45	4.51	4.58	4.62	4.68	4.73	4.75

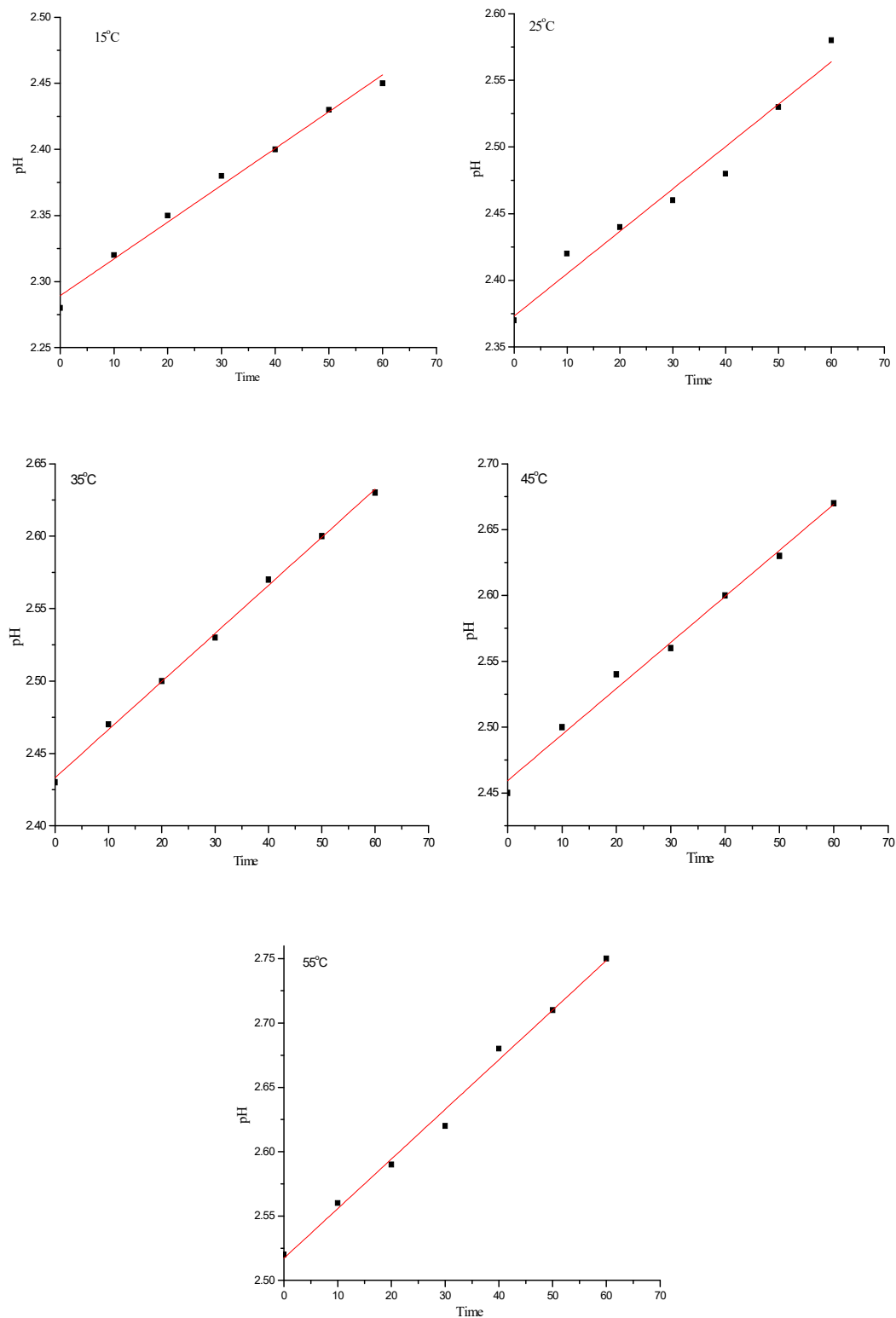
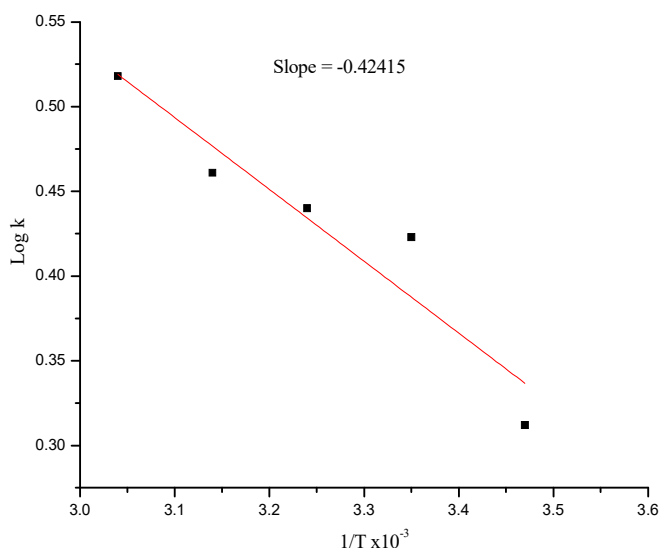


Figure 3.11. Plot of pH and time (10 minutes) for complexation of $[L^2_3PrCl_3]$ (**3.1a**) at different temperatures.

Table 3.7. Rate (k) at different temperature; i.e. 288K, 298K, 308K, 318K, and 328K and Activation energy (Ea) of $[L^2_3PrCl_3]$ (**3.1a**).

Temperature K	1/T K ⁻¹ x10 ⁻³	Rate(k) Mol L ⁻¹ Min ⁻¹	Rate(k) Mol L ⁻¹ S ⁻¹ x10 ⁻³	Log k	Activation Energy (Ea) (KJ)
288	3.47	0.12317	2.05283	0.31235	0.00812
298	3.35	0.15893	2.64883	0.42305	
308	3.24	0.16541	2.75683	0.44040	
318	3.14	0.17345	2.89083	0.46102	
328	3.24	0.19788	3.29800	0.51825	

**Figure 3.12.** Plot of log k versus $(1/T) \times 10^{-3}$ for the complexation of $[L^2_3PrCl_3]$ (**3.1a**) in EtOH.**Table 3.8** Rate (k) and Thermodynamics parameter of the complexation of $[L^2_3PrCl_3]$ (**3.1a**) at different temperature.

Temperature (K)	Rate(k) Mol L ⁻¹ S ⁻¹ x10 ⁻³	ΔH^0 (kJmol ⁻¹)	ΔS^0 (JK ⁻¹ mol ⁻¹)	ΔG^0 (kJmol ⁻¹)
288	2.05283	0.00812	0.00600	-1.72331
298	2.64883		0.00812	-2.41507
308	2.75683		0.00845	-2.59844
318	2.89083		0.00885	-2.80837
328	3.29800		0.00994	-3.25623

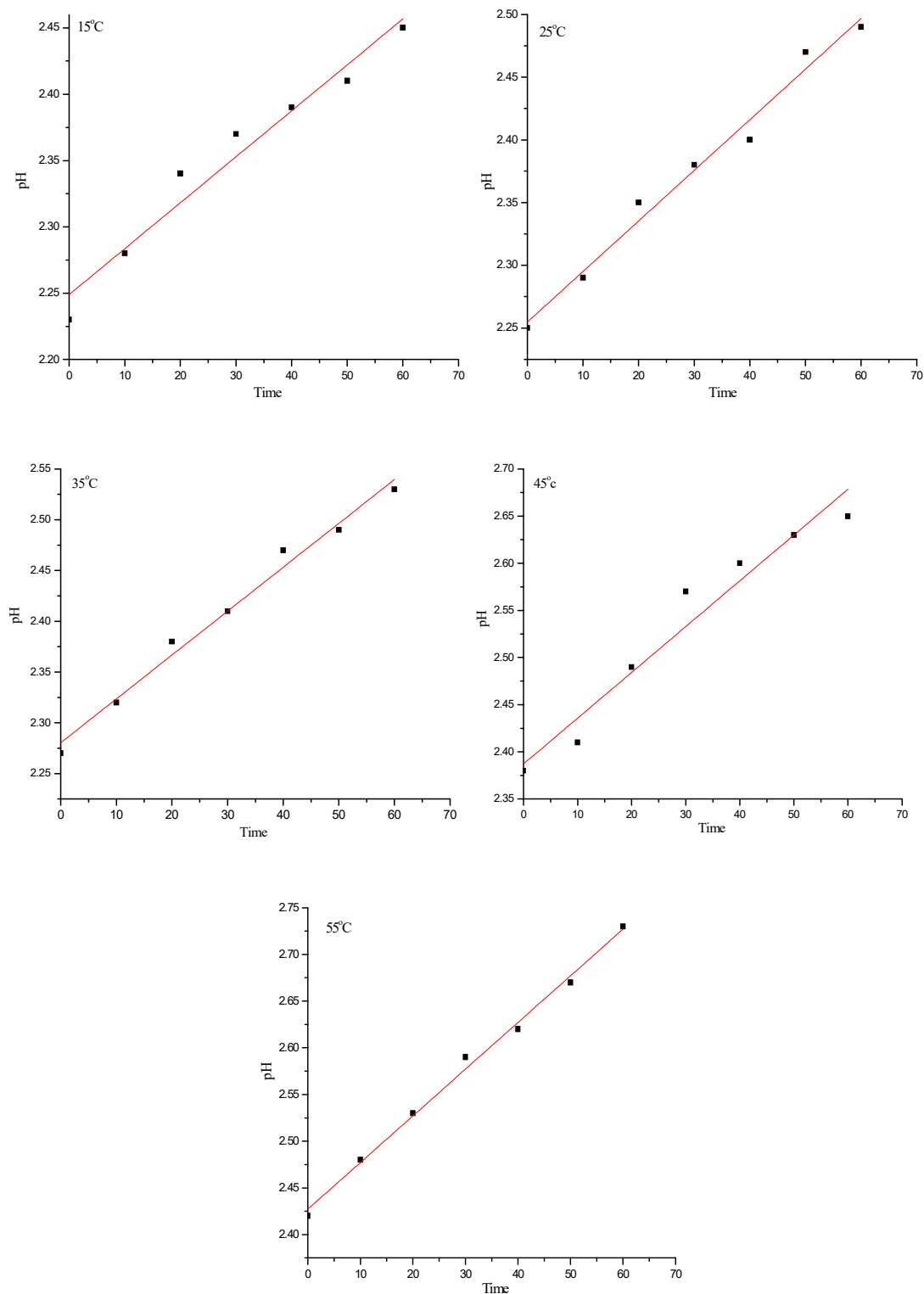
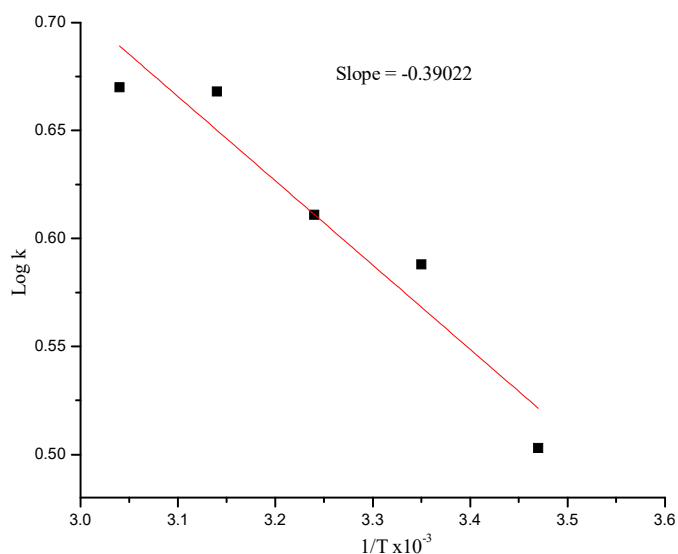


Figure 3.13. Plot of pH and time (10 minutes) for the complex $[L^2_3NdCl_3]$ (3.1b) at different temperatures.

Table 3.9. Rate (k) at different temperature; i.e. 288K, 298K, 308K, 318K, and 328K and Activation energy (Ea) of $[L^2_3NdCl_3]$ (**3.1b**).

Temperature K	1/T K ⁻¹ x10 ⁻³	Rate(k) Mol L ⁻¹ Min ⁻¹	Rate(k) Mol L ⁻¹ S ⁻¹ x 10 ⁻³	Log k	Activation Energy (Ea) (KJ)
288	3.47	0.19109	3.18483	0.50308	0.00747
298	3.35	0.23251	3.87516	0.58828	
308	3.24	0.24549	4.09150	0.61118	
318	3.14	0.27999	4.66650	0.66899	
328	3.04	0.28075	4.67916	0.67016	

**Figure 3.14.** Plot of log k versus $(1/T) \times 10^{-3}$ for the complexation of $[L^2_3NdCl_3]$ (**3.1b**) in EtOH.**Table 3.10.** Rate (k) and Thermodynamics parameter of the complexation of $[L^2_3NdCl_3]$ (**3.1b**) at different temperature.

Temperature (K)	Rate(k) Mol L ⁻¹ S ⁻¹ x 10 ⁻³	ΔH° (kJmol ⁻¹)	ΔS° (JK ⁻¹ mol ⁻¹)	ΔG° (kJmol ⁻¹)
288	3.18483	0.00747	0.00965	-2.77561
298	3.87516		0.01128	-3.35838
308	4.09150		0.01173	-3.61020
318	4.66650		0.01283	-4.07526
328	4.67916		0.01285	-4.21070

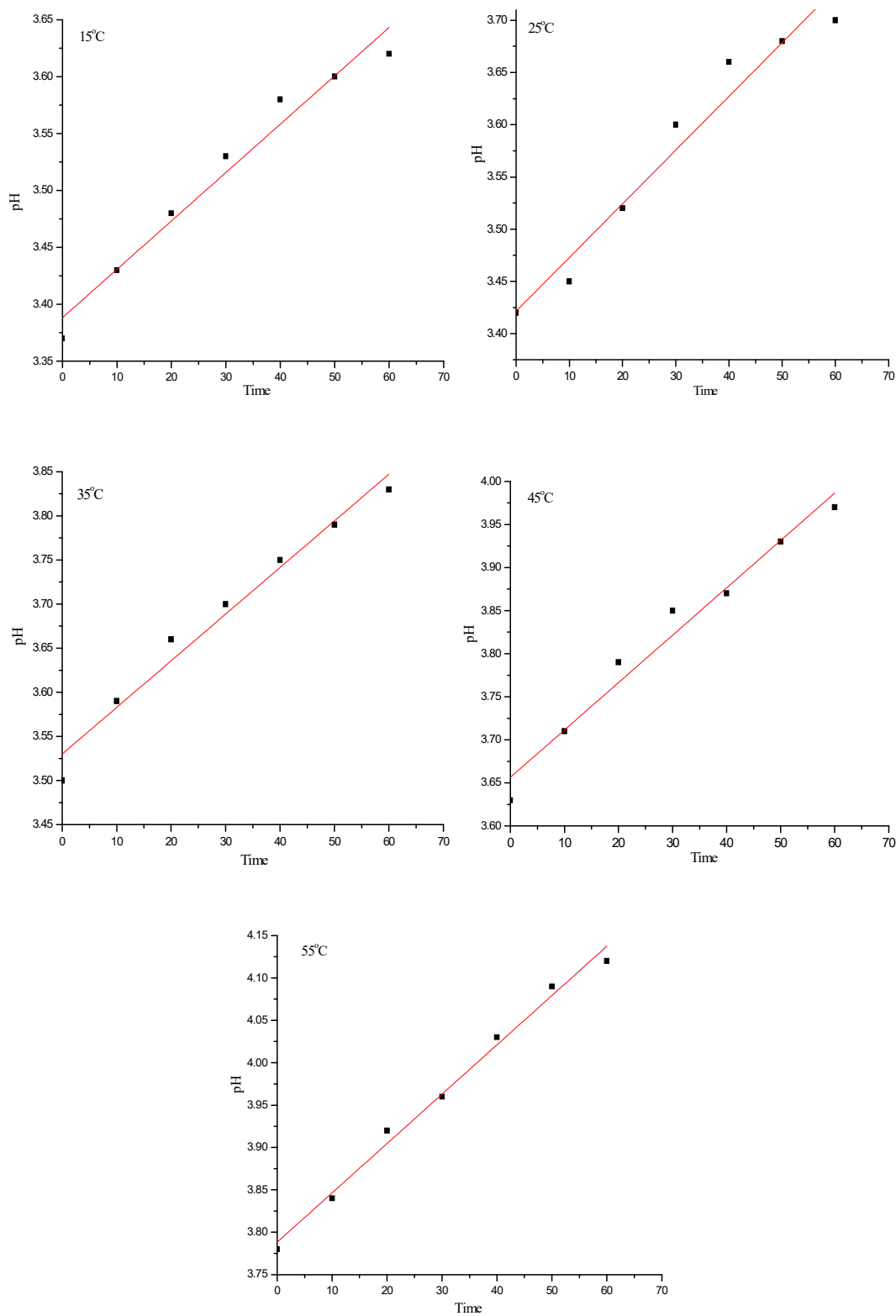
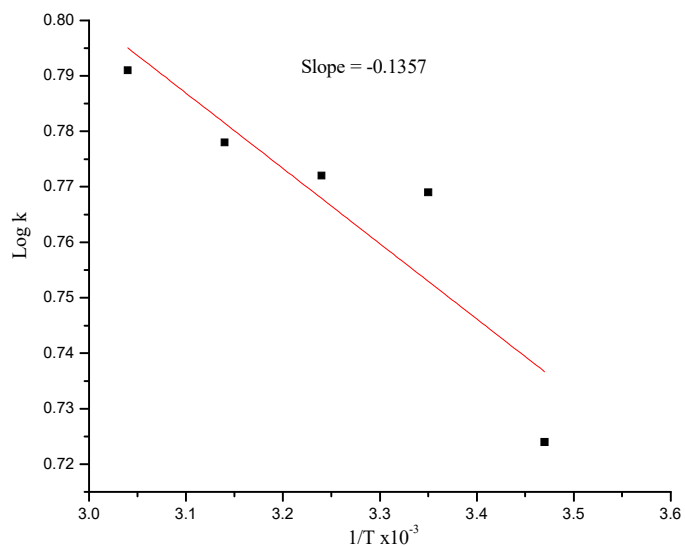


Figure 3.15. Plot of pH and time (10 minutes) for the complex $[L_3EuCl_3]$ (3.1c) at different temperatures.

Table 3.11. Rate (k) at different temperature; i.e. 288K, 298K, 308K, 318K, and 328K and Activation energy (Ea) of $[L^2_3EuCl_3]$ (**3.1c**).

Temperature K	1/T K ⁻¹ x10 ⁻³	Rate(k) Mol L ⁻¹ Min ⁻¹	Rate(k) Mol L ⁻¹ S ⁻¹ x 10 ⁻³	Log k	Activation Energy (Ea) (KJ)
288	3.47	0.30209	5.30348	0.72456	0.00259
298	3.35	0.35326	5.88766	0.76994	
308	3.24	0.35496	5.91600	0.77200	
318	3.14	0.36017	6.00283	0.77835	
328	3.04	0.37143	6.19061	0.79173	

**Figure 3.16.** Plot of log k versus $(1/T) \times 10^{-3}$ for the complexation of $[L^2_3EuCl_3]$ (**3.1c**) in EtOH.**Table 3.14.** Rate (k) and Thermodynamics parameter of the complexation of $[L^2_3EuCl_3]$ (**3.1c**) at different temperature.

Temperature (K)	Rate(k) Mol L ⁻¹ S ⁻¹ x 10 ⁻³	ΔH° (kJmol ⁻¹)	ΔS° (JK ⁻¹ mol ⁻¹)	ΔG° (kJmol ⁻¹)
288	5.30348	0.00259	0.01388	-3.99757
298	5.88766		0.01475	-4.39537
308	5.91600		0.01478	-4.55494
318	6.00283		0.01491	-4.74144
328	6.19061		0.01516	-4.97454

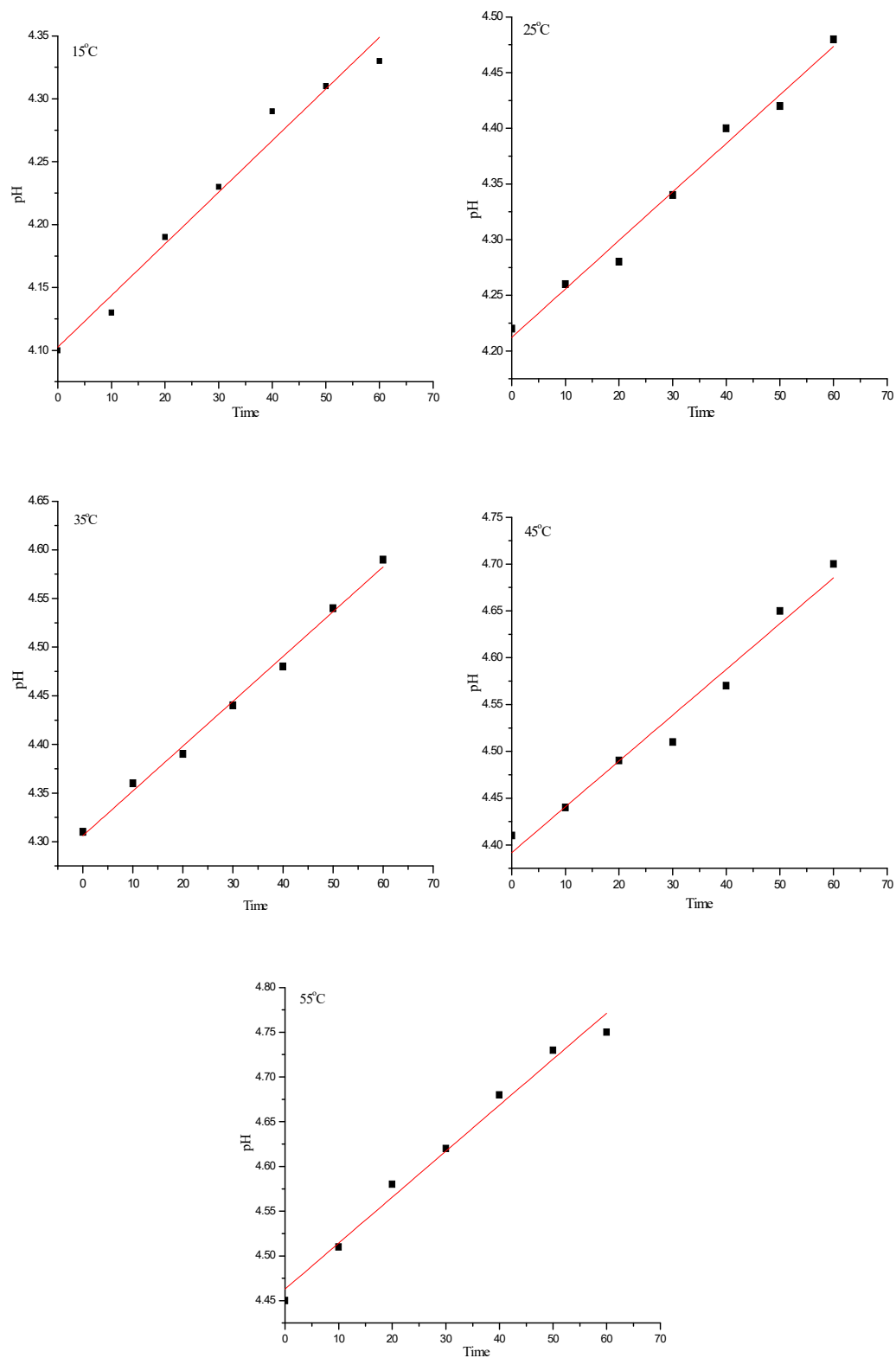
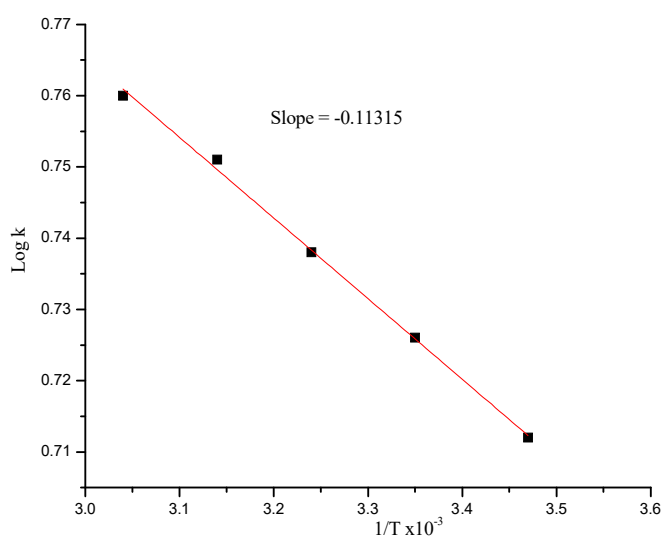


Figure 3.17. Plot of pH and time (10 minutes) for the complex $[L^2_3GdCl_3]$ (3.1d) at different temperatures.

Table 3.13. Rate (k) at different temperature; i.e. 288K, 298K, 308K, 318K, and 328K and Activation energy (Ea) of $[L^2_3GdCl_3]$ (**3.1d**).

Temperature K	1/T K ⁻¹ x10 ⁻³	Rate(k) Mol L ⁻¹ Min ⁻¹	Rate(k) Mol L ⁻¹ S ⁻¹ x 10 ⁻³	Log k	Activation Energy (Ea) (KJ)
288	3.47	0.30949	5.15816	0.71249	0.00216
298	3.35	0.31949	5.32483	0.72630	
308	3.24	0.32839	5.47311	0.73820	
318	3.14	0.33838	5.63966	0.75125	
328	3.04	0.34556	5.75933	0.76000	

**Figure 3.18.** Plot of log k versus $(1/T) \times 10^{-3}$ for the complexation of $[L^2_3GdCl_3]$ (**3.1d**) in EtOH.**Table 3.14.** Rate (k) and Thermodynamics parameter of the complexation of $[L^2_3GdCl_3]$ (**3.1d**) at different temperature.

Temperature (K)	Rate(k) Mol L ⁻¹ S ⁻¹ x 10 ⁻³	ΔH^0 (kJmol ⁻¹)	ΔS^0 (JK ⁻¹ mol ⁻¹)	ΔG^0 (kJmol ⁻¹)
288	5.15816	0.00216	0.01364	-3.93098
298	5.32483		0.01391	-4.14624
308	5.47311		0.01414	-4.35552
318	5.63966		0.01439	-4.57636
328	5.75933		0.01455	-4.77518

3.4. Conclusion

In conclusion, we report the novel synthesis of curcumin thiosemicarbazone (**L**²) and its lanthanide complexes (**3.1a-d**). All the synthesized curcumin thiosemicarbazone lanthanide complexes were well investigated for their various spectroscopic studies. The IR spectra of all complexes were found that there is a chelate band shift and formation of new band in complexes comparing with that of free curcumin thiosemicarbazone ligand which confirm the complexation. The UV-Vis absorption spectra of the complexes increases with the increase in the polarity of the solvents and found that the absorption bands move toward higher wavelength indicating bathochromic shift or the red shift in all the curcumin thiosemicarbazone lanthanide complexes. Interestingly, the fluorescence spectroscopic studies were found that after complexation the intensity of the emission spectra increases comparing with that of free curcumin thiosemicarbazone ligand. The negligibly low value of E_a signified that the reactions involved are fast ones. The negative value of the Gibbs free energy change (ΔG°) indicates that the reaction is a spontaneous and also favorable one. Positive values of Enthalpy change (ΔH°) shows the complexation is endothermic one and the entropy change (ΔS°) value shows the reaction is entropy driven.

3.5. References

1. N. S. H. N Moorthy, N. M. F. S. A. Cerqueira, M. J. Ramos and P. A. Fernandes, Aryl- and Heteroaryl-Thiosemicarbazone Derivatives and Their Metal Complexes: A Pharmacological Template, *Recent Pat. Anticancer Drug Disc.*, 2013, **8**(2), 168-182.
<https://doi.org/10.2174/157489213805290583>
2. G. Pelosi, F. Bisceglie, F. Bignami, P. Ronzi, P. Schiavone, M. C. Re, C. Casoli and E. Pilotti, Antiretroviral Activity of Thiosemicarbazone Metal Complexes, *J. Med. Chem.*, 2010, **53**, 8765-8769. <https://doi.org/10.1021/jm1007616>
3. M. S. More, P. G. Joshi, Y. K. Mishra and P. K. Khanna, Metal Complexes Driven from Schiff bases and Semicarbazones for Biomedical and Allied Applications: a Review, *Mater. Today Chem.*, 2019, **14**, 100195.
<https://doi.org/10.1016/j.mtchem.2019.100195>
4. J. R. Dilworth and R. Hueting, Metal Complexes of Thiosemicarbazones for imaging and Therapy, *Inorg. Chem. Acta.*, 2012, **389**, 1-165.
<https://doi.org/10.1016/j.ica.2012.02.019>
5. M. Baldini, M. B. Ferrari, F. Bisceglie, P. P. D. Aglio, G. Pelosi, S. Pinelli and P. Tarasconi, Copper(II) Complexes with Substituted Thiosemicarbazones of α -Ketoglutaric Acid: Synthesis, X-ray Structures, DNA Binding Studies and Nuclease and Biological Activity, *Inorg. Chem.*, 2004, **43**(22), 7170-7179.
<https://doi.org/10.1021/ic049883b>
6. F. Muleta, T. Alansi and R. Eswaramoorthy, A Review on Synthesis, Characterization Methods and Biological Activities of Semicarbazone, Thiosemi-Carbazone and Their Transition Metal Complexes, *J. Nat. Sci. Res.*, 2019, **9**(17), 33-46.
<https://core.ac.uk/download/pdf/234658265.pdf>
7. A. A. A. Amiery, Y. K. A. Majedy, H. Abdulreazak and H. Abood, Synthesis, Characterization, Theoretical Crystal Structure, and Antibacterial Activities of Some Transition Metal Complexes of the Thiosemicarbazone (Z)-2-(pyrrolidin-2-ylidene)hydrazinecarbothioamide, *Bioinorg. Chem. App.*, 2011, 1-6.
<https://doi.org/10.1155/2011/483101>
8. D. Mishra, S. Naskar, M. G. B. Drew and S. K. Chattopadhyay, Synthesis, Spectroscopic and Redox properties of some Ruthenium(II) Thiosemicarbazone Complexes: Structural Description of four of these Complexes, *Inorg. Chim. Acta.*, 2006, **359**(2), 585-592. <https://doi.org/10.1016/j.ica.2005.11.001>

9. I. Kizilcikli, B. Ulkuseven, Y. Dasdemir, and B. Akkurt, Zn(II) and Pd(II) Complexes of Thiosemicarbazone-S-alkyl Esters Derived from 2/3-formylpyridine, *Synth. React. Inorg. Met. Org. Chem.*, 2004, **34(4)**, 653-665. <https://doi.org/10.1081/SIM-120035948>
10. A. A. Hassan, A. M. Shawky and H. S. Shehatta, Chemistry and Heterocyclization of Thiosemicarbazones, *J. Heterocycl. Chem.*, 2012, **49(1)**, 21-37. <https://doi.org/10.1002/jhet.677>
11. N. P. Prajapati and H. D. Patel, Novel thiosemicarbazone derivatives and their metal complexes: Recent development, *An Inter. J. rapid Comm. Synth. Org. Chem.*, 2019, **49(21)**, 1-38. <https://doi.org/10.1080/00397911.2019.1649432>
12. J. Haribabu, K. Jeyalakshmi, Y. Arun, N. S. P. Bhuvanesh, P. T. Perumal and R. Karvembu, Synthesis of Ni(II) Complexes bearing Indole-based Thiosemicarbazone Ligands for Interaction with Biomolecules and some Biological Applications, *J. Bio. Inorg. Chem.*, 2017, **22**, 461-480. <https://doi.org/10.1007/s00775-016-1424-1>
13. S. Sarkar, T. Mondal, S. Roy, R. Saha, A. K. Ghosh and S. S. Panja, A multi-responsive Thiosemicarbazone-based Probe for Detection and Discrimination of group 12 Metal Ions and its Application in Logic Gates, *New J. Chem.*, 2018, **42**, 15157-15169. <https://doi.org/10.1039/C8NJ02011F>
14. M. K. Bharty, A. Bharti, R. Chaurasia, U. K. Chaudhari, S. K. Kushawaha, P. K. Sonkar, V. Ganesan and R.J. Butcher, Synthesis and characterization of Mn(II) complexes of 4-phenyl(phenylacetyl)-3-thiosemicarbazide, 4-amino-5-phenyl-1,2,4-triazole-3- thiolate, and their application towards electrochemical oxygen reduction reaction, *Polyhedron.*, 2019, **173**, 1-9. <https://doi.org/10.1016/j.poly.2019.114125>
15. B. Kaya, D. Akyüz, T. Karakurt, O. Sahin, A. Koca and B. Ülküseven, Cobalt(II)/(III) Complexes bearing a Tetradentate Thiosemicarbazone: Synthesis, Experimental and Theoretical Characterization and Electrochemical and Antioxidant Properties, *Appl Organomet Chem.*, 2020, 1-12. <https://doi.org/10.1002/aoc.5930>
16. D. Sarker, M. F. Hossen, M. K. Zahan, M. M. Haque, R. Zamir and M. A. Asraf, Synthesis, Characterization, Thermal Analysis and Antibacterial Activity of Cu (II) and Ni(II) Complexes with Thiosemicarbazone Derived from Thiophene-2-aldehyde, *Journal of Materials Science Research and Reviews* 2020, **5(2)**, 15-25. <https://journaljmsrr.com/index.php/JMSRR/article/view/30130>
17. U. M. Osman, S. Silvarajoo, K. H. Kamarudin, M. I. M. Tahir and H. C. Kwong, Ni(II) Complex containing a Thiosemicarbazone Ligand: Synthesis, Spectroscopy, Single-

- crystal X-ray Crystallographic and Conductivity Studies, *J. Mol. Struct.*, 2021, **1223**, 1-9. <https://doi.org/10.1016/j.molstruc.2020.128994>
18. S. Savir, J. W. K. Liew, I. Vythilingam, Y. A. L. Lim, C. H. Tan, K. S. Sim, V. S. Lu, M. J. Maah and K. W. Tan, Nickel(II) Complexes with Polyhydroxybenzaldehyde and O,N,S tridentate Thiosemicarbazone ligands: Synthesis, Cytotoxicity, Antimalarial Activity, and Molecular Docking Studies, *J. Mol. Struct.*, 2021, **1241**.
<https://doi.org/10.1016/j.molstruc.2021.130815>
19. Y. Yue, J. Gu, J. Han, Q. Wu and J. Jiang, Effects of Cellulose/Salicylaldehyde Thiosemicarbazone complexes on PVA based hydrogels: Portable, Reusable, and High-precision Luminescence Sensing of Cu^{2+} , *J. Hazard. Mat.*, 2021, **401**.
<https://doi.org/10.1016/j.jhazmat.2020.123798>
20. T. Khan, S. Dixit, R. Ahmad, S. Raza, I. Azad, S. Joshi and A. R. Khan, Molecular Docking, PASS Analysis, Bioactivity score Prediction, Synthesis, Characterization and Biological Activity evaluation of a Functionalized 2-butanone Thiosemicarbazone Ligand and its Complexes, *J Chem Biol.*, 2017, **10**, 91-104.
<https://doi.org/10.1007/s12154-017-0167-y>
21. I. D. Kostas and B. R. Steele, Thiosemicarbazone Complexes of Transition Metals as Catalysts for Cross-Coupling Reaction Catalysts, 2020, **10(10)**, 1-40.
<https://doi.org/10.3390/catal10101107>
22. N. A. Mathews and M. R. P. Kurup, In vitro Biomolecular Interaction Studies and Cytotoxic Activity of Copper(II) and Zinc(II) Complexes bearing ONS donor Thiosemicarbazones, Applied Organometallic Chemistry, *Appl. Organomet. Chem.*, 2021, **35**, 1-16. <https://doi.org/10.1002/aoc.6056>
23. M. D. Raicopol, N. A. Chira, A. M. Pandele, A. Hanganu, A. A. Ivanov, V. Tecuceanu, I. G. Bugean and G. O. Buica, Electrodes Modified with clickable Thiosemicarbazone Ligands for Sensitive Voltammetric detection of Hg(II) ions, *Sens. Actuators B. Chem.*, 2020, **313**, 128030. <https://doi.org/10.1016/j.snb.2020.128030>
24. B. Zhang, H. Luo, Q. Xu¹, L. Lin and B. Zhang, Antitumor Activity of a *Trans*-Thiosemicarbazone Schiff base Palladium(II) Complex on Human Gastric Adenocarcinoma Cells, *Oncotarget.*, 2017, **8(8)**, 13620-13631.
<https://dx.doi.org/10.18632/oncotarget.14620>

25. O. K. Nehar, R. Mahboub, S. Louhibi, T. Roisnel and M. Aissaoui, New Thiosemicarbazone Schiff base Ligands: Synthesis, Characterization, Catecholase Study and Hemolytic Activity, *J. Mol. Struct.*, 2020, **1204**, 127566.
<https://doi.org/10.1016/j.molstruc.2019.127566>
26. <https://www.britannica.com/science/activation-energy>
27. <https://www.thoughtco.com/arrhenius-equation-4138629>
28. <https://www.priyamstudycentre.com/2019/09/vant-hoff-equation.html>

Synthesis of Curcumin-pyrazole Lanthanide (Pr^{3+} , Nd^{3+} , Eu^{3+} and Gd^{3+}) Complexes and Investigation of their Spectroscopic Studies

Abstract

A series of new lanthanide complexes $[\text{LnCl}_3 \cdot x\text{H}_2\text{O} : (\text{L}^3)_3]$ (where; L^3 =curcumin-pyrazole and $\text{Ln} = \text{Pr}^{3+}$, Nd^{3+} , Eu^{3+} and Gd^{3+}) have been synthesized in ethanol under reflux conditions for 24 hours. The synthesized curcumin-pyrazole lanthanide complexes; $[\text{L}^3_3\text{PrCl}_3 \cdot \text{H}_2\text{O}]$ (**4.1a**), $[\text{L}^3_3\text{NdCl}_3 \cdot 6\text{H}_2\text{O}]$ (**4.1b**), $[\text{L}^3_3\text{EuCl}_3 \cdot 6\text{H}_2\text{O}]$ (**4.1c**), $[\text{L}^3_3\text{GdCl}_3 \cdot 6\text{H}_2\text{O}]$ (**4.1d**) were characterised by elemental analysis, IR, UV-Vis, fluorescence and TGA. The formations of the nona-coordinated lanthanide complexes have been detected through elemental analysis. In IR-spectra, the formation of the new band at 460 cm^{-1} has been assigned to the metal-nitrogen stretching vibration which has conveyed that nitrogen atom of the ligand is being co-ordinated to the lanthanide. Absorption intensity as well as luminescence properties of the synthesized complexes were analysed through UV-Vis and fluorescence spectra. The percentage weight loss of the complexes was studied with TGA analysis. Further the quantum yields of the curcumin-pyrazole ligand (L^3) and its lanthanide complexes (**4.1a-d**) have been analyzed.

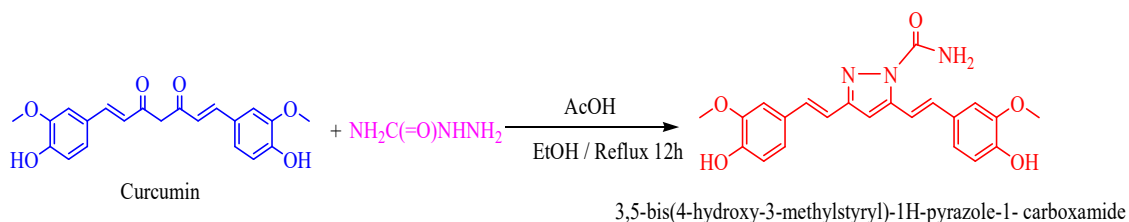
4.1. Introduction

For decades Pyrazole and its derivatives have been attracting many researchers for their diverse properties and application. Traditionally they are used as basis for drug and dyes and with the further studies they were found to be an intermediate for the synthesis of organic compounds.¹ Pyrazoles possess varied biological activities as antifungal, antitumor and antiviral activities as a result of their varied bonding capabilities. The coordination chemistry of pyrazoles has been intensively investigated as Lanthanide chelate.² The synthesis of pyrazole is the on-going attention due to their remarkable applications in pharmaceutical and agrochemical industry. Pyrazole is also well known for its role as anti-inflammatory.³⁻⁶ Pyrazoles are stable thermally and hydrolytically. When they are coordinated to metal to form complexes, they deprotonated to form pyrazolate ion and can be coordinated to the metal or metalloid ion through both the nitrogen atoms as bidentate ligand.⁷

Pyrazole itself has many potentialities but when they react with other compounds, they produce more numerous applications in various fields; pharmacy, agro-chemical, dyes for

food and medicine, colour photography, drug development, catalyst or ligand in organic, inorganic and organometallic reactions as they possessed multiple potentiality such as pharmacophore, anti-cancer, anti-viral, anti-bacterial, anti-microbial, anti-allergy, anti-inflammatory, anti-glycemic chemosensors, corrosion inhibitor, bio-degradable polymer, building blocks for other compounds.⁸⁻¹³ One of the most studied pyrazole derivatives are the curcumin containing pyrazole ring and when this are investigated alone with the various curcumin derivatives, the curcumin based pyrazole showed better biological activity than the parent curcumin.¹⁴⁻¹⁶ Looking into the multiple applications of the pyrazole and its complexes some of the recent indagation are mention below.

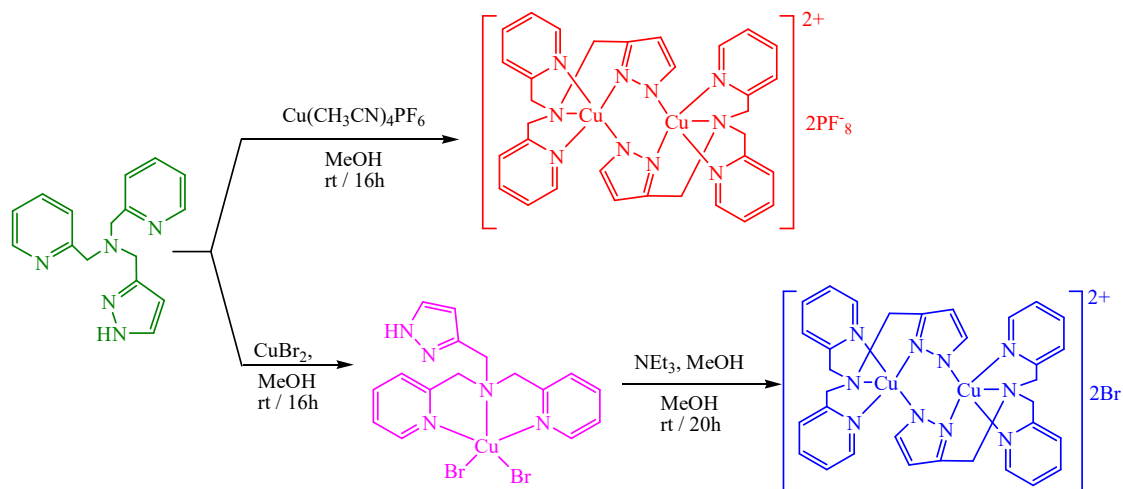
With the increasing cases of cancer with almost 8% death rate (WHO World Cancer Report **2014**), M. J. Ahsan and collaborator in **2015** synthesized curcumin derivative containing pyrazole ring (**Scheme 4.1**) which possessed anti-proliferative activity. The synthesized compounds were characterized with different spectral datas; IR, NMR, and mass. The docking studies show its binding interaction with the epidermal growth factor receptor tyrosine kinase. Against the Leukemia cell 3,5-bis(4-hydroxy-3-methylstyryl)-1H-pyrazole-1-carboxamide was found to have better activity when compared with the standard drug paclitaxel.¹⁷



Scheme 4.1. Synthesis of 3,5-bis(4-hydroxy-3-methylstyryl)-1H-pyrazole-1-carboxamide.

As the metal-organic frameworks (MOFs) has become an encouraging field due to its potentiality as an optical materials, catalyst and energy storage. Organic ligands with good building blocks in structuring MOFs play an important role in the coordination. J. Liu *et al.* (**2016**) derived metal complexes containing pyrazole ring. The synthesized complexes were investigated for crystal structure, luminescence properties and electrolytic properties. At room temperature the complexes were found to exhibit green florescence and they were found to have outstanding catalytic activity for oxygen evolution and oxygen reduction reactions.¹⁸ A mono and binuclear Cu(II) complexes were synthesized (**Scheme 4.2**) and reported by Wenjing ye and group in **2017** which exhibit an

unsymmetrical bipyridine-pyrazole-amine as a ligand. The complexes were characterized by X-ray diffractions and the transition metal complexes were found to possess an excellent catalyst activity. Further studies show their potentiality for preparation of biological compounds.¹⁹



Scheme 4.2. Synthesis of Copper(II) complexes.

For the past few years the detection of the metal in the environment has become a concern as it is a threat to living organisms and human health and with its application of chemical sensor has become an interest. N. Nayak and co-worker in **2018** synthesized and reported two pyrazole Cu(II) complexes exhibiting an excellent colorimetric sensor for the detection of Cu^{2+} ions. Spectral data were analyzed by different spectroscopic methods and proposed a structure for the complexes (**Figure 4.1**).²⁰

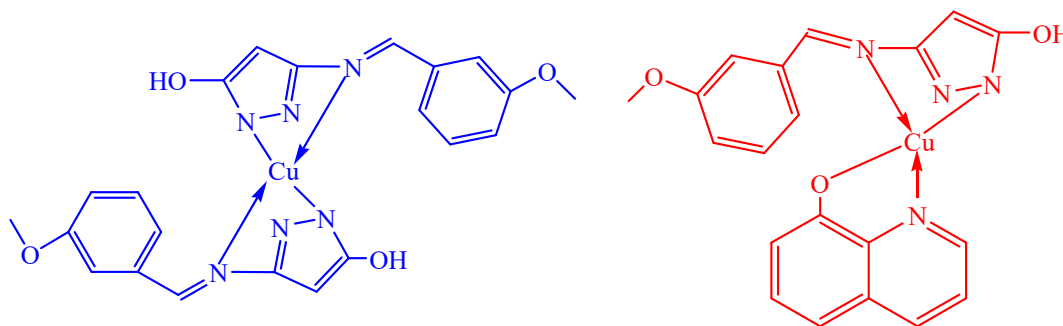
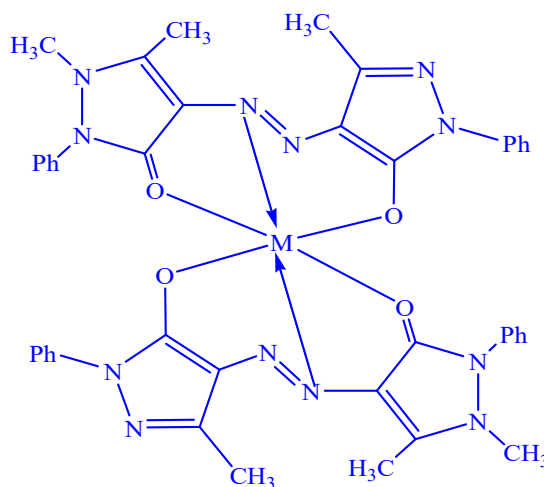


Figure 4.1. Proposed Structure of Cu(II) complexes.

Azo-dyes, an organic compound with chromophoric group plays an important role in industries as color agent and is one of most rapidly developing area of studies as it exhibits multiple applications in various disciplinary. M. N. Matada and K. Jathi in **2019** gave an account on the synthesized embryonic bioactive agents of Pyrazole-based azo-metal(II) complexes. The transition metal complexes were characterized by different spectral and physical approach and studied their anti-microbial activity, showing an increase in activity on coordinating with the metal ions. The DNA binding studies also shows a potent binding quality.²¹



M = Cu(II), Co(II), Ni(II), Mn(II) and Zn(II)

Figure 4.2. Structure of the Pyrazole-based Azo-metal(II) Complexes.

K. Kumarasamy *et al.* (**2020**) synthesized a series of pyrazole and pyridine and their cyclometalated complexes as this variety of complexes mainly complexes of palladium(II) and platinum(II) are attracting the interest of the researcher now days as they can act as the backbone of the catalytic means. The synthesized ligand and complexes (**Figure 4.3**) were specified by different spectroscopic approach such as the NMR, Mass, FT-IR, UV-Vis and elemental analysis. On examining the structure of the compounds with X-ray crystallography the bond length of the ligand was found to be shorter when compared with the coordinated complexes. After the coordination of the ligand and the metal, a red-shift was notice in UV-Vis spectra.²²

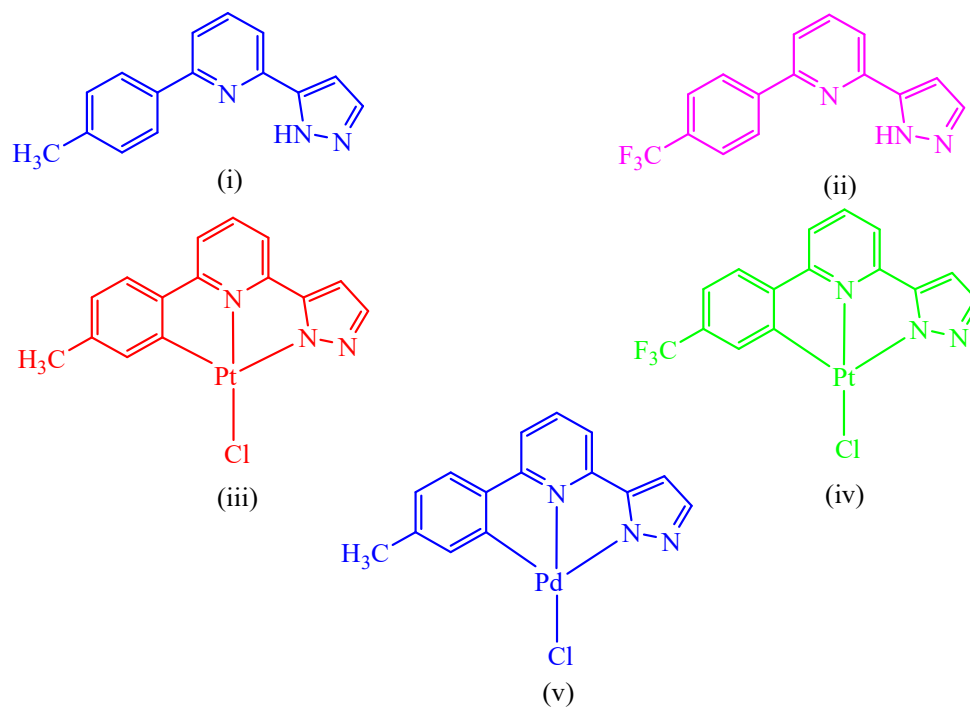


Figure 4.3. Structure of the Pyrazole possessing C, N, N ligand (i and ii) and its Cyclometalated Complexes (iii, iv and v).

Fluorescent substance with multiple application and quantum yield has become one of the main focuses for the researchers and so, C. Amoah *et al.* **2021** has synthesized a complex of palladium metal of pyrazole ligand and specified them with various spectral methods. On addition of the Pd^{2+} ions, there is depletion in quantum yield and intensity of the fluorescence which gives it potentiality to be used as a probe in fluorogenic and for the identification of substances in biological system.²³ A synthesis of Metal complexes of Co(II) and Ni(II) with N, S donor of pyrazole derivatives were reported by B. Saltani and fellow worker. All the synthesized complexes were features by spectroscopic methods, crystal structure and physicochemical. Coordination geometry of a square planner for both the complexes found through X-ray crystallography was reported. The complexes were found to have an excellent anti-bacterial activity.²⁴

J. Khanagwal *et al.* (**2020**) reported four europium(III) complexes (**Figure 4.4**) of carboxylate ligand, 1-(4-methoxyphenyl)-5-(trifluoromethyl)-1*H*-pyrazole-4-carboxylic acid, bathophenanthroline and 1,10-phenanthroline and 2,2-bipyridyl which were synthesized and look into their thermal stability, emission intensity, quantum efficiency, Judd-ofelt parameters, their energy transfer process. The complexes show potentiality for

devices such as display, laser, luminescent and they also shows anti-microbial and anti-oxidant activity.²⁵

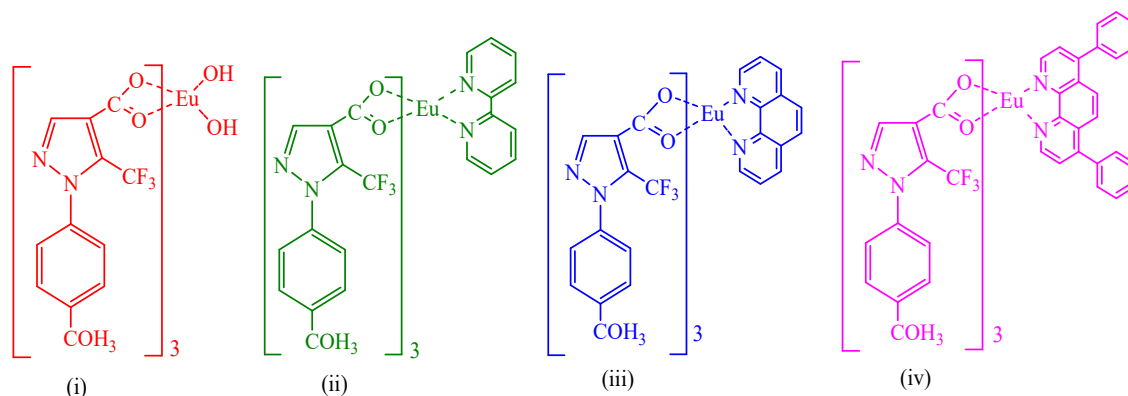


Figure 4.4. Chemical Structures of Ligand in Coordinated to Europium(III) ion.

Coordination polymer is considered as one of the most beneficial material as they shows extensive spectrum of potentiality. D Vlasjuk and R. Lyszczyk in **2021** giving consideration to the applications synthesized and distinguished a series of coordination polymer of pyrazole by-product with some selected lanthanide(III) ions. Mechanochemical and hydrothermal process was implies for the reaction of the complexes and outlined that the complex synthesized from the hydrothermal process were found to be more stable thermally. Degradation of the complexes were found to produce not only H₂O and CO₂ but also pyrazole molecule and so the lanthanide complexes decomposition can be used as a catalyst impact on pyrazole molecule.²⁶

Such important activities of pyrazole and its complexes caught us to synthesis curcumin-pyrazole and utilize it as ligands with Lanthanides which have several unique characteristic properties compared to other elements; since the f-orbital's are filled gradually they have varied coordinating capacities and specify its spectroscopic, physico-chemical and thermally.

4.2. Experimental

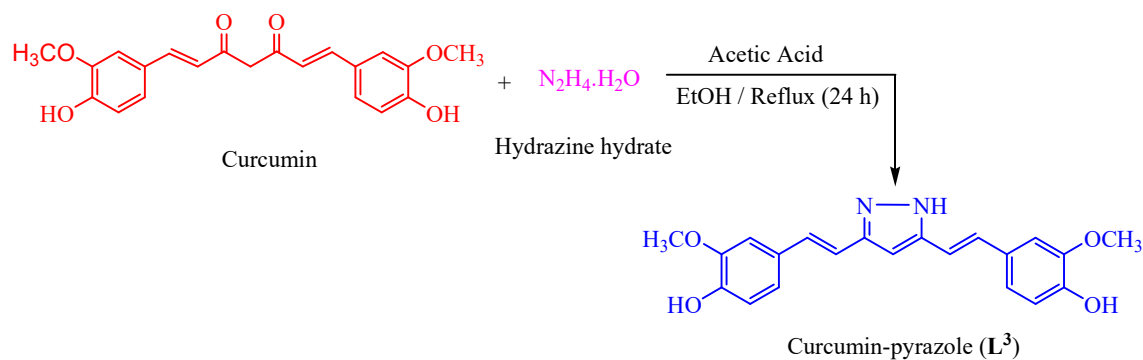
4.2.1. Materials and Methods

All the reagents and solvents were purchased from commercially available sources and used without further purification. FTIR spectra of the curcumin ligand and its lanthanide complexes were recorded on Perkin-Elmer spectrophotometer (Spectrum-Two)

using KBr disk and values are expressed in cm^{-1} . Micro analytical (CHN) data were obtained with a FLASH EA 1112 Series CHNS analyzer. UV-visible spectrophotometer (Double Beam) Perkin Elmer, Lambda-35 is used for recording the absorption bands of the curcumin ligand and its lanthanide complexes. All fluorescence emission spectra of curcumin-pyrazole ligand and its lanthanide complexes were recorded using fluorescence spectrophotometer Shimadzu RF-6000 which is followed by the evaluation of their quantum yields. The TGA-DTA measurements of curcumin ligand and its lanthanide complexes were performed on a Perkin-Elmer analyzer in air over the temperature range of 25-900°C.

4.2.2. Synthesis of Curcumin-pyrazole Ligand (L^3)

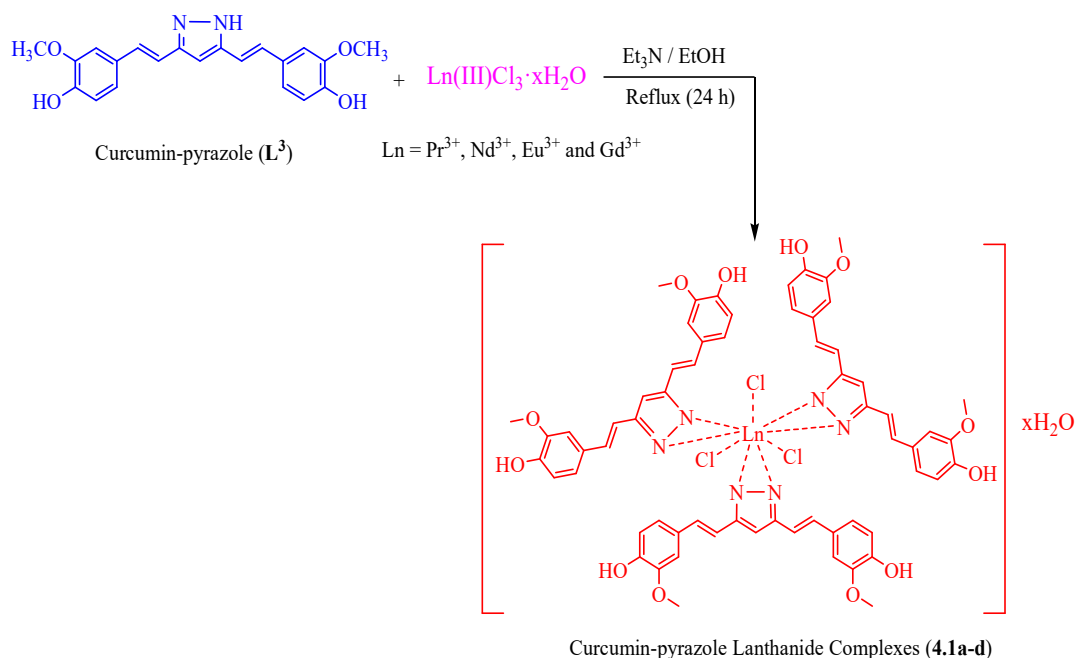
Solution of curcumin [1,7-bis(4-hydroxyl-3-methoxyphenyl)-1,6-heptadiene-3, 5-dione] (0.368g, 1mmol) in ethanol medium was kept with continuous stirring in a magnetic stirrer. Then to the reaction mixture was added hydrazine hydrate (0.050g, 1 mmol) and catalytic amount of acetic acid. The process of the reaction was monitor using thin layer chromatography. The reaction mixture was clear bright orange in colour on addition of the acetic acid which turns to dark orange after 30 minutes of refluxing and on continuing the reaction it turns to dark brown solution. After the completion of the reaction the solvent was allowed to evaporate completely giving a sticky compound to which crushed ice were added forming a pale yellow compound which was collected through normal filtration and air dried after several washing with ice cold water (**Scheme 4.3**).²⁷



Scheme 4.3. Synthesis of Curcumin-pyrazole Ligand (L^3).

4.2.3. General Synthesis of Curcumin-pyrazole Lanthanide(III) Complexes $[L^3LnCl_3 \cdot xH_2O]$ (4.1a-d)

The complex of the lanthanides were synthesized by taken curcumin-pyrazole (3 mmol) in ethanol medium (5 ml) in a round bottom flask at 100°C to it was added $LnCl_3 \cdot xH_2O$; (where; $Ln = Pr^{3+}$, Nd^{3+} , Eu^{3+} and Gd^{3+}) (1 mmol). To the reaction mixture was added catalytic amount of triethylamine (Et_3N) and was kept for refluxing for 24 hours. After which the reaction was allowed to evaporate the solvent completed on evaporation the reaction mixture form dark brown sticky compound which was washed with hexane for several time giving a greenish colored compound which was collected trough filtration. The complexes $[L^3PrCl_3 \cdot H_2O]$ (4.1a), $[L^3NdCl_3 \cdot 6H_2O]$ (4.1b), $[L^3EuCl_3 \cdot 6H_2O]$ (4.1c), $[L^3GdCl_3 \cdot 6H_2O]$ (4.1d) were allowed to air dried (Scheme 4.4).



Scheme 4.4. Synthesis path way of curcumin-pyrazole lanthanide complexes (4.1a-d).

4.3. Results and Discussion

In this chapter, we reported a synthesis of curcumin-pyrazole lanthanide complexes (4.1a-d). The ligand curcumin-pyrazole (L^3) was prepared from a reaction of curcumin and Hydrazine hydrate with a catalytic amount of CH_3COOH in ethanol and reflux for a day which was then used as a ligand (L^3) and curcumin-pyrazole lanthanide metal complexes were then synthesized with selected lanthanide metal chlorides ($LnCl_3 \cdot xH_2O$; $Ln = Pr^{3+}$, Nd^{3+} , Eu^{3+} and Gd^{3+}) in 3:1 ratio in presence of catalytic amount of Et_3N in ethanol and

reaction mixture was kept under reflux condition for 24 hours. The solvent was completely evaporated by removing the condenser after 24 hours of refluxing. The yielded solid which was collected through filtration and the washed with hexane for several times and is allowed to air dried and then collected. The synthesized solid curcumin-pyrazole lanthanide complexes (**4.1a-d**) were stable at room temperature, which were characterized for various spectroscopic properties. The resulting curcumin-pyrazole lanthanide complexes were well studied for FT-IR spectroscopy, UV-Visible spectroscopy, Fluorescence spectroscopy, TGA-DTA analysis and elemental analysis. **Tables 4.1** represent the physico-analytical data of free curcumin-pyrazole ligand (**L³**) and curcumin-pyrazole lanthanide complexes (**4.1a-d**).

Table 4.1. Physico-chemical properties of Curcumin-pyrazole ligand (**L³**) and its Lanthanide Complexes (**4.1a-d**).

Compounds	Yield (%)	Color	CHN Analysis (%) Found(calculated)		
			Carbon	Hydrogen	Nitrogen
Curcumin-pyrazole (L³)	98.93%	Light Brown	66.17 (66.06)	5.58 (5.53)	7.62 (7.69)
[L³ PrCl ₃ ·H ₂ O] (4.1a)	93.47%	Brown	55.36 (55.45)	5.08 (5.02)	6.21 (6.16)
[L³ NdCl ₃ ·6H ₂ O] (4.1b)	86.57%	Brown	51.85 (51.90)	5.32 (5.39)	5.81 (5.76)
[L³ EuCl ₃ ·6H ₂ O] (4.1c)	56.00%	Brown	51.72 (51.63)	5.31 (5.36)	5.78 (5.73)
[L³ GdCl ₃ ·6H ₂ O] (4.1d)	82.11%	Dark Brown	51.32 (51.44)	5.29 (5.34)	5.78 (5.71)

4.3.1. FT-IR Spectral Characterization Studies

4.3.1.1. FT-IR spectra of Curcumin-pyrazole Ligand (L^3)

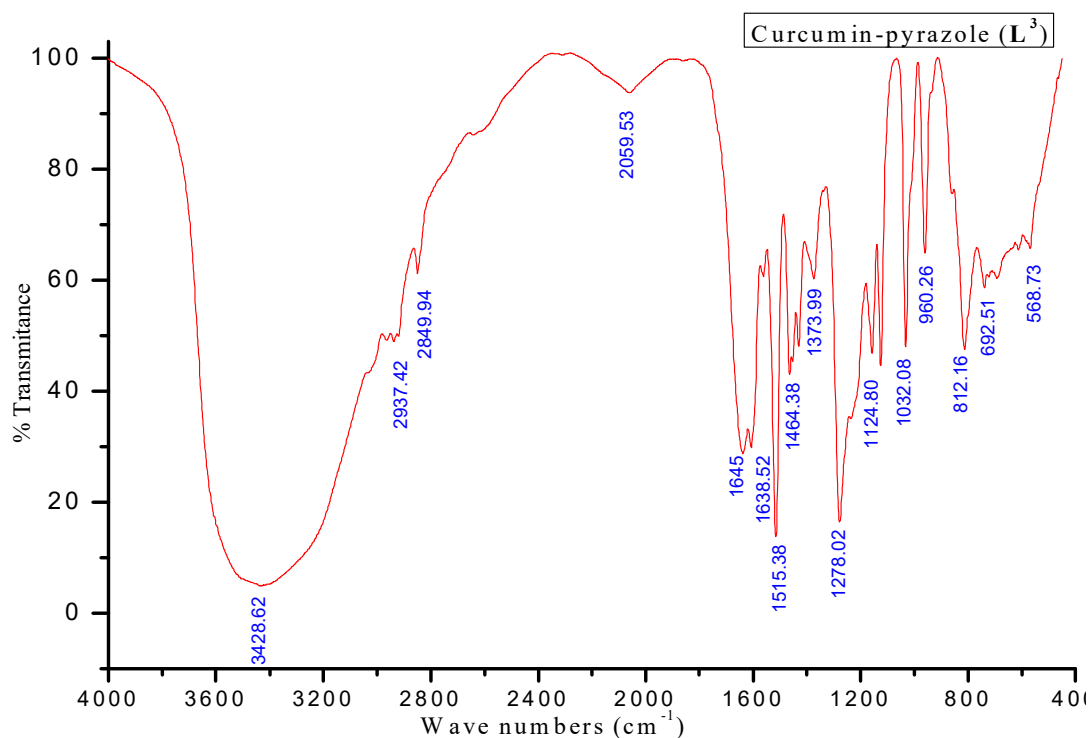


Figure 4.5. FT-IR Spectra of Curcumin-pyrazole ligand (L^3).

The FT-IR spectrum of the curcumin-pyrazole ligand (L^3) (Figure 4.5 and Table 4.1), shows a peak at 3428 cm^{-1} attributing to the OH stretching and absorption at 3325 cm^{-1} and 3000 cm^{-1} attributing to aromatic NH and CH. The band appears at 1638 cm^{-1} is due to the C=N stretching frequencies. A sharp and high intensity band at 1515 cm^{-1} corresponds to the C=C stretching vibrations and another characteristic band appeared at 1278 cm^{-1} attributed to C-N stretching frequencies. The band at 1464 cm^{-1} and 1430 cm^{-1} indicate the aromatic C-C stretching and the bands at 1278 cm^{-1} and 1124 cm^{-1} correspond to phenolic C-O stretching vibrations and a sharp band at 1032 cm^{-1} has been assigned to C-O of the methoxy group. Vibrations band of C-H bond is observed at 955 cm^{-1} and 812 cm^{-1} .

4.3.1.2. FT-IR Spectra of Curcumin-pyrazole Praseodymium Complex $[L^3PrCl_3 \cdot H_2O]$ (4.1a).

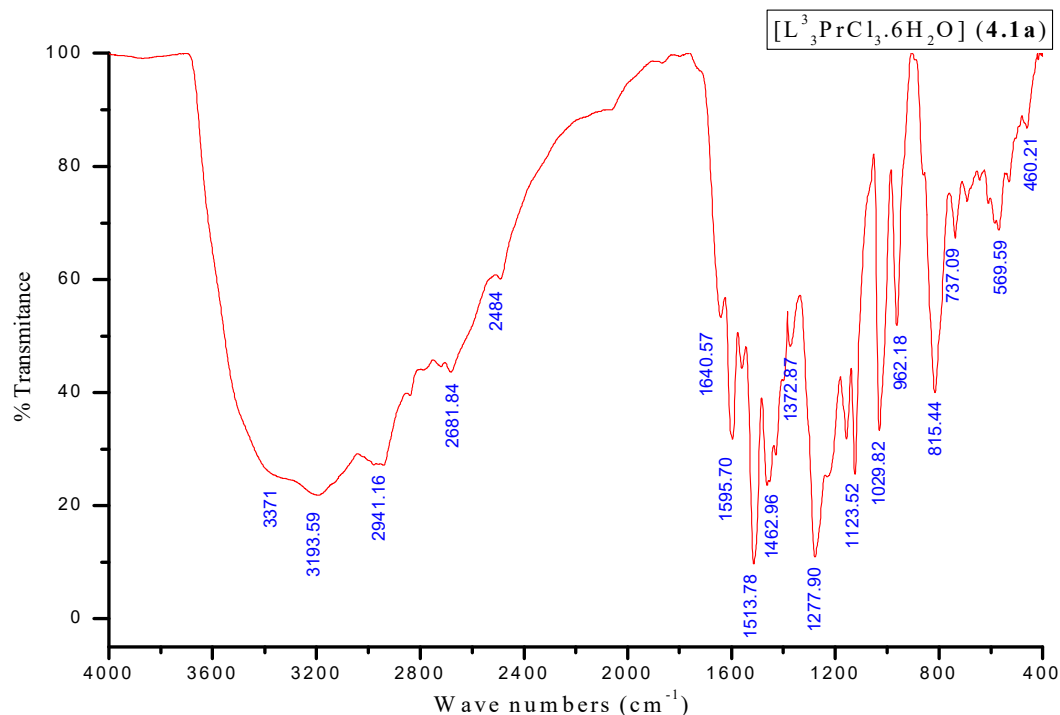


Figure 4.6. FT-IR spectra of Curcumin-pyrazole Praseodymium Complex $[L^3PrCl_3 \cdot H_2O]$ (4.1a).

The FT-IR spectra characterization of curcumin-pyrazole praseodymium complex $[L^3PrCl_3 \cdot H_2O]$ (4.1a) (Figure 4.6 and Table 4.1) shows that the OH stretching at 3428 cm^{-1} which was appeared in the free ligand shifted to a lower wavelength at 3362 cm^{-1} along with a new band at 3193 cm^{-1} which form into a broader band after complexation showing the presence of H_2O in the complex. The prominent bands appeared in the free curcumin-pyrazole ligand indicating the mixed vibrations of C=C and C=N stretching at 1607 cm^{-1} and 1515 cm^{-1} were completely shifted to lower frequencies values at 1595 cm^{-1} and 1513 cm^{-1} and the band at 1638 cm^{-1} shifted to higher wavelength 1640 cm^{-1} . The shifting of the bands in the complex IR spectra is strongly signifying that the praseodymium metal coordinate to curcumin-pyrazole ligand. The band at 3325 cm^{-1} and 3000 cm^{-1} indication the mixed vibration of N-H and C-H in the ligand shifting to a lower frequency at 3321 cm^{-1} and 2999 cm^{-1} and the appearance of a new band at 460 cm^{-1} assigning to the M-N stretching vibrations which was not found in the spectra of free ligand (L^3), clearly suggests that the nitrogen atoms of the ligand are coordinating to the

lanthanide metal leading to the formation of praseodymium lanthanide complex with the curcumin-pyrazole ligand.

4.3.1.3. FT-IR Spectra of Curcumin-pyrazole Neodymium Complex [$L^3NdCl_3 \cdot 6H_2O$] (4.1b).

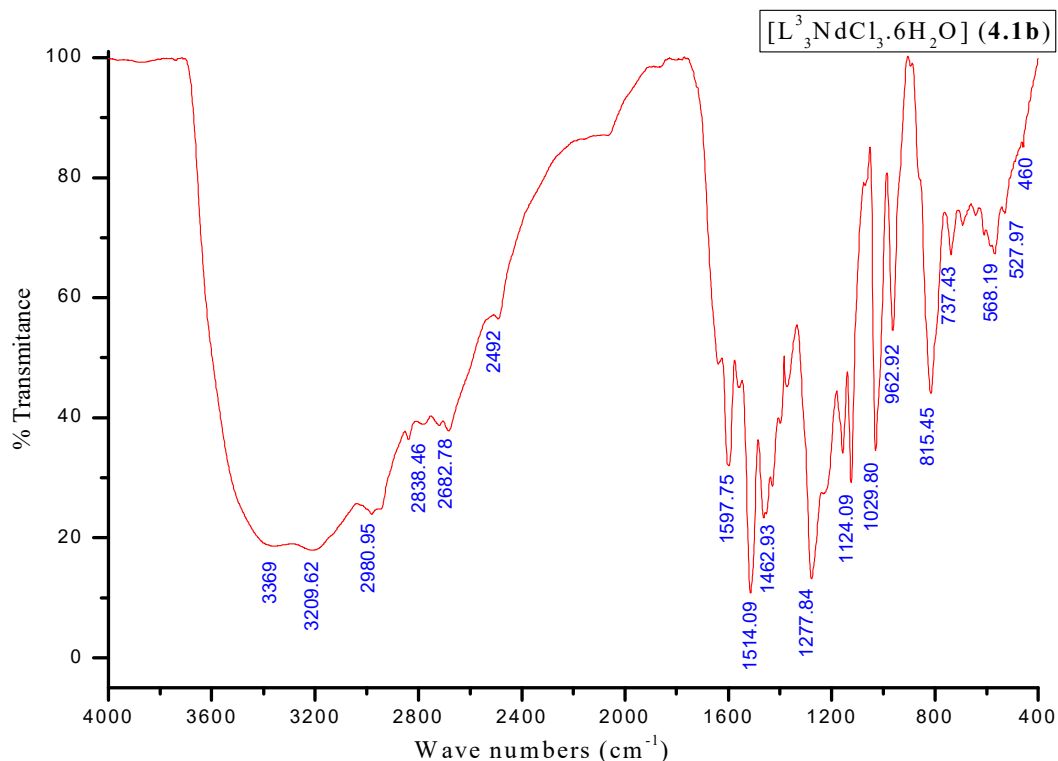


Figure 4.7. FT-IR Spectra of Curcumin-pyrazole Neodymium Complex [$L^3NdCl_3 \cdot 6H_2O$] (4.1b).

Analyzing the FT-IR spectrum of curcumin-pyrazole neodymium complex [$L^3NdCl_3 \cdot 6H_2O$] (4.1a) (Figure 4.7 and Table 4.2) shows that the band at 3428 cm^{-1} assigning to OH stretching which appeared in the free ligand at shifted to a lower frequency at 3368 cm^{-1} in conjunction with a band at 3209 cm^{-1} forming into a broader band after complexation which showing the presence of H_2O in the complex. The prominent bands appeared in the free curcumin-pyrazole ligand (L^3) indicating the mixed vibrations of C=C and C=N stretching at 1607 cm^{-1} and 1515 cm^{-1} were completely shifted to lower frequencies values at 1595 cm^{-1} and 1514 cm^{-1} and the band at 1638 cm^{-1} shifted to higher wavelength 1639 cm^{-1} . The shifting of the bands in the complex IR spectra is strongly signify that the praseodymium metal coordinate to curcumin pyrazole ligand. The band at 3324 cm^{-1} and 2998 cm^{-1} indicating the mixed vibration of N-H and C-H shifted to

a lower frequencies which was shown at 3325 cm^{-1} and 3000 cm^{-1} in the free ligand and the appearance of a new band at 460 cm^{-1} attributing to the M-N stretching vibrations which was not found in the spectra of free ligand (L^3), clearly suggests that the nitrogen atoms of the ligand are coordinating to the lanthanide metal leading to the formation of neodymium lanthanide complexes with the curcumin pyrazole ligand.

4.3.1.4. FT-IR Spectra of Curcumin-pyrazole Europium Complex $[L^3EuCl_3 \cdot 6H_2O]$ (4.1c).

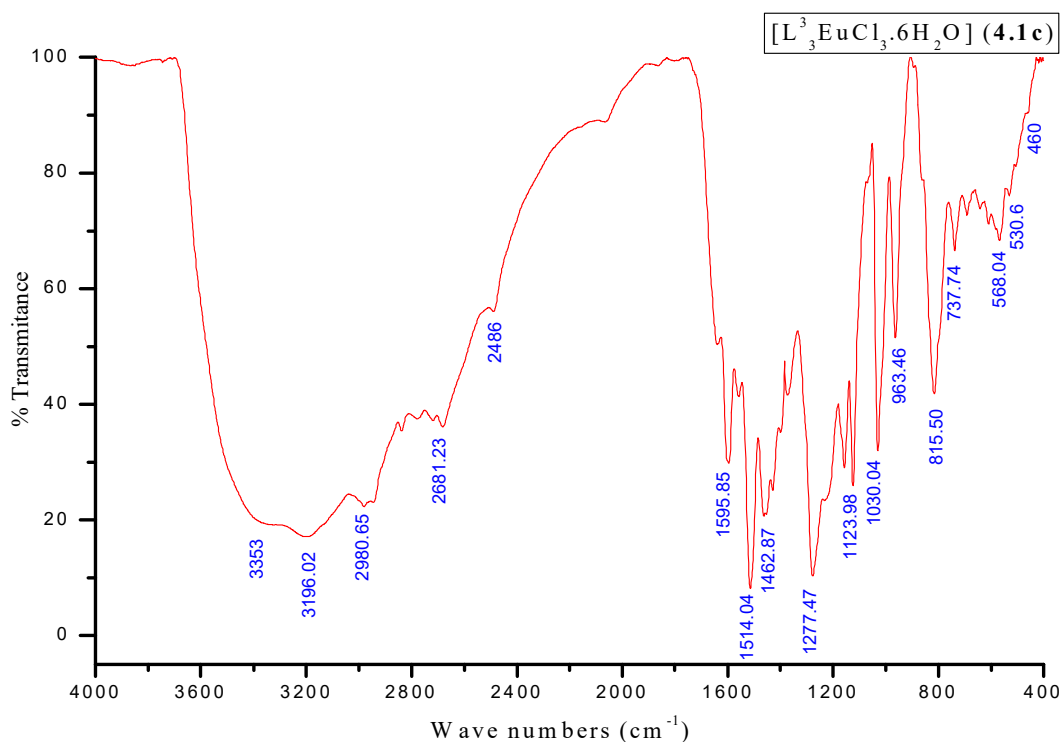


Figure 4.8. FT-IR Spectra of Curcumin-pyrazole Europium Complex $[L^3EuCl_3 \cdot 6H_2O]$ (4.1c).

The FT-IR spectra characterization of curcumin-pyrazole europium complex (Figure 4.8 and Table 4.2) shows that the prominent bands at 1607 cm^{-1} and 1515 cm^{-1} indicating the mixed vibrations of C=C and C=N stretching in the free Curcumin - pyrazole ligand were completely shifted to lower frequencies values at 1597 cm^{-1} and 1514 cm^{-1} and the band at 1638 cm^{-1} shifted to higher wavelength 1639 cm^{-1} which strongly signify that the europium metal coordinate to the N of curcumin-pyrazole ligand (L^3). The OH stretching at 3423 cm^{-1} which appeared in the free ligand shifted to a lower wavelength at 3355 cm^{-1} along with a band at 3196 cm^{-1} forming a broader band indicating the

presence of water molecule in the complex. The appearance of another new band at 459 cm^{-1} assigning to the M-N stretching vibrations and the shifting of the band at 3325 cm^{-1} and 3000 cm^{-1} indicating the mixed vibration of N-H and C-H in curcumin pyrazole ligand (L^3) to a lower wavelength in the $[\text{L}_3\text{EuCl}_3 \cdot 6\text{H}_2\text{O}]$ (**4.1c**) clearly indicating the nitrogen atoms of the ligand coordinating to the europium lanthanide metal leading to the formation of europium lanthanide complexes with the curcumin pyrazole ligand.

4.3.1.5. FT-IR Spectra of Curcumin-pyrazole Gadolinium Complex $[\text{L}_3\text{GdCl}_3 \cdot 6\text{H}_2\text{O}]$ (**4.1d**).

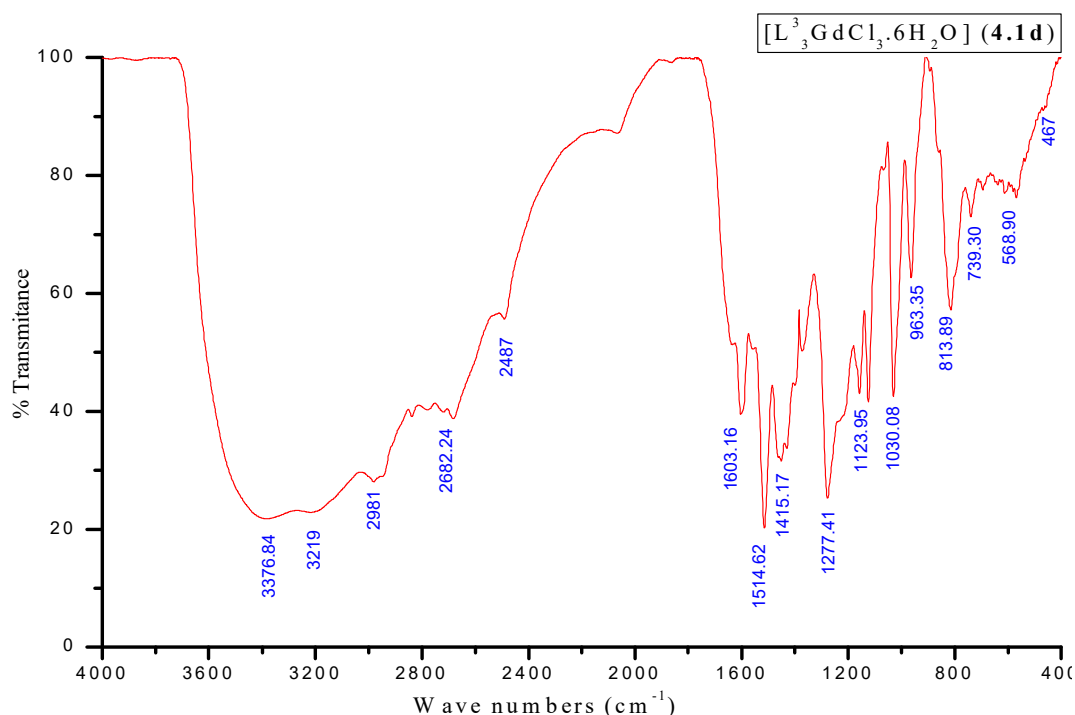


Figure 4.9. FT-IR Spectra of Curcumin-pyrazole Gadolinium complex $[\text{L}_3\text{GdCl}_3 \cdot 6\text{H}_2\text{O}]$ (**4.1d**).

The FT-IR spectra characterization of curcumin-pyrazole gadolinium complex $[\text{L}_3\text{GdCl}_3 \cdot \text{H}_2\text{O}]$ (**4.1d**) shows that the prominent bands appeared in the free curcumin-pyrazole ligand indicating the mixed vibrations of C=C and C=N stretching at 1607 cm^{-1} and 1515 cm^{-1} were completely shifted to lower frequencies values at 1603 cm^{-1} and 1514 cm^{-1} and the band at 1638 cm^{-1} shifted to higher wavelength 1641 cm^{-1} . The shifting of the bands in the complex IR spectra is strongly signifying that the gadolinium metal coordinate to the N of curcumin-pyrazole ligand (L^3). The OH stretching at 3428 cm^{-1} which was appeared in the free ligand shifted to a lower wavelength at 3376 cm^{-1} along with a band at

3192 cm^{-1} giving a broad band indicating the existence of water molecule after formation of complex. The shifting of the band at 3325 cm^{-1} and 3000 cm^{-1} to 2981 cm^{-1} and 2682 cm^{-1} attributing to N-H and C-H bond and appearance of another new band at 467 cm^{-1} assigning to the M-N stretching vibrations which was not found in the spectra of free ligand (L^3), clearly suggests that the nitrogen atoms of the ligand are coordinating to the gadolinium lanthanide metal leading to the formation of gadolinium lanthanide complexes with the curcumin-pyrazole. (**Figure 4.9** and **Table 4.2**).

The results of the FT-IR spectra of all the curcumin-pyrazole lanthanide complexes (**4.1a-d**) along with curcumin-pyrazole ligand (L^3) are tabulated in **Table 4.2**

Table 4.2. Major FT-IR Spectral data of the Curcumin-pyrazole (**L**³) and its Lanthanide Complexes (**4.1a-d**) (cm⁻¹).

Compounds	$\nu(\text{ArOH}, \text{OH})$	$\text{Ar } \nu \text{ CH}$	$\text{Ar}\nu(\text{NH})$ (CH)	$\nu(\text{C}=\text{C})$ (C=N)	$\text{Ar}\nu(\text{CC})$	$\nu(\text{C}-\text{O})$	$\nu(\text{C}-\text{H})$	$\nu(\text{M}-\text{N})$
Curcumin-pyrazole (L ³)	3428	2937, 2849	3325, 3000	1638,1607, 1514	1464, 1430	1278, 1124	812	-
[L ³ PrCl ₃ ·H ₂ O](4.1a)	3362, 3193	2941, 2681	3321, 2999	1640,1595, 1513	1462, 1428	1277, 1123	815	460
[L ³ NdCl ₃ ·6H ₂ O](4.1b)	3368, 3209	2980, 2682	3324, 2998	1639,1595, 1514	1462, 1429	1277, 1123	815	460
[L ³ EuCl ₃ ·6H ₂ O](4.1c)	3355, 3196	2980, 2681	3323, 2998	1639,1597, 1514	1462, 1428	1277, 1123	815	459
[L ³ GdCl ₃ ·6H ₂ O](4.1d)	3376, 3192	2981, 2682	3324, 2999	1641,1603, 1514	1451, 1430	1277, 1123	813	467

4.3.2. UV-Vis Spectral Characterization Studies

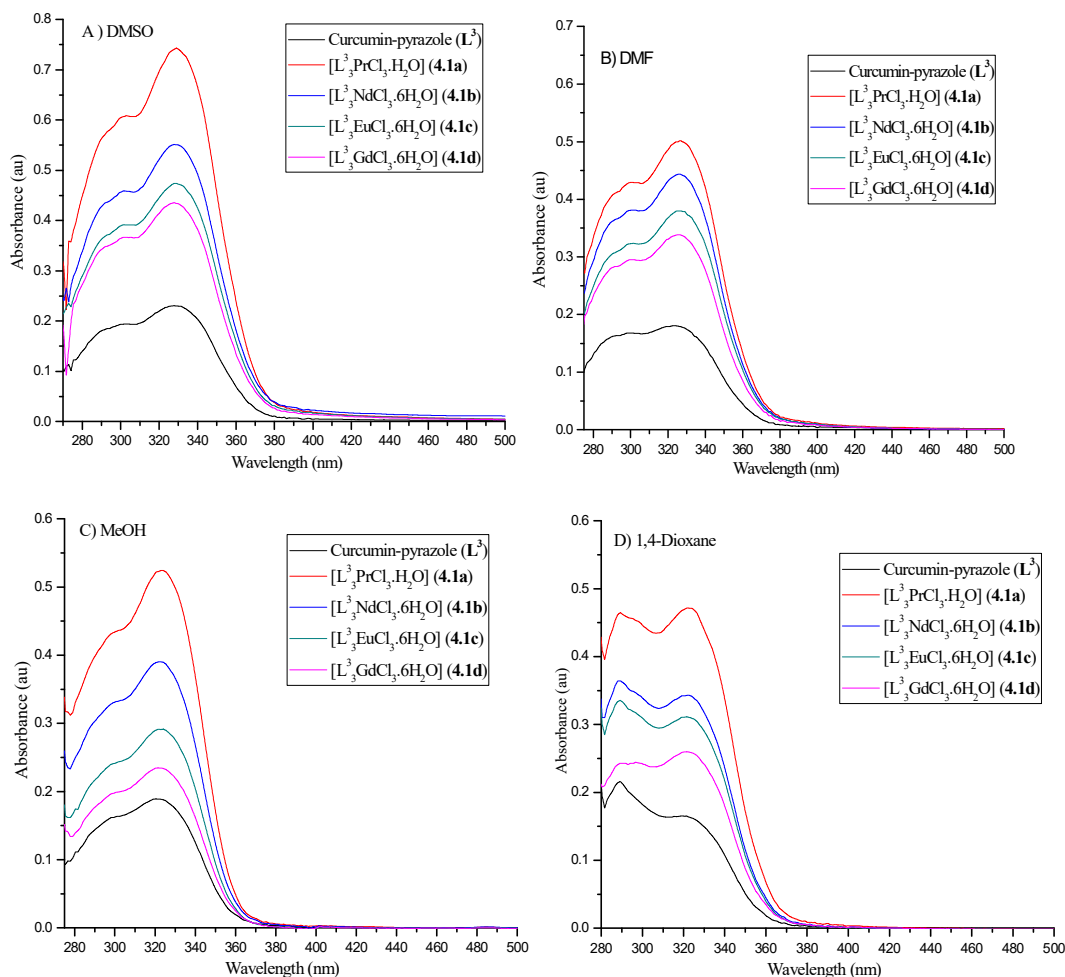


Figure 4.10. UV-Vis spectra of Curcumin-pyrazole ligand (L^3) and its Lanthanide Complexes (**4.1a**) in different solvents (conc. 1×10^{-5} M).

UV-Vis spectra of curcumin-pyrazole ligand (L^3) and its lanthanide complexes (**4.1a-d**) in different solvents such as dimethyl-sulfoxide (DMSO), dimethylformamide (DMF), methanol (MeOH) and 1,4-dioxane were recorded at concentration of 1×10^{-5} M. (**Figure 4.10** and **Table 4.3**) When ligand interacts with the metal ($Ln = Pr^{3+}$, Nd^{3+} , Eu^{3+} and Gd^{3+}) and forms complex, the metal-Ligand bond length is shortened and a strong bond is formed there by increasing the absorption intensity of UV-Vis spectra of the complex compared to the intensity of the absorption spectra of curcumin-pyrazole (Nephelauxetic Effect). In all the solvents (DMF, DMSO, MeOH and 1,4-Dioxane), the intensity of the pure ligand and complexes are in the order $[L^3PrCl_3 \cdot H_2O]$ (**4.1a**) > $[L^3NdCl_3 \cdot 6H_2O]$ (**4.1b**) > $[L^3EuCl_3 \cdot 6H_2O]$ (**4.1c**) > $[L^3GdCl_3 \cdot 6H_2O]$ (**4.1d**) > Curcumin pyrazole ligand (L^3) which

is in the same order of the electronegativity in the periodic table. This trend of sensitivity of absorption intensity of ligand and complexes is shown in the **Figure 4.10** and **Table 4.3**. The sensitivity of the solvents are in the order of 1,4-dioxane < DMF < MeOH < DMSO which may be due to the polarity effect. In the entire medium used the maximum absorption was at around 320 nm-330 nm and a shoulder band at 288 nm-300 nm except for in MeOH medium there is no shoulder band. With the polarity of the solvent there is a shifting in the wavelength which is due to electrostatic interaction between solvent and the curcumin-pyrazole and its complexes, as the solvent incline to stabilized the bond causing $n-\pi^*$ transition and $\pi-\pi^*$ transition.

Table 4.3. UV-Vis Spectral values of Curcumin-pyrazole ligand (L^3) and its Lanthanide complexes (**4.1a-d**).

Compound	DMSO $\lambda_{\max}(\text{a.u})$	DMF $\lambda_{\max}(\text{a.u})$	MeOH $\lambda_{\max}(\text{a.u})$	1,4-Dioxane $\lambda_{\max}(\text{a.u})$
Curcumin-pyrazole (L^3)	299.50(0.1926) 328.55(0.2303)	299.15(0.1676) 325.50(0.1794)	320.80 (0.1897)	288.60(0.2155) 324.35(0.1611)
$[L^3PrCl_3 \cdot H_2O]$ (4.1a)	301.55(0.6061) 329.85(0.7416)	300.45(0.4290) 326.75(0.5018)	322.95 (0.5248)	288.90(0.4649) 322.70(0.4715)
$[L^3NdCl_3 \cdot 6H_2O]$ (4.1b)	302.05(0.4580) 328.10(0.5514)	300.85(0.3803) 325.90(0.4431)	322.10 (0.3902)	289.05(0.3648) 321.40(0.3422)
$[L^3EuCl_3 \cdot 6H_2O]$ (4.1c)	300.75(0.3907) 328.55(0.4733)	300.85(0.3235) 326.35(0.3803)	322.95 (0.2914)	289.50(0.3342) 321.85(0.31154)
$[L^3GdCl_3 \cdot 6H_2O]$ (4.1d)	300.75(0.3952) 328.10(0.4356)	301.30(0.2950) 325.90(0.3387)	322.50 (0.2347)	289.90(0.2423) 321.85(0.2598)

4.3.3. Fluorescence Spectral Characterization Studies

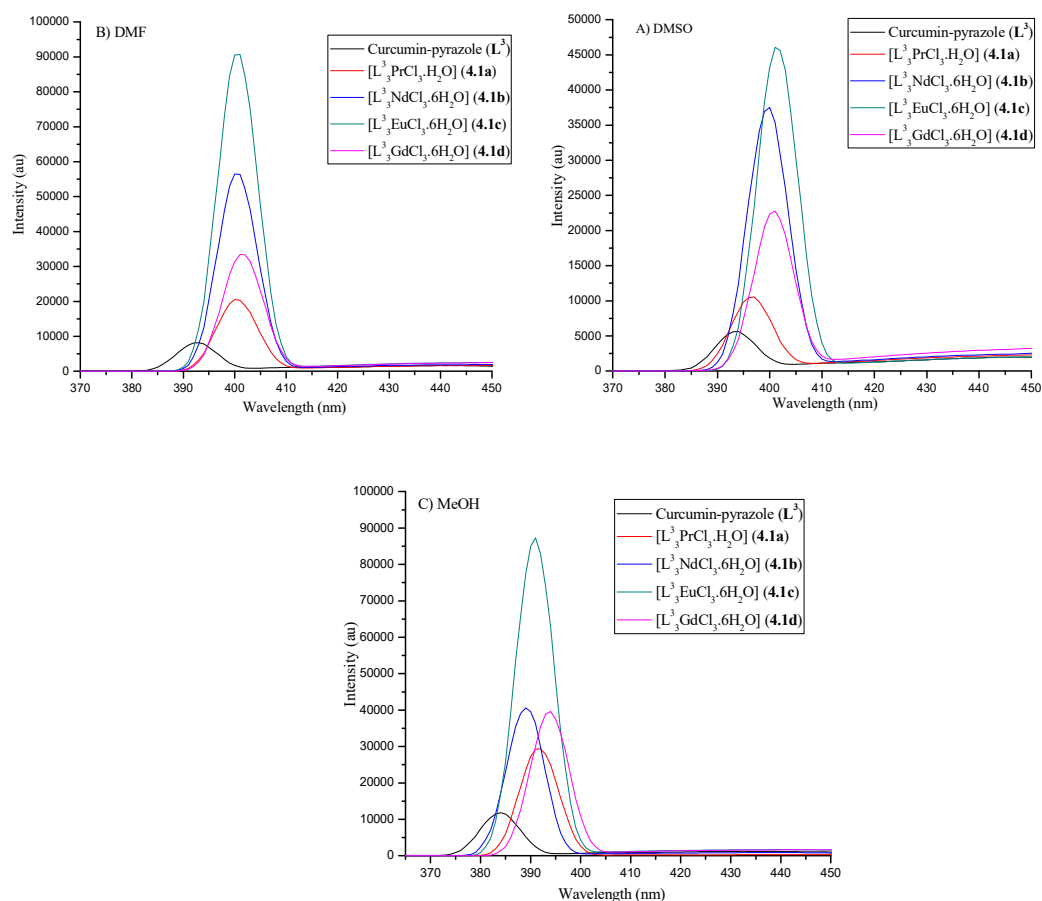


Figure 4.11. Fluorescence Spectra of curcumin-pyrazole ligand (L^3) and its Lanthanide Complexes ($4.1a-d$) in different solvent (conc. 1×10^{-4} M).

The photoluminescence spectra of the curcumin-pyrazole ligand (L^3) and its different lanthanide(III) complexes were recorded in DMSO, DMF and MeOH medium. An organic ligand plays important role to enhance the quantum yield of luminescence emission for the lanthanide metals which is due to the fact that the absorption coefficients of the ligand are manifolds larger than intrinsically low molar absorption coefficient of the Ln(III) ion. It is reflected in the luminescence spectra of pure ligand (L^3) and its lanthanide complexes in the **Figure 4.11**. Analysis of the emission spectra could exhibit the characteristic emission spectra of Pr^{3+} , Nd^{3+} , Eu^{3+} and Gd^{3+} complexes with curcumin-pyrazole ligand (L^3). From which we could easily detect the co-ordination nature as well as the transfer of energy of ligand with lanthanide ions. The fluorescence spectra of a series of lanthanide complexes are found to be red shift (enhancing their wavelengths) shown in

Figure 4.11 and **Table 4.4** it may be due to the complexation of ligand with the rare earth metals.

Referring to the emission values of the Ligand and the corresponding $\text{Ln}^{3+}:(\text{L}^3)_3$ complexes in different solvent (**Table 4.4**) it is reflected that the order of their characteristic emission intensities are in the order $[\text{L}^3\text{EuCl}_3 \cdot 6\text{H}_2\text{O}]$ (**4.1c**) > $[\text{L}^3\text{NdCl}_3 \cdot 6\text{H}_2\text{O}]$ (**4.1b**) > $[\text{L}^3\text{GdCl}_3 \cdot 6\text{H}_2\text{O}]$ (**4.1d**) > $[\text{L}^3\text{PrCl}_3 \cdot \text{H}_2\text{O}]$ (**4.1a**) > L^3 . Again, consequently observing their relative quantum yield value, their luminescence character is in the order of $[\text{L}^3\text{EuCl}_3 \cdot 6\text{H}_2\text{O}]$ (**4.1c**) > $[\text{L}^3\text{NdCl}_3 \cdot 6\text{H}_2\text{O}]$ (**4.1b**) > $[\text{L}^3\text{GdCl}_3 \cdot 6\text{H}_2\text{O}]$ (**4.1d**) > $[\text{L}^3\text{PrCl}_3 \cdot \text{H}_2\text{O}]$ (**4.1a**) > L^3 .

Looking into the luminescent properties, europium complexes particularly act as light conversion molecular devices by absorbing (UV) light and emitting light in the red visible spectral region. The quantum yield of luminescent is defined as the ratio of the number of photons emitted on the number of (UV) photons absorbed. But the higher the quantum yield of luminescent, the higher the sensitivity of the applications. Thus $\text{Eu}^{3+}:(\text{L}^3)_3$ has comparatively higher quantum yield (%) among all the synthesised compounds and higher application may be expected compared to ligand and the other complexes.

Table 4.4. Florescence Spectra and quantum yield for Curcumin-pyrazole ligand (L^3) and its Lanthanide Complexes (**4.1a-d**).

Compound	Solvent	Emission (nm)	Excitation (nm)	Intensity (a.u)	Quantum Yield (Φ_f)
Curcumin – pyrazole (L^3)	DMSO	422	370	12739.9	0.0024
	DMF	417	373	8761.4	0.0017
	MeOH	400	355	2546	0.0010
$[\text{L}^3\text{PrCl}_3 \cdot \text{H}_2\text{O}]$ (4.1a)	DMSO	424	367	14652.3	0.0099
	DMF	418	376	10865.1	0.0036
	MeOH	400	355	3512	0.0022
$[\text{L}^3\text{NdCl}_3 \cdot 6\text{H}_2\text{O}]$ (4.1b)	DMSO	423	370	19961.4	0.0058
	DMF	417	368	11649	0.0023
	MeOH	400	355	4317.1	0.0019
$[\text{L}^3\text{EuCl}_3 \cdot 6\text{H}_2\text{O}]$ (4.1c)	DMSO	421	369	24529.4	0.0038
	DMF	417	364	19558.9	0.0020
	MeOH	400	355	5983.6	0.0018
$[\text{L}^3\text{GdCl}_3 \cdot 6\text{H}_2\text{O}]$ (4.1d)	DMSO	420	366	27406.2	0.0034
	DMF	417	366	23802.4	0.0018
	MeOH	400	355	7651.1	0.0011

4.3.4. Thermogravimetric Analysis

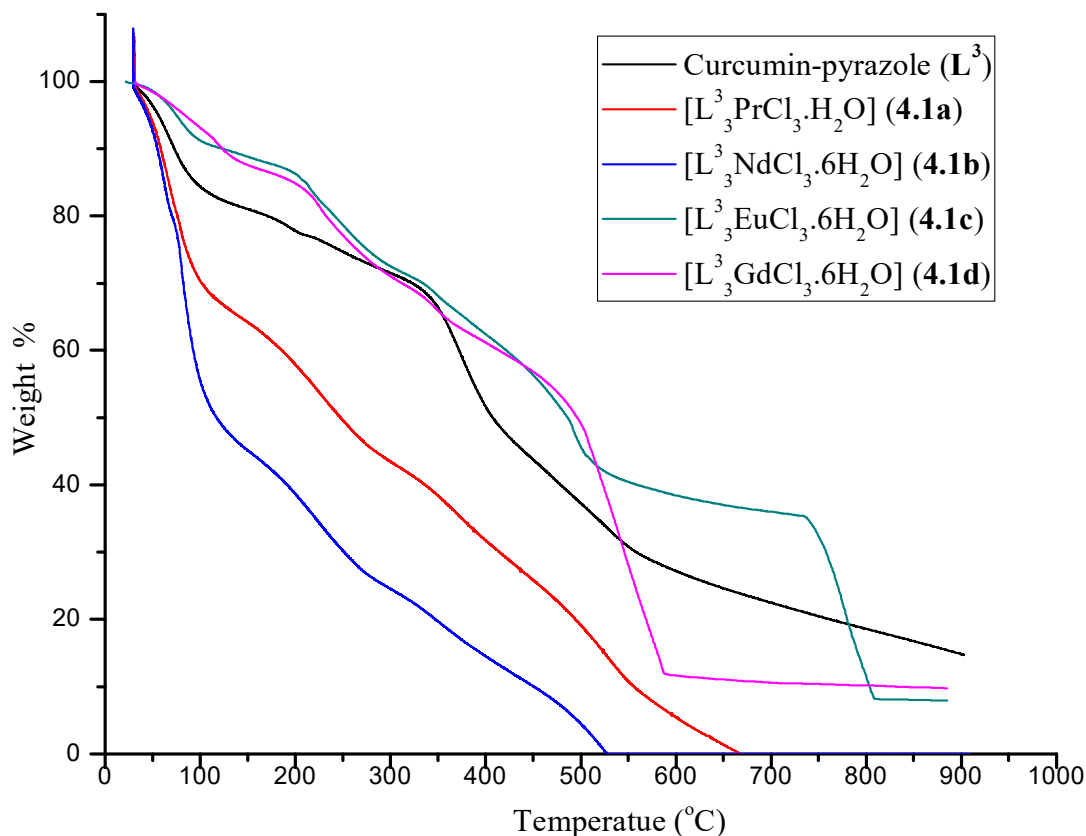


Figure 4.12. TGA curve for the Curcumin-pyrazole ligand (L^3) and its Lanthanide Complexes (**4.1a-d**).

The thermogravimetric analysis of the curcumin pyrazole ligand (L) and its lanthanide complexes $[L^3PrCl_3] \cdot H_2O$ (**4.1a**), $[L^3EuCl_3 \cdot 6H_2O]$ (**4.1b**), $[L^3EuCl_3 \cdot 6H_2O]$ (**4.1c**), $[L^3GdCl_3 \cdot 6H_2O]$ (**4.1d**) were recorded in nitrogen atmosphere at the heating temperature rate of $10^\circ C/min$ and mass loss was measured maintaining the temperature up to $900^\circ C$ shown in **Figure 4.12**. In case of ligand (L^3), with $100^\circ C$ the decomposition was so fast that after reaching certain stage i.e. 72%, decomposes steadily up to $350^\circ C$, then again decomposes very fast up to 5% at $450^\circ C$ and steadily came to 0% at $900^\circ C$.

In case of $[L^3PrCl_3 \cdot H_2O]$ (**4.1a**) complex speedy decomposition is found up to 70% within $100^\circ C$ then steadily decomposes up to 42% at $280^\circ C$ and steadily coming to 0% at around $580^\circ C$ and in case of $[L^3EuCl_3 \cdot 6H_2O]$ (**4.1b**), complex very fast decomposition could be seen up to 48% within $100^\circ C$, then steadily lose weight up to 22% at $230^\circ C$ and coming to 0% at around $500^\circ C$. For the $[L^3EuCl_3 \cdot 6H_2O]$ (**4.1c**), complexes,

decomposition started slowly and it continues steadily up to 42% with 500 °C, then there is constant decomposition up to 77 °C; afterwards suddenly very fast decomposition occurs reaching the weight loss up to 9% from 35% at 800 °C, till it gets its constant value. Considering for the case of $[L^3_3GdCl_3 \cdot 6H_2O]$ (**4.1d**), it could be seen a steady decomposition with weight loss up to 50 % at 480 °C, then speedy decomposition arises losing weight up to 10% at 575 °C after which it remains constant.

The thermal stability of the complexes were specified by the ligand to a great extend and at an average temperature the decomposition of the lanthanide complexes begins step by step and yield a residue of metal complexes even at high temperature showing its thermal stability. From the obtained TGA curve the weight loss of the free ligand and the metal complexes at different temperature were analyzed experimentally and theoretically. The typical thermograms of the curcumin pyrazole ligand (L^3) and its lanthanide complexes $[L^3_3PrCl_3 \cdot H_2O]$ (**4.1a**), $[L^3_3NdCl_3 \cdot 6H_2O]$ (**4.1b**), $[L^3_3EuCl_3 \cdot 6H_2O]$ (**4.1c**), $[L^3_3GdCl_3 \cdot 6H_2O]$ (**4.1d**) are represented in **Figure 4.12** and the detail decomposition of the compounds respected to the temperature is tabulated in **Table 4.5**.

Table 4.5. Thermo Gravimetric Analysis of Curcumin-pyrazole ligand (**L³**) and its Lanthanide Complexes (**4.1a-d**).

Compound	Temperature (° C)	Weight Loss (%) (Experiment/Theoretical)	Decomposed Compound
Curcumin-pyrazole (L³)	30.00 – 109.93	17.18% / 17.18%	2 (CH ₃) and 2 (OH)
	109.93 – 405.43	32.89% / 32.14%	C ₆ H ₃ -CH and 2O
	405.43 – 561.47	20.72% / 20.32%	C ₆ H ₃ and 2H
	561.47.....	29.73% / 28.57%	C-CN- CH ₂ -CNH-CH
[L ³ PrCl ₃ ·6H ₂ O] (4.1a)	30.00 – 98.61	29.31% / 29.61%	H ₂ O, 6 (OCH ₃), 6 (OH), CH and 2 (C ₆ H ₃ -CH)
	98.61 – 204.25	23.28% / 22.80%	3 (C ₆ H ₃ -CH =CH), CH and 4H
	204.25 – 418.89	18.01% / 18.25%	2 (C ₆ H ₃) and 3Cl
	418.89 – 659.49	29.49% / 28.59%	3(CN- CH ₂ -CNH), 4CH and Pr
[L ³ NdCl ₃ ·6H ₂ O] (4.1b)	30.00 – 70.49	20.05% / 20.17%	6 (H ₂ O) and 6 (OCH ₃)
	70.49 – 112.97	29.89% / 29.44%	4 (C ₆ H ₃) ,6(OH) and 3(CH)
	112.97 – 242.88	18.70% / 18.32%	2 (C ₆ H ₃ -CH=CH) ,5 (CH) and 6H
	242.88 – 523.45	31.34% / 30.26%	3(CN- C-CN), and NdCl ₃
[L ³ EuCl ₃ ·6H ₂ O] (4.1c)	30.00 – 106.39	9.22% / 9.23%	6 (H ₂ O) and OCH ₃
	106.39 – 272.94	15.44% /15.90%	5(C ₆ H ₃) and 6OH
	272.94 – 514.22	32.20% / 32.15%	3(C ₆ H ₃ -CH) and 3(C ₆ H ₃)
	514.22 – 786 .40	25.95% / 25.75%	3(C-CN- CH ₂ -CNH-CH) and 3CH
[L ³ GdCl ₃ ·6H ₂ O] (4.1d)	786.40.....	17.19% / 17.47%	Eu Cl ₃
	30.00 – 132.82	11.16% /11.56%	6 (H ₂ O) and 2 (OCH ₃)
	132.82 – 275.87	15.17% /1537%	4 (OCH ₃) and 6(OH)
	275.87 – 367.32	9.80% /9.79%	2(C ₆ H ₃)
	367.32 – 575.48	46.71% /45.85%	2(C ₆ H ₃ -C ₂ H ₂ -CN- CH ₂ -CN-C ₂ H ₂ -C ₆ H ₃) and C ₂ H ₂ -CN-CH ₂ -CN-C ₂ H ₂
	575.48.....	17.16% /17.82%	Nd Cl ₃

4.4. Conclusion

In this chapter, Curcumin-pyrazole ligand (L^3) and its corresponding novel lanthanide complexes $[L^3PrCl_3 \cdot H_2O]$ (**4.1a**), $[L^3NdCl_3 \cdot 6H_2O]$ (**4.1b**), $[L^3EuCl_3 \cdot 6H_2O]$ (**4.1c**), $[L^3GdCl_3 \cdot 6H_2O]$ (**4.1d**) were successfully synthesized and systematically characterized from various spectroscopic studies. From the spectral studies of IR and UV-visible and also from analytical data revealed the formation of complexes of $[L^3PrCl_3 \cdot H_2O]$ (**4.1a**), $[L^3NdCl_3 \cdot 6H_2O]$ (**4.1b**), $[L^3EuCl_3 \cdot 6H_2O]$ (**4.1c**), $[L^3GdCl_3 \cdot 6H_2O]$ (**4.1d**) with curcumin-pyrazole ligand (L^3) and their structures are found as nona-coordination. From the study of luminescence properties of the ligand and its complexes, $[L^3EuCl_3 \cdot 6H_2O]$ (**4.1c**), shows maximum intensities with maximum quantum yield value ($\Phi_f = 0.0498$) providing the possibility of higher application. From the TGA analysis the weight loss process of $[L^3EuCl_3 \cdot 6H_2O]$ (**4.1c**), and $[L^3GdCl_3 \cdot 6H_2O]$ (**4.1d**) complexes are at slower speed compared to other complexes as well as the curcumin pyrazole itself showing comparatively more stable than the curcumin-pyrazole Ligand (L^3), $[L^3PrCl_3 \cdot H_2O]$ (**4.1a**), and $[L^3NdCl_3 \cdot 6H_2O]$ (**4.1b**) complexes. In the fluorescence studies among the solvents quantum yield in the MeOH medium could provide highest value that means MeOH solvent is the most favourable one.

4.5. References

1. A. N. Kost and I. I. Orandberg, Progress in Pyrazole Chemistry, *Adv. Heterocyc. Chem.*, 1966, **6**, 347-42. [https://doi.org/10.1016/S0065-2725\(08\)60579-6](https://doi.org/10.1016/S0065-2725(08)60579-6)
2. A. Amalraj, A. Pius and S. Gopi, Biological Activities of Curcuminoids, Other Biomolecules from Turmeric and their Derivatives - A Review, *J. Trad. Complement. Med.*, 2017, **7 (2)**, 205-233. <https://pubmed.ncbi.nlm.nih.gov/28417091/>
3. C. Liu, M. Li, Z. Lin, M. Zhang, A. Guan, C. Hou, Z. Li, and Y. Jia, Substituted Azole Compounds and its Preparation and Use thereof, (2010) US ,7,795,179 B2. <https://patents.google.com/patent/US7795179B2/en>
4. K. M. Kasiotis, E.N. Tzanetou and Haroutounian, Pyrazoles as Potential Anti-Angiogenesis Agents: a Contemporary Overview, *Front Chem.*, 2014, **2**, 78(1-7). <https://doi.org/10.3389/fchem.2014.00078>
5. C. L. Liu and B.S. Chi, *New Agrochemicals Discovery and Synthesis*. Chemical Industry Press, Beijing, 2013, 251-252.
6. A. A. Bekhita, H. M. A. Ashour, A. E. A. Bekhit and S. A. Bekhit, Synthesis and Biological Evaluation of Novel Pyrazole Derivatives as Anti-Inflammatory Antimicrobial Agents, *Med. Chem.*, 2009, **5**, 103-117. <https://www.ingentaconnect.com/content/ben/mc/2009/00000005/00000002/art00001>
7. S. Trofimenko, Coordination Chemistry of Pyrazole-derived Ligands, *Chem. Rev.*, 1972, **72 (5)**, 497-509. <https://doi.org/10.1021/cr60279a003>
8. B. Poudyal and G. Bharghav, A Review of Pyrazole and its Derivative, *National J. Pharm. Sci.*, 2021, **1(1)**, 34-41. <https://www.pharmajournal.net/article/6/1-1-7-611.pdf>
9. F. K. Keter and J. Darkwa, Perspective: the Potential of Pyrazole-Based Compounds in Medicine, *Biometals*, 2012, **25**, 9-21. <https://doi.org/10.1007/s10534-011-9496-4>
10. A. Tigreros and J. Portilla, Recent Progress in Chemosensors Based on Pyrazole Derivatives, *RSC Adv.*, 2020, **10**, 19693-19712. <https://doi.org/10.1039/D0RA02394A>
11. G. H. Sayed, M. E. Azab, K. E. Anwer, M. A. Raouf, N. A. Negm, Pyrazole, Pyrazolone and Enaminonitrile Pyrazole Derivatives: Synthesis, Characterization and Potential in Corrosion Inhibition and Antimicrobial Applications, *J. Mol. Liq.*, 2018, **252**, 329-338. <https://doi.org/10.1016/j.molliq.2017.12.156>
12. S. Mert, R. Kasimogullari, and S. Ok, A Short Review on Pyrazole Derivatives and their Applications, *J. Postdoc. Res.*, 2014, **2(4)**, 63-72.

- https://www.academia.edu/download/41220001/A_Short_Review_on_Pyrazole_Derivatives_a20160113-1763-1mqawr.pdf[20160115-19908-s0kzqa.pdf](https://www.academia.edu/download/41220001/A_Short_Review_on_Pyrazole_Derivatives_a20160115-19908-s0kzqa.pdf)
13. I. Bouabdallah, L. A. M. Barek, A. Zyad, A. Ramdani, I. Zidane and A. Melhaoui, Anticancer Effect of three Pyrazole Derivatives, *Nat. Prod. Res.*, 2006, **20(11)**, 1024-1030. <https://doi.org/10.1080/14786410600921441>
 14. C. Selvam, S. M. Jachak and R. A. K. Thilagavathi, Design, Synthesis, Biological Evaluation and Molecular Docking of Curcumin Analogues as Antioxidant, Cyclooxygenase Inhibitory and Anti-inflammatory Agents, *Bioorg. Med. Chem. Lett.*, 2005, **15**, 1973-1797. <https://doi.org/10.1016/j.bmcl.2005.02.039>
 15. H. Ohtsu, Z. Xiao, J. Ishida, M. Nagai, H. K. Wang, H. Itokawa, C.-Y. Su, C. Shih, T. Chiang, E. Chang, Y. Lee, M.-Y. Tsai, C. Chang and K. H. Lee, Antitumor Agents. 217. Curcumin Analogues as Novel Androgen Receptor Antagonists with Potential as Anti-Prostate Cancer Agents, *J. Med. Chem.*, 2002, **45**, 5037-5042. <https://doi.org/10.1021/jm020200g>
 16. H. Endo, Y. Nikaido, M. Nakadate, S. Ise and H. Konno, Structure Activity Relationship Study of Curcumin Analogues Toward the Amyloid-beta Aggregation Inhibitor, *Bioorg. Med. Chem. Lett.*, 2014, **24**, 5621-5626. <https://doi.org/10.1016/j.bmcl.2014.10.076>
 17. M. J. Ahsan, K. Choudhary, S. S. Jadav, S. Yasmin, M. Y. Ansari and R. Sreenivasulu, Synthesis, Antiproliferative Activity, and Molecular Docking Studies of Curcumin Analogues bearing Pyrazole Ring, *Med Chem Res.*, 2015, **24**, 4166-4180. <https://doi.org/10.1007/s00044-015-1457-y>
 18. J. Liu, M. L. Cheng, L. L. Yu, S. C. Chen, Y. L. Shao, Q. Liu, C. W. Zhai and F. X. Yin, Three Metal Complexes Derived from 3-methyl-1*H*-pyrazole-4-carboxylic acid: Synthesis, Crystal Structures, Luminescence and Electrocatalytic Properties, *RSC Adv.*, 2016, **6**, 52040-52047. <https://doi.org/10.1039/C6RA10989F>
 19. W. Ye, X. Xiao, L. Wang, S. Hou, and C. Hu, Synthesis of Mono- and Binuclear Cu(II) Complexes Bearing Unsymmetrical Bipyridine-Pyrazole-Amine Ligand and Their Applications in Azide-Alkyne Cycloaddition, *Organometallics.*, 2017, **36**, 2116-2125. <http://dx.doi.org/10.1021/acs.organomet.7b00154>
 20. N. Nayak, K. S. Prasad, R. R. Pillai, S. Armakovic and S. J. Armakovic, Remarkable Colorimetric Sensing Behavior of Pyrazole-based Chemosensor towards Cu(II) ion

- Detection: Synthesis, Characterization and Theoretical Investigations, *RSC Adv.*, 2018, **8**, 18023–18029. <https://doi.org/10.1039/C8RA02905A>
21. M. N. Matada and K. Jathi, Pyrazole-based Azo-metal(II) Complexes as Potential Bioactive Agents: Synthesis, Characterization, Antimicrobial, Anti-tuberculosis, and DNA Interaction Studies, *J. Coord. Chem.*, 2019, **72(12)**, 1994-2014. <https://doi.org/10.1080/00958972.2019.1630613>
22. K. Kumarasamy, T. Devendhiran, M. C. Lin and C. W. Chiu, Synthesis and Physical Property Studies of Cyclometalated Pt(II) and Pd(II) Complexes with Tridentate Ligands Containing Pyrazole and Pyridine Groups, *Polyhedron.*, 2020, **191**, 114799 <https://doi.org/10.1016/j.poly.2020.114799>
23. C. Amoah, C. Obuah, M. K. Aniooson and A. Muller, Synthesis, Characterization and Fluorescent Properties of Ferrocenyl Pyrazole and Triazole Ligands and their Palladium Complexes, *J. Organomet. Chem.*, 2021, **935**, 121664. <https://doi.org/10.1016/j.jorganchem.2020.121664>
24. B. Soltani, M. Ghorbanpour, C. J. Ziegler, M. E. Nahari and R. M. Rezaei, Nickel (II) and Cobalt(II) Complexes with Bidentate Nitrogen-Sulfur Donor Pyrazole Derivative Ligands: Syntheses, Characterization, X-ray structure, Electrochemical Studies, and Antibacterial Activity, *Polyhedron*, 2020, **180**, 114423. <https://doi.org/10.1016/j.poly.2020.114423>
25. J. Khanagwal, S. P. Khatkar, P. Dhankhar, M. Bala, R. Kumar, P. Boora and V. B. Taxak, Synthesis and Photoluminescence Analysis of Europium(III) Complexes with Pyrazole Acid and Nitrogen Containing Auxiliary Ligands, *Spectrosc. Lett.*, 2020, **53(8)**, 625-647. <https://doi.org/10.1080/00387010.2020.1817093>
26. D. Vlasjuk, and R. Lyszczyk, Effect of Different Synthesis Approaches on Structural and Thermal Properties of Lanthanide(III) Metal–Organic Frameworks Based on the 1H-Pyrazole-3,5-Dicarboxylate Linker. *J. Inorg. Organomet. Polym. Mater.*, 2021, **31**, 3534-3548. <https://doi.org/10.1007/s10904-021-02018-w>
27. N. Ahsan, S. Mishra, M. K. Jain, A. Surolia and S. Gupta, Curcumin Pyrazole and its Derivative (N-(3-Nitrophenylpyrazole) Curcumin Inhibit Aggregation, Disrupt Fibrils and Modulate Toxicity of Wild type and Mutant α -Synuclein, *Sci. Rep.*, 2015, **5**, 1-16. <https://www.nature.com/articles/srep09862#citeas>

Synthesis of Curcumin-diethanolimine Lanthanide (Pr^{3+} , Nd^{3+} , Eu^{3+} and Gd^{3+}) Complexes and Investigation of their Spectroscopic Studies

Abstract

In this chapter, a series of new lanthanide complexes $[\text{L}^4\text{LnCl}_3 \cdot x\text{H}_2\text{O}]$ (where; L^4 =curcumin-diethanolimine and $\text{Ln}=\text{Pr}^{3+}$, Nd^{3+} , Eu^{3+} and Gd^{3+}) have been synthesized in ethanol under reflux conditions for 24 hours. The synthesized curcumin-diethanolimine lanthanide complexes; $[\text{L}^4\text{PrCl}_3 \cdot \text{H}_2\text{O}]$ (**5.1a**), $[\text{L}^4\text{NdCl}_3 \cdot 6\text{H}_2\text{O}]$ (**5.1b**), $[\text{L}^4\text{EuCl}_3 \cdot 6\text{H}_2\text{O}]$ (**5.1c**), $[\text{L}^4\text{GdCl}_3 \cdot 6\text{H}_2\text{O}]$ (**5.1d**) were characterised by elemental analysis, IR, UV-Vis, fluorescence and TGA. The formations of the 6-coordinated lanthanide complexes have been detected through the elemental analysis. In IR-spectra, the formation of the new band at around $450\text{--}580\text{ cm}^{-1}$ has been assigned to the metal- nitrogen and metal-oxygen stretching vibration which has conveyed that nitrogen and oxygen atoms of the ligand is being coordinated to the lanthanide. Absorption intensity as well as luminescence properties of the synthesized curcumin-diethanolimine ligand (L^4) and its lanthanide complexes (**5.1a-d**) were analysed through UV-Vis and fluorescence spectra. The quantum yields of the ligand and lanthanide complexes have been analyzed. Further the percentage weight loss of the complexes was studied with TGA analysis.

5.1. Introduction

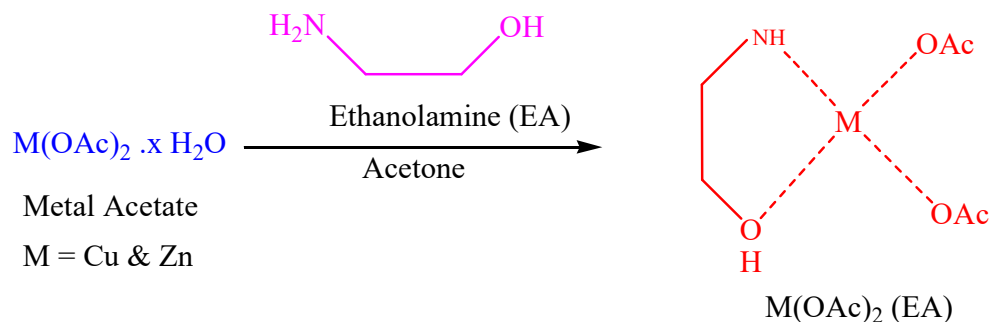
Ethanolamine is a bi-functional organic compound containing both amine and alcohol. Bacteria from the cell membrane can be a source of the carbon and nitrogen to form the ethanolamine. They are base and present in every human cell as phosphatidylethanolamine which is the most abundant phosphate. Ethanolamine is metabolites of amino acids and plays an important role in regeneration of intestinal cell and inflammation of intestine. It was first reported by a Chemist Ludwig Knorr in 1897 by reacting ethylene oxide with ammonia. The presence of both alcohol and amine group makes its potentiality to be used in industries, agricultural chemicals, pharmaceuticals and detergents.¹⁻⁶ When ethanolamine react with equivalent ethylene oxide gives diethanolamine which are poly-functional and are utilized as a corrosion inhibitors, an agent for removal of carbon dioxide and hydrogen sulfide from natural gas.⁷⁻⁸

Diethanolamine when react with other compound (organic, Inorganic and metals) exhibits numerous applications in Pharmaceuticals, Food, Chemical, Agricultural and

Cosmetic industries, Cements, Polymer productions, Lubricants, Fixative, Polishers, Coating, Printings inks, Petroleum, Textile fishing and electroplating. Diethanolamine and its derivatives are also found to have anti-microbial activity, anti-oxidants and also as indirect prevention of cancer, coronary heart diseases and certain kind of sickness. They were also found to possessed promising biological activities such as the anti-cancer, anti-tuberculosis, anti-bacterial, local anesthetic and anti-platelet aggregation.⁹⁻¹⁵ They are also found in nature as a lipids for plants physiological process such as germination, Pathogens interactions, flowering etc.¹⁶ Regarding their multiple applications of ethanolamine and its derivatives some of the recent synthesis and potentiality are quoted below.

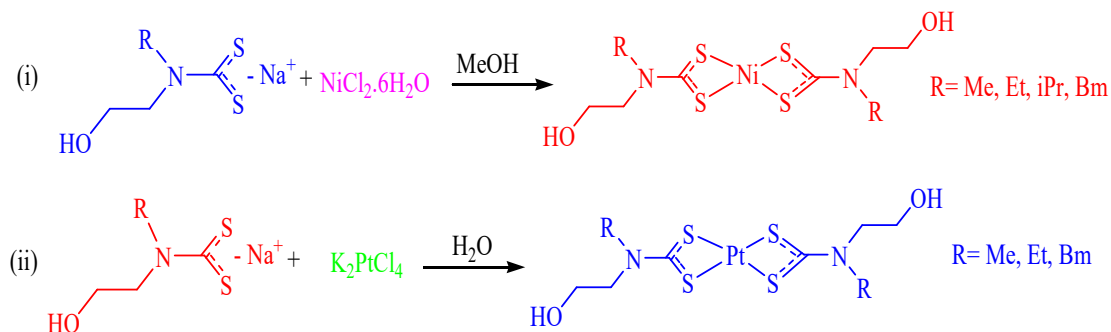
N. Chopin *et al.* (2015) reported a synthesis of Ni(II) and Dy(III)-Cu(II) complexes of ethanolamine. The multinuclear complexes were found to show fascinating magnetic features. Using Pascal's Constant the diamagnetism of the complexes were evaluated and using the Gemini diffraction on the single crystal X-ray the non-hydrogen atoms were clearfied.¹⁷ The same year Zheng Chen and syndicate have reported a synthesis of indium tin oxide nano-crystal using solvothermal dehydration condensation using ethanolamine and metal hydroxide. On addition of ethanolamine, it was discovered that it can decline the size of the nano-crystal constructively and improve their surface chemically which results in a conductive ink for the development of transparent conductive films. The films were also reported to exhibit a better conductivity with low resistance when washed with water.¹⁸

D. Sridaeng and co-workers (2016) designed two metal acetate-ethanolamine complexes (**Scheme 5.1**) which were used as a catalyst for the development of rigid polyurethane. Both the complexes were found to produce a polymerization reaction and when compared with a commercial catalyst (dimethylcyclohexylamine) copper and zinc acetate-ethanolamine complexes were found to exhibit prolonged gel period and a steady rise profile and so the preparation of the rigid polyurethane can be carried out with less hindrance.¹⁹



Scheme 5.1. Synthesis of Metal-ethanolamine Complexes.

Diothiocarbamates have much application in variety of area such as in Biology, Medicine and in material sciences, A. Ramos-Espinosa *et al.* (2017) synthesized a series of complexes using dithiocarbamates as ligand alone with N-(R) ethanolamine where R = Methyl (Me), Ethyl (Et), isopropyl (iPr) and Benzyl (Bn) group and Ni(II) and Pt(II) metal. The Ni(II) complexes were found to have irregular square-planer geometry and the Pt (II) complexes were reported to have cytotoxicity against five cancer cell line namely nervous central system (U251), leukemia (K562), colon (HCT-15), breast (MCF-7) and lung (SKLU-1) (Scheme 5.2).²⁰



Scheme 5.2. Synthesis path way of (i) Ni(II) Complexes and (ii) Pt(II) Complexes.

Removal of heavy metal ions have become one of the necessity and so S. Sahu *et al.* (2018) has synthesized a hybrid molecule thorium ethanolamine for the removal of Cr(VI) from water (Figure 5.1). The product molecule was found to have small pore and particle size, good ion exchange and its surface area was high making it to be a significant agent for removal of Cr(VI). In solution of 10 mgL^{-1} of thorium ethanolamine 99.53% of Cr(VI) was removed.²¹

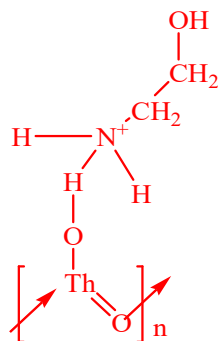


Figure 5.1. Structure of Thorium Ethanolamine.

P. A. Khalf-Allaa *et al* (2019) synthesized a series of seven coordinated iron (III) complex of schiff base as these types of metal complexes exhibit interesting chemical and catalytic activity. The synthesized complexes were found to have anti-bacterial activity while those of the ligand do not show any activity. Some of the complexes were also reported to have an excellent anti-microbial activity against *E.coli* and *aureus*.²² Metal complexes contain the characteristic of both the metal and the ligand and so they possessed variety of applications. In view of the applications and structural characteristic, R. Dubey and group in 2019 have reported a synthesis of Diorganotin(IV) complexes using a mixture of bidentate Schiff base ligand. The complexes were characterized by different spectroscopic techniques. They were found to exhibit average anti-microbial activity and when compare with the free ligand shows more activity.²³

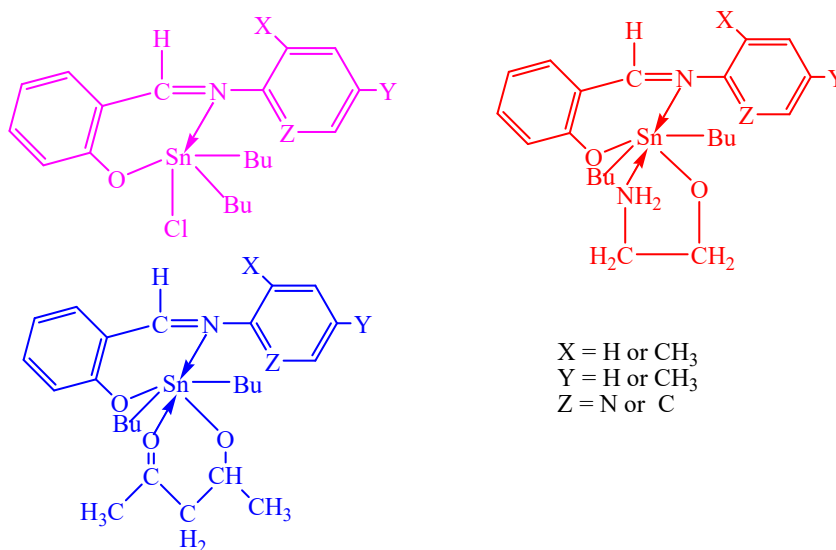


Figure 5.2. Structure of the Diorganotin Complexes.

O. Stetsiuk *et al.* (2020) reported eight polymer manganese(III) complexes which were prepared by direct reaction. The single crystal X-ray of the complex shows a one dimensional polymeric structure and the metal coordinate to the ligand in a tridentate chelate bridging connected by –N-C-C-O- bridges (**Figure 5.2**). The metal complexes were reported to show an antiferromagnetic and the electron paramagnetic resonance analysis show that the zero-field splitting parameters was narrow.²⁴

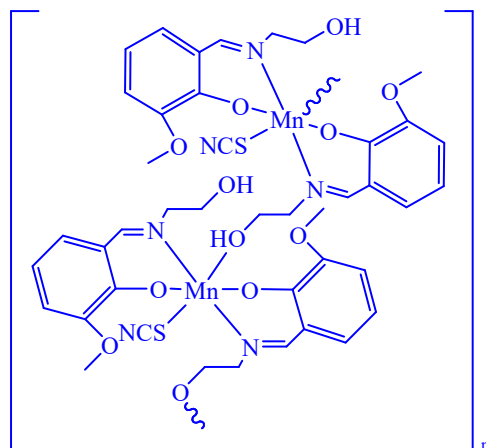


Figure 5.3. Structure of the Mn(III) Complex.

Recently, energy crisis have become one the most concern and so developing energy storage devices is a necessity. Regarding to the need, in 2021 S. Sahu and co-workers developed a nano-structural MnCO_2O_4 . The compounds were reported to have a great electrochemical property in Na_2SO_4 electrolyte with high specific capacitance and excellent cycling stability; therefore the nanostructure material can be a promising application as electrode for high energy density.²⁵ B. Hasanpour *et al* (2021) reported a synthesis of novel Cu (II) complexes of ethanolamine-triazine derivative and their different spectral characterization. The complexes were found to have high oxidation activity and so they can be used as an ideal oxidant and stability of complex.²⁶

Such important applications of ethanolamine and its complexes lead us to synthesis ethanolamine derivative (curcumin-diethanolimine L^4) and utilize it as ligand and developed complexes of lanthanide (**5.1a-d**) as lanthanides have several unique characteristic properties compared to other elements; since the f-orbital's are filled gradually they have varied coordinating capacities and specify its spectroscopic, physico-chemical and thermally.

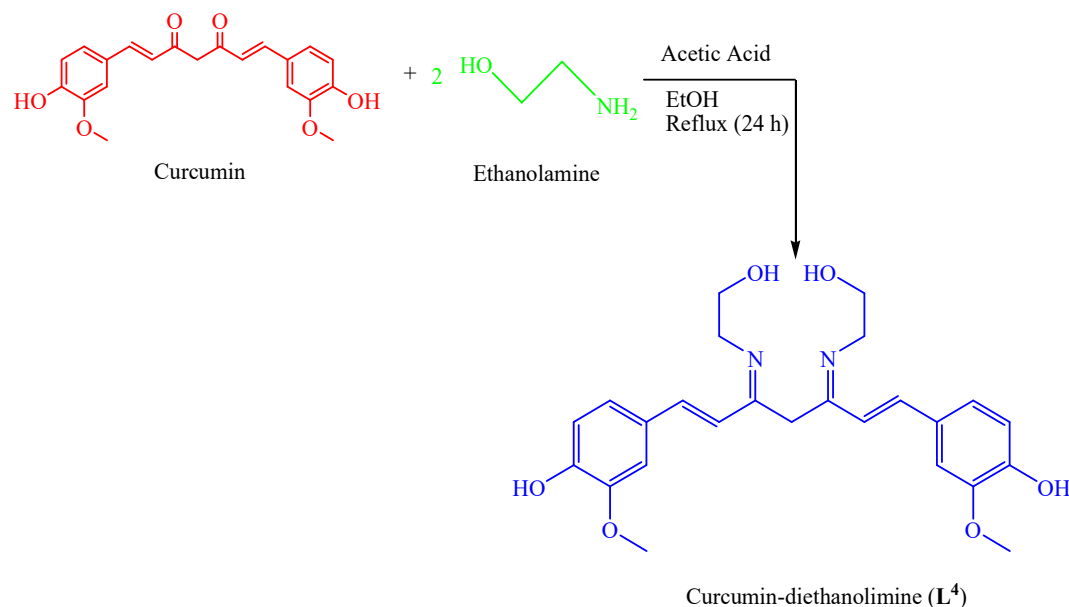
5.2. Experimental

5.2.1. Materials and Methods

All the reagents and solvents utilized were purchased from commercially available sources and used without further purification. FTIR spectra of the curcumin-diethanolimine ligand (**L⁴**) and its lanthanide complexes (**5.1a-d**) were recorded on Perkin-Elmer spectrophotometer (Spectrum-Two) using KBr disk and values are expressed in cm^{-1} . Micro analytical (CHN) data were obtained with a FLASH EA 1112 Series CHNS analyzer. UV-visible spectrophotometer (Double Beam) Perkin Elmer, Lambda-35 is used for recording the absorption bands of the curcumin-diethanolimine ligand and its lanthanide complexes. All fluorescence emission spectra of curcumin-diethanolimine ligand and its lanthanide complexes were recorded using fluorescence spectrophotometer Shimadzu RF- 6000 which is followed by the evaluation of their quantum yields. The TGA-DTA measurements of curcumin-diethanolimine ligand and its lanthanide complexes were performed on a Perkin-Elmer analyzer in air over the temperature range of 30-900 °C.

5.2.2. Synthesis of Curcumin-diethanolimine Ligand (**L⁴**)

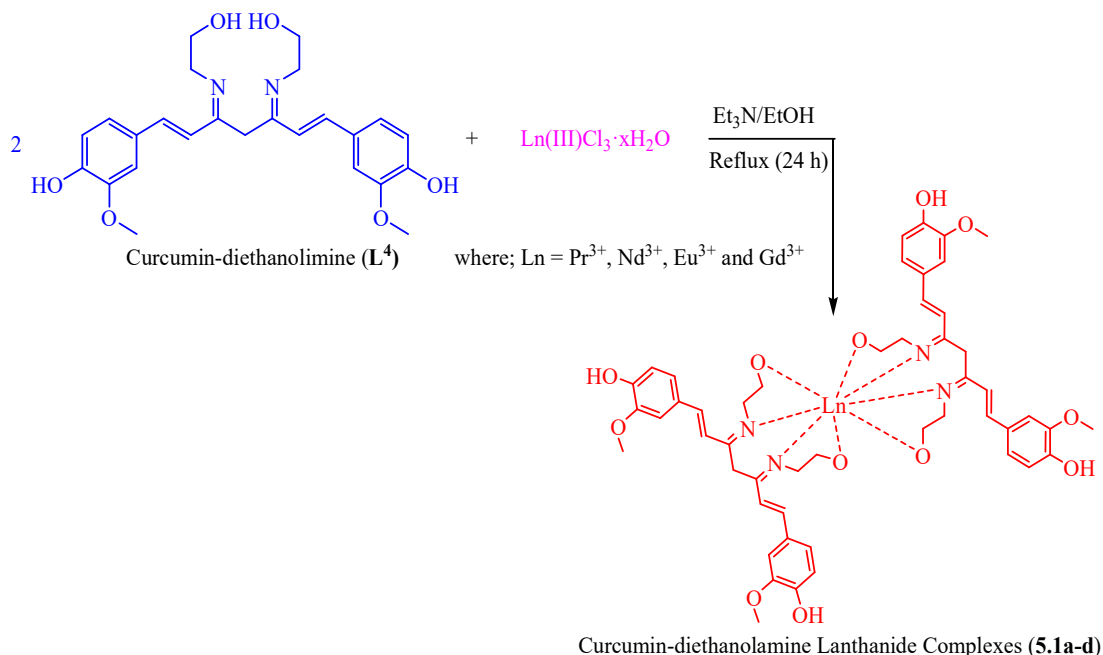
In a solution of curcumin [1,7-bis(4- hydroxyl-3-methoxyphenyl)-1,6- heptadiene-3, 5-dione] (0.368g, 1mmol) in ethanol medium to which added ethanolamine (0.122g, 2 mmol) and kept with continuous stirring in a magnetic stirrer then to the reaction mixture was added a catalytic amount of acetic acid and reflux for 24 hours. The process of the reaction was monitor using thin layer chromatography (TLC). The reaction mixture was dark brown in color, after keeping it under reflux conditions for day and the solvent was allowed to evaporate completely giving a sticky compound to which crushed ice were added forming a pale yellow compound which was collected through normal filtration and air dried after several washing with ice cold water (**Scheme 5.3**).



Scheme 5.3. Synthesis of Curcumin-diethanolimine (L^4).

5.2.3. General Synthesis of Curcumin-diethanolimine Lanthanide(III) Complexes [$L^4_2LnCl_3 \cdot xH_2O$] (5.1a-d)

The complex of the lanthanides were synthesized by taken curcumin-diethanolimine (2 mmol) in ethanol medium (5 ml) in a round bottom flask and to it was added $LnCl_3 \cdot xH_2O$; (where; $Ln = Pr^{3+}$, Nd^{3+} , Eu^{3+} and Gd^{3+}) (1 mmol). To the reaction mixture was added catalytic amount of triethylamine (Et_3N) and was kept for refluxing for 24 hours. After which the reaction was allowed to evaporate the solvent completed on evaporation the reaction mixture form dark brown sticky compound which was washed with hexane for several time giving a brown colored non-sticky compound which was collected trough filtration. The complexes [$L^4_2PrCl_3 \cdot H_2O$] (**5.1a**), [$L^4_2NdCl_3 \cdot 6H_2O$] (**5.1b**), [$L^4_2EuCl_3 \cdot 6H_2O$] (**5.1c**), [$L^4_2GdCl_3 \cdot 6H_2O$] (**5.1d**) were allowed to air dried (**Scheme 5.4**).



Scheme 5.4. Synthesis of Curcumin-diethanolimine Lanthanide Complexes (**5.1a-d**).

5.3. Results and Discussion

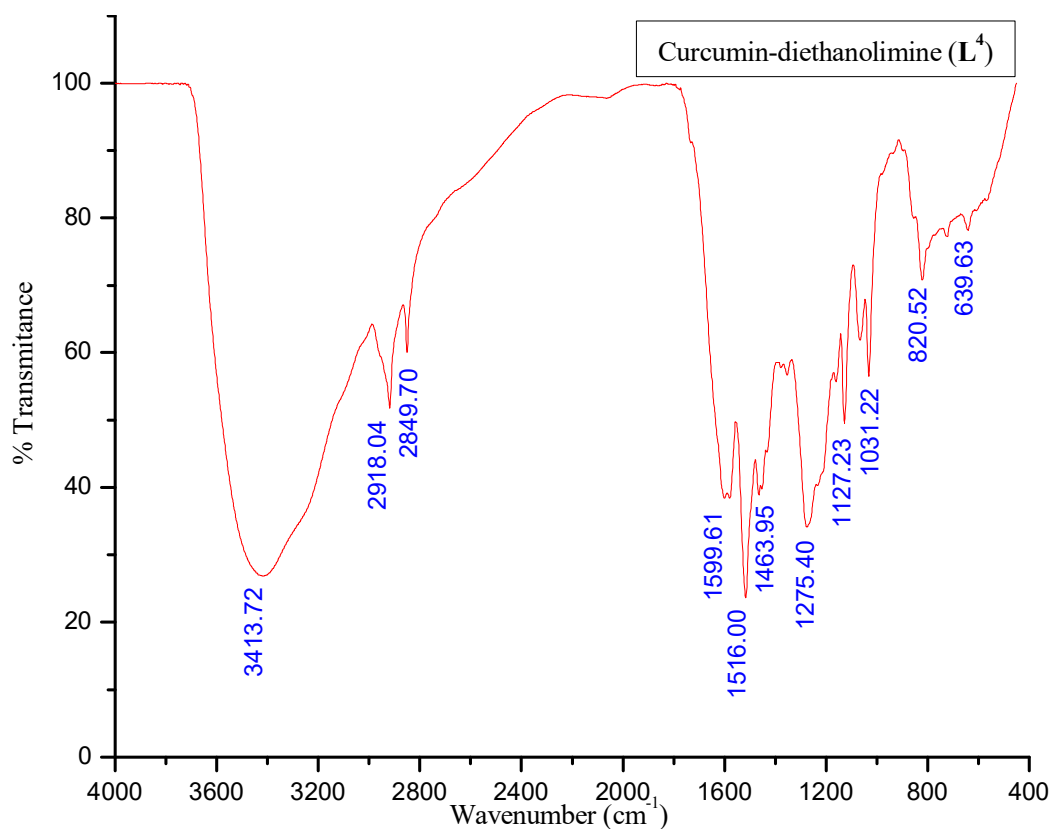
In this chapter, we reported a synthesis of curcumin-diethanolimine lanthanide complexes (**5.1a-d**). The ligand curcumin-diethanolimine (L^4) was prepared from a reaction of curcumin and ethanolamine with a catalytic amount of CH_3COOH in ethanol and reflux for 24 hours which was then used as a ligand (L^4) and curcumin-diethanolimine lanthanide metal complexes were then synthesized with selected lanthanide metal chlorides ($LnCl_3 \cdot xH_2O$; $Ln = Pr^{3+}, Nd^{3+}, Eu^{3+}$ and Gd^{3+}) in 1:3 ratio in presence of catalytic amount of Et_3N in ethanol and reaction mixture was kept under reflux condition for 24 hours. The solvent was completely evaporated by removing the condenser after 24 hours of refluxing. The yielded solid which was collected through filtration and the washed with hexane for several times and is allowed to air dried and then collected. The synthesized solid curcumin-diethanolimine lanthanide complexes (**5.1a-d**) were stable at room temperature, which were characterized for various spectroscopic properties. The resulting curcumin-diethanolimine lanthanide complexes were well studied for FT-IR spectroscopy, UV-Visible spectroscopy, Fluorescence spectroscopy, TGA-DTA analysis and elemental analysis. **Table 5.1** represents the physico-analytical data of free curcumin-diethanolimine ligand (L^4) and curcumin -diethanolimine lanthanide complexes (**5.1a-d**).

Table 5.1. Physicochemical properties of Curcumin-diethanolimine ligand (L^4) and its Lanthanide Complexes (**5.1a-d**).

Compounds	Yield (%)	Color	CHN Analysis (%) Found(calculated)		
			Carbon	Hydrogen	Nitrogen
Curcumin - diethanolamine (L^4)	-	Dark Orange	69.12 (69.22)	6.21 (6.65)	6.59 (6.16)
$[L^4_2PrCl_3 \cdot H_2O]$ (5.1a)	86 %	Dark Brown	56.32 (56.45)	5.23 (5.49)	5.54 (5.27)
$[L^4_2NdCl_3 \cdot 6H_2O]$ (5.1b)	84 %	Dark Brown	51.76 (51.89)	5.87 (5.92)	4.79 (4.84)
$[L^4_2EuCl_3 \cdot 6H_2O]$ (5.1c)	96 %	Dark Brown	51.42 (51.55)	5.82 (5.88)	4.87 (4.81)
$[L^4_2GdCl_3 \cdot 6H_2O]$ (5.1d)	90 %	Dark Brown	51.45 (51.31)	5.82 (5.86)	4.71 (4.79)

5.3.1. FT-IR Spectral Characterization Studies

5.3.1.1. FT-IR spectra of Curcumin-diethanolimine Ligand (L^4)

**Figure 5.4.** FT-IR Spectra of Curcumin-diethanolimine Ligand (L^4).

The FT-IR spectrum of the curcumin-diethanolimine ligand (L^4) (**Figure 5.4** and **Table 5.2**), shows a peak at 3413 cm^{-1} attributing to the OH stretching and absorption at 2918 cm^{-1} and 2849 cm^{-1} attributing to CH stretching. The band appears at 1599 cm^{-1} is and a sharp and high intensity band at 1516 cm^{-1} corresponds to the C=C and C=N stretching vibrations and another characteristic band appeared at 1463 cm^{-1} attributed to C-C stretching frequencies. The bands at 1275 cm^{-1} and 1127 cm^{-1} correspond to phenolic C-O stretching vibrations and a sharp band at 1031 cm^{-1} and 820 cm^{-1} has been assigned to C-H bond.

5.3.1.2. FT-IR Spectra of Curcumin-diethanolimine Praseodymium Complex [$L^4_2\text{PrCl}_3 \cdot \text{H}_2\text{O}$] (5.1a)

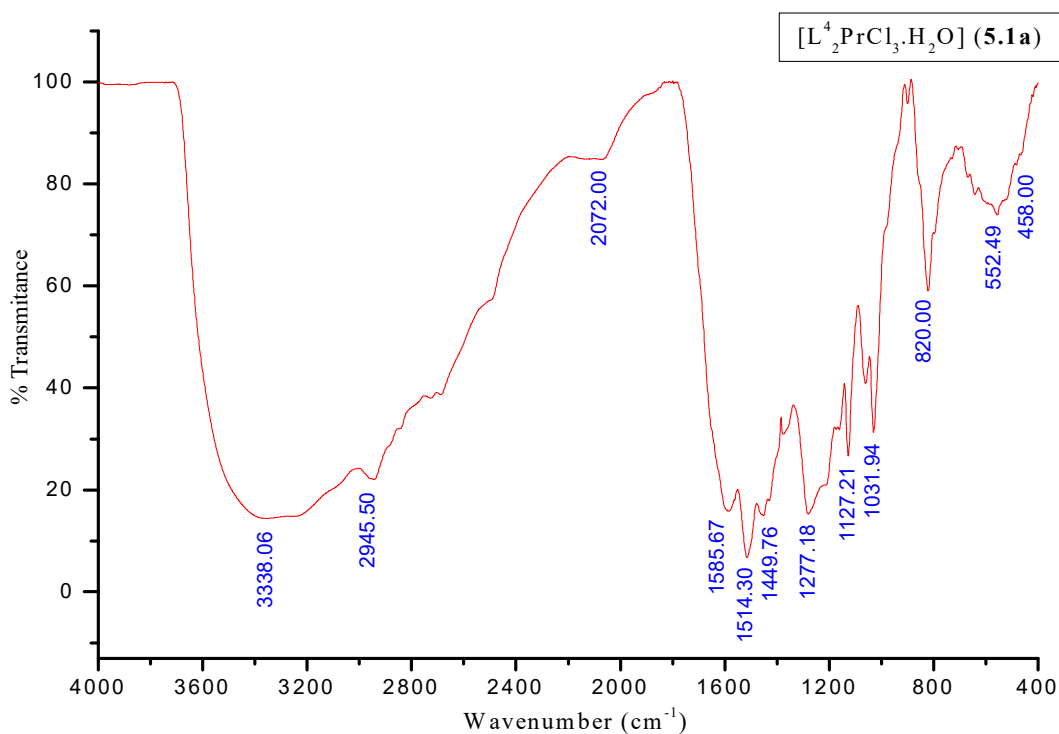


Figure 5.5. FT-IR Spectra of Curcumin-diethanolimine Praseodymium Complex [$L^4_2\text{PrCl}_3 \cdot \text{H}_2\text{O}$] (5.1a).

The FT-IR spectra characterization of curcumin-diethanolimine praseodymium complex [$L^4_2\text{PrCl}_3 \cdot \text{H}_2\text{O}$] (5.1a) (**Figure 5.5** and **Table 5.2**) shows that the OH stretching at 3413 cm^{-1} which appeared in the free ligand shifted to a lower wavelength at 3338 cm^{-1} which form into a broader band after complexation showing the presence of H_2O in the complex. The prominent bands appeared in the free curcumin-diethanolimine ligand indicating the mixed vibrations of C=C and C=N stretching at 1599 cm^{-1} and 1516 cm^{-1} were completely shifted to lower frequencies values at 1585 cm^{-1} and 1514 cm^{-1} and the

band at 1463 cm^{-1} shifted to lower wavelength 1449 cm^{-1} . The band at 2918 cm^{-1} and 2849 cm^{-1} indicating the vibration of C-H in the ligand shifting to a higher and lower frequency at 2945 cm^{-1} and 2839 cm^{-1} . The shifting of the bands in the complex IR spectra strongly signifies that the praseodymium metal coordinate to curcumin-diethanolimine ligand (L^4) and the appearance of a new band at 552 cm^{-1} and 458 cm^{-1} assigning to the M-O and M-N stretching vibrations which was not found in the spectra of free ligand (L^4), clearly suggests that the nitrogen and oxygen atoms of the ligand are coordinating to the lanthanide metal leading to the formation of lanthanide complexes with the curcumin-diethanolimine ligand.

5.3.1.3. FT-IR Spectra of Curcumin-diethanolimine Neodymium Complex $[\text{L}_2^4\text{NdCl}_3 \cdot 6\text{H}_2\text{O}]$ (5.1b)

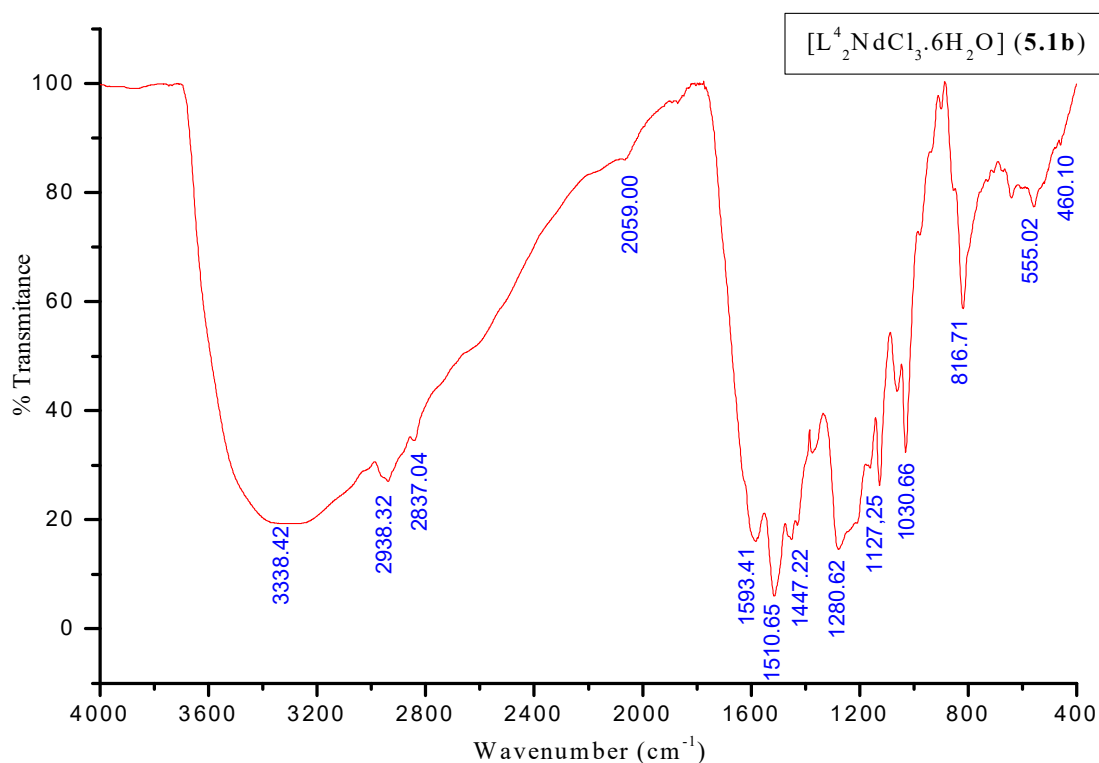


Figure 5.6. FT-IR Spectra of Curcumin-diethanolimine Neodymium Complex $[\text{L}_2^4\text{NdCl}_3 \cdot 6\text{H}_2\text{O}]$ (5.1b).

The FT-IR spectra characterization of curcumin-diethanolimine neodymium complex $[\text{L}_2^4\text{NdCl}_3 \cdot 6\text{H}_2\text{O}]$ (2) (Figure 5.5 and Table 5.2) shows that the OH stretching at 3413 cm^{-1} which appeared in the free ligand shifted to a lower wavelength at 3338 cm^{-1} which form

into a broader band after complexation showing the presence of H₂O in the complex. The band at 2918 cm⁻¹ and 2849 cm⁻¹ indicating the vibration of C-H in the ligand shifting to a higher and lower frequency at 2938 cm⁻¹ and 2837 cm⁻¹. The prominent bands appeared in the free curcumin-diethanolimine ligand indicating the mixed vibrations of C=C and C=N stretching at 1599 cm⁻¹ and 1516 cm⁻¹ were completely shifted to lower frequencies values at 1593 cm⁻¹ and 1510 cm⁻¹ and the band at 1463 cm⁻¹ shifted to lower wavelength 1447 cm⁻¹. The shifting of the bands in the complex IR spectra strongly signifies that the neodymium metal coordinate to curcumin-diethanolimine ligand (**L**⁴) and the appearance of a new band at 555 cm⁻¹ and 460 cm⁻¹ assigning to the M-O and M-N stretching vibrations which was not found in the spectra of free ligand (**L**⁴) clearly suggests that the nitrogen and oxygen atoms of the ligand are coordinating to the lanthanide metal leading to the formation of lanthanide complexes with the curcumin-diethanolimine ligand.

5.3.1.4. FT-IR Spectra of Curcumin-diethanolimine Europium Complex [**L**⁴EuCl₃·6H₂O] (**5.1c**)

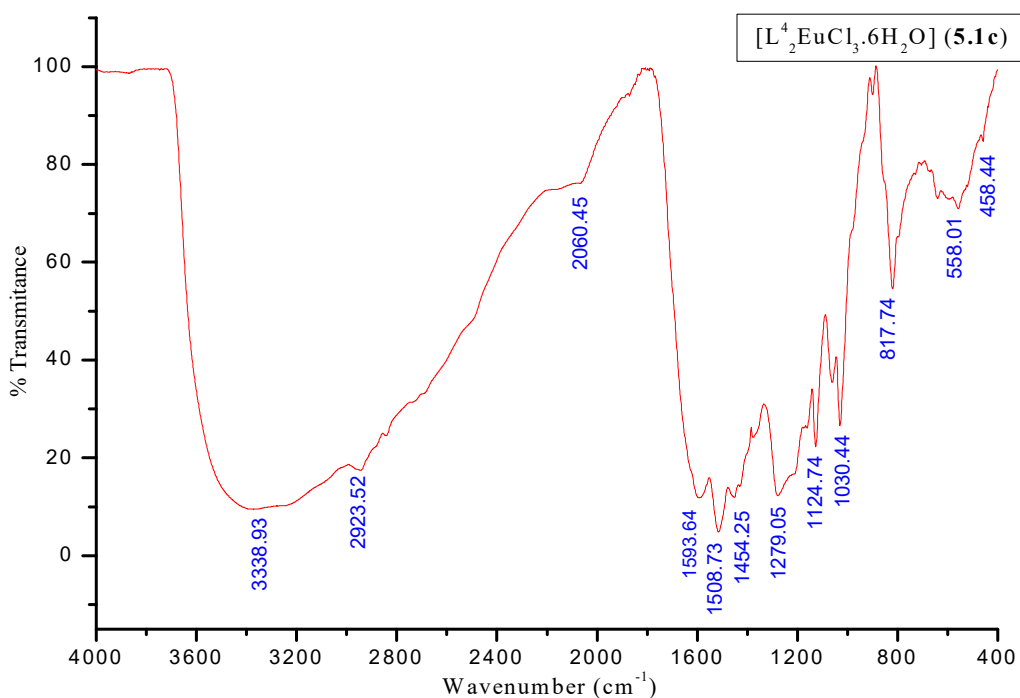


Figure 5.7. FT-IR Spectra of Curcumin-diethanolimine Europium Complex [**L**⁴EuCl₃·6H₂O] (**5.1c**).

In the FT-IR spectra of the curcumin-diethanolamine europium complex; [**L**⁴EuCl₃·H₂O] (**5.1c**), the band at 2918 cm⁻¹ and 2849 cm⁻¹ indicating the vibration of

aromatic C-H bond in the ligand shifting to a higher and lower frequency at 2923 cm^{-1} and 2843 cm^{-1} . The bands attributing to the mixed vibrations of C=N and C=C at 1599 cm^{-1} and 1516 cm^{-1} stretching shown in curcumin-diethanolimine ligand (L^4) was shifted to a lower wavelength at 1585 cm^{-1} and 1511 cm^{-1} after complexation of curcumin-diethanolimine europium complex $[L^4_2EuCl_3 \cdot 6H_2O]$ (**3**) and also the OH stretching at 3413 cm^{-1} which appeared in the free ligand shifted to a lower wavelength at 3338 cm^{-1} indicating the coordination of curcumin-diethanolamine and europium metal. The band at 1463 cm^{-1} shifted to lower wavelength 1454 cm^{-1} . The shifting of the bands in the complex IR spectra strongly signifies that the europium metal coordinate to curcumin-diethanolimine ligand (L^4) and the appearance of a new band at 558 cm^{-1} and 458 cm^{-1} assigning to the M-O and M-N stretching vibrations which was not found in the spectra of free ligand (L^4), clearly suggests that the nitrogen and oxygen atoms of the ligand are coordinating to the europium metal leading to the formation of neodymium complex with the curcumin-diethanolimine ligand.

5.3.1.5. FT-IR Spectra of Curcumin-diethanolimine Gadolinium Complex $[L^4_2PrCl_3 \cdot 6H_2O]$ (**5.1d**)

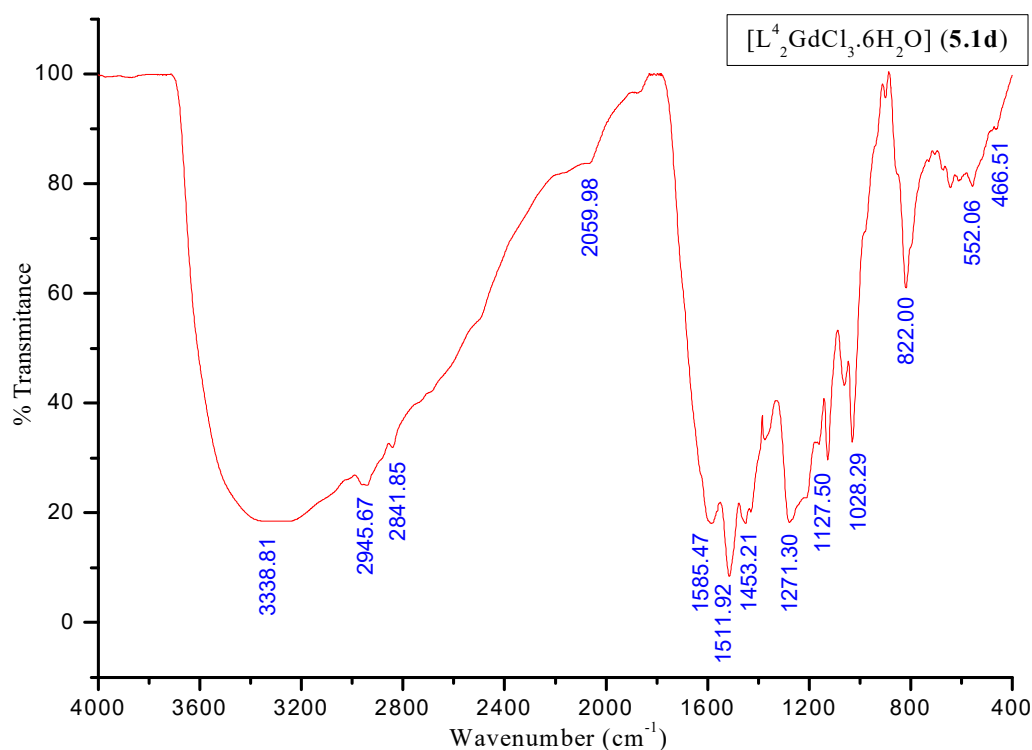


Figure 5.8. FT-IR Spectra of Curcumin-diethanolimine Gadolinium Complex $[L^4_2GdCl_3 \cdot 6H_2O]$ (**5.1d**).

The FT-IR spectra characterization of curcumin-diethanolimine gadolinium complex $[L^4_2GdCl_3 \cdot 6H_2O]$ (**5.1d**) (**Figure 5.8** and **Table 5.2**) shows that the OH stretching at 3413 cm^{-1} which appeared in the free ligand shifted to a lower wavelength at 3338 cm^{-1} forming into a broader band after complexation show the presence of H_2O in the complex. The prominent bands appeared in the free curcumin-diethanolimine ligand indicating the mixed vibrations of C=C and C=N stretching at 1599 cm^{-1} and 1516 cm^{-1} were completely shifted to lower frequencies values at 1585 cm^{-1} and 1511 cm^{-1} . The band at 1463 cm^{-1} shifted to lower wavelength 1453 cm^{-1} , the shifting of the bands in the complex IR spectra strongly signifying that the gadolynium metal coordinate to curcumin-diethanolimine ligand (**L⁴**). The band at 1275 cm^{-1} indicating the vibration of C-O bond in the ligand shifting to a higher frequency at 1277 cm^{-1} and the appearance of a new band at 552 cm^{-1} and 466 cm^{-1} assigning to the M-O and M-N stretching vibrations which was not found in the spectra of free ligand (**L⁴**), clearly suggests that the nitrogen and oxygen atoms of the ligand are coordinating to the gadolinium metal leading to the formation of gadolinium complex with the curcumin-diethanolimine ligand.

The results of the FT-IR spectra of all the complexes; $[L^4_2PrCl_3 \cdot H_2O]$ (**5.1a**), $[L^4_2NdCl_3 \cdot 6H_2O]$ (**5.1b**), $[L^4_2EuCl_3 \cdot 6H_2O]$ (**5.1c**), $[L^4_2GdCl_3 \cdot 6H_2O]$ (**5.1d**) alone with the curcumin-diethanolamine ligand are tabulated in **Table 5.2**.

Table 5.2. Major FT-IR Spectral data of the Curcumin-diethanolimine (**L⁴**) and its Lanthanide Complexes (**5.1a-d**) (cm⁻¹).

Compounds	$\nu(\text{ArOH}, \text{OH})$	$\text{Ar}\nu(\text{CH})$	$\nu(\text{C}=\text{C})$ $(\text{C}=\text{N})$	$\text{Ar}\nu(\text{CC})$	$\nu(\text{C}-\text{O})$	$\nu(\text{C}-\text{H})$	$\nu(\text{M}-\text{O})$	$\nu(\text{M}-\text{N})$
Curcumin- diethanolimine (L⁴)	3413	2918, 2849	1599, 1516	1463	1275, 1127	1031, 820	-	-
[L⁴ ₂ PrCl ₃ ·H ₂ O] (5.1a)	3338	2945, 2839	1585, 1514	1449	1277, 1127	1031, 820	552	458
[L⁴ ₂ NdCl ₃ ·6H ₂ O] (5.1b)	3338	2938, 2837	1593, 1510	1447	1280, 1127	1030, 826	555	460
[L⁴ ₂ EuCl ₃ ·6H ₂ O] (5.1c)	3338	2923, 2843	1585, 1511	1454	1279, 1124	1030, 817	558	458
[L⁴ ₂ GdCl ₃ ·6H ₂ O] (5.1b)	3338	2945, 2841	1585, 1511	1453	1277, 1127	1028, 822	552	466

5.3.2. UV-Vis Spectral Characterization Studies

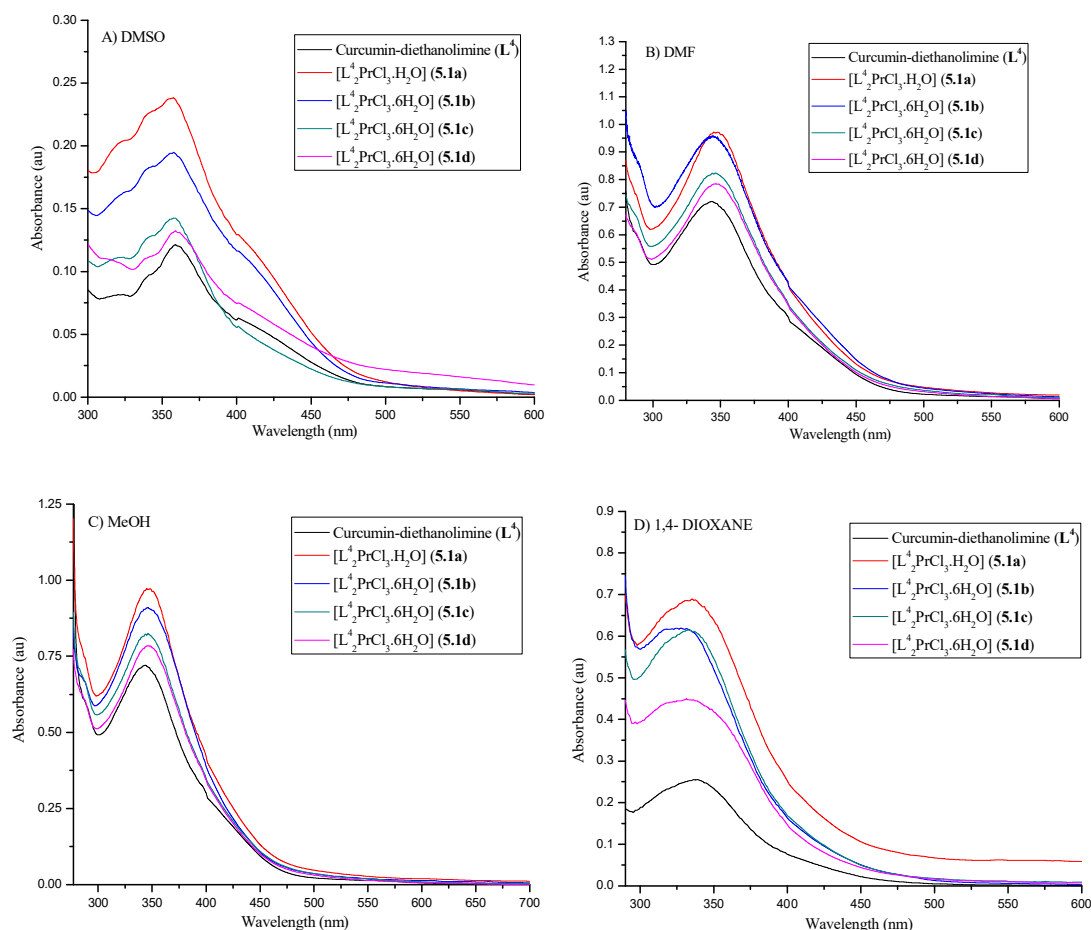


Figure 5.9. UV-Vis spectra of curcumin-diethanolimine ligand (L^4) and its Lanthanide complexes (**5.1a-d**) in different solvents (conc. 1×10^{-5} M).

UV-Vis spectra of curcumin-diethanolimine ligand (L^4) and its lanthanide complexes (**5.1a-d**) in different solvents such as dimethyl-Sulfoxide (DMSO), dimethylformamide (DMF), methanol (MeOH) and 1,4-dioxane were recorded at concentration of 1×10^{-5} M. (**Figure 5.9** and **Table 5.3**) When ligand interacts with the metal ($Ln = Pr^{3+}$, Nd^{3+} , Eu^{3+} and Gd^{3+}) and forms complex, the metal- Ligand bond length is shortened and a strong bond is formed there by increasing the absorption intensity of UV- Vis spectra of the complex compared to the intensity of the absorption spectra of curcumin-diethanolimine (Nephelauxetic Effect). In all the solvents (DMF, DMSO, MeOH and 1,4-Dioxane), the intensity of the pure ligand and complexes are in the order $[L^4_2PrCl_3 \cdot H_2O]$ (**5.1a**) > $[L^4_2NdCl_3 \cdot 6H_2O]$ (**5.1b**) > $[L^4_2EuCl_3 \cdot 6H_2O]$ (**5.1c**) > $[L^4_2GdCl_3 \cdot 6H_2O]$ (**5.1d**) > curcumin-diethanolimine ligand (L^4) which is in the same

order of the electronegativity in the periodic table. This trend of sensitivity of absorption intensity of ligand and complexes is shown in the **Figure 5.9** and **Table 5.3**. The sensitivity of the solvents are in the order of 1,4-dioxane < DMF < MeOH < DMSO which may be due to the polarity effect. In the entire medium used the maximum absorption was at around 330 nm-360 nm. With the polarity of the solvent there is a shifting in the wavelength which is due to electrostatic interaction between solvent and the curcumin-diethanolimine and its complexes, as the solvent incline to stabilized the bond causing $n-\pi^*$ transition and $\pi-\pi^*$ transition.

Table 5.3 UV-Vis spectral values of Curcumin-diethanolimine ligand (**L⁴**) and its Lanthanide Complexes (**5.1a-d**).

Compound	DMSO	DMF	MeOH	1,4-Dioxane
	$\lambda_{\max}(\text{a.u})$	$\lambda_{\max}(\text{a.u})$	$\lambda_{\max}(\text{a.u})$	$\lambda_{\max}(\text{a.u})$
Curcumin-	358.85	344.25	342.90	337.65
diethanolimine(L⁴)	(0.12127)	(0.71959)	(0.71905)	(0.25329)
[L⁴ PrCl ₃ ·H ₂ O] (5.1a)	356.90	347.20	345.45	335.75
	(0.23799)	(0.97068)	(0.97088)	(0.68827)
[L⁴ NdCl ₃ ·6H ₂ O] (5.1b)	357.60	345.35	345.45	331.75
	(0.19474)	(0.95437)	(0.90930)	(0.61804)
[L⁴ EuCl ₃ ·6H ₂ O] (5.1c)	357.60	346.55	344.40	333.25
	(0.14243)	(0.82347)	(0.82133)	(0.614864)
[L⁴ GdCl ₃ ·6H ₂ O] (5.1b)	358.85	346.55	343.25	332.60
	(0.13236)	(0.78437)	(0.77915)	(0.44721)

5.3.3. Fluorescence Spectral Characterization Studies

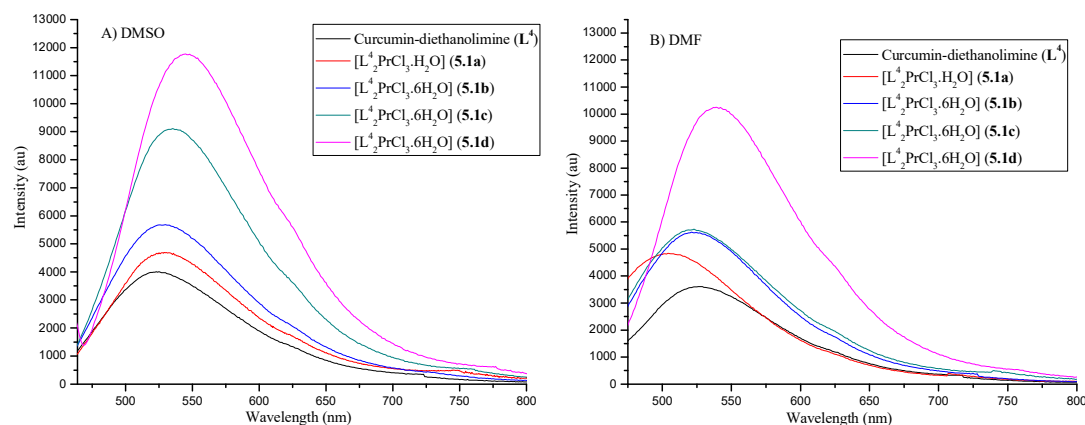


Figure 5.10. Fluorescence Spectra of Curcumin-diethanolimine ligand (L^4) and its Lanthanide complexes (**5.1a-d**) in different solvents.

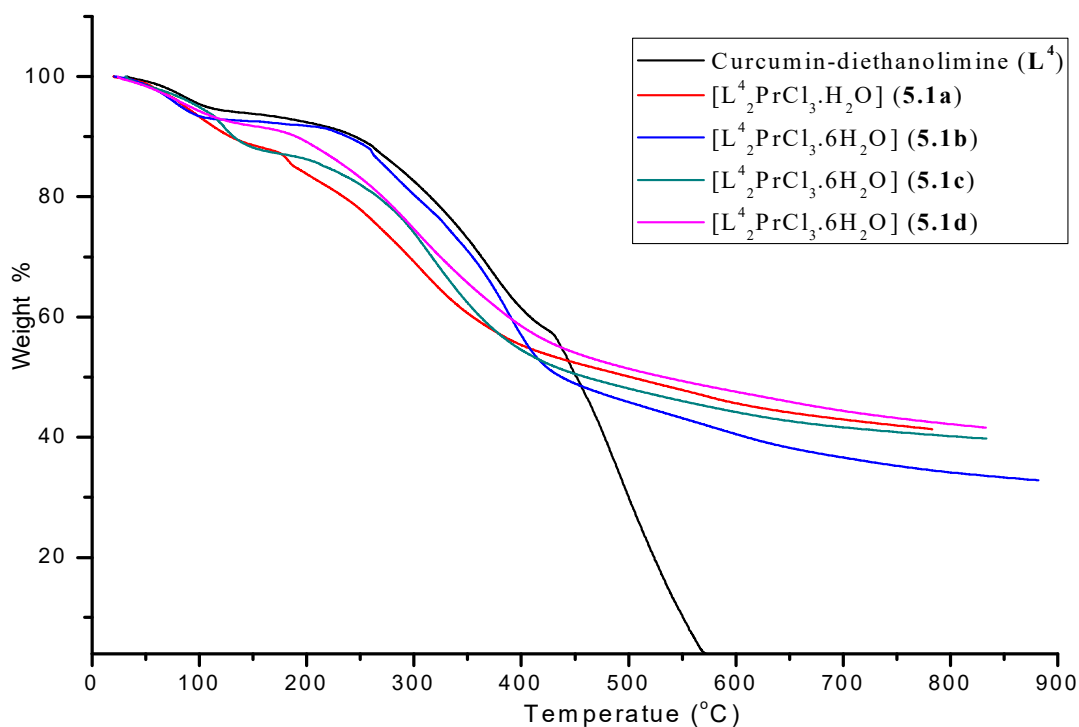
The photoluminescence spectra of the curcumin-diethanolimine ligand (L^4) and its different lanthanide (III) complexes were recorded in DMSO and DMF medium. An organic ligand plays important role to enhance the quantum yield of luminescence emission for the lanthanide metals which is due to the fact that the absorption coefficients of the ligand are manifolds larger than intrinsically low molar absorption coefficient of the Ln(III) ion. It is reflected in the luminescence spectra of pure ligand (L^4) and its lanthanide complexes in the **Figure 5.10**. Analysis of the emission spectra could exhibit the characteristic emission spectra of Pr^{3+} , Nd^{3+} , Eu^{3+} and Gd^{3+} complexes with curcumin-diethanolimine ligand (L^4). From which we could easily detect the coordination nature as well as the transfer of energy of ligand with lanthanide ions. The fluorescence spectra of a series of lanthanide complexes are found to be red shift (enhancing their wavelengths) shown in **Figure 5.10** and **Table 5.4** it may be due to the complexation of ligand with the rare earth metals.

Referring to the emission values of the Ligand and the corresponding $Ln^{3+}:(L^4)_2$ complexes in different solvent **Table 5.4** it is reflected that the order of their characteristic emission intensities are in the order $[L_2GdCl_3 \cdot 6H_2O]$ (**5.1d**) > $[L_2EuCl_3 \cdot 6H_2O]$ (**5.1c**) > $[L_2NdCl_3 \cdot 6H_2O]$ (**5.1b**) > $[L_2PrCl_3 \cdot H_2O]$ (**5.1a**) > L^4 . Again, consequently observing their relative quantum yield value, their luminescence character is in the order of $[L_2GdCl_3 \cdot 6H_2O]$ (**5.1d**) > $[L_2EuCl_3 \cdot 6H_2O]$ (**5.1c**) > $[L_2NdCl_3 \cdot 6H_2O]$ (**5.1b**) > $[L_2PrCl_3 \cdot H_2O]$ (**5.1a**) > L^4 which is due to the increasing of electronegativity of the lanthanides as in periodic table.

Table 5.4. Florescence Spectra and Quantum yield for Curcumin-diethanolimine ligand (L^4) and its Lanthanide Complexes (**5.1a-d**).

Compound	Solvent	Excitation (nm)	Emission (nm)	Intensity (a.u)	Quantum Yield (Φ_f)
Curcumin-diethanolimine (L^4)	DMSO	330	527	6599.2	0.0287
	DMF	320	526	3615.2	0.0212
$[L^4_2PrCl_3 \cdot H_2O]$ (5.1a)	DMSO	329	530	5688.8	0.0392
	DMF	326	530	5497.8	0.0292
$[L^4_2NdCl_3 \cdot 6H_2O]$ (5.1b)	DMSO	329	526	5732.9	0.0408
	DMF	326	521	5625.4	0.0337
$[L^4_2EuCl_3 \cdot 6H_2O]$ (5.1c)	DMSO	329	535	9106.8	0.0416
	DMF	326	529	6952.1	0.0393
$[L^4_2GdCl_3 \cdot 6H_2O]$ (5.1b)	DMSO	329	545	11749.9	0.0639
	DMF	326	539	10252.5	0.0589

5.3.4. Thermogravimetric Analysis

**Figure 5.11.** TGA curve for Curcumin-diethanolimine Ligand (L^4) and its Lanthanide Complexes (**5.1a-d**).

The thermogravimetric analysis of the curcumin-diethanolimine ligand (L^4) and its lanthanide complexes; $[L^4_2PrCl_3 \cdot H_2O]$ (**5.1a**), $[L^4_2NdCl_3 \cdot 6H_2O]$ (**5.1b**), $[L^4_2EuCl_3 \cdot 6H_2O]$ (**5.1c**) and $[L^4_2GdCl_3 \cdot 6H_2O]$ (**5.1d**) were recorded in nitrogen atmosphere at the heating temperature rate of 10 °C/min and mass loss was measured maintaining the temperature up to 900 °C shown in **Figure 5.11**. In case of curcumin -diethanolimine ligand (L^4), it under go three stages of decomposition starting at 118 °C and completing at 581 °C while those of the lanthanide complexes under 5 stages of decomposition. The thermal stability of the complexes were specify by the ligand to a great extend and at an average temperature the decomposition of the lanthanide complexes begins step by step and yield a residue of metal complexes even at high temperature showing its thermal stability. From the obtained TGA curve, the weight loss of the free ligand and the metal complexes at different temperature were analyzed experimentally and theoretically. The typical thermograms of the curcumin-diethanolimine ligand (L^4) and its lanthanide complexes $[L^4_2PrCl_3 \cdot H_2O]$ (**5.1a**), $[L^4_2NdCl_3 \cdot 6H_2O]$ (**5.1b**), $[L^4_2EuCl_3 \cdot 6H_2O]$ (**5.1c**) and $[L^4_2GdCl_3 \cdot 6H_2O]$ (**5.1d**) are represented in **Figure 5.11** and the detail decomposition of the compounds respected to the temperature is tabulated in **Table 5.5**.

Table 5.5. Thermo Gravimetric Analysis of the Curcumin-diethanolimine (L^4) and its lanthanide complexes (**5.1a-d**).

Compound	Temperature (° C)	Weight Loss (%) (Experiment/Theoretical)	Decomposed Compound
Curcumin-diethanolimine (L^4)	30.00 – 118.33	5.53% / 5.72%	2 (OH)
	118.30 – 402.34	33.35% / 33.48%	2(CH ₂ -CH ₂ -OH) and 2(OCH ₃)H and S
	402.34 – 581.90	61.11% / 60.79%	2 (C ₆ H ₃ CH=CH), CH ₂ and 2(C=N)
[L ⁴ ₂ PrCl ₃ ·H ₂ O] (5.1a)	30.00 – 136.57	10.63% / 10.91%	H ₂ O, 4 (OH) and 2(CH ₃)
	136.57 – 186.21	2.99% / 2.82%	2(CH ₃)
	186.21 – 395.16	29.6% / 29.63%	2 (C ₆ H ₃ -CH), CH and 4O
	395.16 – 780.54	14.33% / 14.29%	2 (HC ₆ H ₃)
	780.54.....	41.40% / 42.33%	2 (CO-CN-C-CN-OC) , 2C and Pr
[L ⁴ ₂ NdCl ₃ ·6H ₂ O] (5.1b)	30.00 – 102.10	18.39% / 18.97%	4 (H ₂ O)
	102.10 – 261.21	22.49% / 22.92%	4 (H ₂ O) and 2 (OH)
	261.21 – 448.74	16.48% - 16.73%	4 (OCH ₃), 2(OH) and 4 (C ₆ H ₃)
	448.74 – 604.14	13.66% - 13.10%	4 (CH)
	604.14.....	28.00% - 28.52%	2 (CH-CO-CN-CH ₂ -CN-OC-CH) and Nd
[L ⁴ ₂ EuCl ₃ ·6H ₂ O] (5.1c)	30.00 – 145.51	11.5% / 11.50%	6 (H ₂ O) and 2 (OH)
	145.51 – 255.36	7.14% / 7.55%	2 (OH) and 2 (OCH ₃),
	255.36 – 414.38	28.25% / 27.98%	2 (OCH ₃) and 3 (C ₆ H ₃ CH)
	414.38 – 785.37	12.75% / 12.01%	4 (CH) and C ₆ H ₃ CH
	785.37....	40.36% / 40.94%	2 (CH-CO-CN-CH ₂ -CN-OC-CH) and Eu
[L ⁴ ₂ GdCl ₃ ·6H ₂ O] (5.1d)	30.00 – 119.13	7.46% / 7.69%	5 (H ₂ O)
	119.13 – 204.11	3.99% / 3.76%	H ₂ O and 2 (OH)
	204.11 – 411.32	33.27% / 33.16%	2 (OH), 4 (OCH ₃), 2(C ₆ H ₃) and C ₆ H ₃ CH
	411.32 – 530.11	14.34% / 14.18%	7 (CH) and C ₆ H ₃
	530.11.....	40.94% / 40.19%	2 (CH-CO-CN-CH ₂ -CN-OC-CH) and Gd

5.4. Conclusion

In conclusion, we report the novel synthesis of curcumin-diethanolimine (**L⁴**) and its lanthanide complexes (**5.1a-d**). All the synthesized curcumin-diethanolimine lanthanide complexes were well investigated for their various spectroscopic studies. The IR spectra of all complexes were found that there is a chelate band shift and formation of new band in complexes comparing with that of free curcumin-diethanolimine ligand which confirm the complexation. The UV-Vis absorption spectra of the complexes increase with the increase in the polarity of the solvents. Interestingly, the fluorescence spectroscopic studies were found that after complexation the intensity of the emission spectra increases comparing with that of free curcumin-diethanolimine ligand.

5.5. References

1. <https://www.acs.org/content/acs/en/molecule-of-the-week/archive/e/ethanolamine.html>
2. Garsin, D. Ethanolamine Utilization in Bacterial Pathogens: Roles and Regulation, *Nat. Rev. Microbiol.*, 2010, **8**, 290-295. <https://doi.org/10.1038/nrmicro2334>
3. <https://www.bing.com/search?q=ethanolamine+properties&FORM=QSRE4#>
4. D. Patel and S. N. Wit, Ethanolamine and Phosphatidylethanolamine: Partners in Health and Disease, *Oxidative Medicine and Cellular Longevity*, 2017, 4829180. <https://doi.org/10.1155/2017/4829180>
5. What is ethanolamine? (with pictures) by Ray Hawk <https://www.wisegeek.com/what-is-ethanolamine.htm>
6. J. Zhou, X. Xiong, K. Wang, L. Zou, D. Lv and Y. Yin, Ethanolamine Metabolism in the Mammalian Gastrointestinal Tract: Mechanisms, Patterns, and Importance, *Current Mol. Med.*, 2017, **17**(2), 92-99. <https://doi.org/10.2174/1566524017666170331161715>
7. M. Frauenkron, J. P. Melder, G. Ruider, R. Rossbacher and H. Höke, "Ethanolamines and Propanolamines" in *Ullmann's, Encyclopedia of Industrial Chemistry* by Wiley-VCH, Weinheim, 2002. https://doi.org/10.1002%2F14356007.a10_001
8. K. Weissermel, H. J. Arpe, C. R. Lindley and S. Hawkins, *Oxidation Products of Ethylene*. Industrial Organic Chemistry. Wiley-VCH. 2003, Chapter 7. 159-161. <https://en.wikipedia.org/wiki/Special:BookSources/978-3-527-30578-0>
9. K.H. Beyer, W.F. Bergfeld, W.O. Berndt, R.K. Boutwell, W.W. Carlton, D.K. Hoffmann and A.L. Schroeter, 8 Final Report on the Safety Assessment of Triethanolamine, Diethanolamine, and Monoethanolamine *J. Am. Coll. Toxicol.*, 1983, **2**, 183-235. <https://doi.org/10.3109%2F10915818309142006>
10. E. Lukevics, L. Liberts and M.G. Voronkov, Organosilicon Derivatives of Aminoalcohols, *Russ. Chem. Rev.*, 1970, **39**, 953-963. <http://iopscience.iop.org/article/10.1070/RC1970v039n11ABEH002054/pdf>
11. K. Baillie, A. A. R. Thompson, J.B. Irving, M.G.D. Bates, A.I. Sutherland, W. MacNee, S. R. J Maxwell and D.J. Webb, Oral antioxidant supplementation does not prevent acute mountain sickness: double blind, randomized placebo-controlled trial, *Q. J. Med.*, 2009, 102(5), 341-348. <https://doi.org/10.1093/qjmed/hcp026>

12. Z. D. Petrovic, D. H. Litina, E. Pontiki, D. Simijonovic and V.P. Petrovic, Diethanolamine Pd(II) complexes in bioorganic modeling as model systems of metallopeptidases and soybean lipoxygenase inhibitors, *Bioorg. Chem.*, 2009, **37**, 162-166. <https://doi.org/10.1016/j.bioorg.2009.07.003>
13. H. Bhutani, S. Singh, K.C. Jindal and A.K. Chakraborti, Mechanistic Explanation to the Catalysis by Pyrazinamide and Ethambutol of Reaction between Rifampicin and Isoniazid in Anti-TB FDCs. *J. Pharm. Biomed. Anal.*, 2005, **39**, 892-899. <https://doi.org/10.1016/j.jpba.2005.05.015>
14. C. Fleck, E. Karge, S. Loy, K.J. Wennek, M. Listing and H. Oelschläger, Local Anaesthetic Effects and Toxicity of Seven New Diethanolamine and Morpholine Derivatives of Fomocaine, *Arzneimittelforschung.*, 2003, **253(3)**, 221-228. <https://doi.org/10.1055/s-0031-1297098>
15. P. L. Ferrarini, M. Badawneh, F. Franconi, C. Manera, M. Miceli, C. Mori and G. Saccomanni, Synthesis and antiplatelet activity of some 3-phenyl-1,8-naphthyridine derivatives. *Farmaco.*, 2000, **55(9-10)**, 603-610. [https://doi.org/10.1016/s0014-827x\(00\)00085-9](https://doi.org/10.1016/s0014-827x(00)00085-9)
16. J. Andreani, L. M. Bideau, I. Duflo, P. Jardot, C. Rollanda, M. Boxberger, B. J. Y. Khalil, J. P. Baudouin, N. Wurtz, J. M. Rolain, P. Colson, L. B. Scola and D. Raoult, *In vitro* testing of Combined Hydroxychloroquine and Azithromycin on SARS-CoV-2 shows Synergistic Effect, *Microb Pathog.*, 2020, **145**, 104228. <https://dx.doi.org/10.1016%2Fj.micpath.2020.104228>
17. N. Chopin, G. Novitchi, M. Médebielle and G. Pilet, A Versatile Ethanolamine-Derived Trifluoromethyl Enaminone Ligand for the Elaboration of Nickel(II) and Copper(II)-Dysprosium(III) multinuclear complexes with magnetic properties, *J Fluor. Chem.*, 2015, **179**, 169-174. <https://doi.org/10.1016/j.jfluchem.2015.06.023>
18. Z. Chen, X. Qin, T. Zhou, X. Wu, S. Shao, M. Xi and Z. Cui, Ethanolamine-assisted Synthesis of Size-controlled Indium Tin Oxide Nanoink for Solution Deposited Transparent Conductive Film with Low Annealing Temperature, *J. Mater. Chem. C*, 2015, **3**, 11464-11470. <https://doi.org/10.1039/C5TC00180C>
19. D. Sridaeng, W. Jitaree, P. Thiampanya and N. Chantarasiri, Preparation of Rigid Polyurethane Foams using Low-emission Catalysts Derived from Metal Acetates and Ethanolamine, *e-Polymer*, 2016, **16(4)**, 265-275.

<https://doi.org/10.1515/epoly-2016-0021>

20. A. R. Espinosa, H. Valdés, M. T. R. Apan, S. H. Ortega, B. A. A. Castillo, R. R. Martínez, J. M. G. Acacio and D. M. Morales, N-(R)Ethanolamine Dithiocarbamate Ligands and their Ni(II) and Pt(II) Complexes. Evaluation of the in vitro Anticancer Activity of the Pt(II) Derivatives, *Inorg. Chim. Acta.*, 2017, **466**, 584-590.
<http://dx.doi.org/10.1016/j.ica.2017.07.035>
21. S. Sahu, U. K. Sahu, R. K. Patel, Synthesis of Thorium-Ethanolamine nanocomposite by co-precipitation method and its application for Cr(VI) removal, *New J. Chem.*, 2018, **42**, 5556-5569. <https://doi.org/10.1039/C7NJ05074G>
22. P. A. K. Allaa, S. S. Hassana and M. M. Shoukry, Complex Formation Equilibria, DFT, Docking, Antioxidant and Antimicrobial Studies of Iron(III) complexes involving Schiff Bases Derived from Glucosamine or Ethanolamine, *Inorg. Chim. Acta.*, 2019, **492**, 192–197. <https://doi.org/10.1016/j.ica.2019.04.035>
23. R. K. Dubey, A. P. Singh, N. Jaiswal, D. P. Singh, Meenakshi, A. K. Kushwaha, M. Kumar and A. Anjum, Synthesis, Spectroscopic Characterization, DFT Calculations, and Antimicrobial Activities of Narylsalicylaldiminate Derivatives of Diorganotin(IV), *J. Coord. Chem.*, 2018, **72 (19-20)**, 3371-3384.
<https://doi.org/10.1080/00958972.2019.1689563>
24. O. Stetsiuk, N. Plyuta, N. Avarvari, E. Goreshnik, V. Kokozay, S. Petrusenko and A. Ozarowsk, Mn(III) Chain Coordination Polymers Assembled by Salicylidene-2-ethanolamine Schiff Base Ligands: Synthesis, Crystal Structures, and HFEPR Study, *Cryst. Growth Des.*, 2020, **20(3)**, 1491–1502.
<https://doi.org/10.1021/acs.cgd.9b01150>
25. S. J. Uke, G. N. Chaudhari, Y. Kumar and S. P. Mardikar, Tri-Ethanolamine-Ethoxylate Assisted Hydrothermal Synthesis of Nanostructured MnCo₂O₄ with Superior Electrochemical Performance for High Energy Density Supercapacitor Application, *Mater. Today: Proc.*, 2021, **43(4)**, 2792-2799.
<https://doi.org/10.1016/j.matpr.2020.08.675>
26. B. Hasanpour, M. Jafarpour, F. Feizpour and A. Rezaeifard, Copper(II)-Ethanolamine Triazine Complex on Chitosan-Functionalized Nanomaghemit for Catalytic Aerobic Oxidation of Benzylic Alcohols, *Catal Lett.*, 2021, **151**, 45-55.
<https://doi.org/10.1007/s10562-020-03298-6>

Synthesis of Flavanone-thiosemicarbazone Lanthanide (Pr^{3+} , Nd^{3+} , Eu^{3+} and Gd^{3+}) Complexes and Investigation of their Spectroscopic Studies

Abstract

In this chapter, we report synthesis of $\text{C}_{16}\text{H}_{14}\text{N}_3\text{OSCl}$, a Schiff base derivative of a thiosemicarbazide with a flavanone and lanthanide complexes from flavanone-thiosemicarbazone ligand (L^5) and lanthanide chlorides ($\text{LnCl}_3 \cdot x\text{H}_2\text{O}$; where; $\text{Ln}=\text{Pr}^{3+}$, Nd^{3+} , Eu^{3+} and Gd^{3+}) in presence of triethylamine (Et_3N) in ethanol reflux for 24 hours and investigated their spectroscopic and kinetic studies. The spectroscopic and physic-chemical properties of the flavanone-thiosemicarbazone ligand (L^5) and its lanthanide(III) complexes $[\text{L}_3\text{PrCl}_3 \cdot \text{H}_2\text{O}]$ (**6.1a**), $[\text{L}_3\text{NdCl}_3 \cdot 6\text{H}_2\text{O}]$ (**6.1b**), $[\text{L}_3\text{EuCl}_3 \cdot 6\text{H}_2\text{O}]$ (**6.1c**), $[\text{L}_3\text{GdCl}_3 \cdot 6\text{H}_2\text{O}]$ (**6.1d**) were studied by various means IR, UV-Vis, TGA-DTA and elemental analysis. The FT-IR spectra of flavanone-thiosemicarbazone lanthanide complexes (**6.1a-d**) were well interpreted based on the comparison to free flavanone-thiosemicarbazone ligand (L^5) spectrum.

6.1. Introduction

Flavanones, a subclass of flavonoids, are widely recognized for their nutraceutical values.¹ Flavanones are also known for their potential bioactivities against cancer.² Thiosemicarbazides are a class of versatile ligands exhibiting important physico-chemical properties due to their delocalization and flexibility of coordination modes. Therefore, a combination of flavanones and thiosemicarbazides may lead to compounds having synergistic properties of both classes of compounds. Schiff base derivatives of thiosemicarbazides have been studied for their biological and pharmacological properties.³ Metal-thiosemicarbazone complexes exhibit multiple activities in biology and catalytic application.⁴ and flavanone-metal complexes are also found to have multiple application such as the DNA-binding, anti-cancer, anti-tumor, anti-inflammatory, anti-coagulant, anti-oxidant etc.⁵⁻¹⁰ However, Schiff base derivatives of flavanones with thiosemicarbazides have not been explored extensively.¹¹⁻¹² In particular, structurally characterized flavanone-thiosemicarbazone Schiff bases are rare in the literature. The presence of NH and S moieties in such compounds opens up the possibility of studying the role of the comparatively less explored class of N-H...S interactions in building supramolecular architectures. This is of interest as hydrogen bonding to sulfur is known to play an

important role in biological systems.¹³ Complexes of thiosemicarbazone and flavanone have been frequently studied. Some of the recently reported studies of these complexes were outlined below.

M. M. Kasprzak *et al.* (2015) gives a review on the potentiality and properties of flavonoid metal complexes of different metals as they possessed a wide variety of applications biologically and chemically. This review shows that coordination of the flavonoid molecule depends on the carbonyl and hydroxyl site and when the metal chelate to this site, the properties such as the oxidation state, color, stability etc. are affected. Its application in biological system such as the chemo preventive agent, anti-oxidant, anti-tumor etc are also reported.¹⁴

Flavanones found in citrus fruits are known as naringenin which was found to exhibit inadequate anti-oxidant activity comparing to flavones and flavonols. Naringenin when coordinate to metal the antioxidant activity are enhances and so considering this V. Uivarosi and group in 2016 reported a synthesized oxovanadium(IV) complex (**Figure 6.1**) The complex was characterized by different spectroscopic, molar conductance, elemental and thermal analysis. A square pyramidal stereochemistry was suggested base on the spectral datas and reported that the resultant product can be a promising insulinomimetic agents.¹⁵

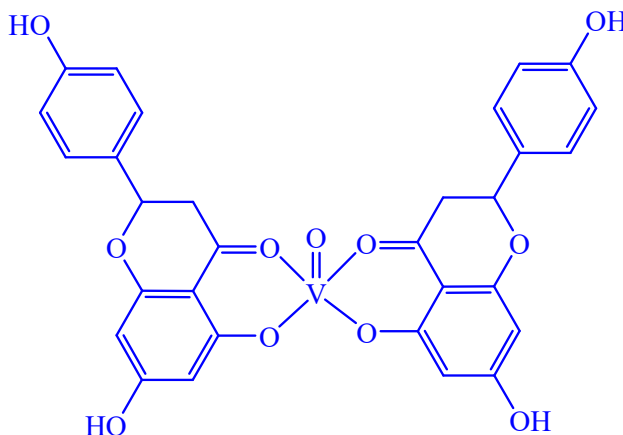
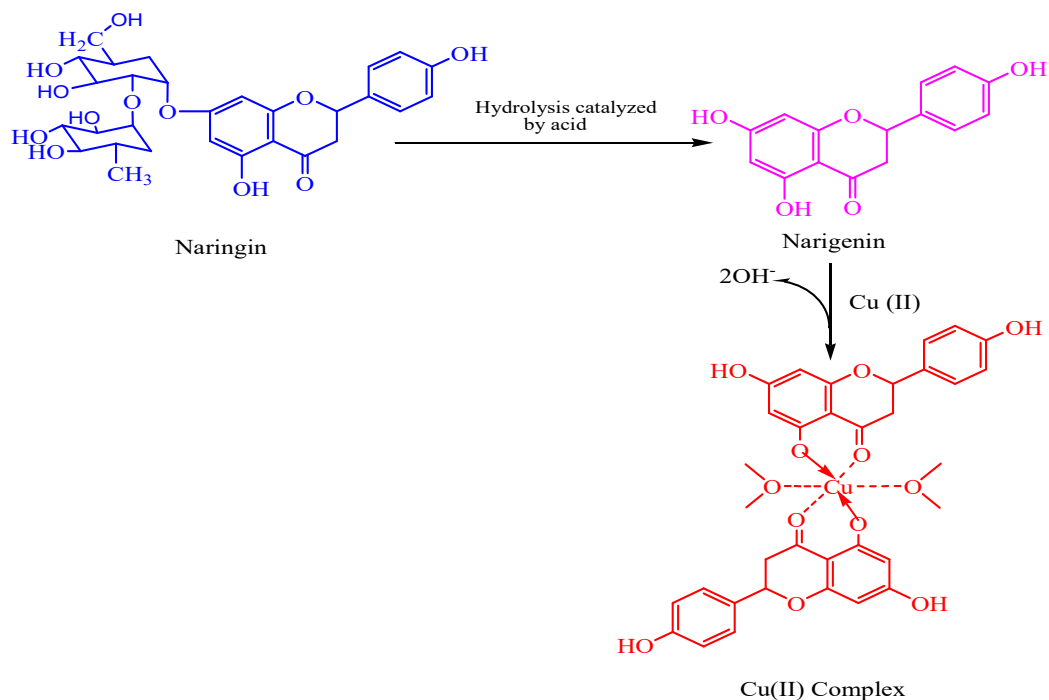


Figure 6.1. Possible structures of metal complex.

G. Celiz *et al.* (2019) reported a synthesis of copper(II) naringenin complexes starting with the extraction of the flavonoid naringin from the waste of grape fruit industry. From the extracted naringenin were obtaining by hydrolysis which was further used for the synthesis of the copper(II) naringenin complex as shown in **Scheme 6.2**. The complex

produce was characterized through different spectroscopic technique and reported their first ever crystal structure. The anti-radical activity of the complexes was found to have more potentiality then that of the free ligand itself.¹⁶



Scheme 6.2. Synthesis of the Cu(II) complex starting from naringin.

The developing of metal-base compound has become one of the rising research areas due to its various activities that they possess. A. S. El-Tabl *et al.* (2020) design a series of new binary metal(II) complexes (**Figure 6.2**) and characterized the complexes using ¹H NMR, Mass spectra, IR, UV-Vis, conductance measurement, elemental and thermal analysis and magnetism measurement. The ligand and some of the metal complexes were found to exhibit anti-tumor activity.¹⁷

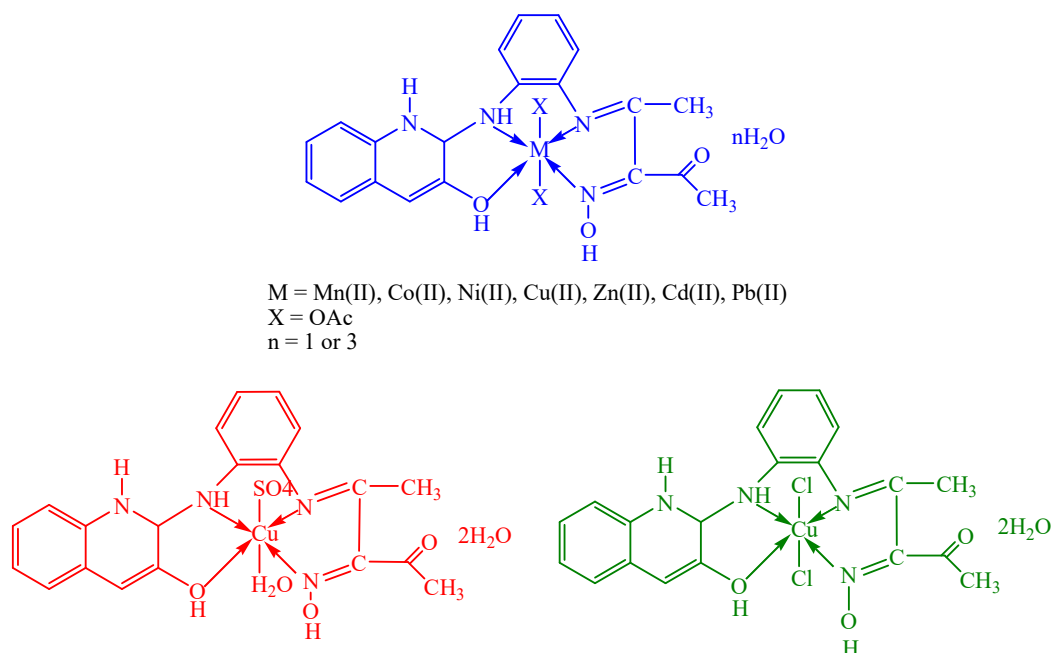


Figure 6.2. Structures of the Metal Complexes.

M. Fabijanska *et al* (2021) outlined the potentiality of some ruthenium(II) and platinum(II) complexes of flavanone (**Figure 6.3**), as the complex base on the flavanone exhibit numerous applications. With the increase of the cancer cases worldwide, the mechanism of the drug resistance plays an important role in proapoptotic activity. The study comfrimed that the Cisplatin-resistant cells increase the glutathione levels showing the mechanism of the cell to resist apoptosis caused by DNA damage. The study also gives the sensitivity of the Cisplatin against human ovarian cancer cell and the complexes of both ruthenium(II) and platinum(II) exhibit cytotoxic effect.¹⁸

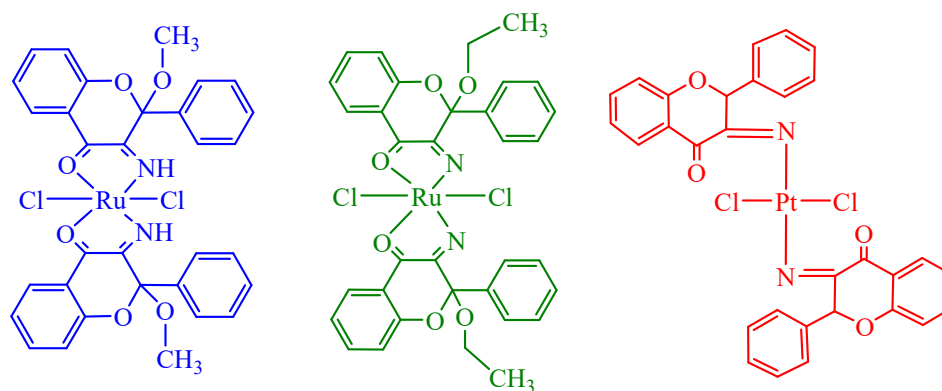


Figure 6.3. Structures of the Flavanoid-base-complexes.

Considering the above, we have synthesized the flavanone-thiosemicarbazone compound through a Schiff base condensation reaction, and report herein on its crystal structure and the Hirshfeld surface analysis and thereby used to synthesize novel lanthanide complexes of flavanone-thiosemicarbazone and characterized its spectroscopic, physico-chemical and kinetics studies.

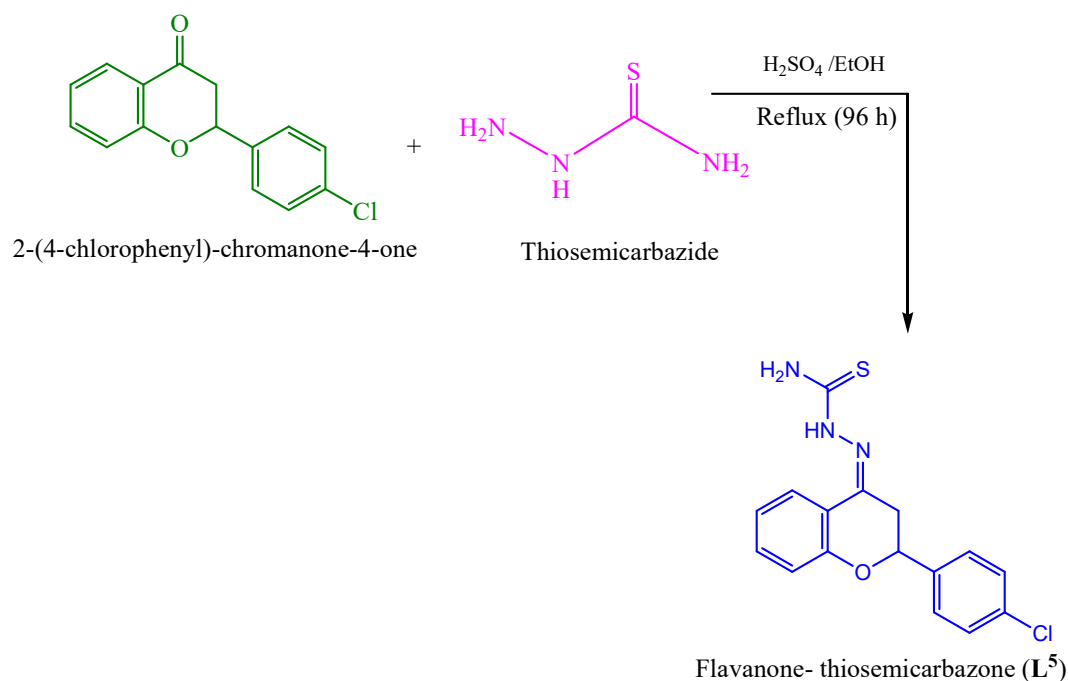
6.2. Experimental

6.2.1. Materials and Methods

All the reagents and solvents were purchased from commercially available sources and used without further purification. FT-IR spectra of the flavanone-thiosemicarbazone ligand and its lanthanide complexes were recorded on Perkin-Elmer spectrophotometer (Spectrum-Two) using KBr disk and values are expressed in cm^{-1} . Micro analytical (CHN) data were obtained with a FLASH EA 1112 Series CHNS analyzer. UV-visible spectrophotometer (Double Beam) Perkin Elmer, Lambda-35 is used for recording the absorption bands of the flavanone-thiosemicarbazone ligand and its Lanthanide complexes. The TGA-DTA measurements of flavanone-thiosemicarbazone ligand (**L⁵**) and its lanthanide complexes (**6.1a-d**) were performed on a Perkin-Elmer analyzer in air over the temperature range of 25-900 °C.

6.2.2. Synthesis of Flavanone-thiosemicarbazone Ligand (**L⁵**)

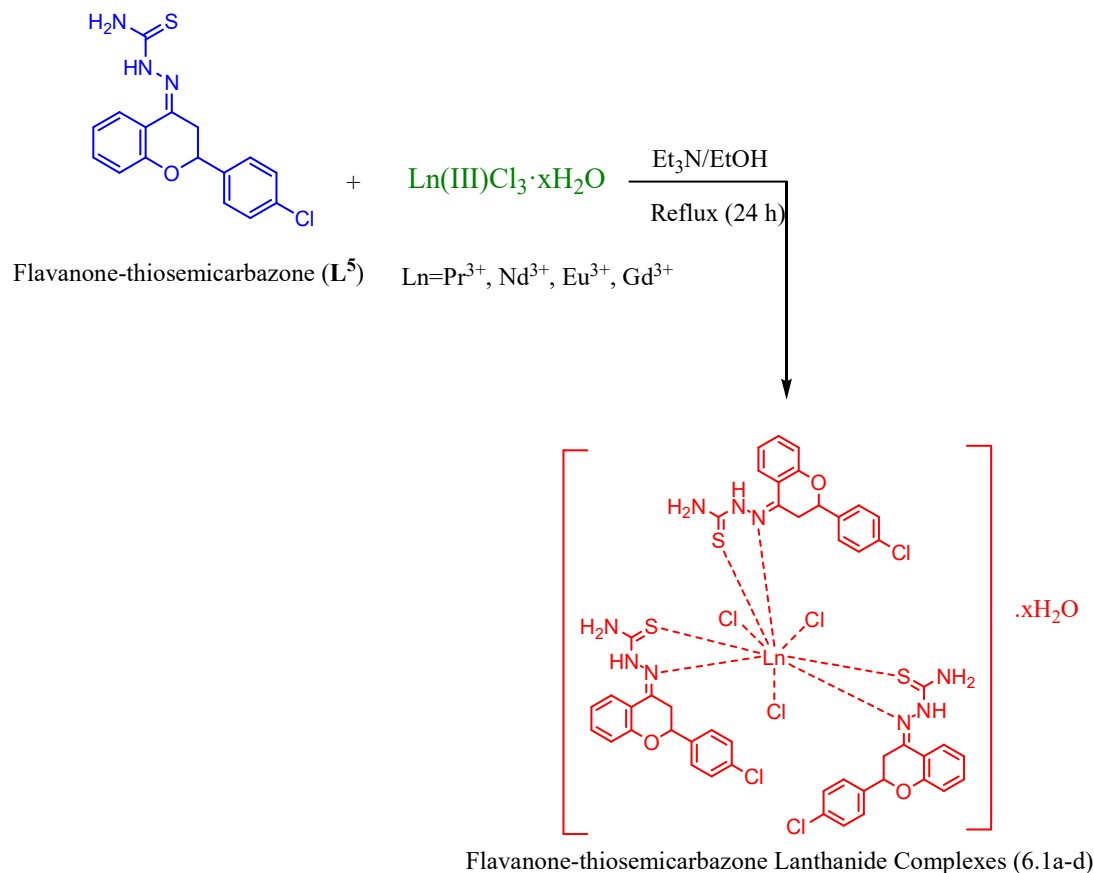
The synthesis of flavanone-thiosemicarbazone was achieved by adding Conc. H_2SO_4 (10 mol %) in ethanol (5 ml) to a stirred solution of 2-(4-chlorophenyl)-chroman-4-one (0.258 g, 1 mmol)²⁰ and thiosemicarbazide (0.091g, 1 mmol). The mixture was refluxed for 96 hours with continuous stirring. After completion of the reaction, as monitored by TLC, the solvent was removed under reduce pressure and then ice-cold water was added. The resulting solid product was collected by filtration, washed with water (3-4 times) and finally with hexane and then dried at room temperature. Pale-yellow plate-like crystals of the title compound were obtained by slow evaporation at room temperature of a solution in acetonitrile (**Scheme 6.2**).



Scheme 6.2. Synthesis of Flavanone-thiosemicarbazone Ligand (L^5).

6.2.3. General Synthesis of Flavanone-thiosemicarbazone Lanthanide(III) Complexes $[\text{L}^5_3\text{LnCl}_3 \cdot x\text{H}_2\text{O}]$ (6.1a-d)

The complex of the lanthanide was prepared by taken flavanone-thiosemicarbazone (3 mmol) in ethanol medium in a round bottom flask and to it was added $\text{LnCl}_3 \cdot x\text{H}_2\text{O}$; (where; $\text{Ln} = \text{Pr}^{3+}$, Nd^{3+} , Eu^{3+} and Gd^{3+}) (1 mmol). To the reaction mixture was added three drops of triethylamine (Et_3N) and was kept for refluxing for 24 hours. After which the reaction was allowed to evaporate the solvent completed on evaporation the reaction mixture form a yellow compound which was washed with hexane for several time gives a pale yellow to yellow compound, which was collected trough filtration. The complexes $[\text{L}^5_3\text{PrCl}_3 \cdot \text{H}_2\text{O}]$ (6.1a), $[\text{L}^5_3\text{NdCl}_3 \cdot 6\text{H}_2\text{O}]$ (6.1b), $[\text{L}^5_3\text{EuCl}_3 \cdot 6\text{H}_2\text{O}]$ (6.1c), $[\text{L}^5_3\text{GdCl}_3 \cdot 6\text{H}_2\text{O}]$ (6.1d) were dried and collected for further investigation (Scheme 6.3).



Scheme 6.3. Schematic Synthesis of Flavanone-thiosemicarbazone Lanthanide (III) Complexes (6.1a-d).

6.3. Results and Discussion

Herein, we report synthesis of flavanone-thiosemicarbazone lanthanide complexes (6.1a-d). The ligand flavanone-thiosemicarbazone (L^5) was prepared from a reaction of flavanone and thiosemicarbazide with a catalytic amount of conc. H_2SO_4 in ethanol and reflux for 96 hours. The flavanone-thiosemicarbazone lanthanide metal complexes were then synthesized using flavanone-thiosemicarbazone ligand (L^5) and lanthanide metal chlorides ($LnCl_3 \cdot xH_2O$; $Ln = Pr^{3+}, Nd^{3+}, Eu^{3+}$ and Gd^{3+}) in 3:1 ratio in presence of catalytic amount of Et_3N in ethanol and reaction mixture was kept under reflux condition for 24 hours. The solvent was completely evaporated and the yielded solid which was collected through filtration and the washed with hexane for several times and is allowed to air dried and then collected. The synthesized solid flavanone-thiosemicarbazone lanthanide complexes (6.1a-d) were stable at room temperature, which were characterized for various

spectroscopic properties. The resulting flavanone-thiosemicarbazone lanthanide complexes were well studied for FT-IR spectroscopy, UV-Visible spectroscopy, TGA-DTA analysis and elemental analysis. The physico-analytical data of free flavanone-thiosemicarbazone ligand (**L⁵**) and flavanone-thiosemicarbazone lanthanide complexes (**6.1a-d**) were represented in **Table 6.1**.

Table 6.1. Physico-analytical data of Flavanone-thiosemicarbazone Ligand (**L⁵**) and its Lanthanide Complexes (**6.1a-d**).

Compounds	Yield (%)	Colour	CHN Analysis (%) Found (calculated)			
			Carbon	Hydrogen	Nitrogen	Sulphur
Flavanone-thiosemicarbazone (L⁵)	-	Pale yellow	57.85 (57.91)	4.28 (4.25)	12.61 (12.66)	9.59 (9.66)
[L⁵ ₃ PrCl ₃ ·H ₂ O] (6.1a)	75.63	Yellow	45.91 (45.84)	3.24 (3.29)	10.08 (10.02)	7.72 (7.65)
[L⁵ ₃ NdCl ₃ ·6H ₂ O] (6.1b)	73.06	Yellow	42.58 (42.67)	3.84 (3.80)	9.25 (9.33)	7.15 (7.12)
[L⁵ ₃ EuCl ₃ ·6H ₂ O] (6.1c)	86.04	Yellow	42.51 (42.43)	3.72 (3.78)	9.21 (9.28)	7.08 (7.15)
[L⁵ ₃ GdCl ₃ ·6H ₂ O] (6.1d)	61.60	Yellow	42.31 (42.26)	3.72 (3.77)	9.18 (9.24)	7.12 (7.05)

6.3.1. Crystal Structure and Hirshfeld Surface Analysis of Flavanone-thiosemicarbazone Ligand (L^5)

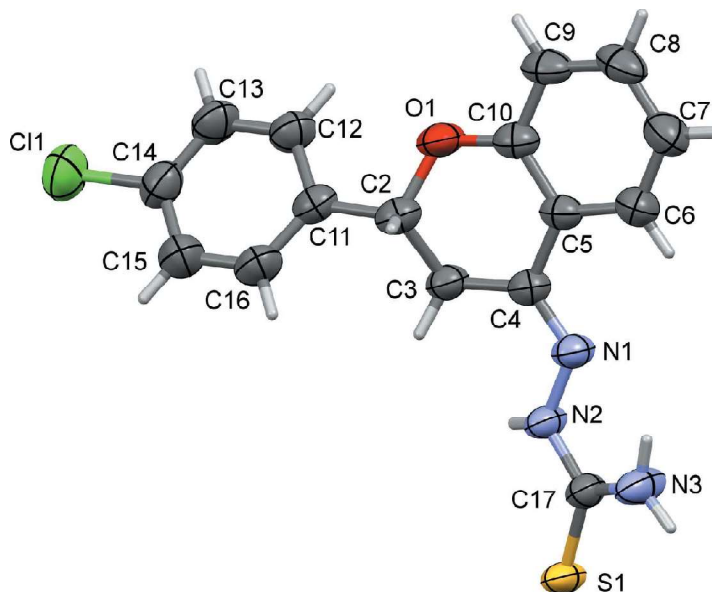


Figure 6.4. Single Crystal X-ray molecular structure of the Flavanone-thiosemicarbazone Ligand (L^5).

The molecular structure of flavanone-thiosemicarbazone is illustrated in **Figure 6.4**. The 4-chlorophenyl ring (C11–C16) is inclined to the benzene ring (C5–C10) of the chromanone ring system by $30.72(12)^\circ$. The pyran ring (O1/C2–C5/C10) has an envelope conformation with atom C2 as the flap, being displaced by $0.655(2)\text{\AA}$ from the mean plane through the other five atoms of the ring. The mean plane of the thiourea unit (N2/C17/S1/N3) is twisted with respect to benzene ring (C5–C10) of the chromane ring system, forming a dihedral angle of $19.78(19)^\circ$.

A strong hydrogen bond often involves highly electronegative second row elements such as N, O and F. However, the less electronegative third row elements (P, S and Cl) are also known to take part in hydrogen-bonding interactions. In the crystal of the flavanone-thiosemicarbazone ligand (L^5), molecules are linked by two pairs of N–H \cdots S hydrogen bonds, forming inversion dimmers enclosing $R_2^2(8)$ ring motifs, which are linked to form ribbons propagating along the b-axis direction (**Table 6.2** and **Figure 6.5**). In the crystal, there are no other significant short intermolecular interactions present

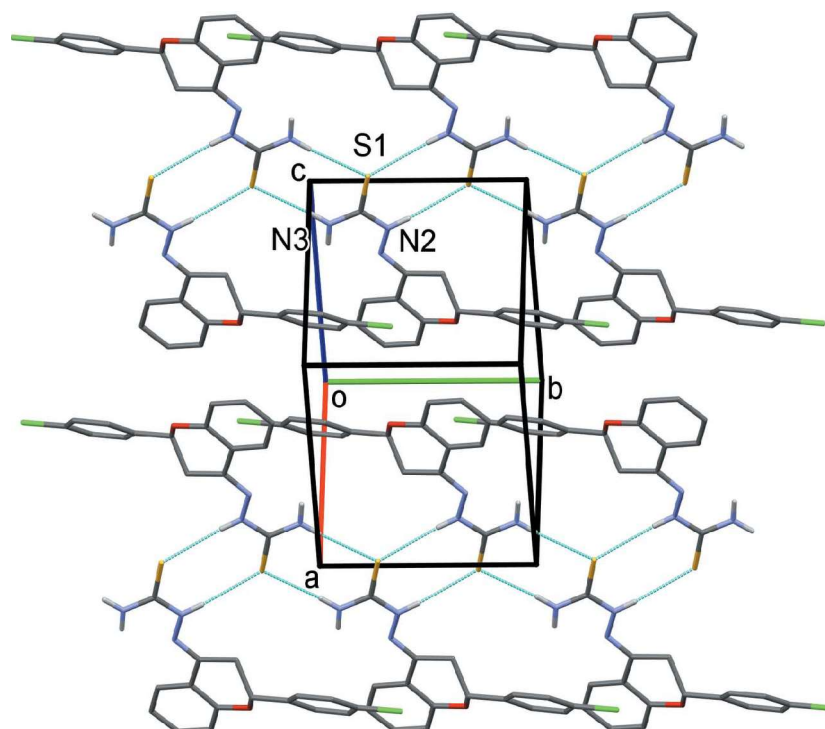


Figure 6.5. Single X-ray diadram of the Flavanone-thiosemicarbazone (L^5).

Table 6.2. Geometrical parameters of hydrogen bonds in Flavanon-thiosemicarbazone (L^5).

D – H \cdots A	D – H	H \cdots A	D \cdots A	D – H \cdots
N2 – H2N \cdots S1 ⁱ	0.85 (3)	2.65 (3)	3.480 (2)	167 (2)
N3 – H3BN \cdots S1 ⁱⁱ	0.88 (3)	2.52 (3)	3.392 (2)	171(2)

Symmetry codes i) – x, -y+1, -z+2; ii) –x, -y, -z+2

The Hirshfeld surface analysis²¹ and the associated two-dimensional fingerprint plots²² were performed with Crystal-Explorer17.²³ A recent article by Tiekink and collaborators²⁴ ‘outlines the various procedures and what can be learned by using Crystal-Explorer’. The Hirshfeld surface of the title compound mapped over d_{norm} is given in **Figure 6.6.a**. The red spots indicate specific points of contact in the crystal. The Hirshfeld surface mapped over the shape-index is given in **Figure 6.6.b**, showing red spots and blue regions indicative of possible C \cdots H/H \cdots C (i.e. C—H \cdots π) contacts. The Hirshfeld surface mapped over the curvedness is given in **Figure 6.6.c**. Here the region around the chromane ring system is fairly flat, indicative of possible π – π interactions. However, these

interactions must be extremely weak as analysis of the structure using PLATON²⁷ did not indicate the presence of any significant C—H \cdots π or offset π – π interactions in the crystal.

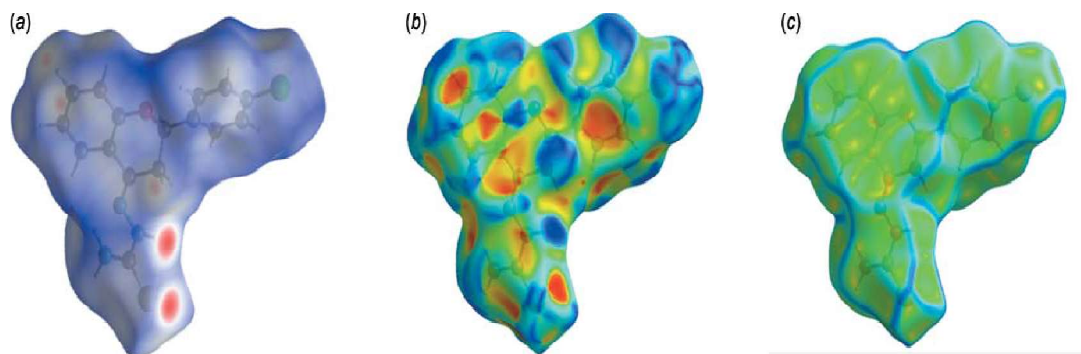


Figure 6.6. The Hirshfeld surface of the title compound mapped over (a) d_{norm} , 0.3525 to 1.4929 arbitrary units, (b) shape-index and (c) curvedness.

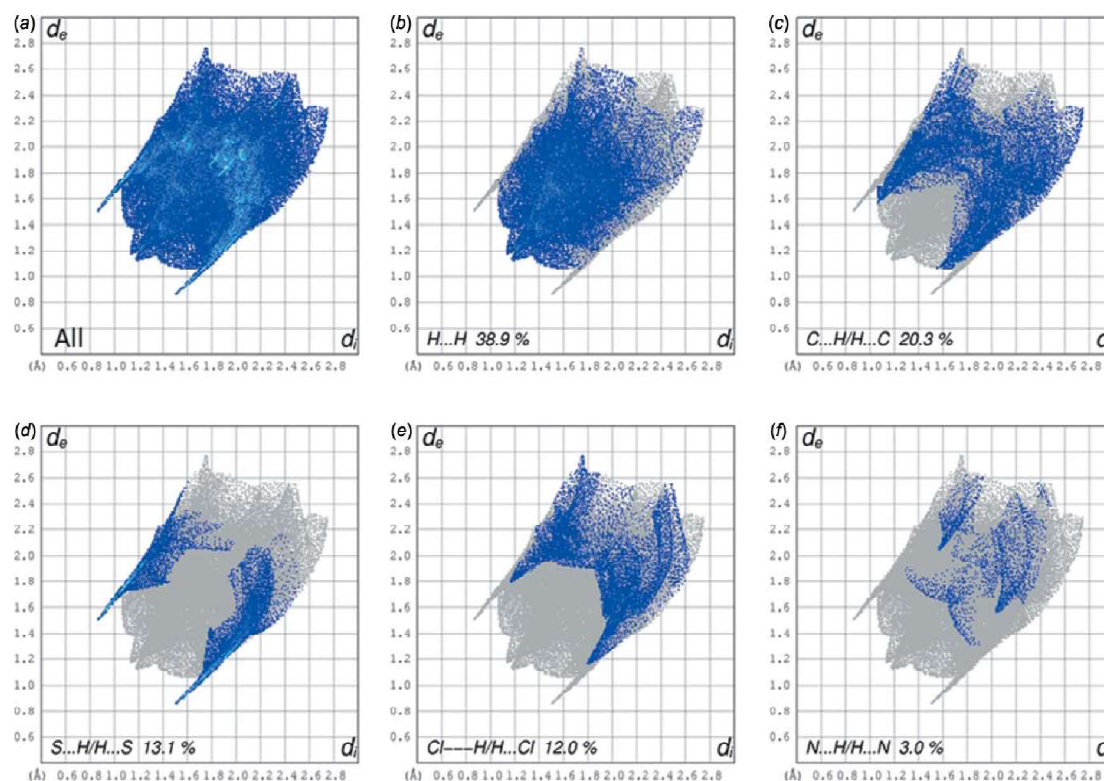


Figure 6.7. (a) The full two-dimensional fingerprint plot for Flavanone-thiosemicarbazone (**L**³) and fingerprint plots delineated into (b) H \cdots H (c) C \cdots H/H \cdots C (d) S \cdots H/H \cdots S (e) Cl \cdots H/H \cdots Cl and (f) N \cdots H/H \cdots N contacts.

The full two-dimensional fingerprint plot for the title compound is given in **Figure 6.7.a**. The principal intermolecular interactions (**Figure 6.7.b-f**) are delineated into H \cdots H (38.9%), C \cdots H/H \cdots C (20.3%), S \cdots H/H \cdots S (13.1%), Cl \cdots H/H \cdots Cl (12.0%) and N \cdots H/H \cdots N (3.0%) contacts. Note that only for the H \cdots H, C \cdots H/H \cdots C and S \cdots H/H \cdots S contacts is $d_e + d_i$ (where d_e and d_i are the distances from a given point on the surface to the nearest atom outside and inside, respectively), less than the sum of the van der Waals radii of the individual atoms.

Crystal data, data collection and structure refinement details are summarized in **Table 6.3**. The NH and NH₂ H atoms were located in a difference-Fourier map and refined freely. The C-bound H atoms were included in calculated positions and treated as riding atoms: C–H=0.93–0.98 Å with $U_{\text{iso}}(\text{H})=1.2U_{\text{eq}}(\text{C})$.

Table 6.3. Experimental Details.

Crystal data	
Chemical formula	C ₁₆ H ₁₄ ClN ₃ OS
M _r	331.81
Crystal system, space group	Triclinic, <i>P</i> $\bar{1}$
Temperature (K)	293
a, b, c (Å)	7.8218 (7), 8.4207 (6), 12.3402 (11)
α , β , γ (°)	99.838 (7), 95.771 (7), 96.515 (7)
V (Å ³)	789.66 (12)
Z	2
Radiation type	Cu K α
μ (mm ⁻¹)	3.41
Crystal size (mm)	0.50 x 0.17 x 0.10
Data collection	Rigaku OD, SuperNova, Dual, Cu
Diffractometer	at zero, Eos
Absorption correction	Gaussian (<i>CrysAlis</i> PRO; Rigaku OD, 2015)
T _{min} , T _{max}	0.464, 1.000
No. of measured, independent and observed [$I > 2\sigma(I)$] reflections	4478, 2766, 2346
R _{int}	0.019
($\sin \theta$) _{max} (Å ⁻¹)	0.596
Refinement	0.042, 0.121, 1.05
R[F ² > 2 σ (F ²)], wR(F ²), S	
No. of reflections	2766
No. of parameters	211
H-atom treatment	H atoms treated by a mixture of independent and constrained refinement
$\Delta\rho_{\max}$, $\Delta\rho_{\min}$ (e Å ⁻³)	0.51, - 0.41

6.3.2. FT-IR Spectral Characterization Studies

6.3.2.1. FT-IR Spectra of Flavanone-thiosemicarbazone Ligand (L^5)

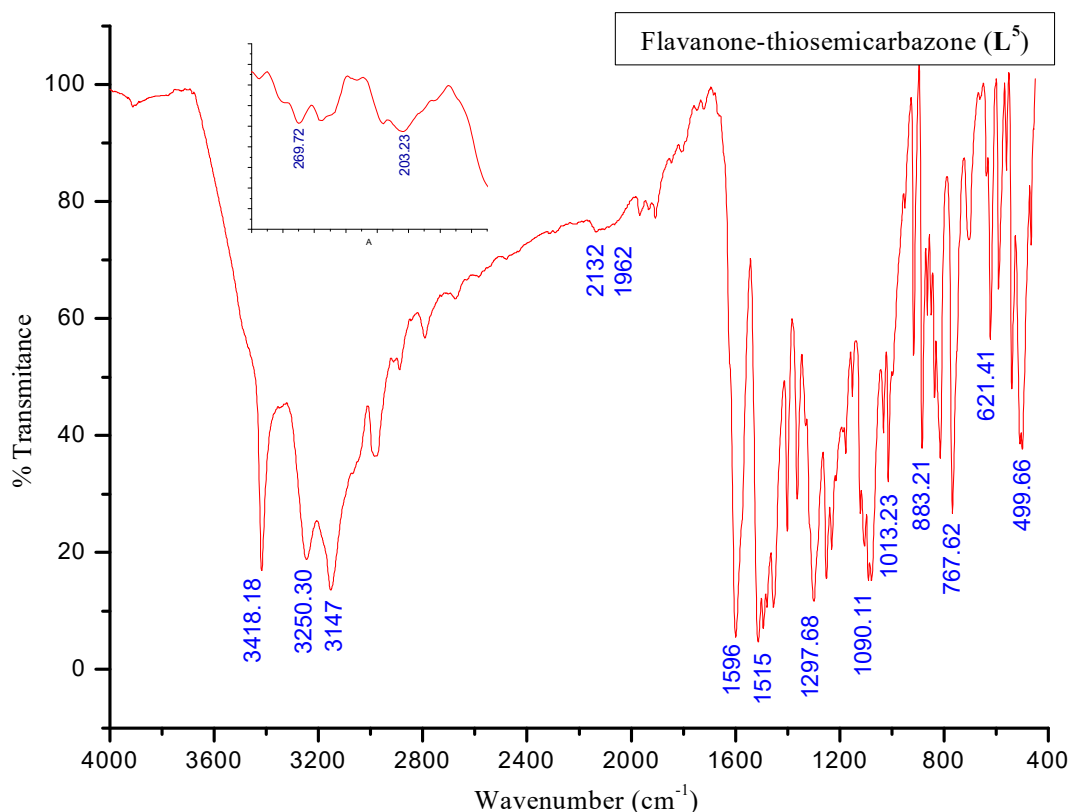


Figure 6.8. FT-IR Spectra of Flavanone-thiosemicarbazone Ligand (L^5).

The FT-IR spectrum of the flavanone-thiosemicarbazone (L^5) shows a peak at 3418 cm^{-1} , 3250 cm^{-1} and 3147 cm^{-1} attributing to NH and CH. The absorption band at 2132 cm^{-1} and 1962 cm^{-1} indicating the thiocyanate i.e. $\nu(\text{N-C=S})$ of the compound. The band observed at 1596 cm^{-1} and 1515 cm^{-1} indicating the mixed vibration of $\nu(\text{C=C})$ and $\nu(\text{C=N})$ and the bands at 1456 cm^{-1} correspond to the vibration of aromatic $\nu(\text{CC})$ bond. The peak observed at 1297 cm^{-1} and 1253 cm^{-1} correspond to C-O stretching and the vibration of the C-H bond is observed at 1090 cm^{-1} , 915 cm^{-1} and 883 cm^{-1} . The band at 767 cm^{-1} attribute to the $\nu(\text{C-Cl})$ bond (**Figure 6.8** and **Table 6.4**).

6.3.2.2. FT-IR Spectra of Flavanone-thiosemicarbazone Praseodymium Complex $[L^5PrCl_3 \cdot H_2O]$ (6.1a)

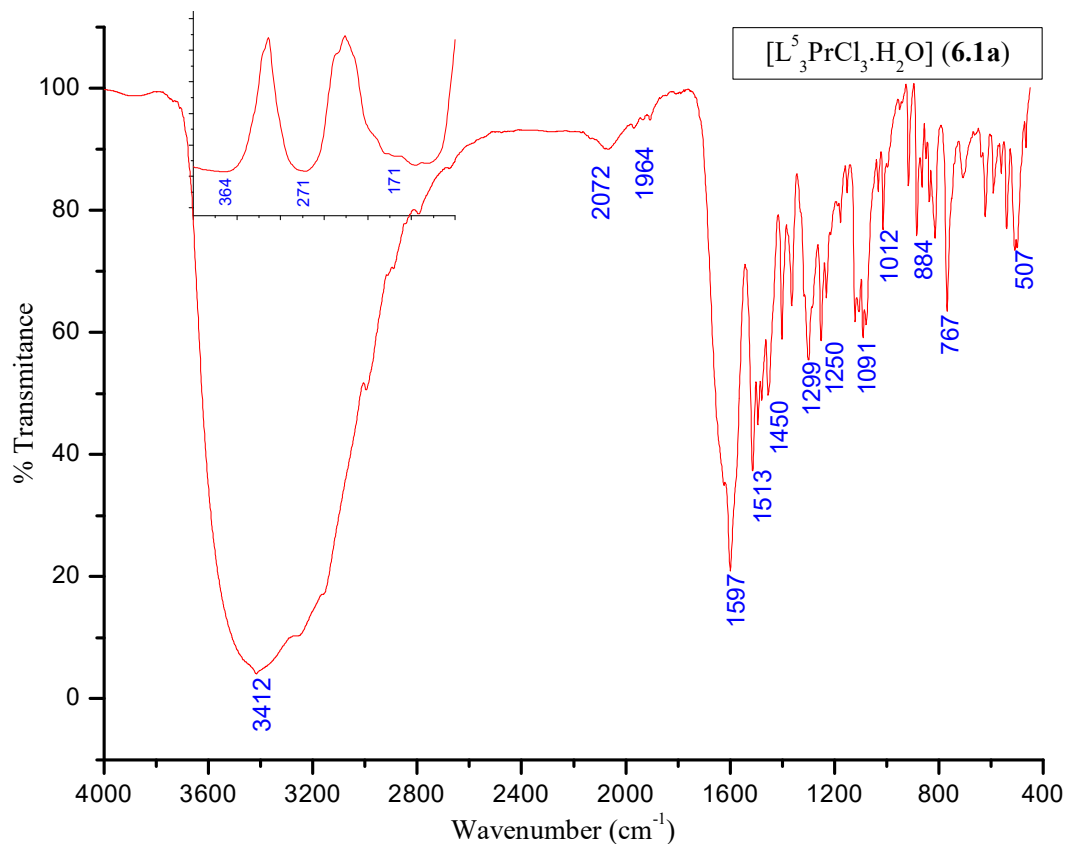


Figure 6.9. FT-IR Spectra of Flavanone-thiosemicarbazone Praseodymium Complex $[L^5PrCl_3 \cdot H_2O]$ (6.1a).

The FT-IR spectra characterization of flavanone-thiosemicarbazone praseodymium complex $[L^5PrCl_3 \cdot H_2O]$ (6.1a) shows the formation of a broad band at 3412 cm^{-1} after complexation indicating the presence of H_2O along with the mixed vibration of NH and CH bond. The prominent bands appeared in the free flavanone-thiosemicarbazone ligand indicating the mixed vibrations of $\nu(C=C)$ and $\nu(C=N)$ stretching at 1596 cm^{-1} and 1515 cm^{-1} were shifted to higher and lower frequencies values at 1597 cm^{-1} and 1513 cm^{-1} . The band at 2132 cm^{-1} and 1962 cm^{-1} in free flavanone-thiosemicarbazone ligand (L^5) shifted to lower and higher frequencies at 2072 cm^{-1} and 1964 cm^{-1} . The shifting of the bands in the complex IR spectra strongly supported the formation of complex with praseodymium metal at N and S coordination site of the flavanone-thiosemicarbazone ligand (L^5) and new bands appearing at 364 cm^{-1} and 171 cm^{-1} supports the formation of the M-N bond and M-

S bond respectively supporting the ligand coordination to the metal where this band was not observed in the free flavanone-thiosemicarbazone ligand (**Figure 6.9** and **Table 6.4**).

6.3.2.3. FT-IR Spectra of Flavanone-thiosemicarbazone Neodymium Complex $[L^5NdCl_3 \cdot 6H_2O]$ (**6.1b**)

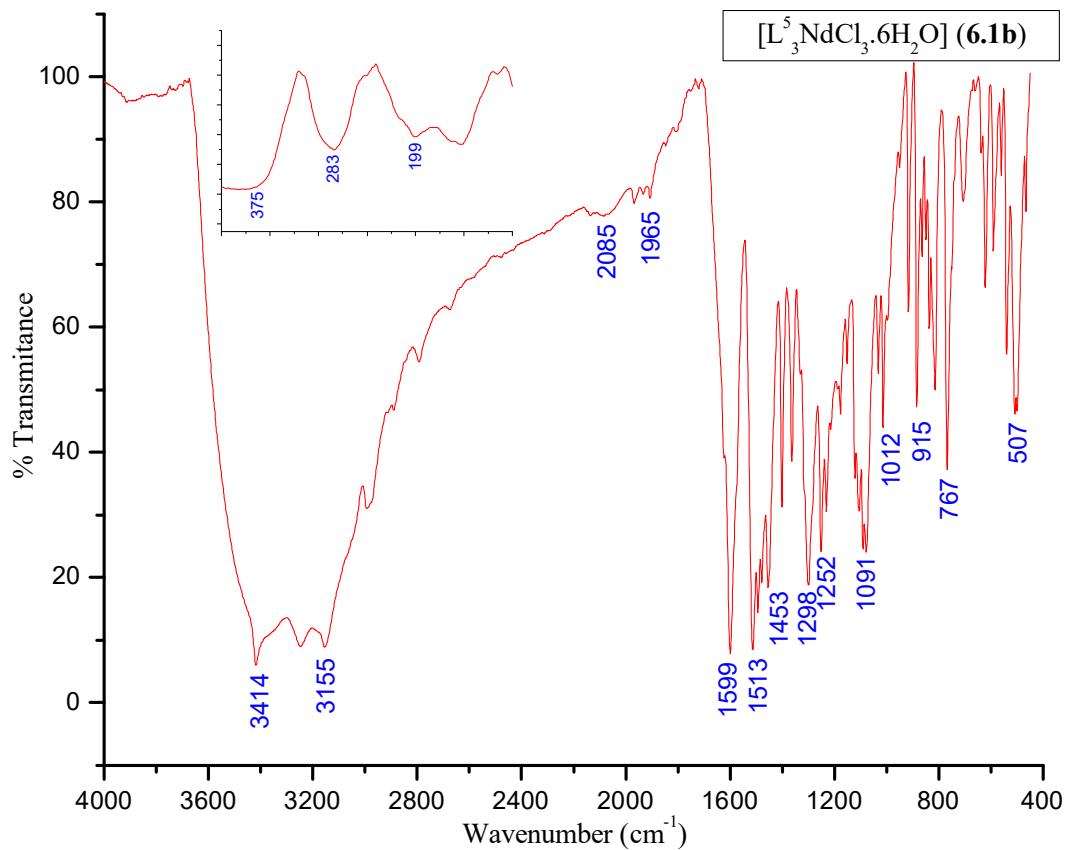


Figure 6.10. FT-IR Spectra of Flavanone-thiosemicarbazone Neodymium Complex $[L^5NdCl_3 \cdot H_2O]$ (**6.1b**).

Analyzing the FT-IR spectra of flavanone-thiosemicarbazone neodymium complex $[L^5NdCl_3 \cdot H_2O]$ (**6.1b**) shows that the formation of a broad band at 3414 cm^{-1} and 3155 cm^{-1} after complexation indicate the presence of H_2O along with the mixed vibration of NH and CH bond. The prominent bands appeared in the free flavanone-thiosemicarbazone ligand indicating the mixed vibrations of $\nu(C=C)$ and $\nu(C=N)$ stretching at 1596 cm^{-1} and 1515 cm^{-1} were shifted to higher and lower frequencies values at 1599 cm^{-1} and 1513 cm^{-1} . The band at 2132 cm^{-1} and 1962 cm^{-1} in free flavanone-thiosemicarbazone ligand (L^5) shifted to lower and higher frequencies at 2085 cm^{-1} and 1965 cm^{-1} . The shifting of the bands in the complex IR spectra strongly supported the

formation of complex with neodymium metal at N and S coordination site of the flavanone-thiosemicarbazone ligand (L^5) and new bands appearing at 375 cm^{-1} and 199 cm^{-1} supports the formation of the M-N bond and M-S bond respectively supporting the ligand coordination to the metal where this band was not observed in the free flavanone-thiosemicarbazone ligand (**Figure 6.10** and **Table 6.4**).

6.3.2.4. FT-IR Spectra of Flavanone-thiosemicarbazone Europium Complex $[L^5_3EuCl_3 \cdot 6H_2O]$ (**6.1c**)

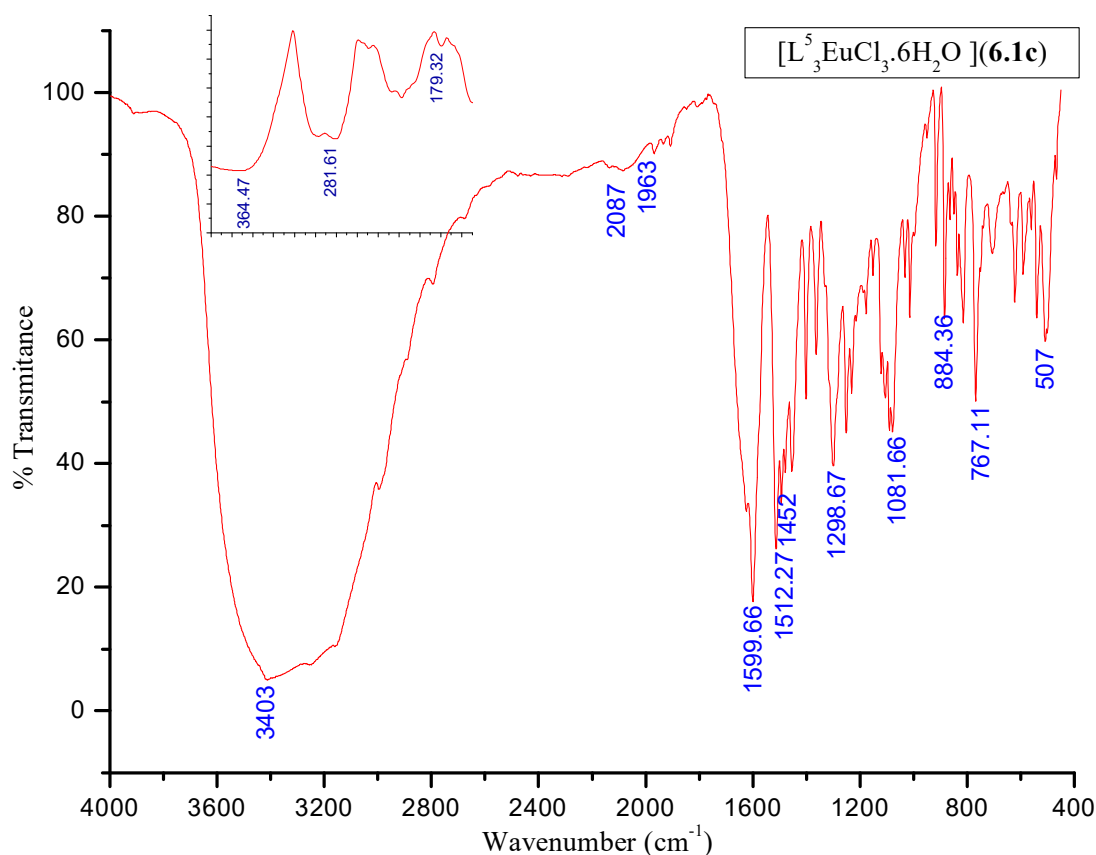


Figure 6.11. FT-IR Spectra of Flavanone-thiosemicarbazone Europium Complex $[L^5_3EuCl_3 \cdot 6H_2O]$ (**6.1c**).

The formation of a broad band at 3403 cm^{-1} after complexation indicates the presence of H_2O along with the mixed vibration of NH and CH bonds in the FT-IR spectrum of the flavanone-thiosemicarbazone europium complex $[L^5_3EuCl_3 \cdot 6H_2O]$ (**6.1c**). The prominent bands attributed to the mixed vibrations of $\nu(C=C)$ and $\nu(C=N)$ stretching at 1596 cm^{-1} and 1515 cm^{-1} in the free flavanone-thiosemicarbazone ligand (L^5) were shifted to higher

and lower wavelength at 1599 cm^{-1} and 1512 cm^{-1} . The shifting of the frequencies values fortify the coordination of flavanone-thiosemicarbazone and europium metal and new bands arising at 364 cm^{-1} and 179 cm^{-1} confirm the formation of the M-N bond and M-S bond respectively supporting the coordination of the lanthanide to the free flavanone-thiosemicarbazone ligand (L^5) (Figure 6.11 and Table 6.4).

6.3.2.5. FT-IR Spectra of Flavanone-thiosemicarbazone Gadolinium Complex $[L^5_3GdCl_3 \cdot 6H_2O]$ (6.1d)

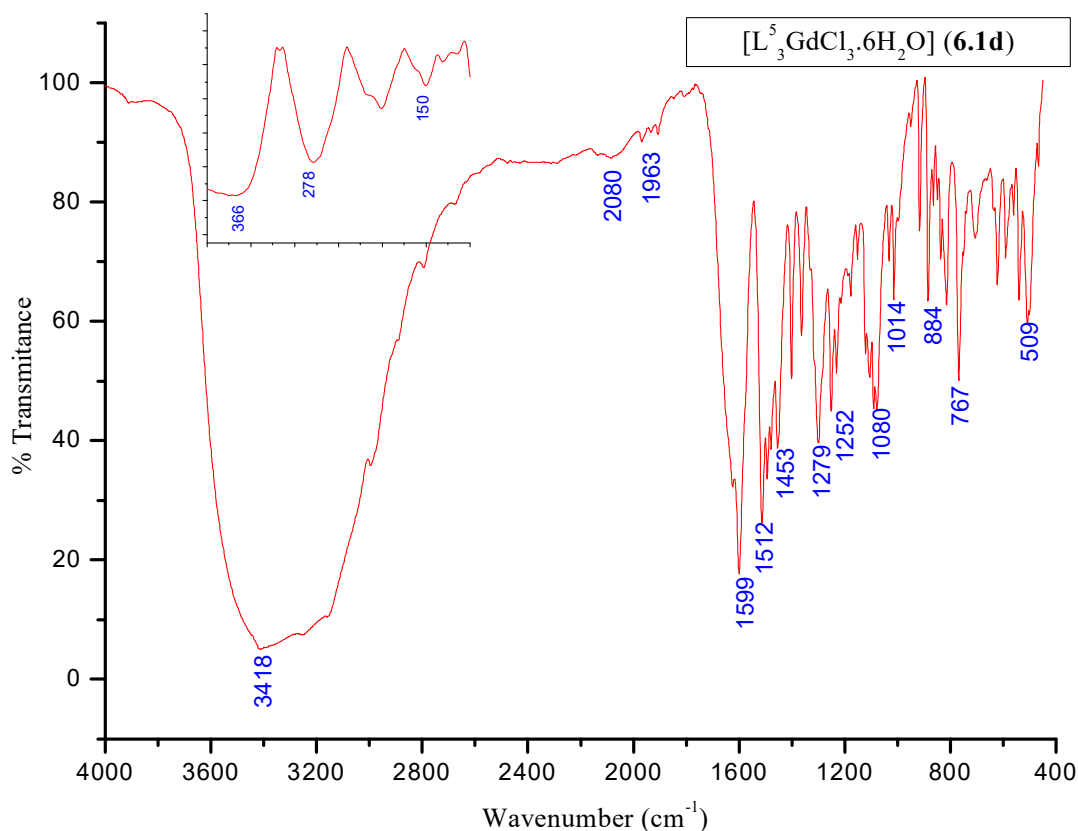


Figure 6.12. FT-IR Spectra of Flavanone-thiosemicarbazone Gadolinium Complex $[L^5_3GdCl_3 \cdot 6H_2O]$ (6.1d).

The FT-IR spectra characterization of flavanone-thiosemicarbazone praseodymium complex $[L^5_3GdCl_3 \cdot 6H_2O]$ (6.1d) shows that after complexation, there is a formation of a broad band at 3418 cm^{-1} indicating the presence of H_2O alone with the mixed vibration of NH and CH bond. The prominent bands appeared in the free flavanone-thiosemicarbazone ligand indicating the mixed vibrations of $\nu(C=C)$ and $\nu(C=N)$ stretching at 1596 cm^{-1} and 1515 cm^{-1} were shifted to higher and lower frequencies values at 1599 cm^{-1} and 1512 cm^{-1} .

The band at 2132 cm^{-1} and 1962 cm^{-1} in free flavanone-thiosemicarbazone ligand (**L**⁵) shifted to lower and higher frequencies at 2080 cm^{-1} and 1963 cm^{-1} . The shifting of the bands in the complex IR spectra strongly supported the formation of complex with gadolinium metal at N and S coordination site of the flavanone-thiosemicarbazone ligand (**L**⁵) and new bands appearing at 364 cm^{-1} and 171 cm^{-1} supports the formation of the M-N bond and M-S bond respectively supporting the ligand coordination to the metal where this band was not observed in the free flavanone-thiosemicarbazone ligand (**Figure 6.12** and **Table 6.4**). The results of the FT-IR spectra of flavanone-thiosemicarbazone ligand (**L**⁵) and its lanthanide complexes (**6.1a-d**) are tabulated in **Table 6.4**.

Table 6.4. Major FT-IR spectral data of the Flavanone-thiosemicarbazone (**L**⁵) and its Lanthanide complexes (**6.1a-d**) (cm⁻¹).

Compound	Arv(NH) (CH)	v(N-C=S)	v(C=N) (C=C)	Arv(CC)	v(C- O)	v(C-H)	v(C-Cl)	v(M-N)	v(M-Cl)	v(M-S)
Flavanone- thiosemicarbazone (L ⁵)	3418, 3250 3147	2132 1962	1596 1515	1456	1297 1253	1090 915, 883	767	-	-	-
[L ⁵ PrCl ₃ ·H ₂ O] (6.1a)	3412	2072 1964	1597 1513	1450	1299 1250	1091, 917, 883	767	364	271	171
[L ⁵ NdCl ₃ ·6H ₂ O] (6.1b)	3414 3155	2085 1965	1599 1513	1453	1298 1252	1091 915, 883	767	375	283	199
[L ⁵ EuCl ₃ ·6H ₂ O] (6.1c)	3403	2087 1963	1599 1512	1452	1279 1252	1081 917, 883	767	364	281	179
[L ⁵ GdCl ₃ ·6H ₂ O] (6.1d)	3413	2080 1963	1599 1512	1453	1279 1252	1080 915, 883	767	366	278	150

6.3.3. UV-Vis Spectral Characterization Studies

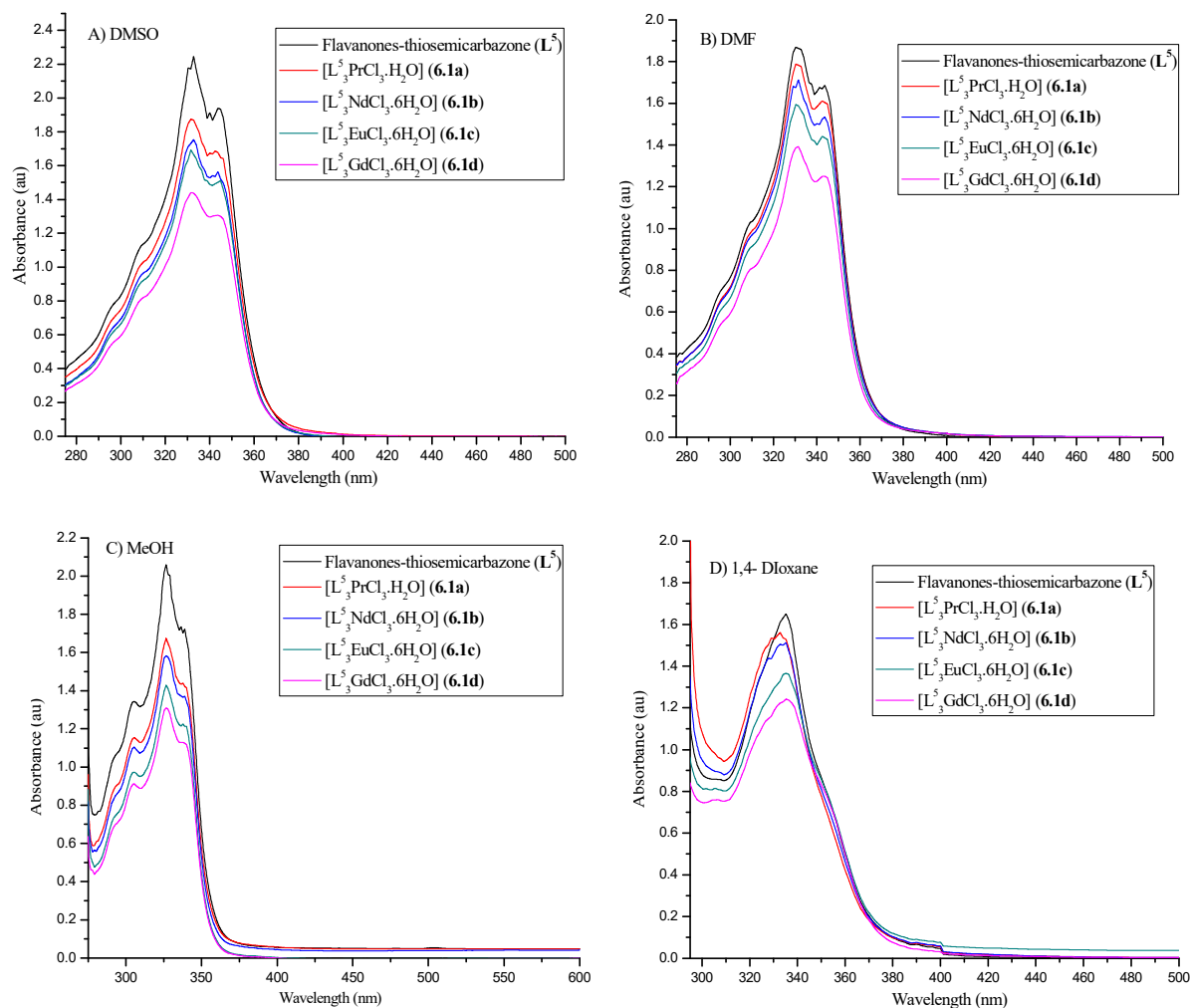


Figure 6.13. UV-Vis spectra of Flavanone-thiosemicarbazone ligand (L^5) and its Lanthanide Complexes ($6.1a-d$) in different solvents (conc. 1×10^{-5} M).

UV-Vis spectra of Flavanone-thiosemicarbazone ligand (L^5) and its Lanthanide complexes ($6.1a-d$) in different solvents such as dimethyl-sulfoxide (DMSO), dimethylformamide (DMF), methanol (MeOH) and 1,4-dioxane were recorded at concentration of 1×10^{-5} M. On recording the electronic spectra of free flavanone-thiosemicarbazone ligand (L^5), a maximum absorption band was observed at around 332 nm, 330 nm, 326 nm and 335 nm in DMSO, DMF, MeOH and 1,4-dioxane respectively. We observed that on increasing the polarity of the solvent the absorption band move toward the higher intensity. Similarly, we have recorded for the flavanone-thiosemicarbazone lanthanide

complexes (**6.1a-d**) in dimethyl-sulfoxide (DMSO), methanol (MeOH), dimethylformamide (DMF) and 1,4-dioxane solvents at same 1×10^{-5} M concentrations and found that with the increase in polarity of the solvent the absorption intensity move toward higher intensity in all the flavanone-thiosemicarbazone lanthanide complexes (**6.1a-d**) as revealed in **Figure 6.13**. and **Table 6.5**. When ligand interacts with the metal ($\text{Ln} = \text{Pr}^{3+}, \text{Nd}^{3+}, \text{Eu}^{3+}$ and Gd^{3+}) and forms complex, the metal- ligand bond length is shortened and a strong bond is formed there by increasing the absorption intensity of UV- Vis spectra of the complex compared to the intensity of the absorption spectra of ligand alone (Nephelauxetic Effect). In all the solvents (DMSO, DMF, MeOH and 1,4-Dioxane), the intensity of the flavanone-thiosemicarbazone ligand and its complexes are in the order $\text{L}^5 > [\text{L}_3\text{PrCl}_3 \cdot \text{H}_2\text{O}]$ (**6.1a**) $> [\text{L}_3\text{NdCl}_3 \cdot 6\text{H}_2\text{O}]$ (**6.1b**) $> [\text{L}_3\text{EuCl}_3 \cdot 6\text{H}_2\text{O}]$ (**6.1c**) $> [\text{L}_3\text{GdCl}_3 \cdot 6\text{H}_2\text{O}]$ (**6.1d**) which signifies the formation of the complexes of lanthanide with flavanone-thiosemicarbazone ligand (L^5) which is in the same order of the electronegativity in the periodic table.

Table 6.5. UV-Vis spectral values of Flavanone-thiosemicarbazone Ligand (L^5) and its Lanthanide Complexes (**6.1a-d**).

Compound	DMSO $\lambda_{\text{max}}(\text{a.u})$	DMF $\lambda_{\text{max}}(\text{a.u})$	MeOH $\lambda_{\text{max}}(\text{a.u})$	1,4-Dioxane $\lambda_{\text{max}}(\text{a.u})$
Flavanone – thiosemicarbazone (L^5)	310 (1.1350) 332 (2.2206) 343 (1.9393)	309 (1.0311) 330 (1.8663) 342 (1.6739)	303 (1.3327) 326 (2.0531) 338 (1.7092)	335(1.6437)
$[\text{L}_3\text{PrCl}_3 \cdot \text{H}_2\text{O}]$ (6.1a)	310 (1.0365) 332 (1.8718) 343 (1.6785)	309 (0.9849) 330 (1.7852) 342 (1.6114)	305 (1.1522) 326 (1.6619) 339 (1.4193)	328 (1.5244) 332 (1.5538)
$[\text{L}_3\text{NdCl}_3 \cdot 6\text{H}_2\text{O}]$ (6.1b)	310 (0.9628) 332 (1.7494) 343 (1.6820)	309 (0.9615) 331 (1.7026) 342 (1.5278)	305 (1.1014) 326 (1.5809) 338 (1.3671)	326 (1.4197) 334 (1.5027)
$[\text{L}_3\text{EuCl}_3 \cdot 6\text{H}_2\text{O}]$ (6.1c)	310 (0.9232) 332 (1.6791) 344 (1.5035)	309 (0.9070) 330 (1.5934) 342 (1.4398)	305 (0.9723) 327 (1.4204) 338 (1.2177)	329 (1.2857) 335(1.3656)
$[\text{L}_3\text{GdCl}_3 \cdot 6\text{H}_2\text{O}]$ (6.1d)	310 (0.8182) 332 (1.4375) 344 (1.3046)	309 (0.8051) 330 (1.3896) 342 (1.2945)	305 (0.9121) 327 (1.3048) 338 (1.1250)	330 (1.1964) 335 (1.2411)

6.3.4. Thermogravimetric Analysis

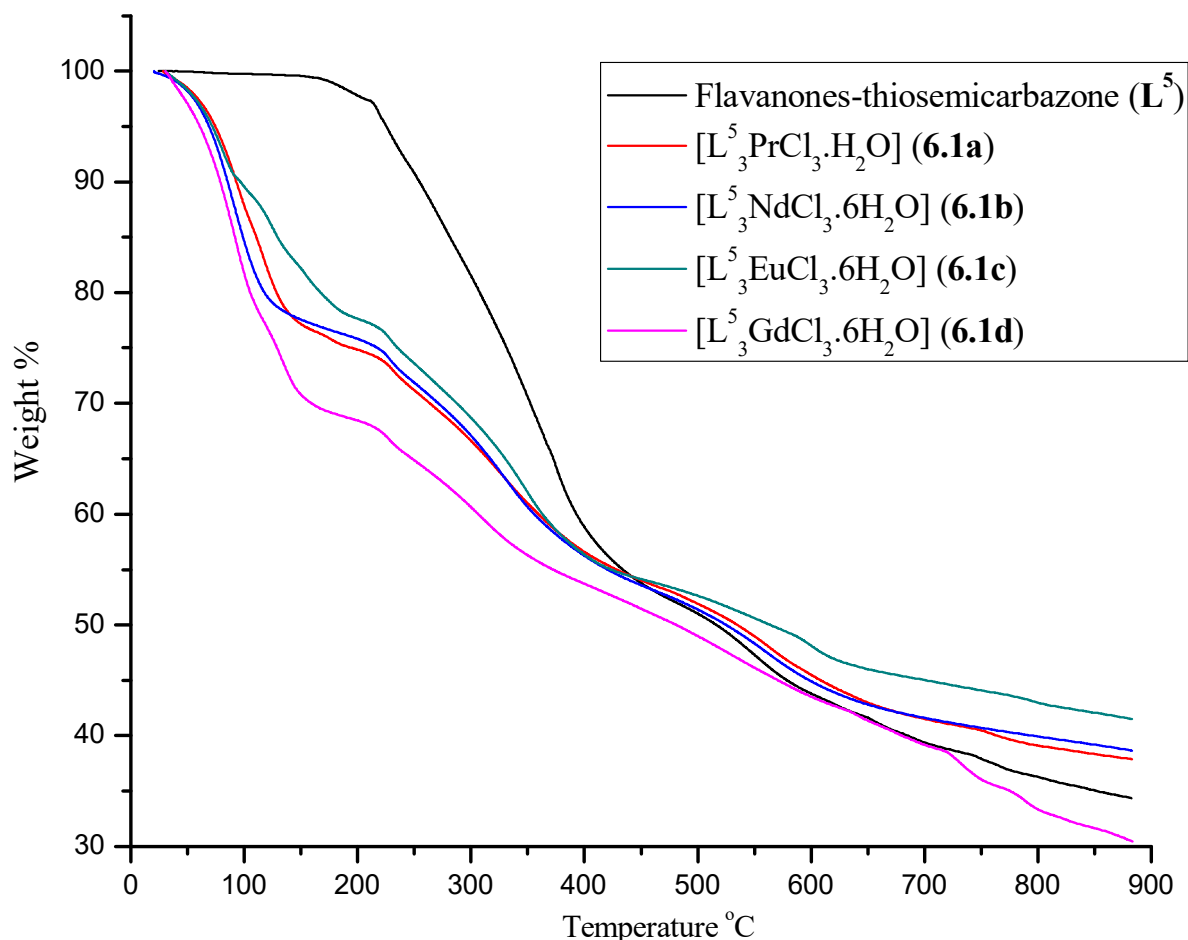


Figure 6.14. TGA curve for Flavanone-thiosemicarbazone Ligand (L^5) and its Lanthanide Complexes (6.1a-d).

Thermogravimetric analyses (weight change) were recorded at 10 °C/minute at a temperature range from 29 °C to 900 °C under nitrogen atmosphere in order to study the thermal behavior of flavanone-thiosemicarbazone ligand (L^5) and its lanthanide(III) complexes (6.1a-d) at different temperature. The thermal stability of the complexes were specify by the ligand to a great extend and at an average temperature the decomposition of the lanthanide complexes begins step by step and yield a residue of metal complexes even at high temperature showing its thermal stability. From the obtained TGA curve the weight loss of the free flavanone-thiosemicarbazone ligand (L^5) and its lanthanide metal complexes (6.1a-d) at different temperature were analyzed experimentally and theoretically. The typical thermograms of the flavanone-thiosemicarbazone ligand (L^5) and its lanthanide metal

complexes; $[L^5_3PrCl_3 \cdot H_2O]$ (**6.1a**), $[L^5_3NdCl_3 \cdot 6H_2O]$ (**6.1b**), $[L^5_3EuCl_3 \cdot 6H_2O]$ (**6.1c**), and $[L^5_3GdCl_3 \cdot 6H_2O]$ (**6.1d**) are represented in **Figure 6.14**. and the detail decomposition of the compounds respected to the temperature is tabulated in **Table 6.6**.

The first decomposition of the flavanone-thiosemicarbazone ligand (L^5) was observed at temperature between 30 °C-425 °C with weight loss of 43.80% followed by second decomposition of 12.38% weight loss at temperature between 425 °C-616 °C. The third decomposition starts at temperature 616 °C with incomplete decomposing of the compound.

While those of the flavanone-thiosemicarbazone lanthanides complexes (**6.1a-d**) shows four stages of decomposition with a residue left at the end supporting the metal contain. In all the complexes the decomposition starts with 21%-26% of weight loss with a temperature range between 30 °C-125 °C, decomposition of the complexes continue till the fourth stage at around 623 °C-776 °C corresponding to the molecules of the organic ligand and shows its thermal stability thereafter with a residue of metal alone with the nitrogen and sulphur of the ligand coordinated to it.

Table 6.6. Thermo gravimetric analysis of Flavanone-thiosemicarbazone Ligand (**L⁵**) and its Lanthanide Complexes (**6.1a-d**).

Compound	Temperature (°C)	Weight Loss (%) (Experiment/Theoretical)	Decomposed Compound
Flavanone – thiosemicarbazone (L⁵)	30.00 – 425.60	44.25% / 43.80%	C ₆ H ₄ , Cl , S and 2H
	425.60 – 616.49	12.04% / 12.38%	CN-NH-N
	616.49...	43.04% / 43.80%	C ₆ H ₄ and C ₃ O
[L ⁵ PrCl ₃ ·H ₂ O] (6.1a)	30.00 – 134.14	21.90% / 21.95%	H ₂ O, 6Cl and 3(NH ₂)
	134.14 – 360.15	18.98% / 18.37%	3 (C ₆ H ₄) and H ₃
	360.15 – 776.51	20.32% / 20.68%	2 (C ₉ H ₆ O)
	77.51...	39.61% / 38.98%	C ₉ H ₆ O , 3(N-N-S) and Pr
[L ⁵ NdCl ₃ ·6H ₂ O] (6.1b)	30.00 – 125.53	23.17% / 23.53%	6 (H ₂ O) and 6Cl
	125.53 – 429.13	24.08% / 24.30%	3(NH ₂) , C ₉ H ₆ O and C ₆ H ₄
	429.13 – 623.56	11.19% / 11.25%	2 (C ₆ H ₄)
	623.56...	43.77% / 43.15%	C ₉ H ₆ O , 3(N-N-S) and Nd
[L ⁵ EuCl ₃ ·6H ₂ O] (6.1c)	30.00 – 114.14	12.21% / 12.66%	6 (H ₂ O) , 3(NH ₂) and 4 Cl
	114.14 – 405.57	21.34% / 21.94%	2 (C ₆ H ₄) and 2 Cl
	405.57 – 609.53	10.38% / 10.57%	C ₉ H ₆ O
	609.53...	47.48% / 48.15%	2(C ₉ H ₆ O) , 3(N-N-S) and Eu
[L ⁵ GdCl ₃ ·6H ₂ O] (6.1d)	30.00 – 136.64	26.44% / 26.83%	6 (H ₂ O), 3(NH ₂) and 2 Cl
	136.16 – 326.50	15.10% / 15.83%	2 Cl and C ₆ H ₄
	326.50 – 742.10	21.83% / 21.11%	2 (C ₆ H ₄) C ₉ H ₆ O and 6 H
	742.10 ...	36.63% / 36.21%	C ₉ H ₆ O , 3(N-N-S) and Gd

6.4. Conclusion

In conclusion, we report the novel synthesis of flavanone-thiosemicarbazone ligand (**L⁵**) and its lanthanide complexes; [**L⁵**PrCl₃·H₂O] (**6.1a**), [**L⁵**NdCl₃·6H₂O] (**6.1b**), [**L⁵**EuCl₃·6H₂O] (**6.1c**) and [**L⁵**GdCl₃·6H₂O] (**6.1d**). All the synthesized flavanone-thiosemicarbazone lanthanide complexes were well investigated for their various spectroscopic studies. The IR spectra of all complexes were found that there is a chelate band shift and formation of new band in complexes comparing with that of free flavanone-thiosemicarbazone ligand which confirm the complexation. The UV-Vis absorption spectra of the complexes increase with the increase in the polarity of the solvents and found that the absorption bands move toward higher intensity in all the flavanone-thiosemicarbazone lanthanide complexes (**6.1a-d**). In future, these newly synthesized flavanone-thiosemicarbazone lanthanide complexes may be of value for numerous applications in various scientific areas.

6.5. References

1. L. Testai and V. Calderone, Nutraceuical Value of Citrus Flavanones and Their Implications in Cardiovascular Disease, *Nutrients.*, 2017, **9**, 502-514.
<https://doi.org/10.3390/nu9050502>
2. B. Bauvois, M. L. Puiffe, J. B. Bongui, S. Paillat, C. Monneret and D. J. Dauzonne, Synthesis and Biological Evaluation of Novel Flavone-8-acetic Acid Derivatives as Reversible Inhibitors of Aminopeptidase N/CD13, *Med. Chem.*, 2003, **46(18)**, 3900-3913. <https://doi.org/10.1021/jm021109f>
3. J. Bai, R. H. Wang, Y. Qiao, A. Wang and C. J. Fang., Schiff Base Derived from Thiosemicarbazone and Anthracene showed high Potential in Overcoming Multidrug Resistance in vitro with Low Drug Resistance Index, *Drug Des. Dev. Ther.*, 2017, **11**, 2227-2237. <https://doi.org/10.2147/dddt.s138371>
4. M. A. Husseina , M. A. Iqbala , M. Asifb , R. A. Haquea , M. B. K. Ahamedb , A. M. S. A. Majidb and T. S. Guana, Asynthesis, Crystal Structures and in vitro Anticancer Studies of New Thiosemicarbazone Derivatives, *J. Coord. Chem.*, 2014, **190 (9)**, 1498-1508. <https://doi.org/10.1080/10426507.2014.995299>
5. A. L. F. Sarria, A. F. L. Vilela, B. M. Frugeri, J. B. Fernandes, R. M. Carlos, M. F. G. Fe. Silva, Q. B.Cass and C. L. Cardoso, Copper (II) and Zinc (II) Complexes with Flavanone Derivatives: Identification of Potential Cholinesterase Inhibitors by on-flow assays, *J. Inorg. Biochem.*, 2016, **164**, 141-149.
<http://dx.doi.org/10.1016/j.jinorgbio.2016.09.010>
6. Y. Li, Z. Y. Yang and M. F. Wang, Synthesis, Characterization, DNA binding Properties, Fluorescence Studies and Antioxidant Activity of Transition Metal Complexes with Hesperetin-2-hydroxy benzoyl hydrazone, *J. Fluoresc.*, 2010, **20**, 91-905. <https://doi.org/10.1007/s10895-010-0635-z>
7. M. Tan, J. Zhu, Y. Pan, Z. Chen, H. Liang, H. Liu, H. Wang, Synthesis, Cytotoxic Activity, and DNA binding properties of Copper (II) Complexes with Hesperetin, Naringenin, and Apigenin, *Bioinorg. Chem. Appl.*, 2009, ID347872, 1-9.
<https://doi.org/10.1155/2009/347872>
8. R. M. Pereira, N. Andrades, N. Paulino, A. C. Sawaya, M. N. Eberlin, M. C. Marcucci, G. M. Favero, E. M. Novak, S. P. Bydlowski, Synthesis and Characterization of a Metal Complex Containing Naringin and Cu, and its Antioxidant, Antimicrobial,

- Antiinflammatory and Tumor Cell Cytotoxicity, *Molecules.*, 2007, **12**, 1352-1366.
<https://www.mdpi.com/1420-3049/12/7/1352/pdf>
9. Y. Li, Z.Y. Yang and T.R. Li, Synthesis, Crystal structure, DNA binding Properties and Antioxidant Activities of Transition Metal Complexes with 3-carbaldehyde-chromone Semicarbazone, *Chem. Pharm. Bull.*, 2008, **56**, 1528-1534.
<https://doi.org/10.1016/j.inoche.2010.07.005>
10. V. Kuntic, I. Filipovic and Z. Vujic, Effects of Rutin and Hesperidin and Their Al(III) and Cu(II) Complexes on *in Vitro* Plasma Coagulation Assays, *Molecules.*, 2011, **16**, 1378-1388. <https://doi.org/10.3390/molecules16021378>
11. S. Bargujar, S. Chandra, R. Chauhan, H. K. Rajor and Bhardwaj, Synthesis, Spectroscopic Evaluation, Molecular Modelling, Thermal Study and Biological Evaluation of Manganese(II) Complexes Derived from Bidentate N, O and N, S donor Schiff Base Ligands, *J. Appl. Organomet. Chem.*, 2018, **32(3)**, 4149-4162.
<https://doi.org/10.1002/aoc.4149>
12. K. Brodowska, A. Sykuła, E. Garribba, E. L. Chruscinska and M. Sojka, Naringenin Schiff Base: Antioxidant activity, Acid-base profile, and Interactions with DNA Transition, *Met. Chem.*, 2016, **41(2)**, 179-189.
<https://link.springer.com/article/10.1007/s11243-015-0010-7>
13. C. L. Andersen, C. S. Jensen, K. Mackeprang, L. Du, S. Jorgensen and H. G. Kjaergaard, Similar Strength of the $\text{NH}\cdots\text{O}$ and $\text{NH}\cdots\text{S}$ Hydrogen Bonds in Binary Complexes, *J. Phys. Chem. A.*, 2014, **118(46)**, 11074-11082.
<https://doi.org/10.1021/jp5086679>
14. M. M. Kasprzak, A. Erxleben and J. Ochocki, Properties and Applications of Flavonoid Metal Complexes, *RSC Adv.*, 2015, **5**, 45853-45877.
<https://doi.org/10.1039/C5RA05069C>
15. V. Uivarosi, M. Badea, R. Olar, B. S. Velescu and V. Aldea, Synthesis and Characterization of a New Complex of Oxovanadium (IV) with Naringenin, as Potential Insulinomimetic Agent, *Farmacia.*, 2016, **64(2)**, 175-180.
https://www.researchgate.net/publication/301552610_Synthesis_and_characterization_of_a_new_complex_of_oxovanadium_IV_with_naringenin_as_potential_insulinomimetic_agent

16. G. Celiz, S. A. Suarez, A. Arias, J. Molina, C. D. Brondino and F. Doctorovich, Synthesis, Structural Elucidation and Antiradical Activity of a Copper (II) Naringenin Complex, *Biometals.*, 2019, **32**, 595-610. <https://doi.org/10.1007/s10534-019-00187-3>
17. A. S. El-Tabl, M. M. A. Wahed, M. I. A. El-Azm and S. M. Faheem, Newly Designed Metal-based Complexes and their Cytotoxic Effect on Hepatocellular Carcinoma, Synthesis and Spectroscopic Studies, *J. Chem. Chem. Sci.*, 2020, **10(1)**, 10-31. <http://chemistry-journal.org/download/Abdou-Saad-El-Tabl-Moshira-Mohamed-Abd-El-Wahed-Maha-Ibrahim-Abo-El-Azm-and-Shaimaa-Mohammed-Faheem-/CHEMISTRY-JOURNAL-CHJV10I01P0010.pdf>
18. M. Fabijanska, M. M. Kasprzak and J. Ochocki, Ruthenium(II) and Platinum(II) Complexes with Biologically Active Aminoflavone Ligands Exhibit In Vitro Anticancer Activity, *Int. J. Mol. Sci.*, 2021, **22**, 1-18. <https://doi.org/10.3390/ijms22147568>
19. X. Zheng, H. Jiang, J. Xie, Z. Yin and H. Zhang, Highly Efficient and Green Synthesis of Flavanones and Tetrahydroquinolones, *Synth. Commun.*, 2013, **43**, 1023-1029. <https://doi.org/10.1080/00397911.2011.621096>
20. M. A. Spackman and D. Jayatilaka, Hirshfeld Surface Analysis, *Cryst. Eng. Comm.*, 2009, **11**, 19-32. <https://doi.org/10.1039/B818330A>
21. J. J. McKinnon, D. Jayatilaka and M. A. Spackman, Towards quantitative analysis of intermolecular interactions with Hirshfeld surfaces, *Chem. Commun.*, 2007, **13**, 3814-3816. <https://doi.org/10.1039/B704980C>
22. P. R. Spackman, M. J. Turner, J. J. McKinnon, S. K. Wolff, D. J. Grimwood, D. Jayatilaka and M. A. Spackman, CrystalExplorer: a program for Hirshfeld Surface Analysis, Visualization and Quantitative Analysis of Molecular Crystals, *J. Appl. Cryst.*, 2021, **54**, 1006-1011. <https://doi.org/10.1107/S1600576721002910>
23. S. L. Tan, M. M. Jotani and E. R. T. Tiekink, Utilizing Hirshfeld Surface Calculations, non-covalent Interaction (NCI) Plots and the Calculation of Interaction Energies in the Analysis of Molecular packing, *Acta. Cryst.*, 2019, **75(3)**, 308-318. <https://doi.org/10.1107/S2056989019001129>
24. A. L. Spek, Structure Validation in Chemical Crystallography, *Acta. Cryst.D.*, 2009, **65(2)**, 14-155. <https://doi.org/10.1107/S090744490804362X>



NAGALAND UNIVERSITY

(A Central University, Estd. By the Act of Parliament No. 35 of 1989)

Lumami – 798627, Nagaland, India

Department of Chemistry

Ph.D. Thesis Certificate on Plagiarism check

Name of the Research Scholar	Ruokuosenuo Zatsu
Ph.D. Registration Number	703/2016 w.e.f 27 th May 2015
Title of PhD thesis	“Synthesis of Lanthanide Complexes with Biologically Active Organic Ligands: their Spectral and Chemical Kinetic Studies”
Name & Institutional Address of the Supervisor / Co-Supervisor	Dr. Maddela Prabhakar Asst. Professor Department of Chemistry, Nagaland University, Lumami
Name & Institutional Address of the Supervisor / Co-Supervisor	Prof. M. Indira Devi Professor Department of Chemistry, Nagaland University, Lumami
Name of the Department and School	Department of Chemistry, School of Sciences
Date of submission	09/06/2021
Date of plagiarism check	09/06/2021
Percentage of similarity detected by the URKUND software	1%

1. We hereby declare that/certify that the Ph.D Thesis submitted by me is complete in all respect as per the guidelines of Nagaland University (NU) for this purpose. I also certify that the Thesis (soft copy) has been checked for plagiarism using **URKUND** similarity checked software. It is also certified that the contents of the electronic version of the thesis are the same as the final hardcopy of the thesis. Copy of the report generated by the **URKUND** software is also enclosed.

Place: *Lumami*
Date: *15/09/2021*

Ruokuosenuo Zatsu
(Name & Signature of the Scholar)



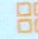
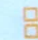

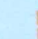

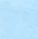


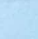
[Signature]
Name & Signature of the Supervisor:
With seal **DR. M. PRABHAKAR**
Asstt. Professor
Department of Chemistry
Nagaland University
Hqtrs: Lumami-798627.Nagaland

[Signature]
(M. INDIRA DEVI)
Professor
Name & Signature of the Co-Supervisor:
With seal Department of Chemistry
Nagaland University
Hqrs: Lumami-798627

Document Information

Analyzed document	Ruokuo-Thesis-for Plagiarism Checking-Draft.pdf (D112136237)
Submitted	9/6/2021 6:00:00 PM
Submitted by	
Submitter email	prabhakem@gmail.com
Similarity	1%
Analysis address	prabhakem.naga@analysis.orkund.com

Sources included in the report

SA	J I N C Y E . M . COMBINED.pdf Document J I N C Y E . M . COMBINED.pdf (D34261122)	 4
W	URL: http://zanotowane.pl/152/3576/ Fetched: 9/6/2021 6:01:00 PM	 1
SA	CHEMISTRY SANJAY RAMKRISHNA PAWAR Thesis.pdf Document CHEMISTRY SANJAY RAMKRISHNA PAWAR Thesis.pdf (D110895253)	 1
W	URL: https://www.researchgate.net/publication/258388283_Synthesis_Characterization_of_LaIII_NdIII_and_ErIII_Complexes_with_Schiff_Bases_Derived_from_Benzopyran-4-one_and_Thier_Fluorescence_Study Fetched: 12/28/2020 9:20:35 AM	 3
SA	Sneha Wankar full thesis chapters.pdf Document Sneha Wankar full thesis chapters.pdf (D21118513)	 5
W	URL: https://docplayer.net/amp/197417572-Transition-metal-complexes-of-6-mercaptopurine-characterization-theoretical-calculation-dna-binding-molecular-docking-and-anticancer-activity.html Fetched: 8/21/2021 2:37:49 PM	 1
W	URL: https://dergipark.org.tr/en/download/article-file/123465 Fetched: 7/21/2020 9:54:47 AM	 1
W	URL: http://www.bsauniv.ac.in/downloadFiles.aspx?file_name=Thesis_L.%20Lekha.pdf Fetched: 2/20/2021 11:11:58 AM	 2
W	URL: https://dx.doi.org/10.21577/0103-5053.20210049 Fetched: 6/28/2021 1:26:33 PM	 2
W	URL: http://www.electrochemsci.org/papers/vol8/81011860.pdf Fetched: 8/24/2021 7:15:14 AM	 1
J	URL: 8b950bc4-b2ca-49bf-892b-c7fe5153938e Fetched: 3/13/2019 1:23:16 AM	 1

List of Publications

- **Ruokuosenuo Zatsu**, Maddela Prabhakar and M. Indira Devi, Synthesis, Characterization and Luminescence Properties of Pr^{3+} , Nd^{3+} , Eu^{3+} and Gd^{3+} Complexes with Curcumin Pyrazole, *J. Mater. Sci.*, 2020, **3(76)**.
<https://dx.doi.org/10.2139/ssrn.3589132>
- **Ruokuosenuo Zatsu**, Prabhakar Maddela M. Indira Devi, Ranjit Singhb and Chullikkattil P. Pradeep, Crystal structure and Hirshfeld surface analysis of rac-2-[2-(4-chlorophenyl)-3,4dihydro-2H-1-benzopyran-4-ylidene]hydrazine-1-carbothioamide, *Acta Cryst.*, 2019, **75**, 707–710.
<https://scripts.iucr.org/cgi-bin/paper?zp2036>
- N. Bendangsenla1, M. Indira Devi, T. Moaienla, **Ruokuosenuo Zatsu**, 4f-4f Transition Spectral Analysis to Probe the Kinetics for the Complexation of Nd(III) with Guanosine and Guanosine Triphosphate (GTP), *J. Adv. Chem. Sci.*, 2018, **4(2)**, 556-561.
<https://www.jacsdirectory.com/journal-of-advanced-chemical-sciences/articleview.php?id=167>
- Maddela Prabhakar, Thechano Merry, **Ruokuosenuo Zatsu**, Shurhovie Tsurho and Ramchander Merugu, Microwave-Assisted Fast and Efficient Green Synthesis of 9-Anthracenyl Chalcones and their Anti-Bacteria Activity, *IOSR J. Pharm.*, 2017, **7(12)**, 24-32.
<http://www.iosrphr.org/papers/vol7-issue12/E0712012432.pdf>
- Maddela Prabhakar, Thechano Merry, Shurhovie Tsurho, **Ruokuosenuo Zatsu**, NishantJain, Aaysha Sataniya and Sreenivas Enaganti, Synthesis, Characterization and Biological Evaluation of 9-Anthracenyl Chalcones as Anti-Cancer Agents; *J. Chem. Pharm. Res.*, 2017, **9(6)**, 185-192.
<https://www.jocpr.com/articles/synthesis-characterization-and-biological-evaluation-of-9anthracenyl-chalcones-as-anticancer-agents.pdf>

Papers communicated/Manuscript under preparation

- **Ruokuosenuo Zatsu**, M. Indira Devi and Maddela Prabhakar, Microwave-Assisted Green Synthesis of Curcumin Lanthanide (Pr^{3+} , Nd^{3+} , Eu^{3+} and Gd^{3+}) Complexes and Investigation of their Spectroscopic and Kinetic Studies (Manuscript Communicated)
- **Ruokuosenuo Zatsu**, Maddela Prabhakar and M. Indira Devi, Synthesis, Characterization and Luminescence Properties of Pr^{3+} , Nd^{3+} , Eu^{3+} and Gd^{3+} Complexes with Curcumin-ethanolimine. (Manuscript under preparation)
- **Ruokuosenuo Zatsu**, M. Indira Devi and Maddela Prabhakar, Synthesis, Characterization and Luminescence Properties of Pr^{3+} , Nd^{3+} , Eu^{3+} and Gd^{3+} Complexes with flavanones-thiosemicarbazone. (Manuscript under preparation)

Conferences/ Workshops/Trainings Attended

- Participated in National e-seminar on “Chemistry in emerging trends of interdisciplinary research (NeSCETIR-2020)” organized by Department of Chemistry, Nagaland University, On 18th -20th November 2020.
- Participated in One day Workshop on “Importance of IPR in Academic Institutions” organized by IPR Cell, Nagaland University held on 29th May, 2019.
- Oral presentation on “Synthesis, Spectral Characterization Studies of Curcumin Lanthanide (Pr^{3+} , Nd^{3+} , Eu^{3+} and Gd^{3+}) Complexes” (Nscir-2018) organized by Department of Chemistry, Nagaland University on 9th -10th November, 2018.
- Participated in workshop on “Liquid Chromatography- Mass Spectrometry and its Applications” organized by at Sophisticated Analytical Instrument Facility (SAIF), North Eastern Hill University (NEHU), Shillong and sponsored by the Department of Science & Technology, Government of India held from 3rd to 5th April, 2018
- Oral presentation on “Natural product ligand synthesis of Lanthanide complex and their spectroscopic studies” (Nscir-2017) organized by Department of Chemistry, Nagaland University held on 16th -17th March, 2017.
- Participated in Science Exhibition on “Water Literacy and Innovation in Water Purification & Conservation” organized by Department of Chemistry, Nagaland University catalyzed and supported by National Council for Science and Technology Communication, DST, New Delhi Under “ECO & WaSH Futures” held on 11th November, 2016.
- Participated in “Innovation Exhibition” organized by Nagaland University Innovation Cell in collaboration with Department of Chemistry, Nagaland University & National Innovation Foundation-India held on 17th November, 2015.
- Participated in Science Exhibition on “Water Literacy & Innovation in Water Purification & Conservation” organized by Department of Chemistry & Innovation Cell, Nagaland University catalyzed and supported by National Council for Science and Technology Communication, DST, New Delhi Under “ECO & WaSH Futures” held on 31st March, 2015.
- Participated in National Seminar on “Globalization, Development and Environment with Special Reference to North-East India” organized by Nagaland University Teachers Association (Lumami), Nagaland University, Lumami Nagaland held on 19th and 20th 2015